

See discussions, stats, and author profiles for this publication at: <https://www.researchgate.net/publication/38058216>

Synthetic therapeutic peptides: science and market. Drug Discov Today

Article in *Drug discovery today* · October 2009

Impact Factor: 6.69 · DOI: 10.1016/j.drudis.2009.10.009 · Source: PubMed

CITATIONS

405

READS

1,813

4 authors:



Patrick Vlieghe

Société d'Accélération du Transfert de Techn...

26 PUBLICATIONS 742 CITATIONS

SEE PROFILE



Vincent Lisowski

Université de Montpellier

60 PUBLICATIONS 959 CITATIONS

SEE PROFILE



Jean Martinez

Université de Montpellier

1,026 PUBLICATIONS 13,274 CITATIONS

SEE PROFILE



Michel Khrestchatisky

Aix-Marseille Université

151 PUBLICATIONS 4,700 CITATIONS

SEE PROFILE



Synthetic therapeutic peptides: science and market

Patrick Vlieghe¹, Vincent Lisowski², Jean Martinez² and Michel Khrestchatisky³

¹ VECT-HORUS S.A.S., Faculté de Médecine Secteur Nord, CS80011, Boulevard Pierre Dramard, 13344 Marseille Cedex 15, France

² Institut des Biomolécules Max-Mousseron (IBMM, UMR5247 CNRS), Universités Montpellier I et II, UFR des Sciences Pharmaceutiques et Biologiques, 15 Avenue Charles Flahault, 34093 Montpellier Cedex 5, France

³ Laboratoire de Neurobiologie des Interactions Cellulaires et Neurophysiopathologie (NICN), UMR6184 CNRS, Université de la Méditerranée, Faculté de Médecine Secteur Nord, CS80011, Boulevard Pierre Dramard, 13344 Marseille Cedex 15, France

The decreasing number of approved drugs produced by the pharmaceutical industry, which has been accompanied by increasing expenses for R&D, demands alternative approaches to increase pharmaceutical R&D productivity. This situation has contributed to a revival of interest in peptides as potential drug candidates. New synthetic strategies for limiting metabolism and alternative routes of administration have emerged in recent years and resulted in a large number of peptide-based drugs that are now being marketed. This review reports on the unexpected and significant number of peptides that are currently available as drugs and the chemical strategies that were used to bring them into the market. As demonstrated here, peptide-based drug discovery could be a serious option for addressing new therapeutic challenges.

Recent pharmaceutical market evolution

The pharmaceutical market is evolving in a context of increasing economic pressure. First, public authorities are pushing for lower healthcare costs through reduced drug pricing and increasing use of generic substitution. Second, regulatory authorities are more demanding in terms of drug efficacy, quality and safety, which – combined with (bio)technological progress – has led to an increase in pharmaceutical R&D costs [1]. At the beginning of the 2000s, the Tufts Center for the Study of Drug Development estimated that the average cost of developing a new prescription drug was US\$ 802 million (US\$ 335 million for preclinical and US\$ 467 million for clinical trials) [2,3]. More recently, these expenses have been estimated at US\$ 1318 billion including costs of capital and failures, the latter representing approximately 70% of the total amount [4]. In fact, 38% of the drug candidates under development are abandoned in phase I clinical trials because of toxicity, 63% of those that reach phase II clinical trials are withdrawn for lack of efficacy or poor bioavailability, 45% of the remaining drug candidates fail in phase III clinical trials, and 23% of those that satisfy the clinical trials are not authorized by

the Food and Drug Administration (FDA) or the European Medicines Agency (EMA) [5]. Attrition owing to lack of efficacy, toxicology and clinical safety are the most common causes of failure in the development of new molecular entities (NMEs). The rate of failure during drug development is, thus, 90% in general and even greater in the case of the central nervous system (CNS) [5,6].

Third, with a decrease in R&D productivity (as shown by the low number of approvals for NMEs in recent years: 17 NMEs and 2 biologic license applications, or BLAs, approved by the FDA in 2007 [7], the lowest number recorded since 1983 and 21 NMEs and 3 BLAs in 2008 [8]) and patent expiry of blockbuster drugs in the past decade, a pipeline problem has emerged in the pharmaceutical industry. To be competitive and profitable in this high-pressure context, pharmaceutical companies need to improve strategies for anticipating and identifying crucial events in development as early as possible to reduce their costs [3]. Pharmaceutical companies also need to be strongly innovative to discover new drugs or technologies and to market innovative products, or at least to give a second life to their molecules through product lifecycle management or new therapeutic applications. There is a convention in the pharmaceutical

Corresponding author: Vlieghe, P. (patrick.vlieghe@vect-horus.com)

industry that to recoup R&D investment and make a reasonable profit, a product needs to bring in peak annual sales of US\$ 500 million [3].

Peptides as drugs: a revival of interest

Peptides are generally considered to be poor drug candidates because of their low oral bioavailability and propensity to be rapidly metabolized. The concept that a drug can be not 'orally available' has become more and more accepted and, as a consequence, some pharmaceutical companies have contributed in recent years to a revival of interest in peptides as potential drug candidates [9]. New synthetic strategies to improve productivity and reduce metabolism of peptides, along with alternative routes of administration, have been developed in recent years, and a large number of peptide-based drugs are now being marketed.

Therapeutic peptides traditionally have been derived from three sources: (i) natural or bioactive peptides produced by plants, animal or human (derived from naturally occurring peptide hormones or from fragments of larger proteins); (ii) peptides isolated from genetic/recombinant libraries and (iii) peptides discovered from chemical libraries [10,11].

Generally, the size of the peptide determines the most suitable technology for its production: chemical synthesis, recombinant DNA technology, cell-free expression systems, transgenic animals and plants or enzymatic synthesis. With the use of unnatural amino acids and pseudo-peptide bonds, chemical synthesis offers access to a much wider chemical diversity than peptide derivatives produced by recombinant technologies, with a diversified potential for intellectual property (in terms of patentable new chemical entities). Large-scale chemical synthesis has become a viable technology for the production of small- and medium-sized peptides ranging from approximately 5 to 50 residues, and the chemical way is now often a better technological option than the biotechnological methods of recombinant DNA or biocatalysis for the synthesis of medium-sized peptides that comprise most of the pharmaceutically relevant molecules. In particular, production of synthetic therapeutic peptides has become possible for the pharmaceutical industry with the development of solid-phase peptide synthesis (SPPS) by Merrifield [12] (Fig. 1). SPPS is crucial in the early steps of preclinical research and in the production of peptide-based active pharmaceutical ingredients (APIs) [13]. The main SPPS strategies are sequential synthesis, convergent synthesis and chemical ligation. Sequential synthesis involves the stepwise addition of amino acids until the desired peptide is achieved. Convergent synthesis involves the independent solid-phase synthesis of peptide sequences (fragments) that are then cleaved from the polymer without N-terminal (or C-terminal) and side-chain protecting group removal and linked by condensation in solution (mixed-phase synthesis). This solid-phase and solution-phase hybrid peptide synthesis is often the most appropriate way to synthesize peptides that contain >50 amino acid residues. Chemical ligation involves coupling of totally deprotected fragments by chemoselective reactions [14]. Several systems for the automated *t*-Boc/Bzl and Fmoc/*t*-Bu SPPS, ranging from 1.5 mg to 5 kg scale, are now available from several companies, including AAPTec, Activotec, Applied Biosystems, CEM, CS Bio, Intavis, Peptide Scientific, Protein Technologies and ThuraMed (CreoSalus group).

Limitations to the use of peptides as drug candidates and key proteolytic enzymes involved in peptide degradation (<http://www.biochem.ucl.ac.uk/bsm/enzymes/ec3/index.html>, <http://www.ebi.ac.uk/thornton-srv/databases/enzymes/>) [15,16]

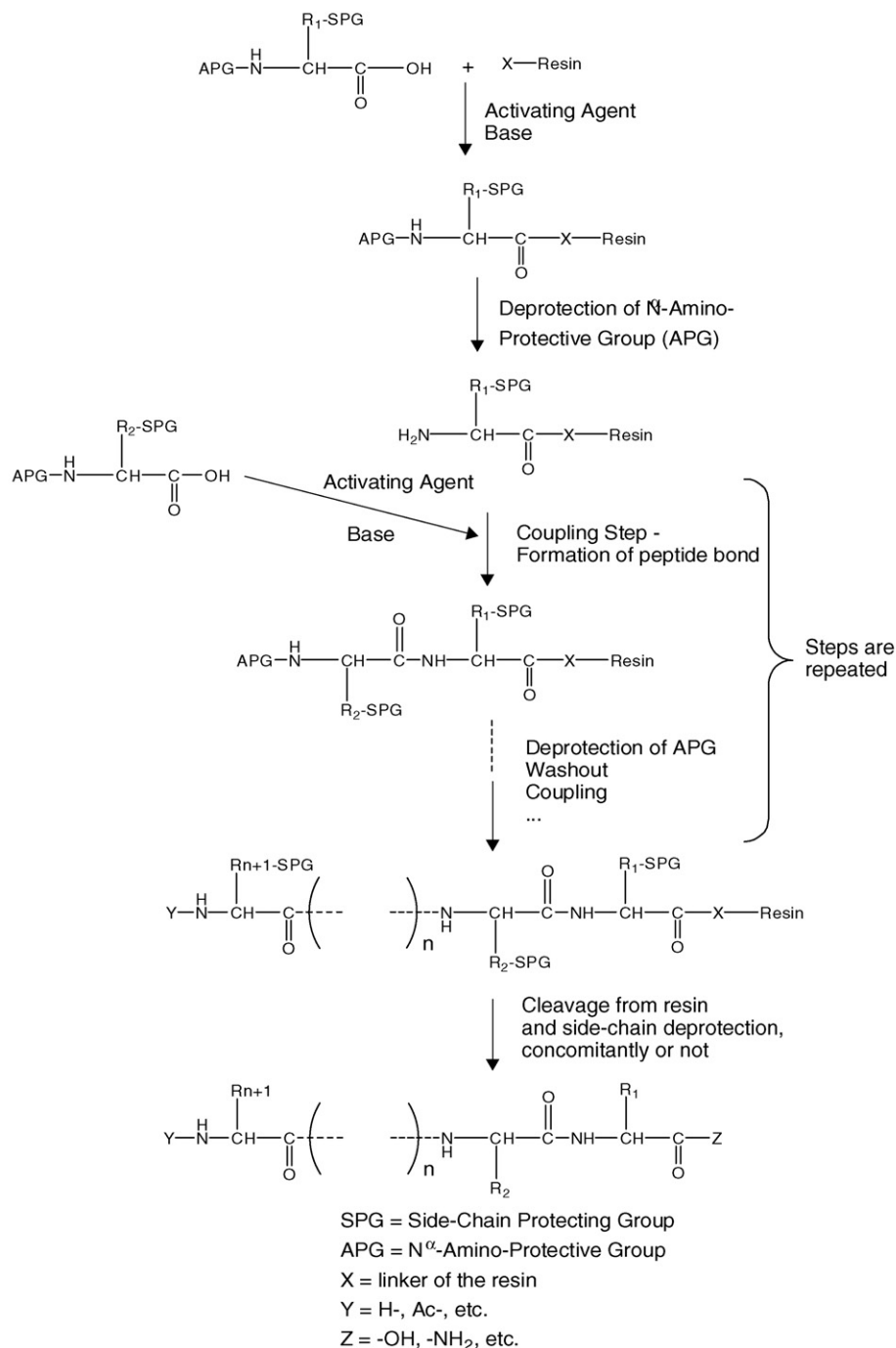
Peptide limitations

Bioavailability and biodistribution of peptide drug candidates, which include absorption, transport, passage of biological membranes and cellular barriers, are determined by a combination of their physicochemical properties, such as aqueous solubility, lipophilicity, H-bond formation, chemical stability and metabolic stability (proteolytic/enzymatic degradation or hydrolysis). With a few exceptions, peptides composed of natural amino acids are not very good drug candidates because of their intrinsic physicochemical properties and pharmacokinetic profiles. When compared with therapeutic proteins and antibodies, peptide drug candidates do have significant drawbacks: they generally have low stability in plasma, are sensitive to proteases and can be cleared from the circulation in a few minutes.

Thus, the main limitations generally attributed to therapeutic peptides [17,18] are: low oral bioavailability (injection is generally required); a short half-life because of their rapid degradation by proteolytic enzymes of the digestive system and blood plasma; rapid removal from the circulation by the liver (hepatic clearance) and kidneys (renal clearance); poor ability to cross physiological barriers because of their general hydrophilicity; high conformational flexibility, resulting sometimes in a lack of selectivity involving interactions with different receptors/targets (poor specific biodistribution), causing activation of several targets and leading to side effects; eventual risk of immunogenic effects; and high synthetic and production costs (the production cost of a 5000 Da molecular mass peptide exceeds the production cost of a 500 Da molecular mass small molecule by more than 10-fold but clearly not 100-fold) [19].

Proteolytic enzymes

As mentioned above, the proteolytic stability of natural peptides is one of the principal limitations of their use as drug candidates. Human blood is composed of 44% red blood cells, 1% white blood cells and 55% plasma. Plasma consists of 91% water, 7% proteins and 2% salts. It contains more than 120 different proteins, including albumin (HSA), immunoglobulin G (IgG), fibrinogen (factor I), alpha-2-macroglobulin (α 2M), alpha-1-antitrypsin (A1AT), transferrin (siderophilin) and lipoproteins and numerous proteolytic enzymes, such as esterases and peptidases. As indicated in Supplementary Table 1, according to the enzyme classification (E.C.), numerous human proteolytic enzymes (peptidases) are involved in peptide degradation. The greatest threat to therapeutic peptides lies in the lumen of the small intestine, which contains gram quantities of peptidases secreted from the pancreas (e.g. α -chymotrypsin, trypsin, pancreatic elastase, carboxypeptidases A, B, D, N and U and so on), as well as cellular peptidases from mucosal cells. The second major enzymatic barrier is the brush border membrane of the epithelial cells, which contains at least 15 peptidases [20] (e.g. dipeptidyl-peptidase IV, prolyl tripeptidyl-peptidase, angiotensin-converting enzyme, leucyl-aminopeptidase, aminopeptidase M, aminopeptidase A and neprilysin), that together have a broad specificity and can degrade both peptides and proteins.



Drug Discovery Today

FIGURE 1

Sequential (or linear) solid-phase peptide synthesis (SPPS). This figure illustrates the repetitive stepwise process (activation, coupling, deprotection, washout and cleavage) of chemical peptide synthesis by solid-phase technique.

Lysosomal peptidases (leukocyte elastase, cathepsins B and D and so on) will also target peptides or proteins endocytosed by epithelial or endothelial cells. In the matrix metalloproteinase family (zinc-dependant endopeptidases) known to degrade extracellular matrix proteins, interstitial collagenase (MMP-1, *E.C.3.4.24.7*) is also able to cleave specific small molecules such as peptides. Amongst proteases, carboxypeptidase C – sometimes referred to as Y

(*E.C.3.4.16.5*) – is the only enzyme that exhibits both the esterase and the amidase activities typical of serine proteases [16]. Many enzymes are also present in different tissues or organs. For example, in brain micro-capillaries, which constitute part of the blood–brain barrier (BBB), gamma-glutamyl transpeptidase (transferase, *E.C.2.3.2.2*), alkaline phosphatase (hydrolase, *E.C.3.1.3.1*), monoamine oxidase (oxidoreductase, *E.C.1.4.3.4*), catechol-O-methyl

transferase (transferase, *E.C.2.1.1.6*), butyrylcholinesterase (hydrolyase, *E.C.3.1.1.8*) and aromatic-L-amino acid carboxylase (or dopa-decarboxylase or aromatic-L-amino acid decarboxylase; lyase, *E.C.4.1.1.28*), are found at high levels [15,21]. Other enzymes, such as epoxidehydrolase (or epoxide hydrolase; hydrolase, *E.C.3.3.2.9*, former *E.C.3.3.2.3*), UDP-glucuronosyl-transferase (glycosyl-transferase, *E.C.2.4.1.17*), benzyloxyresorufin-O-deethylase (cytochrome P-450 CYP2B1; oxidoreductase, *E.C.1.14.14.1*), NADPH cytochrome P-450 reductase (oxidoreductase, *E.C.1.6.2.4*) and glutathione-S-transferase (transferase, *E.C.2.5.1.18*) are also found bound to brain micro-capillaries at high levels [15,21]. The protein-disulfide reductase (oxidoreductase, *E.C.1.8.4.2*), which enables disulfide bridge cleavage by reduction in dithiol, is also abundant in the brain and can alter peptide structures stable in plasma [22,23]. Proteolytic peptide degradation, which results in short half-life (generally, a few minutes or, at best, a few hours), can be countered in various ways, in particular by using new synthetic strategies for limiting metabolism and alternative routes of administration [24]. Thus, it is usually necessary to introduce chemical modifications into peptides containing natural amino acids to adapt them for therapeutic use.

Chemical strategies to improve peptide biological activity, specificity and stability

As discussed previously, the low bioavailability of peptides is partly because of high biodegradability by gastrointestinal, plasma and tissue peptidases. Moreover, their rapid removal from the circulation can also limit their therapeutic use. Absorption, distribution, metabolism and excretion processes play a pivotal part in defining the disposition of a drug candidate and, thus, its therapeutic effect [25]. To develop a peptide as a therapeutic agent, its biological effect, pharmacokinetic profile and low immunogenicity are crucial parameters. Therefore, various chemical strategies have been developed to try and overcome the limitations of peptides to increase their *in vivo* plasma residence time. Many cyclic peptides, pseudo-peptides (modification of the peptide bond) and peptidomimetics (nonpeptide molecules) preserving the biological properties of peptides have been and are widely developed to increase their resistance to degradation and elimination, their bioavailability and their selectivity (targeting of protein–receptor interactions) to become good drug candidates. In fact, from a model peptide of interest (lead peptide), it is often necessary to optimize its chemical structure (cyclization, bioisosteric replacement of peptide bonds, changing the stereochemistry of an amino acid and so on) to obtain a compound that can be used therapeutically, even for parental administration (e.g. subcutaneous, intramuscular or intravenous injection).

The chemical optimization strategy of a therapeutic peptide is based on structure–activity relationship and/or quantitative structure–activity relationship studies of newly synthesized peptide derivatives, with the aim of improving bioavailability, reducing elimination and biodegradation and increasing selectivity or affinity to its receptor/target. As detailed in Box 1, lead peptide chemical optimization usually requires different strategies developed by peptide chemists [15,17,18,26,27]. As previously discussed, the main reasons for the low oral bioavailability of peptide drugs are pre-systemic enzymatic degradation and poor penetration of the intestinal mucosa. According to Lipinski's 'rule of five' [28–31] completed by Veber *et al.*'s analysis [32], peptides

BOX 1

Lead peptide chemical optimization

- Search for the minimum active sequence (MAS) from N- and/or C-terminal truncated analogues (Fig. 2).
- Significance of the N- and C-terminus.
- Deletion of one or more consecutive amino acid(s) and combinatorial deletion with two or more positions omitted independently throughout the sequence (Fig. 2).
- Simplification/optimization of the structure after alanine scanning (Ala-scan) and/or D-scanning (D-scan) to eliminate potential sites of cleavage (notably by endopeptidases) and to determine important functional groups involved in the interaction with the target of interest (Fig. 2).
- Cyclization of the peptide sequence (between side chains or ends of the peptide sequence: head to tail, N-backbone to N-backbone, end to N-backbone, end to side chain, side chain to N-backbone, side chain to side chain) [36] through disulfide (disulfide-bond cyclization scan, Fig. 2), lanthionine, dicarba, hydrazine or lactam bridges [37] to decrease the conformational flexibility of linear peptides, to reduce hydrogen bonding, to enhance membrane permeability and, importantly, to increase their stability to proteolysis by endo- and exopeptidases.
- Substitution of a natural amino acid residue by an unnatural amino acid (D-configuration), an N-methyl- α -amino acid, a non-proteogenic constrained amino acid or a β -amino acid, to increase plasma stability (e.g. resistance to endopeptidases) of the peptide and/or affinity (activity) for its target.
- Isosteric, or not, amide bond replacement between two amino acids: NH-amide alkylation, the carbonyl function of the peptide bond can be replaced by CH₂ (reduced bond: –CH₂–NH–), C(=S) (endothiopeptide, –C(=S)–NH–) or PO₂H (phosphonamide, –P(=O)OH–NH–). NH-amide bond can be exchanged by O (depsipeptide, –CO–O–), S (thioester, –CO–S–) or CH₂ (ketomethylene, –CO–CH₂–). The peptide bond can also be modified: retro-inverso bond (–NH–CO–), methylene-oxy bond (–CH₂–), thiomethylene bond (–CH₂–S–), carba bond (–CH₂–CH₂–), hydroxyethylene bond (–CHOH–CH₂–) and so on, to increase plasma stability of the peptide sequence (notably towards endopeptidases).
- Blocking N- or C-terminal ends by N-acylation, N-pyroglutamate, C-amidation and so on, or addition of carbohydrate chains (glycosylation: glucose, xylose, hexose, etc.) to increase plasma stability (notably, resistance towards exopeptidases).
- N-terminal esterification (phosphoester) or pegylation modifications to enhance plasma stability (e.g. resistance to exopeptidases) and to reduce immunogenicity. Pegylation is also designed to make the peptide larger (generally >50 kDa) to retard excretion through the kidneys (renal clearance).

are poor candidates to move from the digestive tract to the circulatory system because of their physicochemical properties. For these reasons, until a few years ago, therapeutic peptides were generally administered by subcutaneous, intramuscular or intravenous routes (which inevitably cause discomfort for the patient) to circumvent the gut barrier. The paths of molecules in animals or humans are as follows: (i) heart (right ventricle), lungs, heart (left ventricle), then distribution to the various organs, including liver,

Q17

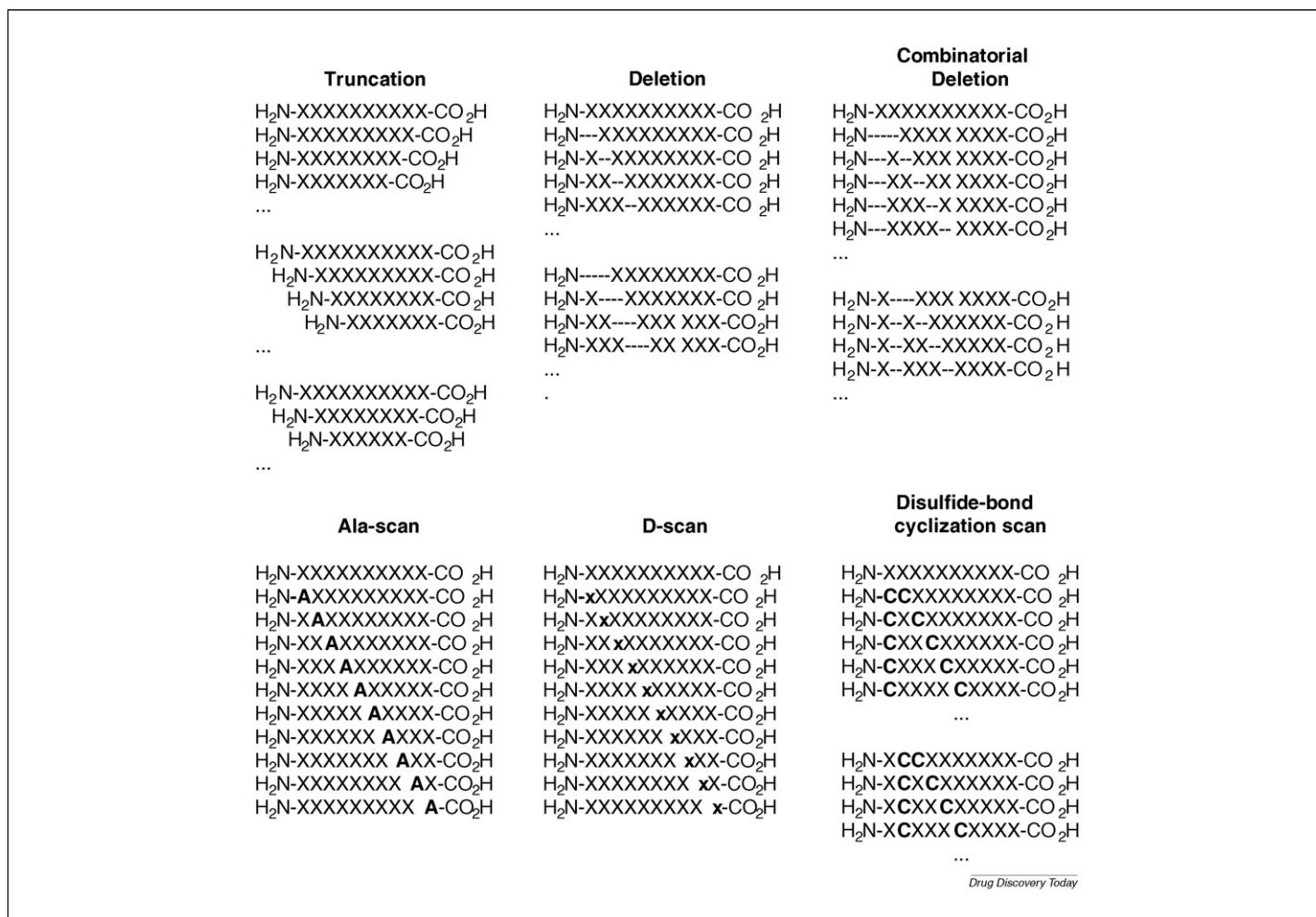


FIGURE 2

Q16 Chemical optimization strategies of peptides. This figure illustrates the main strategies developed by peptide chemists for lead peptide optimization. Adapted, with permission, from Ref. [36].

intestine, brain, kidneys and muscles, if injected intravenously; and (ii) stomach, intestine, liver, blood, kidneys and tissues, if administered orally [33]. In the latter case, peptides have to face a strongly acidic gastric environment, high levels of intestinal proteolytic activity and a high intestinal permeability barrier [20]. Consequently, alternative routes for the administration of peptide-based drugs have been improved in recent years, and novel peptide delivery technologies have emerged, including controlled-release parenteral route (subcutaneous, intramuscular or intravenous), mucosal route (nasal spray, pulmonary delivery or sublingual delivery), oral route (penetration enhancers, protease inhibitors or carriers) and transdermal route (patches) [24]. The biodistribution study of a therapeutic peptide is essential to determine its uptake by various organs and its selectivity for its targeted site of action. Despite these recent advances in oral delivery, the bioavailability of therapeutic peptides with any of the current technologies is much lower than that obtained by injection. The speed of action and the low side effects of a peptide injection are unbeatable in case of emergency treatments [34]. In spite of some limitations and thanks to progress in chemical synthesis and routes of administration, synthetic therapeutic peptides present numerous advantages compared with their homologous com-

pounds (proteins and antibodies) and with small organic molecules.

Advantages of peptides over other drug candidates

Compared with proteins and antibodies, peptides have the potential to penetrate further into tissues owing to their smaller size. Moreover, therapeutic peptides, even synthetic ones, are generally less immunogenic than recombinant proteins and antibodies [35]. Peptides have other advantages over proteins and antibodies as drug candidates, including lower manufacturing costs (synthetic versus recombinant production), higher activity per unit mass (15–60-fold, assuming 75 kDa for one combining site of an antibody and 10–50 amino acids for a therapeutic peptide), lower royalty stack than antibodies because of a simpler intellectual property landscape during discovery and manufacturing, greater stability (lengthy storage at room temperature acceptable), reduced potential for interaction with the immune system (assuming the peptide contains no known immune-system signalling sequence) and better organ or tumour penetration [26].

Therapeutic peptides also offer several advantages over small organic molecules that make up traditional medicines. The first advantage is that often representing the smallest functional part of

a protein, they offer greater efficacy, selectivity and specificity (limited non-specific binding to molecular structures other than the desired target) [36] than small organic molecules. A second advantage is that the degradation products of peptides are amino acids, thus minimizing the risks of systemic toxicity (minimization of drug–drug interactions) [34]. Third, because of their short half-life, few peptides accumulate in tissues (reduction of risks of complications caused by their metabolites). Most therapeutic peptides, which are mainly derived from natural peptides, are receptor agonists [37]. Generally small quantities of these peptide agonists are necessary to activate the targeted receptors [38]. Few peptide antagonists, inhibiting ligand–receptor interactions, have reached the market so far [26]. As a general rule, antagonists must occupy more than 50% of the receptor population to be effective, in contrast to agonists, which require lower levels of receptor occupancy to be effective (normally between 5% and 20%) [6].

Since the advent of SPPS [12], chemical synthesis of therapeutic peptides can be considered as the most mature technology available [39]. Compared with synthetic therapeutic peptides, the quality/purity of recombinant molecules is not always optimal and peptides produced by enzymatic routes have low productivity [14]. The system of choice can be dictated by the cost of production or the modifications of the peptide sequence (for example, glycosylation, phosphorylation or proteolytic cleavage) that are required for biological activity [40]. Production systems for recombinant peptides or proteins include bacteria, yeast, insect cells, mammalian cells and transgenic animals and plants. Inability to incorporate unnatural amino acids or C-terminal amidation is another drawback of genetic engineering during the synthesis of therapeutic peptides. Moreover, the application of recombinant DNA technology typically requires a long and expensive R&D phase. Despite the technological advances in peptide synthesis by biocatalysis, the low productivity, the low yield and the high cost of enzymes could hamper competitiveness in a broad spectrum of cases. SPPS is especially suited for medium-size peptides (up to 100 amino acid residues) that comprise most of the peptides of therapeutic relevance. Moreover, a key advantage of the chemical synthesis in solid-phase is that the peptide product can be easily separated from impurities and side products. In addition, synthetic therapeutic peptides are now less expensive to produce than peptides or proteins obtained by recombinant technology (applicable only for peptide sequences including natural amino acids) or enzymatic route. As an example, even if it takes six to eight months and 106 steps to chemically synthesize at a multi-tonne per year scale the 36-mer anti-HIV peptide Fuzeon[®] (enfuvirtide, the first fusion inhibitor on the market for HIV treatment), its development has helped reduce costs of large-scale good manufacturing practices peptide synthesis to less than US\$ 1 per gram per amino acid residue [19].

Market for synthetic therapeutic peptides

The market for synthetic therapeutic peptides rose from €5.3 billion in 2003 to €8 billion in 2005. It has been estimated that it will reach €11.5 billion in 2013 [18]. This excludes peptides, proteins and antibodies extracted from natural sources or produced by recombinant DNA technology, cell-free expression systems, transgenic animals and plants and enzyme technology.

As described in **Supplementary Table 2**, more than 60 synthetic therapeutic peptides (comprising those used for medical diagnostics or imaging), with a size <50 amino acids, have reached the American, European and/or Japanese pharmaceutical markets through a marketing authorization as APIs, even if some of them are generics or discontinued (<http://www.biam2.org/>, <http://www.documed.ch>, <http://www.fda.gov/>, <http://www.fdaapproveddrugs.us>, <http://www.rxlist.com> and <http://www.vidal.fr>) [14,19,34,41].

Peptides and their homologous compounds (proteins and antibodies) can be used in multiple pathologies, including allergy and asthma, arthritis, baldness, cardiovascular diseases (coronary syndrome and angina), diabetes, gastrointestinal dysfunction, growth problem, haemostasis, immunity disease, impotence, incontinence, infective diseases (bacterial, fungal and viral), inflammation, obesity, oncology (cancer and tumour imaging), osteoporosis (calcium metabolism dysfunction), pain, vaccines and so on [34,41], which represent important markets. In this context, the CNS is certainly a paradox: it is a major therapeutic area with unmet medical needs, for which the therapeutic peptide market potential is immense. To achieve therapeutic efficacy, a potential CNS drug has to cross the BBB by one of two transcellular mechanisms: passive diffusion or active (catalyzed) transport. Passive diffusion comprises mechanisms as transcellular lipophilic diffusion, which requires no energy. Carrier-mediated transport (CMT) and receptor-mediated transport or transcytosis (RMT) are active transport mechanisms, which require energy. Unfortunately, most small molecules and virtually all peptide and protein therapeutics are generally excluded from passive transport because of their hydrophilicity and/or molecular mass, even if some commercial synthetic therapeutic peptides (thyrotropin-releasing hormone, argipressin, luteinizing-hormone-releasing hormone and so on) have been demonstrated to cross the BBB by saturable transport mechanisms [42]. Peptides will probably be used intensively in the near future for various applications in the treatment of CNS diseases, notably in the design of peptide regulators of protein activity, if they are able to cross the BBB. Peptide-based vectors (cationic or cationized peptides or proteins, which cross the BBB by adsorptive-mediated transport [43,44], and CMT- or RMT-based peptides [45–49]) developed for CNS drug targeting will certainly contribute to the development of peptide-based drugs with facilitated access to the CNS.

In 2004, more than 20% of drugs belonging to the top 200 sales were based on peptides, proteins or antibodies, with sales reaching US\$ 40 billion and, hence, approximately 10% of the overall figure for the pharmaceutical industry [50]. According to the review of Leader *et al.* [40], which gives an interesting new functional classification of protein therapeutics, we provide herein in **Supplementary Table 3** a list of peptide derivatives or homologous compounds (proteins or antibodies) used for medical diagnostics or imaging, produced by other means (recombinant DNA and so on) than chemical synthesis, and having reached the American, European and/or Japanese pharmaceutical markets (some of them are generics or discontinued) (<http://www.biam2.org/>, <http://www.documed.ch>, <http://www.fda.gov/>, <http://www.fdaapproveddrugs.us>, <http://www.rxlist.com> and <http://www.vidal.fr>) [51]. As described here, more than 200 peptide drugs and homologous compounds (proteins or antibodies) containing peptide bonds are marketed now (or have been marketed) on same pharmaceutical markets.

Concluding remarks

As stated by Loffet [34], peptides (or proteins) still suffer from a deficit in image because they (generally) have to be injected, but erythropoietin and insulin are blockbusters even though they cannot be taken orally. We are sure that chronic treatment with new formulations or routes of administration will give a new impetus to the therapeutic peptide field. The majority of marketed peptide products and homologous compounds (proteins and antibodies) are peptide hormones or peptide derivatives that simulate the action of hormones. Peptides that are agonists or antagonists for receptors implicated in oncology and inflammation, peptides as antibiotics, or peptides that act as enzyme inhibitors in a variety of therapeutic indications are increasingly being tested for efficacy at the discovery and preclinical stages, suggesting that this class of drugs might soon occupy a larger niche in the marketplace. In France, the 2008 MEDEC prize of the year (recognizing the provision of innovative molecules by pharmaceutical companies for physicians and their patients) was awarded to a synthetic therapeutic peptide: the new antidiabetic drug Byetta[®] (exenatide, 39 amino acids) of Eli Lilly (<http://www.gazettelabo.fr/2002breves/0608/medec.htm>

and <http://www.lemedec.com/website-medec-web/prix-medec.do>). Other therapeutic peptides, such as antimicrobial peptides, with broad-spectrum antimicrobial activity against bacteria, viruses and fungi, are promised a great future, especially in counteracting the loss of efficiency of conventional antibiotics [52–54].

The decreasing number of approved drugs produced by the pharmaceutical industry, accompanied by expanding expenses for R&D, demands alternative approaches to improve pharmaceutical R&D productivity. As discussed here, peptide-based drug discovery could be a serious option for addressing as yet unresolved problems. To date, hundreds of synthetic therapeutic peptides are in clinical development, and even more are in advanced stages of preclinical development in the pipeline of pharmaceutical companies. This augurs a promising future for the marketing of innovative synthetic therapeutic peptides in the coming years.

Appendix A. Supplementary data

Supplementary data associated with this article can be found, in the online version, at doi:10.1016/j.drudis.2009.10.009.

References

- Schmid, E.F. and Smith, D.A. (2005) Is declining innovation in the pharmaceutical industry a myth? *Drug Discov. Today* 10, 1031–1039
- DiMasi, J.A. *et al.* (2003) The price of innovation: new estimates of drug development costs. *J. Health Econ.* 22, 151–185
- Rawlins, M.D. (2004) Cutting the cost of drug development? *Nat. Rev. Drug Discov.* 3, 360–364
- DiMasi, J.A. and Grabowski, H.G. (2007) The cost of biopharmaceutical R&D: is biotech different? *Manag. Decis. Econ.* 28, 469–479
- Kola, I. and Landis, J. (2004) Can the pharmaceutical industry reduce attrition rates? *Nat. Rev. Drug Discov.* 3, 711–715
- Pangalos, M.N. *et al.* (2007) Drug development for CNS disorders: strategies for balancing risk and reducing attrition. *Nat. Rev. Drug Discov.* 6, 521–532
- Hughes, B. (2008) 2007 FDA drug approvals: a year of flux. *Nat. Rev. Drug Discov.* 7, 107–109
- Hughes, B. (2009) 2008 FDA drug approvals: a year of flux. *Nat. Rev. Drug Discov.* 8, 93–96
- Marx, V. (2005) Watching peptide drugs grow up. *Chem. Eng. News* 83, 17–24
- Latham, P.W. (1999) Therapeutic peptides revisited. *Nat. Biotechnol.* 17, 755–757
- Sato, A.K. *et al.* (2006) Therapeutic peptides: technological advances driving peptides into development. *Curr. Opin. Biotechnol.* 17, 638–642
- Merrifield, B. (1963) Solid phase peptide synthesis. I. The synthesis of a tetrapeptide. *J. Am. Chem. Soc.* 85, 2149–2154
- Bruckdorfer, T. *et al.* (2004) From production of peptides in milligram amounts for research to multi-ton quantities for drugs of the future. *Curr. Pharm. Biotechnol.* 5, 29–43
- Guzman, F. *et al.* (2007) Peptide synthesis: chemical or enzymatic. *J. Biotechnol.* 10, 279–314
- Witt, K.A. *et al.* (2001) Peptide drug modifications to enhance bioavailability and blood–brain barrier permeability. *Peptides* 22, 2239–2243
- Kumar, D. and Bhalla, T.C. (2005) Microbial proteases in peptide synthesis: approaches and applications. *Appl. Microbiol. Biotechnol.* 68, 726–736
- Guichard, G. (2004) Du peptide à l'analogie peptidique: stratégies de stabilisation de la conformation active, amélioration du profil pharmacocinétique (cyclisation, acides aminés non naturels, mimes de repliement, modification du squelette). *Du peptide naturel... au médicament* (Atelier de Formation Inserm 150)
- Pichereau, C. and Allary, C. (2005) Therapeutic peptides under the spotlight. *Eur. Biopharm. Rev.* 88–91
- Bray, B.L. (2003) Large-scale manufacture of peptide therapeutics. *Nat. Rev. Drug Discov.* 2, 587–593
- Woodley, J.F. (1994) Enzymatic barriers for GI peptide and protein delivery. *Crit. Rev. Ther. Drug Carrier Syst.* 11, 61–95
- Anderson, B.D. (1996) Prodrugs for improved CNS delivery. *Adv. Drug Deliv. Rev.* 19, 171–202
- Letvin, N.L. *et al.* (1986) *In vivo* administration of lymphocyte-specific monoclonal antibodies in nonhuman primates. *In vivo* stability of disulfide-linked immunotoxin conjugates. *J. Clin. Invest.* 77, 977–984
- Rousselle, C. *et al.* (2003) Improved brain uptake and pharmacological activity of dalargin using a peptide-vector-mediated strategy. *J. Pharmacol. Exp. Ther.* 306, 371–376
- Pettit, D.K. and Gombotz, W.R. (1998) The development of site-specific drug-delivery systems for protein and peptide biopharmaceuticals. *Trends Biotechnol.* 16, 343–349
- Pajouhesh, H. and Lenz, G.R. (2005) Medicinal chemical properties of successful central nervous system drugs. *NeuroRx* 2, 541–553
- Ladner, R.C. *et al.* (2004) Phage display-derived peptides as therapeutic alternatives to antibodies. *Drug Discov. Today* 9, 525–529
- Witt, K.A. and Davis, T.P. (2006) CNS drug delivery: opioid peptides and the blood–brain barrier. *AAPS J.* 8, E76–E88
- Lipinski, C.A. *et al.* (1997) Experimental and computational approaches to estimate solubility and permeability in drug discovery and development settings. *Adv. Drug Deliv. Rev.* 23, 3–25
- Lipinski, C.A. (2000) Drug-like properties and the causes of poor solubility and poor permeability. *J. Pharmacol. Toxicol. Methods* 44, 235–249
- Lipinski, C.A. *et al.* (2001) Experimental and computational approaches to estimate solubility and permeability in drug discovery and development settings. *Adv. Drug Deliv. Rev.* 46, 3–26
- Lipinski, C.A. (2004) Lead- and drug-like compounds: the rule-of-five revolution. *Drug Discov. Today Technol.* 1, 337–341
- Veber, D.F. *et al.* (2002) Molecular properties that influence the oral bioavailability of drug candidates. *J. Med. Chem.* 45, 2615–2623
- Kerns, E.H. and Di, L. (2003) Pharmaceutical profiling in drug discovery. *Drug Discov. Today* 8, 316–323
- Loffet, A. (2002) Peptides as drugs: is there a market? *J. Pept. Sci.* 8, 1–7
- McGregor, D.P. (2008) Discovering and improving novel peptide therapeutics. *Curr. Opin. Pharmacol.* 8, 616–619
- Hummel, G. *et al.* (2006) Translating peptides into small molecules. *Mol. Biosyst.* 2, 499–508
- Hruby, V.J. (2002) Designing peptide receptor agonists and antagonists. *Nat. Rev. Drug Discov.* 1, 847–858
- Lien, S. and Lowman, H.B. (2003) Therapeutic peptides. *Trends Biotechnol.* 21, 556–562
- Amblard, M. *et al.* (2006) Methods and protocols of modern solid phase peptide synthesis. *Mol. Biotechnol.* 33, 239–254

- 40 Leader, B. *et al.* (2008) Protein therapeutics: a summary and pharmacological classification. *Nat. Rev. Drug Discov.* 7, 21–39
- 41 Stevenson, C.L. (2009) Advances in peptide pharmaceuticals. *Curr. Pharm. Biotechnol.* 10, 122–137
- 42 Tamai, I. and Tsuji, A. (2000) Transporter-mediated permeation of drugs across the blood–brain barrier. *J. Pharm. Sci.* 89, 1371–1388
- 43 Temsamani, J. and Vidal, P. (2004) The use of cell-penetrating peptides for drug delivery. *Drug Discov. Today* 9, 1012–1019
- 44 Hervé, F. *et al.* (2008) CNS delivery via adsorptive transcytosis. *AAPS J.* 10, 455–472
- 45 Pardridge, W.M. (2003) Blood–brain barrier drug targeting: the future of brain drug development. *Mol. Interv.* 3, 90–105
- 46 de Boer, A.G. and Gaillard, P.J. (2007) Drug targeting to the brain. *Annu. Rev. Pharmacol. Toxicol.* 47, 323–355
- 47 de Boer, A.G. and Gaillard, P.J. (2007) Strategies to improve drug delivery across the blood–brain barrier. *Clin. Pharmacokinet.* 46, 553–576
- 48 Demeule, M. *et al.* (2008) Involvement of the low-density lipoprotein receptor-related protein in the transcytosis of the brain delivery vector angiopep-2. *J. Neurochem.* 106, 1534–1544
- 49 Régina, A. *et al.* (2008) Antitumour activity of ANG1005, a conjugate between paclitaxel and the new brain delivery vector Angiopep-2. *Br. J. Pharmacol.* 155, 185–197
- 50 Decaffmeyer, M. *et al.* (2008) Les médicaments peptidiques: mythe ou réalité? *Biotechnol. Agron. Soc. Environ.* 12, 81–88
- 51 Baty, D. and Chames, P. (2006) Approved antibodies for imaging and therapeutic: an update. *IBS* 21, 255–263
- 52 Jessen, H. *et al.* (2006) Peptide antimicrobial agents. *Clin. Microbiol. Rev.* 19, 491–511
- 53 Rotem, S. and Mor, A. (2008) Antimicrobial peptide mimics for improved therapeutic properties. *Biochim. Biophys. Acta* 1788, 1582–1592
- 54 Rossi, L.M. *et al.* (2008) Research advances in the development of peptide antibiotics. *J. Pharm. Sci.* 97, 1060–1070

UNCORRECTED PROOF

spectrum was being taken in deuteriochloroform the sample tube popped its cork and vigorous gas evolution was noted. The spectrum was run several times during the first 15 min. after which it became constant and appeared to be that of 9,10-dihydrophenanthrene contaminated by an unidentified impurity which exhibited a strong peak at approximately 7.3 δ . Positive identification was made by comparison of the infrared spectrum with that of an authentic sample.

Thermal Decomposition of 1,4-Dihydronaphtho[1,8-d,e][1,2]-diazepine (XX).—In a semimicro distillation apparatus 0.4 g. of XX was heated gently with a free flame. The solid melted to an orange liquid and on continued heating sudden and vigorous decomposition occurred with the release of a cloud of smoke. The black liquid remaining in the pot was distilled into the receiver by means of the free flame. The distillate solidified as a black solid (0.2 g., 59.2%). Recrystallization from ethanol-water (decolorizing carbon) gave nearly white crystals, m.p. 93.5–94.5°. The melting point was not depressed on admixture with an authentic sample of acenaphthene.

When the azo compound was heated in diglyme (b.p. 162°) or triglyme (b.p. 210°), isomerization to XXI was noted as proved by mixture melting point determination.

Isomerization of 1,4-Dihydronaphtho[1,8-d,e][1,2]diazepine (XX).—A solution of 0.5 ml. of concentrated hydrochloric acid and 3 ml. of water was warmed with 0.2 g. of XX for 2–3 min.

until solution occurred. Excess solid potassium hydroxide was added and the cream-colored powder filtered and dried in air. The yield was 0.17 g. (85%), m.p. 129–130°, identified as XXI by comparison with a sample prepared by selenium dioxide oxidation of X.

1-Benzal-2-benzylhydrazine.—A mixture of 10.4 g. of benzalazine, 4.66 g. of dry lithium chloride, 5.94 g. of potassium borohydride and 80 ml. of tetrahydrofuran was refluxed for 24 hours with stirring.³³ The mixture was decomposed by the addition of water and the tetrahydrofuran layer separated and allowed to evaporate spontaneously. Snow-white flakes (9.5 g., 91%) remained, m.p. 64–72° dec. Recrystallization from methanol gave 7.6 g. (72%) of the pure hydrazone, m.p. 70–73.5° dec. (softening at 69.5°, lit.³⁴ m.p. 69–70°). Since the hydrazone decomposed readily on standing as noted by previous workers, the n.m.r. spectrum was run at once.

Acknowledgment.—We are indebted to Prof. Thomas Stengle for the n.m.r. spectra and discussions concerning their interpretation.

(33) The procedure is based on the work of M. Davis [*J. Chem. Soc.*, 3981 (1956)], who showed that tertiary amides could be reduced under these conditions.

(34) A. Wohl and C. Oesterlin, *Ber.*, **33**, 2736 (1900).

[CONTRIBUTION FROM THE ROCKEFELLER INSTITUTE, NEW YORK 21, N. Y.]

Solid Phase Peptide Synthesis. I. The Synthesis of a Tetrapeptide¹

BY R. B. MERRIFIELD

RECEIVED JANUARY 31, 1963

A new approach to the chemical synthesis of polypeptides was investigated. It involved the stepwise addition of protected amino acids to a growing peptide chain which was bound by a covalent bond to a solid resin particle. This provided a procedure whereby reagents and by-products were removed by filtration, and the recrystallization of intermediates was eliminated. The advantages of the new method were speed and simplicity of operation. The feasibility of the idea was demonstrated by the synthesis of the model tetrapeptide L-leucyl-L-alanyl-glycyl-L-valine. The peptide was identical with a sample prepared by the standard *p*-nitrophenyl ester procedure.

The classical approach to peptide synthesis has yielded impressive successes in recent years in the preparation of several biologically active peptides.² With the development of new reagents and techniques the synthesis of most small peptides has been placed within easy reach.³ However, these procedures are not ideally suited to the synthesis of long chain polypeptides because the technical difficulties with solubility and purification become formidable as the number of amino acid residues increases. A new approach to peptide synthesis has been investigated in an effort to overcome some of these difficulties. The present report deals with the basic idea behind the new method and with a demonstration of its feasibility through the synthesis of a simple model tetrapeptide.

The general concept underlying the new method is outlined in Fig. 1. It depends on the attachment of the first amino acid of the chain to a solid polymer by a covalent bond, the addition of the succeeding amino acids one at a time in a stepwise manner until the desired sequence is assembled, and finally the removal of the peptide from the solid support. The reason for this approach is that when the growing peptide chain is

firmly attached to a completely insoluble solid particle it is in a convenient form to be filtered and washed free of reagents and by-products. Thus the intermediate peptides are purified, not by the usual recrystallization procedures, but by dissolving away the impurities. This greatly simplifies the manipulations and shortens the time required for the synthesis of the peptides. It is hoped that such a method will lend itself to automation and provide a route to the synthesis of some of the higher molecular weight polypeptides which have not been accessible by conventional procedures.

The Polymer.—The first requirement was for a suitable polymer. It had to be insoluble in all of the solvents which were used and have a stable physical form which permitted ready filtration. It also had to contain a functional group to which the first protected amino acid could be firmly linked by a covalent bond. Many polymers and modes of attachment were investigated. Among the polymers were cellulose, polyvinyl alcohol, polymethacrylate and sulfonated polystyrene. The one which worked best was a chloromethylated copolymer of styrene and divinylbenzene. The resin, in the form of 200–400 mesh beads, possessed a porous gel structure which allowed ready penetration of reagents, especially in the presence of swelling solvents. Although diffusion and steric hindrance were no doubt important factors, they were not serious enough to prevent the desired reactions from proceeding to completion. The reaction rates were slower than corresponding ones in solution, but conditions were found which permitted all of the reactions to occur at useful rates in spite of the fact that the growing peptide chain was in the completely insoluble solid phase at all times. It was for this reason that the term solid phase peptide synthesis was introduced to describe the new method.

(1) (a) Supported in part by Grant A 1260 from the U. S. Public Health Service. (b) An abstract of this work was presented at the 46th Annual Meeting of the Federation of American Societies for Experimental Biology, April, 1962; R. B. Merrifield, *Fed. Proc.*, **21**, 412 (1962).

(2) (a) V. du Vigneaud, C. Ressler, J. M. Swan, C. W. Roberts, P. G. Katsoyannis and S. Gordon, *J. Am. Chem. Soc.*, **75**, 4879 (1953); (b) R. B. Merrifield and D. W. Woolley, *ibid.*, **78**, 4646 (1956); (c) H. Schwarz, M. Bumpus and I. H. Page, *ibid.*, **79**, 5697 (1957); (d) R. A. Boissonas, S. Guttmann and P. A. Jaquenoud, *Helv. Chim. Acta*, **43**, 1349 (1960); (e) K. Hofmann, H. Yajima, N. Yanaiharu, T. Liu and S. Lande, *J. Am. Chem. Soc.*, **83**, 487 (1961); (f) C. H. Li, J. Meienhofer, E. Schnabel, D. Chung, T. Lo and J. Ramachandran, *ibid.*, **83**, 4449 (1961); (g) H. Kappeler and R. Schwyzler, *Helv. Chim. Acta*, **44**, 1136 (1961).

(3) See J. P. Greenstein and M. W. Winitz, "Chemistry of the Amino Acids," Vol. 2, John Wiley and Sons, Inc., New York, N. Y., 1961.

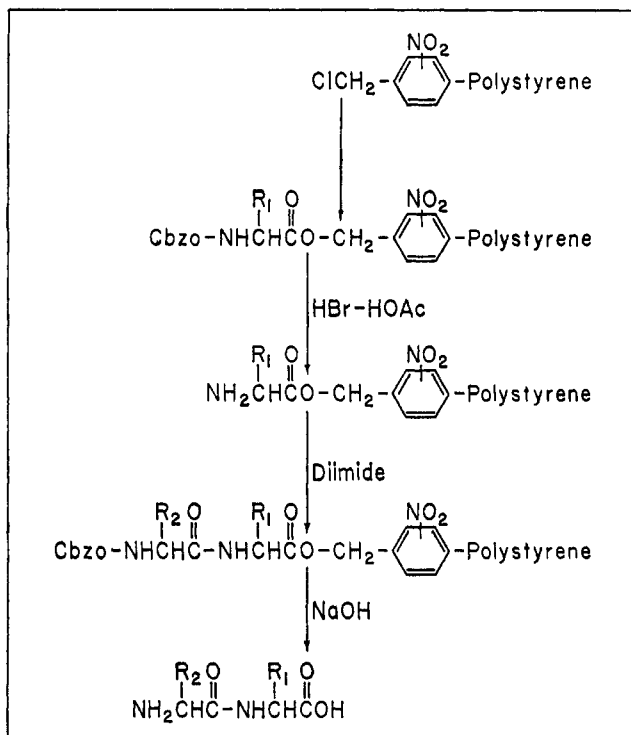


Fig. 1.—The scheme for solid phase peptide synthesis.

Attachment of the First Amino Acid to the Polymer.—

To provide a point of attachment for the peptide the polystyrene resin was partially chloromethylated.⁴ For reasons to be discussed later the product was then nitrated or brominated. The resulting substituted chloromethyl polystyrene was treated with the triethylammonium salt of the first protected amino acid in the proposed peptide chain to give a substituted benzyl ester linkage. This was the stable covalent bond which held the growing peptide chain in the solid phase on the supporting resin. The reaction was shown to go to completion with carbobenzoxyglycine at refluxing temperatures in dry solvents such as ethyl acetate, benzene or dioxane giving carbobenzoxyglycyl polymer.⁵ It was also demonstrated to proceed with carbobenzoxy-L-valine and carbobenzoxy-L-arginine. Racemization of the C-terminal amino acid was not observed during the reaction. The quantity of amino acid attached to the resin was purposely limited to approximately 0.5 mmole per gram of substituted polymer. To avoid undesired alkylations in subsequent steps the unreacted chloromethyl groups were then esterified with an excess of triethylammonium acetate. Complete reaction was indicated by the fact that the product was nearly free of halogen.

Cleavage of the Amino-Protecting Group.—The protecting group which was used throughout the syntheses to be reported was the carbobenzoxy group. It was selected because it could be removed readily and completely by hydrogen bromide in glacial acetic acid.⁶ Since the latter reagent also attacked the benzyl ester at a slow rate the loss of peptide from the resin was a serious problem. The difficulty was largely overcome by nitration or bromination of the polymer after the

(4) K. W. Pepper, H. M. Paisley and M. A. Young, *J. Chem. Soc.*, 4097 (1953).

(5) The abbreviated name carbobenzoxyglycyl polymer was used to designate the compound in which carbobenzoxyglycine was bound in ester linkage to the aromatic rings of the styrene-divinylbenzene copolymer through hydroxymethyl side chains. The number of substituents per molecule of polymer varied and the exact location on the ring or distribution among the rings was not known. The other polymer derivatives were named in an analogous manner.

(6) D. Ben-Ishai and A. Berger, *J. Org. Chem.*, **17**, 1564 (1952).

chloromethylation step. Table I shows that while the carbobenzoxy group cleaved rapidly from the unsubstituted carbobenzoxy-L-valyl polymer even in 10% HBr-acetic acid there was also considerable loss of ester. After nitration the rate of removal of carbobenzoxy was decreased, but the loss of ester was reduced to a very small level. With 30% HBr the carbobenzoxy group was removed in 2 to 4 hr., while the ester cleavage remained at a low level for at least 6 hr. In fact, the peptides could not be removed completely from the nitrated resin even with prolonged HBr treatment. The carbobenzoxy-L-valyl bromopolymer had properties intermediate between the nitrated and unsubstituted derivatives with respect to the stability of the carbobenzoxy and ester bonds. The carbobenzoxy group could be removed from it with dilute (10%) HBr and the ester could be cleaved with concentrated (30%) HBr.

TABLE I
CLEAVAGE OF CARBOBENZOXY AND ESTER GROUPS BY
HBr-ACETIC ACID

Time, min.	Extent of cleavage, %								
	Cbz-val- polymer		Cbz-val- nitropolymer				Cbz-val- bromopolymer		
	10% HBr	Ester	10% HBr	Ester	30% HBr	Ester	10% HBr	Ester	30% HBr
5	52	6					8	0.5	8
10	73	8			14		17	1.1	13
20	90	12			28		32	2.2	21
30	100	15	19		43	1.2			28
60	100	18	38	1.2	67		77	6	46
90			57	2.0	90	3.8			52
120			67	2.5	100	4.3	87	10	58
180			83		99		91	14	
240			94	3.2	108	5.4			69
300			99	3.2	98	4.8	100	18	

The Peptide-Forming Step.—After removal of the N-terminal protecting group by HBr the hydrobromide was neutralized with excess triethylamine and the free base was coupled with the next protected amino acid. Although the *p*-nitrophenyl ester method⁷ at first appeared to be ideal for this step it finally proved to be unsatisfactory after many experiments. The yields were not high enough even with elevated temperatures (80°) and there was evidence for partial racemization (Table II). The *N,N'*-dicyclohexylcarbodiimide method,⁸ on the other hand, proved to be very satisfactory. The reaction went in virtually quantitative yield in about 30 minutes at room temperature. The relatively insoluble by-product dicyclohexylurea and the rearrangement product carbobenzoxyaminoacyldicyclohexylurea, which was formed in appreciable quantities, were both easily removed by thorough washing. In conventional syntheses this is not always the case, especially when the peptide derivatives have become large and relatively insoluble themselves. The choice of solvent for the condensation was very important. Of the several solvents which were examined dimethylformamide was the best, methylene chloride was satisfactory, but dioxane, benzene, ethanol, pyridine and water gave very low yields and were not useful. The effectiveness of the solvent depended partly on its ability to swell the resin and partly on other factors. For example, the two effective solvents (dimethylformamide and methylene chloride) had high dielectric constants and also swelled the resin whereas benzene, which swelled the resin but had a low dielectric constant, was ineffective.

The coupling reaction was shown to occur between glycylvalyl polymer and the carbobenzoxy derivatives

(7) M. Bodanszky, *Nature*, **175**, 685 (1955).

(8) J. C. Sheehan and G. P. Hess, *J. Am. Chem. Soc.*, **77**, 1067 (1955).

TABLE II

AMINO ACID ANALYSES OF L-LEUCYL-L-ALANYLGLYCYL-L-VALINE

Polymer subst.	Coupling method	Cleavage method	Ratio ^a $\frac{\text{enzyme hydrolysate}}{\text{acid hydrolysate}}$			
			Leu	Ala	Gly	Val
NO ₂	Active ester	NaOH	0.83	0.73	0.61	0.58
NO ₂	Diimide	NaOH	1.00	1.05	0.97	..
Br	Diimide	HBr	1.06	1.00	1.02	1.01

^a The concentration of each amino acid in a leucine aminopeptidase digest divided by the corresponding value in a 6 N HCl hydrolysate.

of leucine, isoleucine, valine, alanine, glycine, phenylalanine, O-benzyltyrosine, proline, serine, threonine, methionine, S-benzylcysteine, *im*-benzylhistidine, nitroarginine, γ -methyl glutamate and asparagine. Lysine and tryptophan derivatives were not studied.

Since it was very important that no unreacted amine remain after the peptide-forming reaction,⁹ several precautions were taken. First, an excess of carbobenzoxy-amino acid and of diimide was used and each condensation step was repeated with fresh reagents. Finally, after the coupling reactions were completed any trace of unreacted amine was acetylated with a large excess of acetic anhydride and triethylamine. This reduced the free amine to less than 0.1% of that originally present. The acetamido bond was completely resistant to 30% HBr-acetic acid for 18 hours at 25°. Consequently, the danger of re-exposure of these amino groups during subsequent steps was eliminated.

The steps described to this point completed one cycle, *i.e.*, the peptide chain was lengthened by one amino acid residue. Further cycles were carried out in the same way by alternately deprotecting and coupling with the appropriate carbobenzoxyamino acid. The completed protected peptides were finally decarbobenzoxylated by HBr and the free peptides were liberated from the polymer by saponification, or, in the case of the brominated resin, by more vigorous HBr treatment. The liberated peptides were desalted and purified by ion-exchange chromatography, countercurrent distribution or other suitable procedures.

In order to establish the optimal conditions for the various reactions and to test the feasibility of the method as outlined, the simple tetrapeptide L-leucyl-L-alanyl-glycyl-L-valine was synthesized. Carbobenzoxy-L-leucyl-L-alanyl-glycyl-L-valyl polymer was made by the stepwise procedures described, using first the nitrophenyl ester method and later the more suitable diimide reaction. The latter was used on both nitrated and brominated polymer. The best procedure was with the nitropolymer using dicyclohexylcarbodiimide in dimethylformamide for the coupling reaction and saponification for the liberation of the free peptide.

Isolation and Purification of the Peptides.—The crude peptide product liberated from the resin was chromatographed on a Dowex 50-X4 column using 0.1 M pH 4.0 pyridine acetate buffer. The eluate was analyzed by the quantitative ninhydrin reaction of Moore and Stein¹⁰ and by dry weight after evaporation of the volatile buffer from pooled fractions. Figure 2 shows the chromatogram resulting from the separation of the peptides prepared on 10 g. of polymer. A total of 332 mg. of tetrapeptide was isolated which accounted for 80% of the free amino acids and peptides

(9) If any amine remained unacylated after reaction with the carbobenzoxyamino acid it would be liable to react with the subsequent carbobenzoxyamino acids. In this way a peptide chain lacking one or more of the internal amino acid residues would begin to grow. A family of closely related peptides, difficult to separate, would thus result.

(10) S. Moore and W. H. Stein, *J. Biol. Chem.*, **211**, 907 (1954).

present in the crude product. In addition, an acetylated peptide fraction weighing 57 mg. passed through the column almost unretarded. It contained acetylvaline, acetylglycylvaline and acetylalanyl-glycylvaline in approximately equal amounts. It was concluded that the coupling reactions were not quite quantitative, but that the unreacted amine was available to acetic anhydride and could be prevented from further reactions in this way. The presence of small amounts of acetylated derivatives was not a serious difficulty, however, since these could be separated readily from the desired tetrapeptide. On the other hand, the presence of small amounts of the intermediate dipeptides (20 mg.) and tripeptides (33 mg.) was more serious and required the chromatographic separation for their removal from the tetrapeptide. Their presence indicated that either the acetylation step, or more likely, the cleavage of the carbobenzoxy group was incomplete. Thus the appearance of leucylalanylvaline and leucylvaline must mean that some carbobenzoxyvaline remained after the first HBr-acetic acid treatment and was then deprotected by the second or third treatments. This could, of course, become serious if the synthesis of large polypeptides were contemplated. The presence of two peaks (at 1.25 l. and 1.34 l.) both containing leucine, alanine, glycine and valine also deserves some comment. The main component (92.5%) was shown by carboxypeptidase and leucine aminopeptidase digestions to be the desired all-L-peptide and the minor peak (7.5%) was found to be L-leucyl-L-alanyl-glycyl-D-valine. The explanation was clear when it was subsequently found that the sample of commercial carbobenzoxy-L-valine from which the peptides in this particular run were made contained 12% of carbobenzoxy-D-valine.

The purity and identity of the tetrapeptide was established in the following ways: (1) Rechromatography on Dowex 50 gave a single homogeneous peak. (2) Countercurrent distribution¹¹ for 100 transfers gave a single symmetrical peak which agreed closely with the calculated theoretical curve. (3) Paper chromatography gave a single spot in three solvent systems.¹² (4) The ratios of amino acids determined by quantitative amino acid analysis¹³ of an acid hydrolysate were leucine 1.00, alanine 1.00, glycine 0.99, valine 1.00. (5) Optical purity was demonstrated by digestion with two enzymes. Leucine aminopeptidase completely digested the peptide (Table II). This showed the optical purity of L-leucine and L-alanine. Carboxypeptidase A completely liberated L-valine, demonstrating the optical purity of this amino acid. (6) The final proof was a comparison with the same tetrapeptide synthesized by conventional methods. The two peptides were identical by chromatography, optical rotation and infrared spectra.

For the conventional synthesis the stepwise *p*-nitrophenyl ester method of Bodanszky⁷ was used. L-Valine methyl ester was coupled with carbobenzoxyglycine *p*-nitrophenyl ester and the product hydrogenated to give glycyl-L-valine methyl ester which was condensed with carbobenzoxy-L-alanine *p*-nitrophenyl ester. The protected tripeptide was hydrogenated and coupled with carbobenzoxy-L-leucine *p*-nitrophenyl ester to give analytically pure carbobenzoxy-L-leucyl-

(11) L. C. Craig, J. D. Gregory and G. T. Barry, *Cold Spring Harbor Symposia on Quant. Biol.*, **14**, 24 (1949).

(12) The sprays used would have detected any impurities of free or protected amino acids or peptides. The first was the ninhydrin spray, made by dissolving 2 ml. of acetic acid, 3 ml. of pyridine and 200 mg. of ninhydrin in 100 ml. of acetone. The second was the hypochlorite-KI spray for amides; see C. G. Greig and D. H. Leaback, *Nature*, **188**, 310 (1960), and R. H. Mazur, B. W. Ellis and P. S. Cammarata, *J. Biol. Chem.*, **237**, 1619 (1962).

(13) S. Moore, D. H. Spackman and W. H. Stein, *Anal. Chem.*, **30**, 1185 (1958).

L-alanylglycyl-L-valine methyl ester. Carbobenzoxy-L-leucyl-L-alanylglycyl-L-valine was also obtained analytically pure after saponification of the methyl ester. Catalytic hydrogenation over palladium-on-carbon gave the free tetrapeptide L-leucyl-L-alanylglycyl-L-valine.

These experiments demonstrate the feasibility of solid phase peptide synthesis. For the new method to be of real value it must, of course, be applied to the synthesis of much larger peptides, preferably to those with biological activity. It must also be automated if large polypeptides of predetermined sequence are to be made. Encouraging experiments along these lines are now under way.

Experimental

The Polymer.—Copolymers of styrene and divinylbenzene of varying degrees of cross linking were obtained from the Dow Chemical Co.¹⁴ The preparations were in the form of 200–400 mesh beads. The degree of cross linking determined the extent of swelling, the effective pore size and the mechanical stability of the beads, and these properties in turn determined the suitability of the polymers for peptide synthesis. The 1% cross-linked beads were somewhat too fragile and became disrupted during the peptide synthesis to an extent which made filtration difficult. On the other hand, the 8 and 16% cross-linked beads were too rigid to permit easy penetration of reagents, causing slower and less complete reactions. The 2% cross-linked resin was most useful and was employed for all the reactions reported here. The commercial product was washed thoroughly with *M* NaOH, *M* HCl, H₂O, dimethylformamide and methanol and dried under vacuum at 100°. The resulting material consisted of nearly white spheres ranging from approximately 20 to 80 μ in diameter. No attempt was made to obtain particles of more uniform size.

Chloromethylpolymer.⁴—Copolystyrene–2% divinylbenzene (50 g.) was swelled by stirring at 25° for 1 hr. in 300 ml. of chloroform and then cooled to 0°. A cold solution of 7.5 ml. of anhydrous SnCl₄ in 50 ml. of chloromethyl methyl ether was added and stirred for 30 min. at 0°. The mixture was filtered and washed with 1 l. of 3:1 dioxane–water, and then with 1 l. of 3:1 dioxane–3 *N* HCl. The cream-colored beads were washed further with a solution which changed gradually from water to pure dioxane and then progressively to 100% methanol. Abrupt changes of solvent composition were avoided. The product was dried under vacuum at 100°; yield 55.0 g. The product contained 1.89 mmoles of Cl/g., from which it could be calculated that approximately 22% of the aromatic rings of the polymer were chloromethylated. Conditions which would give this degree of substitution were purposely selected in order to minimize cross linking and to avoid starting peptide chains at the more difficultly accessible sites.

Nitrochloromethylpolymer.—A 50-g. sample of the dry chloromethylpolymer (1.89 mmole of Cl/g.) was added slowly with stirring to 500 ml. of fuming nitric acid (90% HNO₃, sp. gr. 1.5) which had been cooled to 0°. The mixture was stirred 1 hr. at 0° and then poured into crushed ice. The light tan beads were filtered and washed as described above with water, dioxane and methanol and dried; yield 69.9 g. The nitrogen content was 6.38 mmoles/g. by Dumas analysis. This was equivalent to 1.03 nitro groups per aromatic ring.

Bromochloromethylpolymer.—An 8.00-g. sample of chloromethylpolymer (4.92 mmoles of Cl/g.) was suspended in 25 ml. of carbon tetrachloride containing 100 mg. of iodine. A solution of 5 ml. of bromine in 10 ml. of CCl₄ was added and the mixture was stirred for 3 days in the dark at 25°. The deep red suspension was filtered and the polymer was washed with CCl₄, dioxane, water, sodium bicarbonate, water and methanol and dried; yield 12.5 g. The extent of substitution was 4.56 mmoles of Br/g., which was equivalent to 0.97 bromine atom per aromatic ring.

The Esterification Step. Carbobenzoxy-L-valyl Nitropolymer.—A solution of 15.5 g. (61.7 mmoles) of carbobenzoxy-L-valine and 8.65 ml. (61.7 mmoles) of triethylamine in 350 ml. of ethyl acetate was added to 40.0 g. of chloromethylnitropolymer and the mixture was stirred under reflux. After 48 hr., a solution of 12 ml. of acetic acid and 28 ml. of triethylamine in 100 ml. of ethyl acetate was added and the stirring and heating continued for another 4 hr. The resin was filtered and washed thoroughly with ethyl acetate, ethanol, water and methanol by gradual change of solvent composition and dried under vacuum; yield 46.9 g. A 30-mg. sample of the resulting esterified resin was hydrolyzed by refluxing for 24 hr. in a mixture of 5 ml. of acetic acid and 5 ml. of 6 *N* HCl. Valine in the filtrate was determined

by the ninhydrin method and found to be 0.56 mmole/g. A chlorine determination (Parr fusion) indicated that only 0.08 mmole of Cl/g. remained. When carbobenzoxy-L-arginine was used in the corresponding reaction, ethyl acetate was replaced by dioxane as solvent because of the increased solubility of the triethylammonium salt.

The Reaction Vessel.—A reaction vessel was designed to make possible the process of automatic synthesis. The remaining reactions to be described were conducted within this vessel. It consisted of a 45 × 125 mm. glass cylinder, sealed at one end and fitted with a 40-mm. medium porosity fritted disk filter at the other end. Immediately beyond the disk the tubing was constricted sharply and sealed to a 1.5-mm. bore stopcock through which solvents could be removed under suction. A side arm, fitted with a drying tube, was used to introduce reagents and to remove solid samples for analysis. The apparatus was attached to a mechanical rocker which rotated the vessel 90° between the vertical and horizontal positions and provided gentle but efficient mixing of solvents and polymer. At the end of each reaction the vessel was stopped in the vertical position with the fritted disk at the bottom so that opening the stopcock allowed the solvents to be removed by suction.

The Deprotection Step. L-Valyl Nitropolymer.—Carbobenzoxy-L-valyl nitropolymer (10 g., 5.6 mmoles of valine) was introduced into the reaction vessel and 30 ml. of 30% HBr in acetic acid was added. After shaking for 5 hr. at 25°, the suspension was diluted with 50 ml. of acetic acid, filtered and washed with acetic acid, ethanol and dimethylformamide (DMF). The resulting hydrobromide was then neutralized by shaking for 10 min. in 30 ml. of DMF containing 3 ml. of triethylamine. The solvent containing the triethylammonium bromide was removed by suction and the polymer was washed with DMF. The filtrate contained 5.4 mmoles of halogen (Volhard titration), indicating a quantitative removal of the carbobenzoxy group.

The time required for the deprotection step was determined in two ways. In the first method 100-mg. samples of carbobenzoxy-L-valyl polymers (either nitrated, brominated or unsubstituted) were treated with 1 ml. of 10% or 30% HBr–HOAc. At intervals the samples were filtered and washed with acetic acid, ethanol and water. The resulting valyl polymer hydrobromides were then analyzed for halogen by Volhard titration. A measure of the rate of ester cleavage during the reaction was obtained by analyzing the filtrates for valine by the ninhydrin reaction.¹⁰ These data are summarized in Table I. Completion of the reaction with 30% HBr–HOAc on carbobenzoxy-L-valyl nitropolymer required about 2 hr. and resulted in a loss of 4.3% of valine. The second determination of the rate of the reaction depended on coupling the free α -amino derivatives with another carbobenzoxyamino acid according to the procedures to be described below. The amount of the new amino acid thus added to the peptide was determined by hydrolysis and quantitative measurement of the amino acids. For this purpose the tripeptide derivative carbobenzoxy-L-alanylglycyl-L-valyl nitropolymer was used and carbobenzoxy-L-leucine was coupled to it. The leucine in the resulting tetrapeptide derivative was found to be 0.05 mmole/g. for the 0.5-hr. deprotection time. For times of 2, 4 and 6 hr., the leucine values were 0.14, 0.31 and 0.29 mmole/g. These results showed that removal of the carbobenzoxy group was maximal under these conditions within 4 hr. In order to ensure a complete reaction at this step a standard time of 5 hr. was adopted.

The Peptide-Forming Step. Carbobenzoxyglycyl-L-valyl Nitropolymer. A. The Diimide Method.—Carbobenzoxy-L-valyl nitropolymer (10 g., 5.6 mmoles of valine) was deprotected and neutralized as described above. Immediately thereafter a solution containing 2.34 g. (11.2 mmoles) of carbobenzoxyglycine in 20 ml. of dimethylformamide was added and shaken for 10 min. to allow for penetration of the reactant into the solid. A solution of 2.31 g. (11.2 mmoles) of dicyclohexylcarbodiimide in 4.6 ml. of DMF was then added and the suspension was shaken for 18 hr. at 25°. The polymer beads were sucked dry, washed with DMF, and an additional portion (1.17 g.) of carbobenzoxyglycine in 20 ml. of DMF was added. After 10 min., 1.16 g. of dicyclohexylcarbodiimide was added, the mixture was shaken for 2 hr. and then filtered and washed. A solution of 3 ml. of acetic anhydride and 1 ml. of triethylamine in 20 ml. of DMF was then added. After 2 hr., the resin was filtered and washed four times each with DMF, ethanol and acetic acid to remove excess reagents and by-products. Although dicyclohexylurea is a relatively insoluble compound, it was readily removed in this manner (solubility about 4, 10 and 17 mg./ml. respectively, in DMF, ethanol and acetic acid). A hydrolysate of a dried sample of the product showed glycine 0.53 mmole/g. and valine 0.53 mmole/g.

The reaction time allowed for the peptide-forming step could probably be reduced to much less than the 18 hr. employed here, although the exact reaction rate will depend on the particular amino acid derivative, the length of the peptide chain and perhaps other factors. To determine the approximate rate of the coupling

(14) Obtained from the Technical Service and Development Dept. of the Dow Chemical Co., Midland, Mich.

reaction, glycyl-L-valyl nitropolymer was condensed as just described with a twofold excess of carbobenzoxy-L-alanine and dicyclohexylcarbodiimide in DMF. Portions of the suspension were removed at intervals, filtered, washed and dried. Weighed samples were hydrolyzed in 6 *N* HCl-acetic acid and analyzed quantitatively for amino acids by column chromatography.¹³ Alanine was found to be 0.1, 0.2 and 0.4 mmole/g. after coupling times of 5, 10 and 30 min., and remained at this level up to 18 hr.

B. The Nitrophenyl Ester Method.—A solution of 3.70 g. (11.2 mmoles) of carbobenzoxyglycine *p*-nitrophenyl ester in 30 ml. of benzene was added to 10 g. of L-valyl nitropolymer hydrobromide (5.6 mmoles of valine) and stirred 1 hr. at 25° to allow swelling of the resin and penetration of the reagent. The swelling step was particularly important in order to get a satisfactory yield in this reaction. A solution of 5 ml. of triethylamine in 15 ml. of benzene was added and the mixture was stirred for 18 hr. at 80°. The mixture was cooled, 3 ml. of acetic anhydride was added, and the mixture was stirred for 2 hr. at 25°. The product was then filtered, washed with benzene, ethanol, water, and methanol and dried. A hydrolysate showed glycine 0.29 mmole/g., and valine 0.43 mmole/g.

The effectiveness of the acetylation step in blocking free α -amino groups was demonstrated in the following way. Samples (100 mg.) of L-valyl nitropolymer were stirred with acetic anhydride (0.3 ml.) and triethylamine (0.1 ml.) in DMF (2 ml.) for various lengths of time at 25°. The products were filtered, washed, and then saponified in ethanol (1 ml.) and 2 *N* NaOH (0.3 ml.) at 25° for 2 hr. Free valine was determined in the filtrate by the ninhydrin reaction.¹⁰ The unacetylated control contained 0.72 mmole/g., while the 1.5-hr. and 24-hr. acetylation samples each contained only 0.0029 mmole/g.

The stability of the acetylated product to HBr-HOAc was determined by treating samples (100 mg.) with 30% HBr-HOAc (0.4 ml.) at 25° for 1 to 24 hr. The samples were then saponified as before and analyzed for free valine. In this experiment the untreated control showed 0.0015 mmole/g. and the 24-hr. sample 0.0015 mmole/g.

Carbobenzoxy-L-leucyl-L-alanyl-glycyl-L-valyl Nitropolymer.—The peptide chains were extended in a manner exactly analogous to the general procedures just described for the dipeptides. Carbobenzoxy-glycyl-L-valyl nitropolymer (from part A above), still in the reaction vessel, was treated with HBr-HOAc, neutralized with triethylamine and coupled with carbobenzoxy-L-alanine to give the tripeptide derivative. Without further manipulations another cycle was carried out using carbobenzoxy-L-leucine to give the desired tetrapeptide derivative. The same protected tetrapeptide polymer was also made by the nitrophenyl ester method.

The Peptide Liberation Step. L-Leucyl-L-alanyl-glycyl-L-valine.—The carbobenzoxy-L-leucyl-L-alanyl-glycyl-L-valyl nitropolymer described above was decarboxylated with HBr-HOAc in the usual way. It was then saponified by shaking for 1 hr. at 25° in a solution of 40.5 ml. of ethanol and 4.5 ml. of 2 *N* aqueous NaOH. The filtrate, withdrawn through the fritted disk of the reaction vessel by suction, was neutralized at once with HCl and the saponification step was repeated on the resin with more ethanolic sodium hydroxide for another hour. The resin was washed with ethanol and water and the neutralized filtrates were combined. Quantitative ninhydrin analysis of the filtrate gave a total of 1.98 mmoles (leucine equivalents) and analysis of an acid hydrolysate gave 6.92 mmoles. The ratio of 3.49 instead of the 4.0 expected for a tetrapeptide indicated that some amino acids or shorter chain peptides were also present. Since the ninhydrin value of an acid hydrolysate of the carbobenzoxy tetrapeptide polymer before saponification was 12.8 mmoles, the yield in the saponification step was 54%.

The tetrapeptide was purified and isolated by ion-exchange chromatography on a 2 × 120 cm. column of Dowex 50-X4 (200–400 mesh) resin using 0.1 *M* pH 4 pyridine acetate buffer. It was eluted at 1 ml./min. and collected in 5.4-ml. fractions. Aliquots (0.2 ml.) of the fractions were analyzed by the ninhydrin method. Tubes comprising the peaks were pooled and their contents were weighed after evaporation of the buffer. The fractions were identified by paper chromatography of their acid hydrolysates. The results are summarized in Fig. 2. The acetylated peptides emerged after only slight retardation as a group of four poorly resolved fractions. They were thus easily and completely separated from the desired tetrapeptide which emerged at 1.25 l. The portion of the fraction between 1.12 and 1.29 l. was combined, evaporated to dryness, dissolved in 20 ml. of ethanol, filtered and precipitated with 100 ml. of dry ether. The product was centrifuged, washed, and dried under vacuum at 60°. The yield was 265 mg. of a cream-colored, hygroscopic powder. Rechromatography on the same column gave a single sharp peak at 1.20 l. which indicated that L-leucyl-L-alanyl-glycyl-L-valine had been completely removed.

A 200-mg. sample of the tetrapeptide was counter-currented for 100 transfers in a solvent (10 ml. each phase) made from 2000 ml. of redistilled *sec*-butyl alcohol, 22.2 ml. of glacial acetic acid

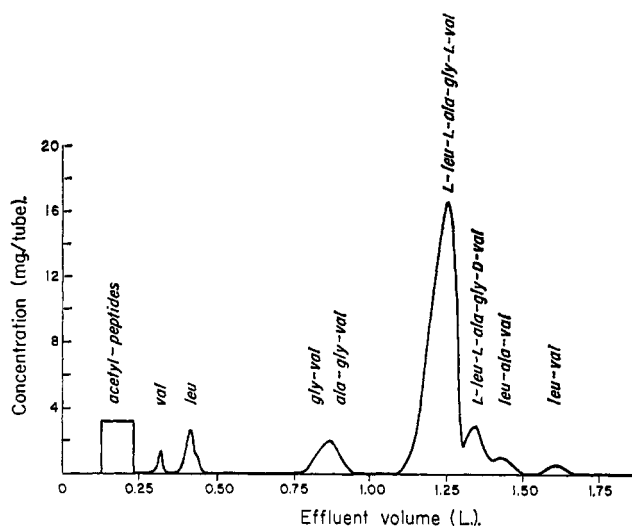


Fig. 2.—Chromatographic separation of the tetrapeptide L-leucyl-L-alanyl-glycyl-L-valine on a 2 × 120 cm. column of Dowex 50-X4 resin. Elution was with 0.1 *M* pyridine acetate buffer, pH 4.0. The concentration was calculated from the ninhydrin analysis of individual tubes and dry weight of pooled fractions.

and 1977 ml. of doubly distilled water. A single symmetrical peak resulted which was located by ninhydrin analysis on 0.2-ml. aliquots of both phases. The distribution coefficient was 0.32 and was constant between tubes 16 and 33. This fraction was combined and evaporated to dryness; yield 195 mg. The peptide was dissolved in 2 ml. of ethanol and crystallized by the addition of 5 ml. of dioxane; yield 76 mg., $[\alpha]_D^{25} + 18.0^\circ$ (*c* 2, ethanol); R_f 0.71 (propanol-H₂O, 2:1), 0.73 (*sec*-BuOH-formic acid),¹⁵ 0.49 (*sec*-BuOH-ammonia)¹⁵; amino acid ratios¹³: leucine 1.00, alanine 1.00, glycine 0.99, valine 1.00.

*Anal.*¹⁶ Calcd. for C₁₈H₃₀N₄O₆: C, 53.6; H, 8.4; N, 15.6. Found: C, 52.6; H, 8.2; N, 15.2.

Optical Purity of the Peptides.—The possibility of racemization of the leucine and alanine residues was examined with use of leucine aminopeptidase (LAP) by a method similar to that described by Hofmann.¹⁷ The peptide was incubated with Worthington LAP (1 mg./20 mg. of peptide) for 2 days at 37°. The digest was analyzed on a quantitative amino acid column and a comparison of the ratios of amino acids found after enzymatic hydrolysis to those found after acid hydrolysis was used as a measure of racemization (Table II). Within the experimental error of about 5% it was found that the diimide method caused no racemization in the synthesis of the tetrapeptide. On the other hand, the nitrophenyl ester procedure gave a product containing approximately 17% of *D*-leucine and 12% of *D*-alanine. Because the tetrapeptide isolated from the diimide route showed no evidence of racemized residues and because 92.5% of the total tetrapeptides in the reaction mixture was isolated as pure product, it was clear that racemization was not a problem with synthesis by the diimide method.

The configuration of valine was established by carboxypeptidase digestion using Worthington carboxypeptidase A.¹⁸ In this case, hydrolysis was followed by paper chromatography in *sec*-butyl alcohol-ammonia.¹⁵ The spot for tetrapeptide (R_f 0.49) progressively decreased while spots for valine (R_f 0.29) and leucyl-alanyl-glycine (R_f 0.33) increased. After 3 hr., the reaction was essentially complete and the total ninhydrin value had doubled, indicating that the glycylvaline bond was completely digested and therefore that the valine had not been racemized. The second tetrapeptide isolated from this run (peak at 1.34 l.) which represented 7.5% of the total was resistant to carboxypeptidase. After 20 hr. only unchanged tetrapeptide (R_f 0.49) was present. It therefore contained *D*-valine. This was presumed to have originated from the commercial carbobenzoxyvaline used as starting material in this run since the latter was subsequently shown to be 12% racemized.

(15) W. Hausmann, *J. Am. Chem. Soc.*, **74**, 3181 (1952).

(16) The several samples of L-leucyl-L-alanyl-glycyl-L-valine prepared both by the new method and by the conventional procedure have, in every case, given analytical values for C, H and N which were a few per cent lower than theory. The data for the different preparations, however, have always agreed well with one another. The values given were for samples dried for 18 hr. at 100° under vacuum over P₂O₅. Other conditions were tried but did not change the results.

(17) K. Hofmann and H. Yajima, *J. Am. Chem. Soc.*, **83**, 2289 (1961).

(18) H. Neurath, E. Elkins and S. Kaufman, *J. Biol. Chem.*, **170**, 221 (1947).

Conventional Synthesis of the Tetrapeptide. A. Carbobenzyloxyglycyl-L-valine Methyl Ester.—To 7.13 g. (0.0425 mole) of L-valine methyl ester hydrochloride in 30 ml. of methylene chloride at 0° was added 12 ml. (0.085 mole) of triethylamine, followed by a solution of 14 g. (0.042 mole) of carbobenzyloxyglycine *p*-nitrophenyl ester in 50 ml. of methylene chloride. After standing 24 hr. at room temperature the clear yellow solution was washed with *N* ammonium hydroxide until colorless, then with *N* hydrochloric acid and water. The dried product was an oil weighing 10.3 g. (75%). Thin layer chromatography on silicic acid in chloroform-acetone (10:1) gave one spot, R_f 0.75, by the hypochlorite-KI spray for amides.¹² The oil was used directly for the next step.

B. Carbobenzyloxy-L-leucyl-L-alanyl-glycyl-L-valine Methyl Ester.—Carbobenzyloxy-glycyl-L-valine methyl ester (5.1 g., 15.8 mmoles) was hydrogenated for 2 hr. at 25° in 50 ml. of methanol containing 15.8 ml. of *N* HCl and 500 mg. of 5% palladium-on-carbon. The product was dissolved in 20 ml. of methylene chloride, cooled to 0° and 4.4 ml. of triethylamine was added. Carbobenzyloxy-L-alanine *p*-nitrophenyl ester (5.44 g., 15.8 mmoles) in 20 ml. of methylene chloride was added and the mixture was stirred for 3 days at 25°. The solution was washed with NH_4OH , HCl and water and dried. The solution of carbobenzyloxy-L-alanyl-glycyl-L-valine methyl ester was evaporated to dryness and the oil (3.43 g., 55%) was dissolved in methanol for hydrogenation. The product was then coupled with 2.88 g. (7.65 mmoles) of carbobenzyloxy-L-leucine *p*-nitrophenyl ester in a manner similar to that described for the previous step. The yield of crude carbobenzyloxy-L-leucyl-L-alanyl-glycyl-L-valine methyl ester was 2.80 g. (64% from the protected tripeptide), m.p. 155–157°. For analysis the product was recrystallized twice from ethyl acetate-petroleum ether; m.p. 160–161°, $[\alpha]^{25}_D$ –31.8° (*c* 2, ethanol).

Anal. Calcd. for $C_{25}H_{38}N_4O_7$: C, 59.25; H, 7.57; N, 11.07. Found: C, 59.21; H, 7.26; N, 11.08.

C. Carbobenzyloxy-L-leucyl-L-alanyl-glycyl-L-valine.—Carbobenzyloxy-L-leucyl-L-alanyl-glycyl-L-valine methyl ester (662 mg., 1.3 mmoles) was dissolved in 2.5 ml. of ethanol and 0.28 ml. of 5 *N* NaOH was added. After 60 min. at 25° the solution was diluted with water and extracted with ethyl acetate. The aqueous phase was acidified with HCl and the product extracted into ethyl acetate. Evaporation of the dried solution gave 520 mg. (81%), m.p. 194°. Two recrystallizations from ethanol-water raised the m.p. to 199–200°, $[\alpha]^{25}_D$ –23.8° (*c* 2, ethanol).

Anal. Calcd. for $C_{24}H_{36}N_4O_7$: C, 58.52; H, 7.37; N, 11.37. Found: C, 58.55; H, 7.00; N, 11.30.

D. L-Leucyl-L-alanyl-glycyl-L-valine.—Carbobenzyloxy-L-leucyl-L-alanyl-glycyl-L-valine (493 mg., 1.0 mmole) was dissolved in 50 ml. of ethanol and hydrogenated for 24 hr. in the presence of 50 mg. of 5% palladium-on-carbon. The mixture was filtered and evaporated to dryness. The residue was redissolved in 2 ml. of ethanol and filtered again and the tetrapeptide was then precipitated with dry ether; yield 343 mg. (96%), $[\alpha]^{25}_D$ +17.5° (*c* 2, ethanol); R_f 0.71 (propanol-H₂O), 0.73 (*sec*-butyl alcohol-formic acid),¹⁴ 0.49 (*sec*-butyl alcohol-ammonia¹⁵); amino acid ratios¹³: leucine 0.98, alanine 1.00, glycine 1.00, valine 1.01.

*Anal.*¹⁶ Calcd. for $C_{16}H_{30}N_4O_5$: C, 53.6; H, 8.4; N, 15.6. Found: C, 52.7; H, 8.1; N, 14.9.

Acknowledgments.—The author wishes to express his sincere appreciation to Dr. D. W. Woolley for his interest and advice during this work. The author also is grateful to Dr. John Stewart for many helpful suggestions and discussions and to Miss Angela Corigliano and Miss Gretchen Grove for their technical assistance.

[CONTRIBUTION FROM THE INSTITUTE OF INDUSTRIAL MEDICINE OF NEW YORK UNIVERSITY MEDICAL CENTER, NEW YORK 16, N. Y.]

Beryllium Binding by Bovine Serum Albumin at Acid pH

BY SIDNEY BELMAN

RECEIVED AUGUST 2, 1962

The binding of beryllium by bovine serum albumin was investigated, at three temperatures, in the pH region 5 and below, where beryllium salts are soluble and dialyzable. Reversible association was studied by the method of equilibrium dialysis in solutions containing nitrate ion at an ionic strength of 0.15. The amount of binding increased with increasing pH and temperature. The constancy of the intrinsic association constant ($K = 36.2$) and the variation of n , the number of binding sites, suggest that environmental conditions modify the structure of the protein so that a varying number of a single class of binding sites become available for reaction. Considerations of the effect of pH and temperature on beryllium ion hydrolysis and albumin structure support this interpretation. Esterified serum albumin exhibited no beryllium binding which is evidence for the carboxyls as the reacting groups. The results of potentiometric titrations agreed with those obtained from equilibrium dialysis. Albumin denatured by dodecyl sulfate showed greatly increased beryllium binding which was attributed to the electrostatic effect of the bound anion. The cooperative behavior of the beryllium binding was ascribed to the structural effects induced by dodecyl sulfate bound to albumin. Although the beryllium species in equilibrium with the protein is unknown, the data suggest that Be^{2+} is one reacting species.

Introduction

The interaction of beryllium with proteins is important for several reasons. Beryllium toxicity in the lung disease, berylliosis, is of unexplained mechanism^{1,2} but may involve interaction of beryllium with tissue proteins.³ In addition, studies of metal-protein complex formation can be used to elucidate protein structure.⁴

Beryllium-protein interactions have been qualitatively examined by several procedures. Thus, beryllium precipitates serum and nucleoproteins^{5–10} and

inhibits heat denaturation of trypsin.¹¹ Binding in calf serum at pH 7.5 at about 10^{-9} *M* beryllium is indicated by the dialysis experiment of Feldman, *et al.*¹²

In another study the strong inhibition of alkaline phosphatase by beryllium was used by Schubert and Lindenbaum¹³ to measure the formation constants between this metal and chelating agents. The agreement of their values with those in the literature demonstrated that alkaline phosphatase binds beryllium.¹⁴

(9) W. Jacobson and M. Webb, *Exptl. Cell Research*, **3**, 163 (1952).

(10) L. M. Gilbert, W. G. Overend and M. Webb, *ibid.*, **2**, 349 (1951).

(11) W. G. Crewther, *Australian J. Biol. Sci.*, **6**, 597 (1953).

(12) I. Feldman, J. R. Havill and W. F. Neuman, *Arch. Biochem. Biophys.*, **46**, 443 (1953).

(13) J. Schubert and A. Lindenbaum, *J. Biol. Chem.*, **208**, 359 (1954).

(14) These authors err, however, in assuming that a 1:1 complex forms between beryllium and chelating agent. Meek and Banks¹⁵ have shown that sulfosalicylic acid forms a 2:1 complex with beryllium at alkaline pH. The data in Fig. 1 and 3 of Schubert and Lindenbaum's paper can be used to determine which complex is formed. Theoretical curves based on data in Fig. 1 were plotted for the 1:1 and 2:1 complex of sulfosalicylic acid. The curve for the 2:1 complex coincided with the experimental curve in Fig. 3. The curve for the 1:1 complex did not. Furthermore the calculation of the formation constant for the 2:1 complex was $K = 1.74 \times 10^{-9}$, which is to be

(1) H. L. Hardy and I. R. Tabershaw, *J. Ind. Hyg. Toxicol.*, **28**, 197 (1946).

(2) J. H. Sterner and M. Eisenbud, *Arch. Ind. Hyg. and Occupational Med.*, **4**, 123 (1951).

(3) W. N. Aldridge, J. M. Barnes and F. A. Denz, *Brit. J. Exptl. Pathol.*, **30**, 375 (1949).

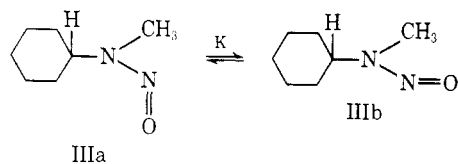
(4) I. M. Klotz, J. M. Urquhart, T. A. Klotz and J. Ayers, *J. Am. Chem. Soc.*, **77**, 1919 (1955).

(5) U. Richter, *Inaug. Diss.*, Wurzburg, 1930, described in ref. 6.

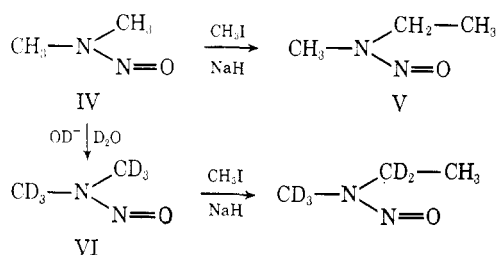
(6) H. Steidle, *Arch. Exper. Path. Pharmacol.*, **187**, 553 (1937).

(7) L. T. Fairhall, F. Hyslop, E. D. Palmes, W. C. Alford and A. R. Monaco, *Natl. Inst. Health. Bull.*, **181** (1943).

(8) S. V. Volter, *Farmakol. i. Toksikol.*, **3**, 82 (1940).



mg of sodium hydride for 3 hr. That the methyl-ethyl-nitrosamine (V) produced in this reaction was the result of direct displacement of iodide, rather than carbene insertion, was demonstrated by subjecting dimethylnitrosamine- d_6 (VI)⁶ to these conditions; the isolation of product with a molecular weight of 93 (mass spectrometry) implies that cleavage of the nitrosamine C-D bond preceded the reaction with the alkylating species.



It is noteworthy that canonical structures involving resonance delocalization of the formal negative charge at carbon cannot be formulated, and the facility of the reaction must be attributable entirely to inductive effects. Such a situation was once thought to be impossible,⁷ but several groups have amply demonstrated the viability of inductively stabilized carbanions⁸ analogous to the one proposed here. It is presumed that polarization of the N-N-O group, as in IIb, is more important in the carbanion than in the nitrosoamine itself, since the formal positive charge at the heterocyclic nitrogen would contribute to the inductive stabilization of the carbanionic center. It is hoped that kinetic studies currently in progress will shed further light on the mechanistic details of this reaction.

Acknowledgment. The authors wish to thank Drs. C. A. Kingsbury and W. Lijinsky for helpful discussions, and Messrs. J. Loo, F. Watson, and D. E. Johnson for able technical assistance. The financial support of the U. S. Public Health Service, Contract No. 43-68-959, is gratefully acknowledged.

(6) Dimethylnitrosamine- d_6 (VI) was prepared by exchange with deuterium oxide in the presence of sodium deuterioxide. The isotopic purity of the redistilled product, bp 149°, was estimated to be 99% using mass spectrometry. No trace of any impurity could be detected by glc or nmr.

(7) E. S. Gould, "Mechanism and Structure in Organic Chemistry," Holt, Rinehart and Winston, New York, N. Y., 1959, p 388.

(8) Several other types of carbanions have been alleged to be purely inductively stabilized, including the α -fluoro- and α -aryloxy carbanions,⁹ the quaternary ammonium methylides,¹⁰ and the carbanion derived from 7-ketonorborene.¹¹

(9) J. Hine, L. G. Mahone, and C. L. Liotta, *J. Amer. Chem. Soc.*, **89**, 5911 (1967).

(10) W. v. E. Doering and A. K. Hoffmann, *ibid.*, **77**, 521 (1955).

(11) P. G. Gassman and F. V. Zalar, *ibid.*, **88**, 3070 (1966).

(12) Address correspondence to this author.

Larry K. Keefer,¹² Connie H. Fodor

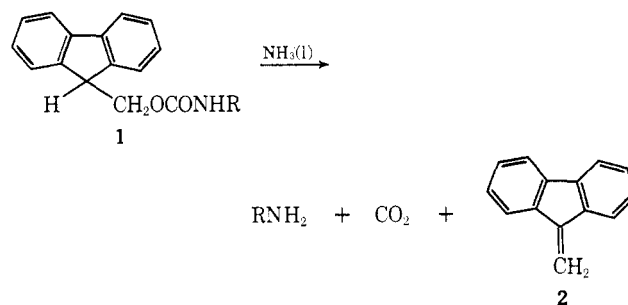
The Eppley Institute for Research in Cancer
University of Nebraska Medical Center
Omaha, Nebraska 68105

Received May 16, 1970

The 9-Fluorenylmethoxycarbonyl Function, a New Base-Sensitive Amino-Protecting Group

Sir:

In contrast to the variety of amino-protecting groups which can be cleaved under nonhydrolytic conditions by acids of varying strengths, there is currently no complementary set of groups cleavable by basic reagents of graded activity. Making use of the process of β elimination,¹⁻⁴ we have developed one such hydrocarbon-derived protective function, the 9-fluorenylmethoxycarbonyl group (Fmoc), which can be cleaved under extremely mild conditions, most conveniently simply by allowing a solution in liquid ammonia⁵ to stand for several hours. Other convenient deblocking conditions involve dissolution in ethanalamine, morpholine, or a similar amine. In addition the group is potentially capable of being modified for greater or lesser sensitivity toward basic reagents.



The Fmoc group may be readily introduced by treatment of the parent amine with 9-fluorenylmethyl chloroformate (**3a**) or the corresponding azidoformate (**3b**) in aqueous dioxane in the presence of sodium carbonate or bicarbonate. The chloroformate (mp 61.5-63°; ir (CHCl₃) 1770 cm⁻¹; nmr (CDCl₃) δ 4-4.6 (m, 3, CHCH₂), 7.1-7.8 (m, 8, aryl)) is obtained (86%) by reaction of 9-fluorenylmethanol⁶ with phosgene in methylene dichloride without added base. The azidoformate (mp 83-85°; ir (CHCl₃) 2135, 1730 cm⁻¹; nmr (CDCl₃) δ 4-4.5 (m, 3, CHCH₂), 7.1-7.9 (m, 8, aryl)) is best obtained (82%) by reaction of **3a** with sodium azide in aqueous acetone. Fortunately, for purposes of selectivity in the synthesis of polyfunctional compounds

(1) A. T. Kader and C. J. M. Stirling [*J. Chem. Soc.*, 258 (1964)] have recommended use of the related β -tosylethoxycarbonyl group, although removal conditions involved use of sodium hydroxide or ethoxide and prior acidification to decompose the first-formed carbamate. The β -nitroethoxycarbonyl group has also been examined but found unsuitable for various reasons.^{2,3}

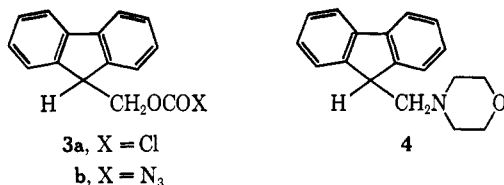
(2) P. J. Crowley, M.S. Thesis, University of Massachusetts-Amherst, Amherst, Mass., 1958; L. A. Carpino, unpublished work, 1967-1968.

(3) Th. Wieland, G. J. Schmitt, and P. Pfaender, *Justus Liebigs Ann. Chem.*, **694**, 38 (1966).

(4) The 9-fluorenylmethyl system was first suggested to us in conversations with Professor A. Cecon regarding the ease of β elimination from 9-fluorenyl thiocyanates and analogous systems relative to the corresponding benzhydryl derivatives [compare A. Cecon, U. Miotti, U. Tonellato, and M. Padovan, *J. Chem. Soc. B*, 1084 (1969); U. Miotti, A. Sinico and A. Cecon, *Chem. Commun.*, 724 (1968)]. For recent studies showing that even 9-fluorenylmethanol undergoes ready β elimination (mechanism E1cB), see R. A. More O'Ferrall, and S. Slae, *J. Chem. Soc. B*, 260 (1970); R. A. More O'Ferrall, *ibid.*, **B**, 268, 274 (1970).

(5) One of the classic deblocking systems in peptide chemistry involves reduction of tosyl and other protective groups by means of a solution of sodium in liquid ammonia. Presence of sodium is, however, a distinct disadvantage both in terms of possible competing reactions and isolation difficulties due to the presence of inorganic salts.

(6) W. G. Brown and B. A. Bluestein, *J. Amer. Chem. Soc.*, **65**, 1082 (1943).



or complex polypeptides, the Fmoc group is stable under conditions involved in the removal of most of the commonly used protective groups such as hydrogen bromide or chloride in various organic solvents, trifluoroacetic acid, and catalytic hydrogenolysis over palladium-carbon. Cleavage by-products (monomeric or polymeric dibenzofulvene (**2**) or an amine-dibenzofulvene adduct such as **4**) depend on both reaction conditions and the reagent used and in all cases are easily separated from the desired amine. As an example, a solution of Fmoc-glycine (**1**, R = CH₂CO₂H), mp 174–176°, in liquid ammonia is allowed to stand for 10–12 hr, the ammonia evaporated, and the residue treated with ether to remove **2**. The residue is treated with water to remove a trace of dibenzofulvene polymer and evaporation gives glycine in quantitative yield. Similarly a solution of Fmoc-aniline (**1**, R = C₆H₅), mp 189–190°, in morpholine is allowed to stand at room temperature for 25 min, diluted with water, filtered to remove adduct **4**, mp 172.5–174° (95%), and extracted with ether to give aniline (96%). If ethanolamine is substituted for morpholine as solvent and cleavage reagent the by-product is **2** rather than an analog of **4**. Authentic **2** was shown to react with morpholine to give **4**.

Acknowledgments. This work was supported by Grant No. GM-09706 from the National Institutes of Health. In addition, we wish to thank Professors E. Scoffone and A. Ceccon of the Istituto di Chimica Organica, Università di Padova, for discussions leading to the inception of this work.

(7) Address correspondence to this author.

Louis A. Carpino,⁷ Grace Y. Han

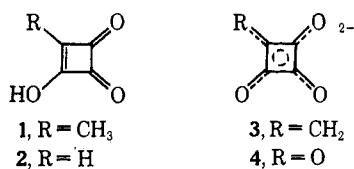
Department of Chemistry, University of Massachusetts-Amherst
Amherst, Massachusetts 01002

Received July 6, 1970

Methylhydroxycyclobutenedione

Sir:

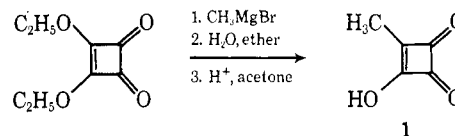
We wish to report the synthesis of methylhydroxycyclobutenedione (**1**), the first simple homolog of hydroxycyclobutenedione (**2**). On the basis of previous work on the phenyl analog,¹ **1** was expected to be a strong monoprotic acid. In addition, abstraction of another proton by base would lead to a new species (**3**)



(1) E. J. Smutny and J. D. Roberts, *J. Amer. Chem. Soc.*, **77**, 3420 (1955); E. J. Smutny, M. C. Caserio, and J. D. Roberts, *ibid.*, **82**, 1793 (1960).

isoelectronic with the aromatic squarate anion (**4**).² Simple Hückel calculations performed on **3** suggest that a substantial amount of the stability exhibited by **4** should also be found in **3**.³ In this report we wish to communicate the synthesis of **1** and the formation of **3** under relatively mild conditions.

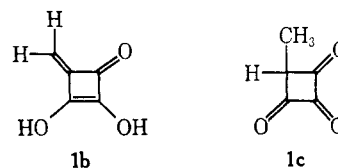
Treatment of diethoxycyclobutenedione^{2a} (4.7 g, 27.6 mmol) with methyl magnesium bromide (2.95 M,



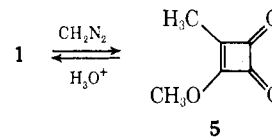
32 mmol) in ether at –78° followed by hydrolysis and extraction afforded a residue which was treated with an aqueous acid-acetone mixture and allowed to evaporate. Trituration with ether afforded **1** (1.34 g, 44%) as colorless crystals after sublimation and recrystallization;⁴ mp 162–164° (acetone-heptane); nmr (acetone-*d*₆, TMS) τ 1.98 (0.99 H, s), 7.82 (3 H, s); ν_{\max} (Nujol) 2650–2150 (broad), 1800, 1725, 1540, 1070, 755 cm⁻¹; λ_{\max} (H₂O) 260 (ϵ 11,000), 230 m μ (24,000).

Anal. Calcd for C₅H₄O₃: C, 53.58; H, 3.60; mol wt, 112. Found: C, 53.70; H, 3.48; *m/e*, 112, neut equiv, 115.

The presence of only two resonances in the nmr spectrum of **1** coupled with the absence of any appreciable amount of H/D exchange in the methyl group (acetone-*d*₆, D₂O, HCl) precludes the presence of tautomer **1b**. Keto-enol tautomers such as **1c** in rapid equilibrium with **1**, however, cannot be ruled out at present.



Treatment of **1** (720 mg, 6.43 mmol) with excess diazomethane afforded the crystalline methyl ether derivative **5** (680 mg, 84%); mp 49–51°; ν_{\max} (Nujol) 1820, 1800, 1760 cm⁻¹; λ_{\max} (CH₃OH) 228 m μ (ϵ



17,000); nmr (CDCl₃, TMS) τ 5.53 (2.96 H, s), 7.75 (3 H, s). Acid-catalyzed hydrolysis of **5** gave back **1** (90%). The mass spectrum of **5** consisted of four major

(2) (a) G. Maahs and P. Hegenberg, *Angew. Chem., Int. Ed. Engl.*, **5**, 888 (1966); (b) R. West, H. Y. Niu, D. L. Powell, and M. V. Evans, *J. Amer. Chem. Soc.*, **82**, 6204 (1960); (c) R. West and D. L. Powell, *ibid.*, **85**, 2577 (1963); (d) M. Ito and R. West, *ibid.*, **85**, 2580 (1963); (e) R. West and H. Y. Niu in "Non-Benzenoid Aromatics," Vol. I, J. P. Snyder, Ed., Academic Press, New York, N. Y., 1969, pp 311–345.

(3) Using Coulomb and resonance integrals of $\alpha + \beta$ and 0.8β for oxygen,^{2b} these calculations indicate that about 80% of the delocalization of **4** would be retained by **3**.

(4) A small amount of dimethylcyclobutenedione was also isolated from the ether-soluble portion (dinitrophenylhydrazone derivative, mp 204° (lit. 205–208° dec)): A. T. Blomquist and R. A. Vierling, *Tetrahedron Lett.*, **19**, 655 (1961).

Methods and Protocols of Modern Solid Phase Peptide Synthesis

Muriel Amblard, Jean-Alain Fehrentz, Jean Martinez, and Gilles Subra*

Abstract

The purpose of this article is to delineate strategic considerations and provide practical procedures to enable non-experts to synthesize peptides with a reasonable chance of success. This article is not encyclopedic but rather devoted to the Fmoc/tBu approach of solid phase peptide synthesis (SPPS), which is now the most commonly used methodology for the production of peptides. The principles of SPPS with a review of linkers and supports currently employed are presented. Basic concepts for the different steps of SPPS such as anchoring, deprotection, coupling reaction and cleavage are all discussed along with the possible problem of aggregation and side-reactions. Essential protocols for the synthesis of fully deprotected peptides are presented including resin handling, coupling, capping, Fmoc-deprotection, final cleavage and disulfide bridge formation.

Index Entries: Solid phase peptide synthesis (SPPS); resin; Fmoc SPPS; coupling reagents; protecting groups; anchoring; side reaction.

1. Introduction

Currently, “peptide synthesis” includes a large range of techniques and procedures that enable the preparation of materials ranging from small peptides to large proteins. The pioneering work of Bruce Merrifield (1), which introduced solid phase peptide synthesis (SPPS), dramatically changed the strategy of peptide synthesis and simplified the tedious and demanding steps of purification associated with solution phase synthesis. Moreover, Merrifield’s SPPS also permitted the development of automation and the extensive range of robotic instrumentation now available. After defining a synthesis strategy and programming the amino acid sequence of peptides, machines can automatically perform all the synthesis steps required to prepare multiple peptide samples. SPPS has now become the method of choice to produce peptides, although solution phase synthesis can still be useful for large-scale production of a given peptide.

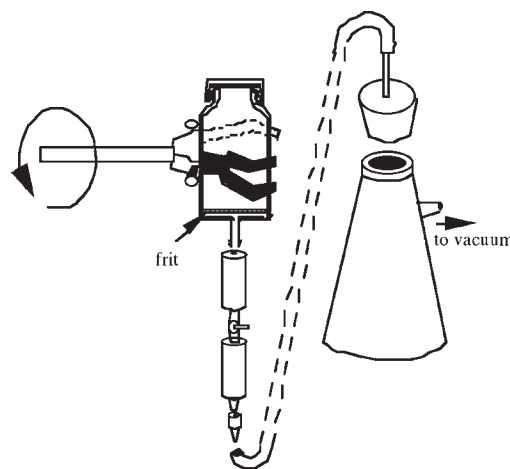


Fig. 1. Basic equipment for SPPS.

2. Materials

1. Reaction vessel (Fig. 1).
2. Polytetrafluoroethylene (PTFE) stick (15-cm length, 0.6–0.8-cm diameter).
3. Rotor.

*Author to whom all correspondence and reprint requests should be addressed. Laboratoire des Amino Acides, Peptides et Protéines–UMR-CNRS 5810. Faculté de Pharmacie. B.P. 14491, 15, Avenue Charles Flahault, 34093 Montpellier cedex 5, France. E-mail: muriel.amblard@univ-montp1.fr

4. Filtration flask.
5. Porous frit.
6. Lyophilizer.
7. High-performance liquid chromatography (HPLC) equipped with reverse phase C 18 column.
8. pH-Indicating paper.
9. Solvents (*N,N*-dimethylformamide [DMF], methanol [MeOH], dichloromethane [DCM]) in wash bottles.
10. Di-isopropylethylamide (DIPEA).
11. Piperidine solution in DMF (20:80).
12. Kaiser test solutions (ninhydrin, pyridine, phenol) (**Note 1**).
13. Fmoc-amino-acids with protected side-chains (**Table 1**).
14. Trifluoroacetic acid (TFA).
15. Tri-isopropylsilane (TIS).
16. *tert*-butyl methyl ether (MTBE).

3. Methods

3.1. Principles of SPPS

As peptide synthesis involves numerous repetitive steps, the use of a solid support has obvious advantages. With such a system a large excess of reagents at high concentration can drive coupling reactions to completion. Excess reagents and side products can be separated from the growing and insoluble peptide simply by filtration and washings, and all the synthesis steps can be performed in the same vessel without any transfer of material.

The principles of SPPS are illustrated in **Fig. 2**. The *N*-protected C-terminal amino-acid residue is anchored via its carboxyl group to a hydroxyl (or chloro) or amino resin to yield respectively an ester- or amide- linked peptide that will ultimately produce a C-terminal acid or a C-terminal amide peptide. After loading the first amino acid, the desired peptide sequence is assembled in a linear fashion from the C-terminus to the N-terminus (the C→N strategy) by repetitive cycles of *N*^α deprotection and amino acid coupling reactions.

Side-chain functional groups of amino acids must be masked with permanent protecting groups (P_n) that are stable in the reaction conditions used during peptide elongation. The α -amino group is protected by temporary protecting group (T) that

is usually a urethane derivative. The temporary protecting group (T) can be easily removed under mild conditions that preserve peptide integrity and reduces the rate of epimerization, which can occur via 5(4*H*)-oxazolone formation of the activated amino acid during coupling step (2,3) as indicated in **Fig. 3**. The protective role of urethanes against epimerization also explains the predominance of the C→N strategy.

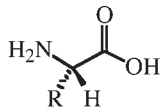
After coupling, the excess of reactants is removed by filtration and washings. The temporary *N*-terminal protecting group is removed allowing the addition of the next *N*-urethane-protected amino acid residue by activation of its α -carboxylic acid. This process (deprotection/coupling) is repeated until the desired sequence is obtained. In a final step, the peptide is released from the resin and the side-chain protecting groups (P_n) concomitantly removed.

3.2. Fmoc/*t*Bu SPPS

In SPPS, two main strategies are used: the Boc/Bzl and the Fmoc/*t*Bu approaches for T/ P_n protecting groups. The former strategy is based upon the graduated acid lability of the side-chain protecting groups. In this approach, the Boc group is removed by neat trifluoroacetic acid (TFA) or TFA in dichloromethane and side-chain protecting groups and peptide-resin linkages are removed at the end of the synthesis by treatment with a strong acid such as anhydrous hydrofluoric acid (HF). Although this method allows efficient syntheses of large peptides and small proteins, the use of highly toxic HF and the need for special polytetrafluoroethylene-lined apparatus limit the applicability of this approach to specialists only. Moreover, the use of strongly acidic conditions can produce deleterious changes in the structural integrity of peptides containing fragile sequences.

The Fmoc/*t*Bu method (4) is based upon an orthogonal protecting group strategy. This approach uses the base-labile *N*-Fmoc group for protection of the α -amino function, acid-labile side-chain protecting groups and acid-labile linkers that constitute the C-terminal amino acid protecting group. This latter strategy has the advantage that temporary and permanent orthogonal protections are re-

Table 1
Proteinogenic Amino Acids



Amino acid	Three-letter code	One-letter code	Side-chain
Glycine	Gly	G	H-
Alanine	Ala	A	CH ₃ -
Valine	Val	V	(CH ₃) ₂ CH-
Leucine	Leu	L	(CH ₃) ₂ CHCH ₂ -
Isoleucine	Ile	I	CH ₃ CH ₂ (CH ₃)CH-
Acide aspartique	Asp	D	HOOC-CH ₂ -
Asparagine	Asn	N	H ₂ NOC-CH ₂ -
Acide glutamique	Glu	E	HOOC-CH ₂ CH ₂ -
Glutamine	Gln	Q	H ₂ NOC-CH ₂ CH ₂ -
Lysine	Lys	K	H ₂ N-CH ₂ CH ₂ CH ₂ CH ₂ -
Arginine	Arg	R	$\begin{array}{c} \text{HN} \\ \diagdown \\ \text{C} \\ \diagup \\ \text{H}_2\text{N} \end{array} \text{-NH-CH}_2\text{CH}_2\text{CH}_2\text{-}$
Histidine	His	H	
Serine	Ser	S	HO-CH ₂ -
Threonine	Thr	T	CH ₃ -CH(OH)-
Phenylalanine	Phe	F	
Tyrosine	Tyr	Y	
Tryptophane	Trp	W	
Cysteine	Cys	C	HS-CH ₂ -
Methionine	Met	M	CH ₃ -S-CH ₂ CH ₂ -
Proline	Pro	P	

Note: All the 20 DNA-encoded or proteinogenic α -amino acids are of L stereochemistry

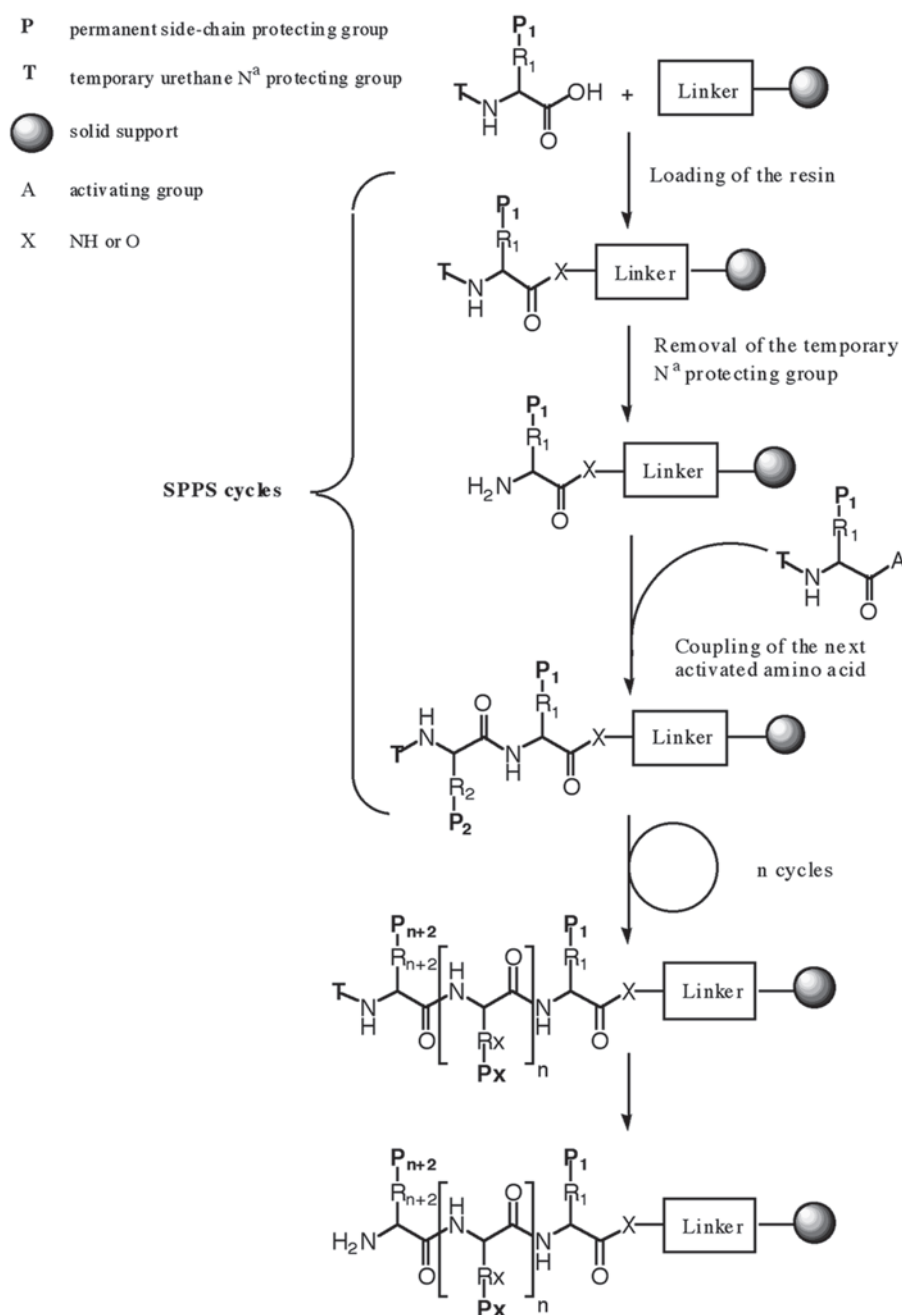


Fig. 2. Principles of SPPS.

moved by different mechanisms allowing the use of milder acidic conditions for final deprotection and cleavage of the peptide from the resin. For all these reasons, Fmoc-based SPPS method is now the method of choice for the routine synthesis of peptides.

3.3. Solid Supports

The matrix polymer and the linker can characterize solid supports (5). Often the term “resin” is improperly used in place of the linker system, ignoring the fact that the matrix polymer is as important in supported chemistry as the solution

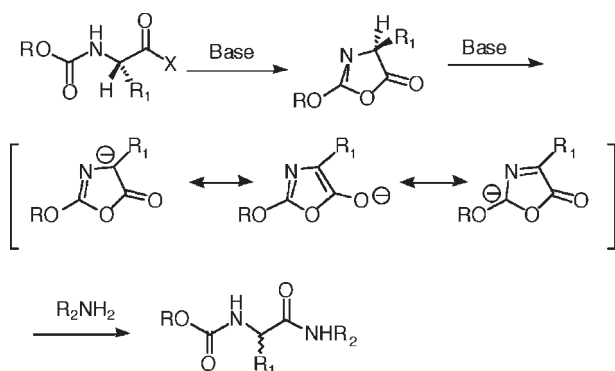


Fig. 3. Epimerization by oxazolone formation.

phase (6). As hundreds of different resins are commercially available, some of them carrying the same linkers, special care should be taken to properly choose the most suitable linker for the synthesis.

3.3.1. Matrix Polymers

Crosslinked polystyrene (PS)-based resins are most commonly used for routine SPPS. Beads of 200- to 400-mesh size distribution (corresponding to a diameter of about 50 μm) and a loading of 0.5 to 0.8 mmol/g present good characteristics for polymer swelling in solvents such as DMF and DCM, diffusion of reactants into the polymer matrix, and accessibility of linker sites buried into the bead. For larger peptides (more than 25 amino acids) or more difficult sequences, a lower loading is required (0.1–0.2 mmol/g).

Crosslinked polyamide-based resins (PA) and composite PS-Polyethylene glycol (PEG)-based resins are much more hydrophilic supports than PS resins. They exhibit different physical properties at microscopic and macroscopic levels (7). These supports, often with a lower loading capacity, may represent an alternative to standard crosslinked PS resins for the synthesis of difficult sequences and large peptides.

3.4. Resin Handling

3.4.1. SPPS Reaction Vessels

SPPS can be performed in classical glass reaction vessels that can be made by glassblowers or purchased from manufacturers (Fig. 1). Alternatively,

syringes equipped with PTFE or glass frits may also be used.

Reaction vessel size should be in relation to the amount of resin used, according to Table 2.

3.4.2. Solvents

As 99% of coupling sites are not at the surface but inside the resin beads, swelling of beads carrying the growing peptide chain is essential for the optimal permeation of activated *N*-protected amino acids within the polymer matrix, thus improving coupling yields. Before starting the solid phase synthesis, the resin has to be swollen in an adequate solvent such as DCM or DMF for 20 to 30 min (Protocol 1). For crosslinked polystyrene beads used in SPPS, DCM presents optimal swelling properties. For coupling steps, polar aprotic solvents such as DMF or NMP are preferred to improve solubility of reactants. Alcohols and water are not adequate solvents for PS resins (see Note 2). Nevertheless, methanol or isopropanol can be used during the washing steps (Protocol 2) to shrink PS resin beads. This shrinking will efficiently remove reactants in excess. After such treatment, PS beads should be swollen in DCM or DMF.

3.4.3. Stirring and Mixing

It is not necessary to agitate the reaction vessel vigorously, as diffusion phenomena dictate the kinetic reaction in SPPS. Moreover, most types of resin beads used for peptide synthesis are fragile, so magnetic stirring is not recommended. An old rotary evaporator rotor can be used for stirring during coupling and deprotection steps or alternately any apparatus enabling smooth agitation by rocking or vortexing is appropriate. As beads usually stick to glass, the important condition is that all surfaces of the reactor must be in contact with the reaction mixture during stirring.

3.4.4. Washing

Washing steps are essential to remove soluble side products and the excess of reactants used during coupling and deprotection steps. Filling the reactor with solvent contained in a wash bottle and emptying it under a vacuum is an appropriate and simple method. If necessary, stirring and mixing of the resin in the washing solvent can be performed with a PTFE stick.

Table 2
Type of SPPS Reaction Vessels

Vessel length (cm)	Vessel diameter (cm)	Max. resin weight (mg)	Working volume (mL)
5	2	0.5	10
11	2.6	2	40
15	3.4	4	90

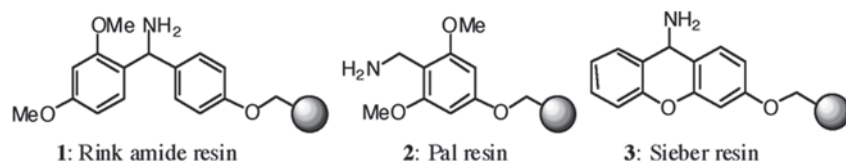


Fig. 4. Resins for peptide amide synthesis.

PROTOCOL 1: RESIN SWELLING

1. Place the dry resin in the appropriate reaction vessel (*see Subheading 3.4.1.*).
2. Fill the reactor with DCM until all resin beads are immersed. Resin suspension can be gently mixed with a PTFE stick.
3. Leave for 20 to 30 min.
4. Remove DCM by filtration under vacuum.

PROTOCOL 2: STANDARD WASHING PROCEDURES

1. Fill the reaction vessel with DMF.
2. Leave for 10 s and remove the solvent by filtration.
3. Carefully wash the screw cap and the edge of the reactor with DMF.
4. Repeat **steps 1 and 2** twice with DMF.
5. Repeat **steps 1 and 2** with MeOH.
6. Repeat **steps 1 and 2** with DCM.
7. Repeat **steps 1 and 2** with DMF.

3.5. Linkers and Resins for Fmoc-Based SPPS

The first step of SPPS is the anchoring (or loading) of the *N*-protected C-terminal amino acid residue to the solid support via an ester or an amide bond depending of the C-terminal functional group of target peptide (respectively acid or amide). Most of the linkers are commercially available anchored on the different matrixes (PS, PA, PEG-PS). The bead (ball) symbol used in the

following paragraph is generic and does not refer to a particular matrix.

3.5.1. Peptide Amides

For the synthesis of C-terminal peptide amides, the commonly used resins are 1 to 3 (**Fig. 4**) (8–10). These resins are compatible with Fmoc chemistry and final TFA cleavage. For attachment of the first urethane *N*-protected residue, standard peptide coupling procedures (**Protocol 5**) can be used. These resins are usually supplied Fmoc-protected and should be deprotected before incorporation of the first residue. With bulky C-terminal amino acids, a double coupling step can be necessary.

3.5.2. Peptide Acids

The anchoring of an amino acid to the solid support by esterification is often more difficult, and even hazardous, for some residues and can lead to epimerization, dipeptide formation and low substitution. Thus, we recommend the purchase of resins preloaded with the first C-terminal *N*-protected amino acid; these are commercially available from various manufacturers.

Commonly used resins in Fmoc/*t*Bu strategy for the synthesis of C-terminal peptide acid are reported in **Fig. 5** (11–14). Anchoring reactions must be performed in an anhydrous medium and amino acids containing water should be dried before use.

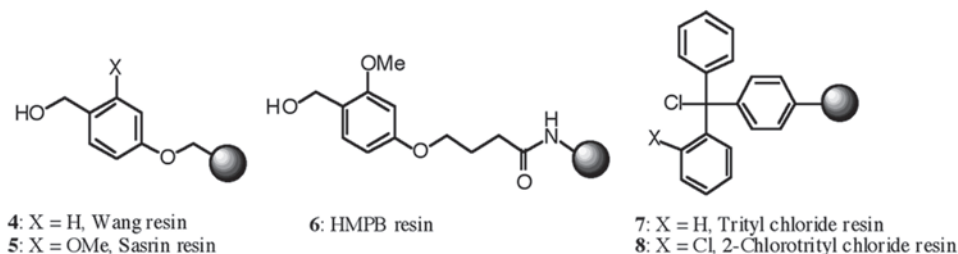


Fig. 5. Resins for peptide acid synthesis.

3.5.3. Hydroxymethyl-Based Resins

For hydroxymethyl-based resins 4 to 6, formation of the ester linkage is easier with unhindered resins such as Wang resin 4 compared with resins possessing withdrawing methoxy groups 5 and 6. The most commonly used esterification process is the symmetrical anhydride method (**Protocol 3**). Determination of the loading can be performed by Fmoc release measurement (*see Note 3*). In the case of difficult anchoring, the esterification step can be repeated with fresh reactants. Arginine derivatives can need three esterification steps to achieve correct loading. After anchoring, unreacted resin-bound hydroxyl groups should be capped by benzoic anhydride or acetic anhydride (*see Protocol 3, step 8*).

PROTOCOL 3: ATTACHMENT TO HYDROXYMETHYL-BASED RESIN

1. Place the resin in the appropriate SPPS reactor.
2. Swell the resin as described in **Protocol 1**.
3. The desired Fmoc-amino-acid (10 equivalents relative to resin substitution) is placed in a dry, round-bottom flask with a magnetic stirrer and dissolved in dry DCM at 0°C (3 mL/mmol). Some drops of dry DMF may be useful to achieve complete dissolution.
4. Add DIC (5 equivalents) and stir the mixture for 10 min at 0°C. If a precipitate is observed, add DMF until dissolution and stir for 10 min more.
5. Add the solution to the hydroxymethyl resin.
6. Dissolve dimethylaminopyridine (DMAP) (0.1–1 equivalent) in DMF and add the solution to the reaction mixture.
7. After 1-h stirring, wash the resin with DMF (three times) and finally with DCM.

8. Dry the resin in vacuo for 18 h before performing Fmoc release measurement on a sample (*see Note 3*). When the loading is less than 70%, repeat the esterification step.
9. When the desired substitution is achieved, cap the remaining hydroxyl groups by adding benzoic or acetic anhydride (5 eq) and pyridine (1 eq) in DMF to the resin (previously swelled) and stir for 30 min.
10. Wash the resin (**Protocol 2**) and start classical elongation with *N*-protected amino acid after Fmoc deprotection (**Protocol 7**).

3.5.4. Trityl-Based Resins

Trityl-based resins are highly acid-labile. The steric hindrance of the linker prevents diketopiperazine formation and these resins are recommended for Pro and Gly C-terminal peptides. Extremely mild acidolysis conditions enable the cleavage of protected peptide segments from the resin. These resins are commercially available as their chloride or alcohol precursors. The trityl chloride resin is extremely moisture-sensitive, so reagents and glassware should be carefully dried before use to avoid hydrolysis into the alcohol form. It is necessary to activate the trityl alcohol precursor and it is highly recommended to reactivate the chloride just before use (*see Note 4*). After activation, attachment of the first residue occurs by reaction with the Fmoc amino acid derivative in the presence of a base. This reaction does not involve an activated species, so it is free from epimerization. Special precautions should be taken for Cys and His residues that are particularly sensitive to epimerization during activation (**Table 2**).

PROTOCOL 4: ATTACHMENT TO TRITYL-BASED RESIN

1. Place 1 g of trityl-based resin (1.0–2.0 mmol chloride/g resin) in a SPPS reaction vessel.
2. Swell the resin as described in **Protocol 1**.
3. Add a solution of 3 eq of Fmoc amino acid and 7.5 eq of DIPEA in dry DCM (10-mL/g resin).
4. Stir the mixture for 30 to 60 min at room temperature.
5. Wash the resin with DMF (two to three times).
6. Add 10 mL of a mixture of DCM/MeOH/DIPEA (80:15:5) to cap any remaining reactive chloride group.
7. Mix for 15 min and filter.
8. Wash the resin three times with DMF and DCM. After drying in vacuo, the substitution can be measured from Fmoc release (*see Note 3*).

3.6. Side-Chain Protecting Groups

We will limit the description of side-chain protecting groups (**5**) to those that have been found most effective for the preparation of a large number of classical peptide sequences in Fmoc SPPS and are commercially available from most of the protected amino acid providers. For routine synthesis, TFA-labile protecting groups are usually used. However, for selective modifications of a particular residue on the solid support (e.g., side-chain cyclized peptides, biotinylated peptides), special orthogonal protecting groups are needed (**15**). Some of the most commonly used side-chain protecting groups are reported in **Table 3**.

3.7. Coupling Reaction

The most simple and rapid procedure for the stepwise introduction of *N*-protected amino acids in SPPS is the in situ carboxylic function activation (**Protocol 5**). A large excess of the activated amino acid is used (typically 2–10 times excess compared to the resin functionality, which is provided by the manufacturer or empirically determined; *see Note 3*). This excess allows a high concentration of reactants (typically 60–200 mM) to ensure effective diffusion.

The time required for a complete acylation reaction depends on the nature of the activated species, the peptide sequence that is already linked to the resin, and the concentration of reagents. This last parameter must be as high as possible

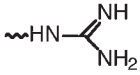
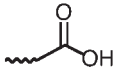
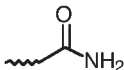

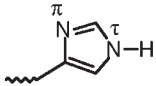


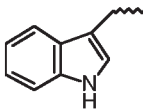
and is in connection with the volume of the reaction vessel and the resin substitution (**Table 2**). The preferred coupling reagents for in situ activation are benzotriazol-1-yl-oxytripyrrolidino phosphonium hexafluorophosphate PyBOP (**16**) for phosphonium-based activation and O-(benzotriazol-1-yl)-1,1,3,3-tetramethyluronium tetrafluoroborate TBTU (**17**) or *N*-[(1H-benzotriazol-1-yl) (dimethylamino)methylene]-*N*-methylmethanaminium hexafluorophosphate *N*-oxide HBTU (**18**) for aminium/uronium-based activation (**Fig. 6**). These coupling reagents convert *N*-protected amino acids into their corresponding OBt esters. A tertiary amine (generally diisopropylethylamine) is required to produce the carboxylate of *N*-protected amino acids which reacts with coupling reagents. More recently, *N*-[(dimethylamino)-1H-1,2,3-triazolo[4,5-*b*] pyridin-1-ylmethylene]-*N*-methylmethanaminium hexafluorophosphate *N*-oxide HATU (**19**) and PyAOP (**20**), that generate OAt esters, have been reported to be more efficient and to reduce epimerization.

Uronium/aminium-based reagents (HBTU, HATU, TBTU) are thought to mechanistically function in a similar way to their phosphonium analogs but unlike them, they can irreversibly block the free *N*-terminal amino function of the peptide-resin by forming tetramethylguanidinium derivatives (**Fig. 7**) (**21**). To avoid this side-reaction, it is recommended to generate the carboxylate of the amino acid before adding these coupling reagents at a slightly reduced equivalent compared to the amino acid.

PROTOCOL 5: STANDARD COUPLING PROCEDURE WITH HBTU

1. After Fmoc deprotection and washings (or properly conditioning and swelling when the resin is dry), wash the resin once with DMF.
2. Add the *N*- α Fmoc protected amino acid as a powder (usually 3 eq).
3. Fill the SPPS reaction vessel (at least 2/3 of volume) with DMF and stir with a PTFE stick for 10–20 s.
4. Add DIPEA to the vessel (usually slight excess, 3.5–4 eq) and stir with a PTFE stick until complete dissolution of the *N*-protected amino acid

Table 3
Side-Chain Protecting Groups in Fmoc-Based SPPS

Amino acid and side-chain functionality	Protecting groups	Removal condition	Remarks and side reactions
Arg 	Pmc Pbf	95% TFA 95% TFA	Presence of thiols may accelerate the cleavage
Asp/Glu 	OtBu OAll ^a	95% TFA Pd(Ph ₃ P) ₄ /PhSiH ₃	Aspartimide formation (§ 12.2)
Asn/Gln 	Trt	95% TFA	Protections avoid dehydration of the carboxamide side-chain during activation and help to solubilize Fmoc-Asn-OH and Fmoc-Gln-OH. pyrGlu formation for <i>N</i> -terminal glutamine peptides (Note 5)
Cys 	Trt	95% TFA	High level of epimerization can occur during activation (Note 6). Participate in the folding of peptides and proteins by disulfide bridge formation (§ 11).
His 	Trt (NHτ) Mtt ^a	TFA 1% TFA	Even with protection of the imidazole ring, problems of epimerization can occur during activation.
Lys 	Boc Mtt ^a Aloc ^a	TFA 1% TFA Pd(Ph ₃ P) ₄ /PhSiH ₃	
Ser/Thr/Tyr 	tBu Trt ^a	TFA 1% TFA	
Trp 	Boc	TFA	Trp can be used unprotected. However if Arg(Pmc) or Arg(Pbf) is present in the sequence, side-reaction can occur.

^a Protection used for on-resin derivatization

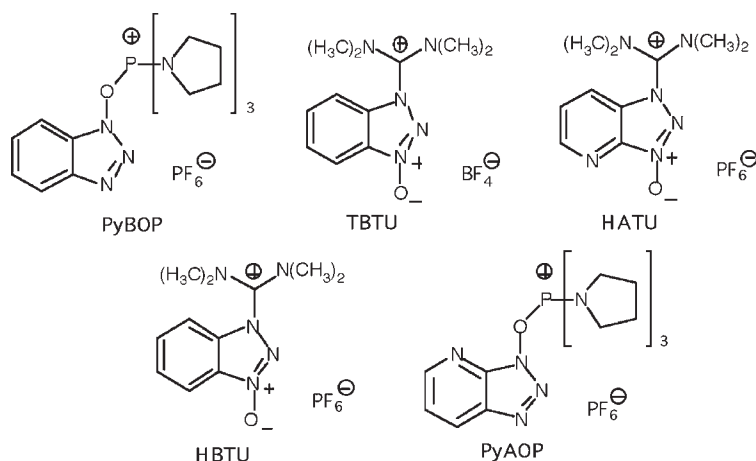


Fig. 6. Phosphonium and uronium/aminium coupling reagents.

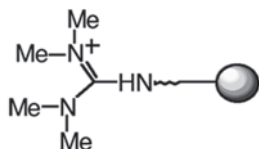


Fig. 7. N-terminal tetramethylguanidated peptides.

occurs. Other tertiary amines can be used such as *N*-methyl morpholine or triethylamine.

5. Add HBTU (2.9 eq compared with 3 eq of amino acid), screw the cap, and stir for 30 min. For difficult sequences it is recommended to preactivate the *N*-protected amino acid before coupling to the free *N*^α-amino function to limit the guanylation side-reaction.
6. Remove the coupling solution by filtration.
7. Wash the resin properly according to washing **Protocol 2**.
8. Perform qualitative monitoring of the coupling reaction using a colorimetric test (*see Note 1*).

In some cases coupling is not complete and a colorimetric test will reveal the presence of free amino groups. On these occasions a double coupling with fresh reagents must be performed. When acylation is incomplete after a second coupling, a capping procedure through acetic anhydride (**Protocol 6**) can be performed to stop the elongation of these less-reactive amino groups. When the colorimetric test still reveals the pres-

ence of free amine functions after capping, aggregation can be suspected.

PROTOCOL 6: CAPPING

1. Swell the resin in DCM.
2. Remove the DCM by filtration.
3. Fill the SPPS reactor (at least 2/3 of volume) with a 50/50 DCM/acetic anhydride solution (in case of trityl linker, *see Note 7*) and mix for 3 min.
4. Remove the capping solution by filtration and repeat **step 3** for 7 min.
5. Wash three times with DCM.
6. Check the disappearance of free amino groups by a convenient colorimetric test (*see Note 1*) and repeat the operation if necessary.

3.8. Difficult Sequences and Aggregation

When *N*^α-deprotection reactions and amino acid coupling steps do not go to completion or proceed in low yields, repeated or prolonged reaction times should overcome these problems. Nevertheless, this is not always sufficient. The cause of this failure is thought to be self-association of the peptide chain by hydrogen bond formation leading to aggregation. This aggregation results in incomplete solvation of the peptide-resin and inaccessibility of the reagents to the N-terminal amino group. This phenomenon is sequence-dependent with particular propensity for sequences containing high proportions of hydrophobic residues

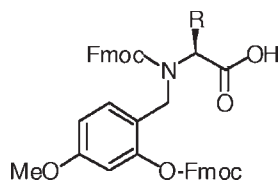


Fig. 8. Fmoc-(FmocHmb) amino acid.

and can start from the fifth-coupled residue. Two general methods can be used to disrupt the formation of secondary structures. The first consists of changing the peptide environment by adding chaotropic salts such as potassium thiocyanate or lithium chloride at a 0.4 M concentration, detergent solvents at 1% (v/v), or solvents such as DMSO, trifluoroethanol, hexafluoroisopropanol to the reaction medium (22–28). The second approach involves structural changes in the peptide backbone itself by the introduction of protecting groups to selected amide bonds. This is usually achieved by using the 2-hydroxy-4-methoxybenzyl (Hmb) derivative of glycine. Other amino acids can also be incorporated as their *N,O*-bis(Fmoc)-*N*-(Hmb) derivatives approximately every 6–7 residues (Fig. 8) (29,30). The incorporation of (Hmb) amino acids can be performed through their corresponding pentafluorophenyl esters, which are commercially available, or by standard coupling methods. For optimal *N*-acylation of the terminal Hmb residue that can be slow, it is recommended to use powerful coupling methods such as symmetrical anhydrides or preformed acid fluorides in DCM. The O-Fmoc protection of the Hmb derivatives is cleaved under piperidine treatment and the Hmb group in the final TFA cleavage. For Cys-, Ser-, and Thr-containing peptides their pseudoproline derivatives, also known to disrupt aggregation, can also be used (31–33).

3.9. Fmoc Deprotection

Removal of the temporary Fmoc protecting group from the N-terminus of the peptidyl-resin is normally achieved by short treatment with 20% piperidine in DMF (Protocol 7). The reaction is generally complete within 10 min, but can be longer in some cases. For safe removal a 20-min deprotection time is recommended. The

deprotection results in formation of a dibenzofulvene–piperidine adduct that strongly absorbs in the UV range (see Note 3). Fmoc removal can be monitored by UV spectroscopy. This is a common procedure with automatic synthesizers but not in standard manual SPPS. When incomplete deprotection is suspected, the use of 20% piperidine containing 1 to 5% DBU in DMF is recommended. However, DBU can promote aspartimide formation, thus its use should be avoided in Asp- or Asn-containing sequences.

PROTOCOL 7: REMOVAL OF *N*^α FMOC PROTECTION

1. After coupling reaction and washings, resin is washed once with DMF.
2. Fill the SPPS reaction vessel (at least 2/3 of volume) with an 80/20 DMF/piperidine solution and stir for 20 min (see Note 8).
3. Remove the DMF/piperidine solution by filtration.
4. Wash the resin properly according to Protocol 2.

3.10. Final Cleavage

Concentrated trifluoroacetic acid is widely used for the simultaneous cleavage of the peptide from the resin and removal of side-chain protecting groups. In these conditions, side-chain protecting groups produce stabilized carbocations, which can readily react with the electron rich side-chain of amino acids (Cys, Met, Tyr, Thr, Ser, Trp), leading to unwanted byproducts. To minimize this phenomenon, scavengers are added to the cleavage cocktail to trap carbocations. Numerous cocktails have been described to optimize the cleavage conditions of particular sequences. Silane-based cocktails that generally provide good results are nonodorous and less toxic than thiol-based cocktails (34). Special care should be taken to prepare and to use cleavage cocktails. All operations should proceed under a fume hood using gloves and safety glasses.

PROTOCOL 8: STANDARD TFA CLEAVAGE

1. Weigh the resin and place it in a round bottom flask. When the resin is dry, swell it as described in Protocol 1.
2. Add 10 mL of cleavage cocktail (trifluoroacetic acid/water/triisopropyl silane 95/2.5/2.5) per 100 mg of resin.

3. Resin is cleaved for 90 min under gentle stirring (see **Note 9**).
4. Filter the resin on a glass frit and wash it twice with fresh cleavage cocktail. Recover the filtrate in a round-bottom flask.
5. Concentrate the cleavage cocktail in vacuo to approximately one-fourth of its original volume.
6. Under vigorous stirring, add MTBE to precipitate the peptide. At least 10 times the initial TFA volume of MTBE should be added to precipitate the unprotected peptide. When the peptide does not precipitate, concentrate the solution in vacuo and go directly to **step 9**.
7. Filter the precipitate on a 4-porosity glass frit.
8. Triturate and wash by filtration the precipitated peptide on the frit three times with MTBE.
9. Solubilize the peptide in acetonitrile/water/TFA 50/50/0.1 and lyophilize. Solvent used for this step can be changed to increase solubility. Lyophilization can be repeated twice when scavengers are detected after reverse phase HPLC analysis of the peptide.

3.11. Disulfide Bridge Formation

One of the simplest ways to form disulfide bonds is oxidation of the fully deprotected linear peptide obtained after cleavage from the resin (in some cases, disulfide bridges began to form during the cleavage step) before or after preparative HPLC purification. The cyclization has to be performed using high dilution conditions to promote intramolecular disulfide bond formation versus intermolecular dimerization. Dimethyl sulfoxide is used to accelerate the oxidation reaction (**35**).

PROTOCOL 9: STANDARD FORMATION OF DISULFIDE BRIDGES BY AIR OXYDATION

1. Dissolve the lyophilized peptide at 0.5 mM concentration in a 5% acetic acid solution.
2. Add 10% volume of DMSO in a large beaker. Adjust the pH to 6.0 to 7.0 if necessary with a 0.5 M ammonium acetate solution.
3. Stir the solution vigorously at room temperature for 12 h to incorporate atmospheric oxygen into the solution. Ideally, disulfide bridge formation should be monitored by reverse phase HPLC. Purification (**step 4**) should be performed immediately after the end of the reaction.

4. Purify the peptide by preparative reverse phase HPLC after acidification with a TFA solution (pH 2.0).
5. Lyophilize the solution containing the fractions.

For peptides having more than two cysteines, orthogonal protection of these residues can be used to allow selective and sequential disulfide bridge formation (**5**). However, especially if the peptide sequence is a natural one, simultaneous deprotection/bridge formation can be attempted in an adequate redox buffer. The equilibrium between the different disulfide bridge arrangements during “oxidative folding” leads, in most of cases, to the native folding.

PROTOCOL 10: FORMATION DISULFIDE BRIDGES USING OXIDATIVE FOLDING IN REDOX BUFFER

1. Dissolve the linear peptide at a 0.05 to 0.1 mM concentration in a buffer (0.1–0.2 M Tris-HCl, pH 7.7–8.7) containing 1 mM EDTA and reduced (1–10 mM) and oxidized (0.1–1 mM) glutathione.
2. Stir the solution at 25–35°C and monitor the reaction by HPLC, normally from 16 to 48 h.
3. Lyophilize the solution after acidification with a TFA solution (pH 2.0).
4. Purify the oxidized peptide by preparative reverse phase HPLC.
5. Lyophilize the solution containing the fractions.

3.12. Side Reactions

Several residue- or sequence-dependent side reactions can occur during SPPS.

3.12.1. Diketopiperazine Formation

Diketopiperazine formation occurs at the C-terminal deprotected dipeptide stage by intramolecular cleavage of the resin ester linkage by the free amino function of the penultimate amino acid under basic conditions. This side reaction is particularly favored in Fmoc SPPS strategy as the base-induced deprotection of the Fmoc group releases a free amino group. The extent of its formation depends on the nature of the C-terminal amino acid and the type of peptide-linker ester anchor. Peptides containing proline or glycine in the C-terminal dipeptide sequence are especially

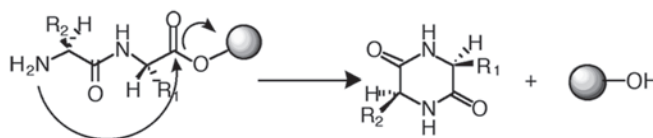


Fig. 9. DKP formation.

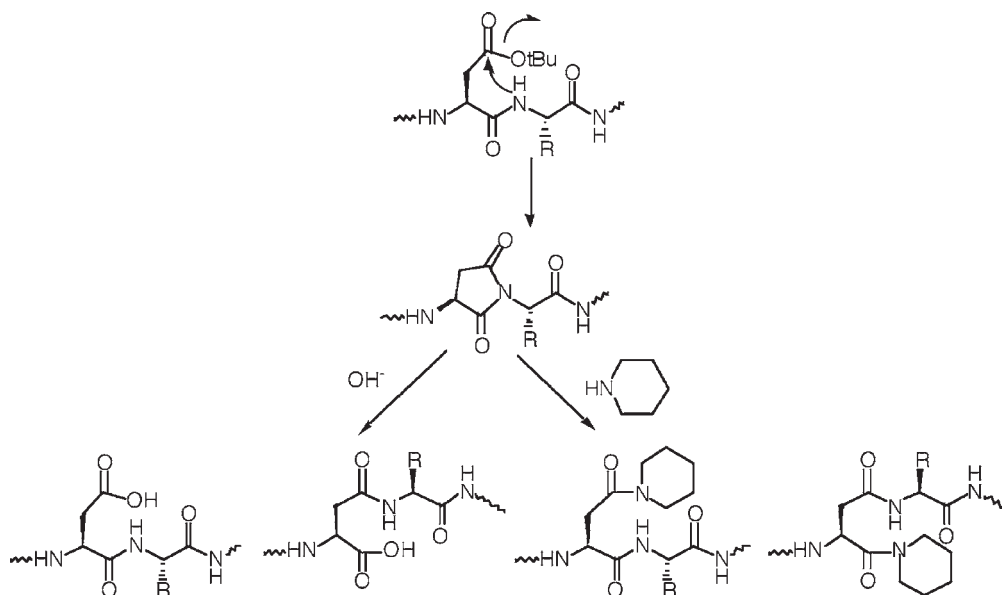


Fig. 10. Aspartimide formation and succinimide ring re-opening in basic medium.

sensitive to DKP formation. In such cases, hindered trityl-based resins should be used to avoid its formation and consequently the loss of the C-terminal dipeptide from the resin (Fig. 9).

3.12.2. Aspartimide Formation

The cyclization of aspartic acid residues to form aspartimide is the most likely side-reaction observed in routine SPPS (Fig. 10). This is a sequence-dependent side reaction that occurs either during chain elongation or during final TFA cleavage when Asp(OtBu)-AA sequence (AA = Ala, Gly, Ser, Asn[Trt]) is present in the peptide. Hydrolysis of the aspartimide ring leads to a mixture of both α- and β-peptides. Its reaction with piperidine used for Fmoc removal also leads to the formation of α- and β-piperidides. Normally, in Fmoc based SPPS, Asp(OtBu) provides sufficient protection. However, for particular

sequences such as Asp(OtBu)-Asn(Trt) particularly sensitive to aspartimide formation, addition of HOBt to the piperidine solution or protection of the aspartyl amide bond with the 2-hydroxy-4-methoxybenzyl (Hmb) group should be considered (36).

4. Notes

1. Kaiser test. Solution A: 5% ninhydrin in ethanol (w/v); solution B: 80% phenol in ethanol (w/v); solution C: KCN in pyridine (2 mL 0.001 M KCN in 98-mL pyridine). After washings, sample a few resin beads in a small glass tube and add 2 drops of each of the above solutions. Heat to 120°C for 4–6 min. Blue resin beads indicate the presence of resin-bound free amines.
TNBS test. Solution A: 5% DIPEA in DMF (v/v); Solution B: 1% TNBS in water (w/v) commercially available from Fluka (St. Quentin-

- Fallavier, France), and 1% in DMF. Sample a few resin beads in a small glass tube, add 1 drop of each of the above solutions, and watch the sample under a microscope. The presence of resin-bound free amines is indicated within 10 min by yellow or red resin beads.
2. Polyamide-based and composite PEG-PS resin beads present a larger scope of solvent compatibility than PS beads, even allowing the use of water solutions. However, for routine peptide synthesis, solvents are the same than those used for PS-resin.
 3. Fmoc determination: (1) Weigh duplicate samples of 5- to 10-mg loaded resin in an Eppendorf tube and add 1.0 mL 20% piperidine/DMF, stir for 20 min, and centrifuge down the resin. (2) Transfer 100 μ L of the above solution to a tube containing 10 mL DMF and mix. (3) Set the spectrophotometer at 301 nm. Transfer 2 mL DMF into each of the two cells of the spectrophotometer (reference and sample cells), set spectrophotometer to zero. Empty the sample cell, transfer 2 mL of the solution to measure, check absorbance. (4) Substitution of the resin = $[101 \times (\text{Absorbance})]/[7.8 \times (\text{weight in mg})]$. Check absorbance three times at 301 nm; calculate average substitution.
 4. Reactivation of trityl resins: After swelling and washing the resin with toluene (five times), place the resin in a round-bottom flask and cover with toluene. Add freshly distilled acetyl chloride (1 mL/g resin) and fit a reflux condenser on the flask. Heat the reaction mixture at 60°C for 3 h. Allow to cool to room temperature, filter the resin on a frit, and wash six times with DCM. Load it immediately as described in **Protocol 4**.
 5. To avoid the intramolecular cyclization of N-terminal Gln peptide leading to the formation of N-terminal pyroglutamic acid peptide, it is recommended to cleave the peptide from the support before removing the N-Fmoc terminal protection. The DMF/piperidine treatment has to be performed in solution followed by concentration of the mixture. The target peptide is then precipitated by MTBE and filtered.
 6. To minimize epimerization during N-protected cysteine coupling, some coupling methods are recommended:
 - a. Preferably use a hindered or weaker base such as 2,4,6-trimethylpyridine (TMP) or 2,6-di-tert-butyl-4-(dimethylamino) pyridine (**37**).
 - b. Use 50/50 DMF/DCM coupling solvent instead of neat DMF.
 - c. Avoid preactivation.
 7. When a particularly acid-sensitive linker such as trityl is used, 50/50 DCM/acetic anhydride solution should be replaced by a 0.5 M solution of acetic anhydride and DIPEA in DMF. This will prevent premature cleavage of the linker by acetic acid released in the medium.
 8. Some linkers, such as Rink amide linker, are sold N-Fmoc protected. The first removal of the Fmoc group may require a longer deprotection time particular with highly loaded resin (>0.9 mmol/g). In these cases it should be useful to repeat **steps 2 and 3 of Protocol 7**.
 9. Longer reaction times can be required to fully deprotect bulky side-chain protecting groups (Pbf, Trt...) and especially when several protecting groups are closed to each other in the sequence. When uncompleted deprotection is detected, the partially deprotected peptide should be cleaved in solution using larger cocktail volume and/or longer reaction time.

References

1. Merrifield, R. B. (1963) Solid phase peptide synthesis. I. The synthesis of a tetrapeptide. *J. Am. Chem. Soc.* **85**, 2149–2154.
2. Bergmann, M. and Zervas, L. (1928) Über katalytische racemisation von aminosäuren und peptiden. *Biochem. Z.* **203**, 280–292.
3. Goodman, M. and Levine, L. (1964) Peptide synthesis via active esters. IV. Racemization and ring-opening reactions of optically active oxazolones. *J. Am. Chem. Soc.* **86**, 2918–2922.
4. Carpino, L. A. and Han, G. Y. (1972) 9-Fluorenylmethoxycarbonyl amino-protecting group. *J. Org. Chem.* **37**, 3404–3409.
5. For review. Lloyd-Williams, P., Giralt, E. and Albericio F. (eds.) (1997) *Chemical Approaches to the Synthesis of Peptides and Proteins*. CRC LLC, NY.

6. Czarnik, A. W. (1998) Solid-phase synthesis supports are like solvents. *Biotechnol. Bioeng. (Comb. Chem.)* **61**, 77–79.
7. Sherrington, D. C. (1998) Preparation, structure and morphology of polymer supports. *Chem. Commun.* 2275–2286.
8. Rink H. (1987) Solid-phase synthesis of protected peptide fragments using a trialkoxy-diphenyl-methylester resin. *Tetrahedron Lett.* **28**, 3787–3790.
9. Bernatowicz, M. S., Daniels, S. B. and Köster, H. (1989) A comparison of acid labile linkage agents for the synthesis of peptide C-terminal amides. *Tetrahedron Lett.* **30**, 4645–4648.
10. Sieber, P. (1987) A new acid-labile anchor group for the solid-phase synthesis of C-terminal peptide amides by the Fmoc method. *Tetrahedron Lett.* **28**, 2107–2110.
11. Wang, S.-S. (1973) p-Alkoxybenzyl alcohol resin and p-alkoxybenzyloxycarbonylhydrazide resin for solid phase synthesis of protected peptide fragments. *J. Am. Chem. Soc.* **95**, 1328–1333.
12. Mergler, M., Nyfeler, R., Tanner, R., Gosteli, J., and Grogg, P. (1988) Peptide synthesis by a combination of solid-phase and solution methods II synthesis of fully protected peptide fragments on 2-methoxy-4-alkoxy-benzyl alcohol resin. *Tetrahedron Lett.* **29**, 4009–4012.
13. Flörsheimer, A. and Riniker, B. (1991) Solid-phase synthesis of peptides with the highly acid-sensitive HMPB linker. in *Peptides 1990: Proceedings of the 21st European Peptide Symposium* (Giralt, E. and Andreu, D. eds.) ESCOM, Lieden., 131–133.
14. Barlos, K., Gatos, D., Kallitsis, J., Papaphotiu, G., Sotiriu, P., Wenqing, Y. and Schäfer, W. (1989) Darstellung geschützter peptid-fragmente unter einatz substituierter triphenylmethyl-harze. *Tetrahedron Lett.* **30**, 3943–3946.
15. Albericio, F. (2000) Orthogonal Protecting groups for N α -amino and C-terminal carboxylic functions in solid-phase peptide synthesis. *Biopolymers (Peptide Science)* **55**, 123–139.
16. Coste, J., Le Nguyen, D. and Castro, B. (1990) PyBOP[®]: A new peptide coupling reagent devoid of toxic by-product. *Tetrahedron Lett.* **31**, 205–208.
17. Knorr, R., Trzeciak, A., Bannwarth, W. and Gillissen, D. (1989). New coupling reagents in peptide chemistry. *Tetrahedron Lett.* **30**, 1927–1930.
18. Dourtoglou, V., Ziegler, J. C. and Gross, B. (1978) L'hexafluorophosphate de O-benzotriazolyl-N,N-tetramethyluronium: un réactif de couplage peptidique nouveau et efficace. *Tetrahedron Lett.* **19**, 1269–1272.
19. Carpino, L. A. (1993) 1-Hydroxy-7-azabenzotriazole. An efficient peptide coupling additive. *J. Am. Chem. Soc.* **115**, 4397–4398.
20. Carpino, L. A., El-Faham, A., Minor, C. A. and Albericio, F. (1994) Advantageous applications of azabenzotriazole (triazolopyridine)-based coupling reagents to solid-phase peptide synthesis. *J. Chem. Soc. Chem. Commun.* 201–204.
21. Story S. C. and Aldrich J. V. (1994) Side-product formation during cyclization with HBTU on a solid support. *Int. J. Pept. Protein Res.* **43**, 292–296.
22. Westall, F. C. and Robinson A. B. (1970) Solvent modification in Merrifield solid-phase peptide synthesis. *J. Org. Chem.* **35**, 2842–2844.
23. Yamashiro, D., Blake, J. and Li, C. H. (1976) The use of trifluoroethanol for improved coupling in solid-phase peptide synthesis. *Tetrahedron Letters* **17**, 1469–1472.
24. Milton, S. C. and Milton, R. C. (1990) An improved solid-phase synthesis of a difficult-sequence peptide using hexafluoro-2-propanol. *Int. J. Pept. Protein Res.* **36**, 193–196.
25. Hendrix, J. C., Halverson, K. J., Jarrett, J. T and Lansbury, P. T. (1990) A novel solvent system for solid-phase synthesis of protected peptides: the disaggregation of resin-bound antiparallel beta-sheet. *J. Org. Chem.* **55**, 4517–4518.
26. Hyde, C. B., Johnson, T. and Sheppard, R. C. (1992) Internal Aggregation during Solid Phase Peptide Synthesis. Dimethyl Sulfoxide as a Powerful Dissociating Solvent. *J. Chem. Soc. Chem. Commun.* 1573–1575.
27. Stewart, J. M. and Klis, W. A. (1990) Peptides, polypeptides and oligonucleotides. Macro-organic reagents and catalysts and biomedical applications, in *Innovation and Perspectives in solid phase synthesis and related technologies* (Epton, R., ed.); Mayflower Worldwide Ltd, Birmingham, pp. 1–9.
28. Zhang, L., Goldhammer, C., Henkel, B., Zühl, F., Panhaus, G., Jung, G. and Bayer, E. (1994) Peptides, proteins and nucleic acids. Biological and biomedical applications, in *Innovation and Perspectives in solid phase synthesis* (Epton, R., ed.); Mayflower Worldwide Ltd, Birmingham, pp. 711–716.
29. Bedford, J., Hyde C., Johnson, T., Jun, W., Owen, D., Quibell, M. and Sheppard, R. C. (1992) Amino acid structure and “difficult sequences” in solid phase peptide synthesis. *Int. J. Pept. Protein Res.* **40**, 300–307.
30. Hyde, C., Johnson, T., Owen, D., Quibell, M. and Sheppard, R. C. (1994) Some difficult sequences made easy. A study of interchain association in solid-phase peptide synthesis. *Int. J. Pept. Protein Res.* **43**, 431–440.
31. Mutter, M., Nefzi, A., Sato, T., Sun, X., Wahl, F. and Wöhr, T. (1995) Pseudo-prolines (psi Pro) for accessing “inaccessible” peptides. *Peptide Res.* **8**, 145–153.
32. Wöhr, T., Wahl, F., Nefzi, A., Rohwedder, B., Sato, T., Sun, X. and Mutter, M (1996) Pseudo-Prolines as a Solubilizing, Structure-Disrupting Protection Tech-

- nique in Peptide Synthesis. *J. Am. Chem. Soc.* **118**, 9218–9227.
33. Guichou, J. F., Patiny, L. and Mutter, M. (2002) Pseudo-prolines (Pro): direct insertion of Pro systems into cysteine containing peptides. *Tetrahedron Lett.* **43**, 4389–4390.
34. Pearson, D. A., Blanchette, M., Baker, M. L. and Guindon, C. A. (1989) Trialkylsilanes as scavengers for the trifluoroacetic acid deblocking of protecting groups in peptide synthesis. *Tetrahedron Lett.* **30**, 2739–2742.
35. Tam, J. P., Wu, C. R., Liu, W. and Zhang, J. W. (1991) Disulfide bond formation in peptides by dimethyl sulfoxide: scope and applications. *J. Am. Chem. Soc.* **113**, 6657–6662.
36. Quibell, M., Owen, D., Packman, L. C., Johnson, T. (1994) Suppression of piperidine-mediated side product formation for Asp(OBut)-containing peptides by the use of N-(2-hydroxy-4-methoxybenzyl)(Hmb) backbone amide protection. *J. Chem. Soc. Chem. Commun.* **20**, 2343–2344.
37. Han, Y., Albericio, F. and Barany, G. (1997) Occurrence and minimization of cysteine racemization during stepwise solid-phase peptide synthesis. *J. Org. Chem.* **62**, 4307–4312.

Synthesis and Biological Effects of c(Lys-Lys-Pro-Tyr-Ile-Leu-Lys-Lys-Pro-Tyr-Ile-Leu) (JMV2012), a New Analogue of Neurotensin that Crosses the Blood–Brain Barrier

Pierre Bredeloux,[†] Florine Cavelier,[‡] Isabelle Dubuc,[†] Bertrand Vivet,^{*,§} Jean Costentin,[†] and Jean Martinez^{*,‡}

CNRS FRE 2735, Unité de Neuropsychopharmacologie de la dépression, IFRMP 23, Faculté de Médecine et de Pharmacie, 22 Bd Gambetta, 76183 Rouen cedex, France, and CNRS UMR 5247, IBMM, Universités Montpellier 1 & 2, Place E. Bataillon, 34095 Montpellier, France

Received July 30, 2007

The central administration of neurotensin (NT) or of its C-terminal hexapeptide fragment NT(8-13), produces strong analgesic effects in tests evaluating acute pain. The use of NT-derived peptides as pharmaceutical agents to relief severe pain in patients could be of great interest. Unfortunately, peptides do not readily penetrate the blood–brain barrier. We have observed that the cyclic NT(8-13) analogue, c(Lys-Lys-Pro-Tyr-Ile-Leu-Lys-Lys-Pro-Tyr-Ile-Leu) (JMV2012, compound **1**), when peripherally administered to mice produced analgesic and hypothermic effects, suggesting the peptide penetrates the blood–brain barrier and functions effectively like a drug. Moreover, dimeric compounds show increased potency compared to their corresponding monomer. We present the synthesis of the cyclic dimer compound **1** (JMV2012). In mice, compound **1** induced a profound hypothermia and a potent analgesia, even when peripherally administered. Compound **1** appears to be an ideal lead compound for the development of bioactive NT analogues as novel analgesics drugs.

Introduction

Neurotensin (NT,^a pGlu-Leu-Tyr-Glu-Asn-Lys-Pro-Arg-Arg-Pro-Tyr-Ile-Leu-OH) is a tridecapeptide first isolated by Caraway and Leeman (1973)¹ from bovine hypothalami. This peptide, which fulfills the major criteria attributed to a neuro-modulator/neurotransmitter, exerts a wide range of biological actions when injected in the central nervous system, including modulation of dopamine transmissions in the nigro-striatal and mesocorticolimbic systems,² hypothermia,³ and analgesia.⁴ This last effect is of particular interest because this analgesia was shown to be more potent than morphine⁵ and principally naloxone-insensitive^{4,6,7} on a molar basis. For this reason, NT agonists might be useful as nonopioid analgesics from a therapeutic point of view.

Several receptors are involved in NT biological activity. So far, three NT receptors have been cloned and designated NTS1, NTS2, and NTS3. NTS1⁸ and NTS2^{9,10} belong to the family of G protein coupled receptors, while NTS3,¹¹ constituted by a single transmembrane domain, corresponds to the gp95/sortilin.¹² Although it was recently shown that stimulation of the NTS1 receptor was required for the full expression of NT analgesia when a thermal stimulus was used to induce

nociception,^{13–15} several studies demonstrate that NTS2 receptors are the main receptors involved in NT analgesia, independently of the nature of the nociceptive stimulus (thermal, mechanical, or chemical) used to evaluate nociception.^{15–22} The development of NT agonists able to cross the blood–brain barrier and selective for the NTS2 receptors is of significant interest as potential novel analgesic agents. In this way, the C-terminal hexapeptide fragment of NT [NT(8-13)], which corresponds to the shorter fragment of NT that maintains full biological activities²³ is an obvious lead compound for development.

Thus, peptide NT1 or “Eisai peptide”,^{24–26} a modified analogue of NT(8-13), was the first agonist able to induce biological activity, such as analgesia, hypothermia, and hypolocomotion, after systemic administration in animals.^{27,28} More recently, the group of Richelson was interested in peptidase-resistant NT agonists able to cross the blood–brain barrier and presenting high binding affinity for the NTS1 receptor. Among the different peptides they developed, NT69L was the most studied. This peptide exhibits high affinity for the neurotensin receptor (0.82 nM for the rat NTS1; 1.55 nM for the human NTS1; 2.1 nM for the human NTS2 receptor) and induces potent analgesia and hypothermia after intraperitoneal injection in rats.²⁹

A different strategy to obtain agonist that cross the blood–brain barrier is the development of cyclic analogues. A few years ago, a structure–activity relationship study revealed that a cyclic analogue (JMV1193) comprising the minimal effective NT fragment was able to cross the blood–brain barrier.³⁰ This cyclic compound has the sequence c(Lys-Lys-Pro-Tyr-Ile-Leu) and displays an affinity in the 0.3 μ M range for mouse brain NT receptors. The i.v. administration of this compound induces the same hypothermic and analgesic effects as icv injection. However, like NT and NT(8-13), compound JMV1193 was inactivated by the endopeptidase neprilysin. It has been shown that dimeric compounds were usually able to show increased potency compared to their corresponding monomer.³¹ We then decided to synthesize the dimeric compound of Lys-Lys-Pro-

* To whom correspondence should be addressed: Phone: +33 (0)4 67 14 38 44. Fax: +33 (0)4 67 14 48 66. E-mail: martinez@univ-montp1.fr.

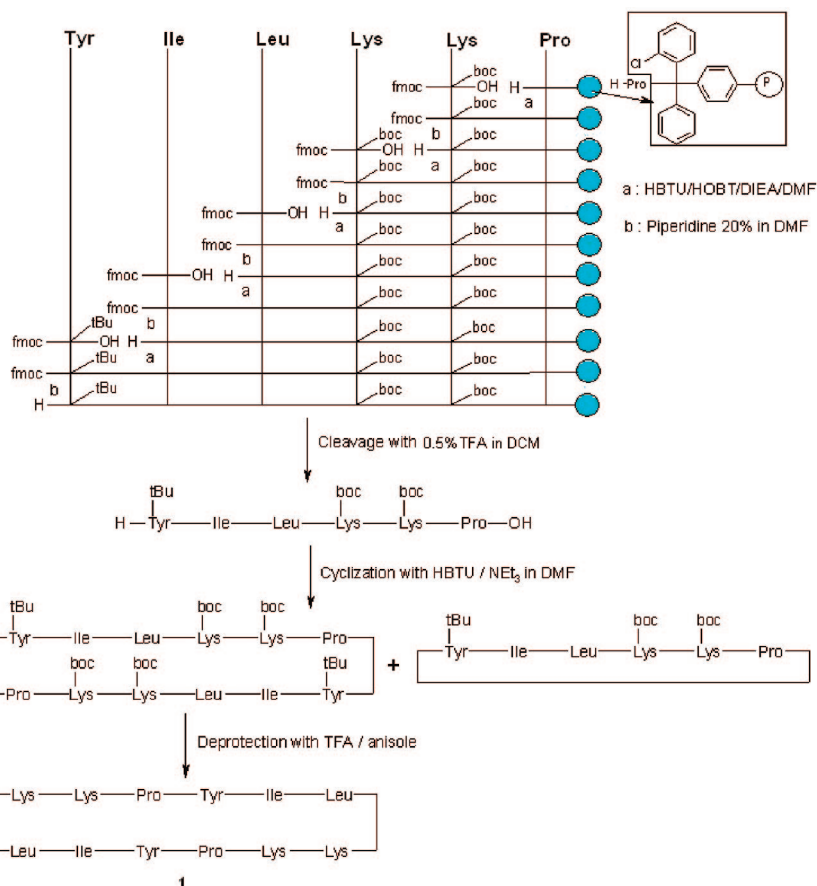
[†] CNRS FRE 2735.

[‡] CNRS UMR 5247.

[§] Present address: Sanofi-aventis, recherche & développement, 16 rue d'Ankara, 67080 Strasbourg, France.

^a Abbreviations: Boc, *N*^α-*tert*-butyloxycarbonyl; DCM, dichloromethane; DE₃₅, dose that brings the mean body temperature to 35 °C over 4 h; DIEA, diisopropylamine; DMF, dimethylformamide; DMSO, dimethylsulfoxide; ED₅₀, effective dose 50; Fmoc, 9-fluorenylmethyloxycarbonyl; HBTU, *O*-(benzotriazol-1-yl)-*N,N,N'*-tetramethyluronium hexafluorophosphate; HOBt, *N*-hydroxybenzotriazole; icv., intracerebroventricular; i.v., intravenous; NT, neurotensin; NTS1, neurotensin receptor type 1; NTS2 neurotensin receptor type 2; NTS3, neurotensin receptor type 3; per os, oral route of administration; s.c., subcutaneous; tBu, *tert*-butyl; TEA, triethylamine; TFA, trifluoroacetic acid. The symbols and abbreviations are in accordance with recommendations of the IUPAC-IUB Joint Commission on Biochemical Nomenclature and Symbolism for Amino Acids and Peptides. *Biochem J.* 1984, 219, 345–373.

Scheme 1. Synthetic Procedure for Cyclic Peptide Compound 1



Tyr-Ile-Leu, maintaining the cyclic character of this molecule. We synthesized compound JMV2012 (compound **1**), c(Lys-Lys-Pro-Tyr-Ile-Leu-Lys-Lys-Pro-Tyr-Ile-Leu). The cyclization conditions were modulated to favor dimerization starting from the hexapeptide Lys-Lys-Pro-Tyr-Ile-Leu.

Initial studies performed *in vitro* showed that this peptide was able to bind to both human NTS1 and NTS2 receptors with a similar affinity close to 150 ± 100 nM. Under the same experimental conditions, NT was found to bind to the human NTS1 receptor with an affinity of 0.16 nM and to the human NTS2 receptor with an affinity of 1.10 nM. Furthermore, it has been shown that NT(8-13) binds to the rat and human NTS1 receptor with an affinity of 0.16 and 0.14 nM, respectively.³² Nevertheless, we decided to evaluate the *in vivo* activity (hypothermia and analgesia) of compound **1** after various routes of administration in mice.

In mice, compound **1** was able to induce a profound hypothermia and an NTS2-dependent analgesia in the acetic acid-induced writhing and hot plate test after *icv* injection. Consequently, compound **1** was further characterized with respect to its ability to cross the blood-brain barrier. For this purpose, we studied its ability to trigger hypothermia and analgesia observed with the help of acetic acid-induced writhing test after various routes of administration such as the intravenous (*i.v.*), subcutaneous (*s.c.*), and oral routes (*per os*) in mice.

Results

Chemistry. The linear hexapeptide precursor was synthesized by solid-phase using the 2-chlorotrityl chloride resin preloaded with proline residue (Scheme 1). The 9-fluorenylmethoxy-

Table 1. Optimization of the Cyclization Reaction

coupling reagent	base	concentration (linear peptide)	reaction time	yields ^a (mono/dimer)
HBTU (1.5 equiv)	TEA (10 equiv)	1 mmol/L	1 h 30 min	87/0%
HBTU (1.5 equiv)	TEA (10 equiv)	100 mmol/L	1 h 30 min	0/85%

^a Yields after purification on preparative HPLC.

carbonyl (Fmoc) protection was used as temporary protection of the *N*-terminal amino groups, and *N*^α-*tert*-butyloxycarbonyl (Boc) and *tert*-butyl (tBu) were used for the side-chain protections. Couplings of protected amino acids were carried out with a solution of HBTU/HOBt reagents.

The use of the 2-chlorotrityl resin, as well as of mild conditions (0.5% trifluoroacetic acid (TFA) in DCM) for cleaving the peptide from the resin, allowed the release of the protected peptide from the resin. Cyclization of the resulting protected linear hexapeptide was achieved using *O*-(benzotriazol-1-yl)-*N,N,N',N'*-tetramethyluronium hexafluorophosphate (HBTU) and triethylamine (TEA) in dimethylformamide. We modulated the cyclization conditions to favor dimerization. The linear precursor concentration was used at a high concentration to obtain the desired cyclic peptide **1** (Table 1).

Finally, the protected cyclic analogue was deprotected with TFA in the presence of anisole as scavenger. The free cyclic analogue **1** was purified by preparative reverse-phase HPLC on a C₁₈ column, and its structure was confirmed by ESI mass spectrometry. To confirm the structure of this compound, we prepared the corresponding linear dodecapeptide stepwise on the same solid support, followed by cyclization, deprotection, and purification. The cyclic compound obtained by this way

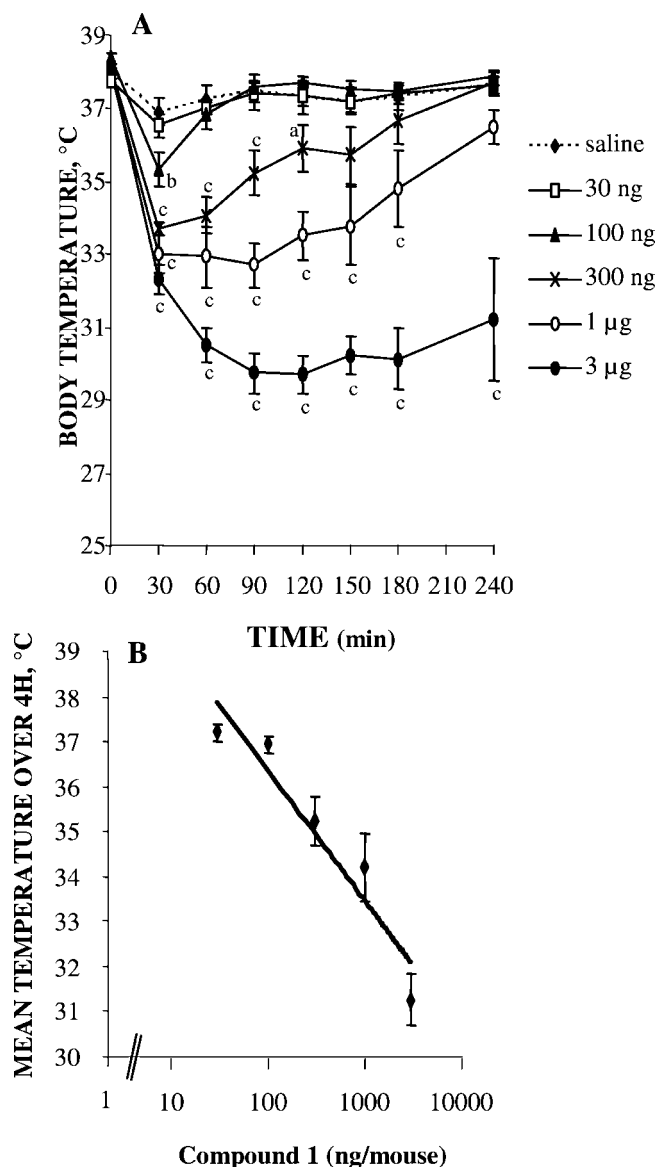


Figure 1. Time course and dose–response relationships for the hypothermic effect of icv injected compound **1** in the mouse. (A) Body temperature as a function of time after icv injections of saline or compound **1** at the indicated doses. (B) Mean body temperature over 4 h after icv injection of compound **1** at various doses. $M \pm SEM$ from eight mice per group; (a) $p < 0.05$, (b) $p < 0.01$, and (c) $p < 0.001$ vs saline controls.

has the same chemical and physical properties than compound **1** prepared previously.

The biological profile of the cyclic peptide was then evaluated by its ability to induce analgesic and hypothermic activities after various systemic routes of administration.

Biological Results. Effects of Compound 1 on Body Temperature and Nociception in Mice after icv Administration. In a first series of experiments, compound **1** was injected icv for studying its ability to trigger hypothermia and analgesia in mice.

Hypothermia. The two-way repeated measures analysis of variance performed on the results of this experience indicates a statistically significant interaction between the different doses of compound **1** icv administered and the different time of the measure ($F(35,238) = 16.699$; $p < 0.001$). Thus, compound **1** icv administered between the dose of 30 ng and 3 µg reduced dose and time-dependent mice body temperature (Figure 1A).

This hypothermia was significant from the dose of 100 ng at 30 min postinjection ($p = 0.006$ vs saline). At the highest tested dose (3 µg), a profound hypothermia occurred with a maximal effect at 90 min postinjection ($p < 0.001$ vs saline). This hypothermia was prolonged because at 4 h postinjection the body temperature of mice treated with compound **1** (3 µg) remained significantly lower than that of the saline controls ($p < 0.001$). To integrate the intensity of the hypothermia and its duration into one parameter, the mean body temperature over 4 h was calculated as the area under the time–response curve for each mouse over a period of 240 min (4 h) divided by 240 min (Figure 1B). From this dose–response curve, we determined that the ED_{35} for compound **1** (dose of compound **1** that brings the mean body temperature to 35 °C over 4 h) was 300 ng. Moreover, this hypothermia was not potentiated by the mixed multipetidase inhibitor JMV390-1 (data not shown), indicating that compound **1** is resistant to the major NN/NT degrading enzymes, such as aminopeptidase N and endopeptidases 24.11, 24.15, and 24.16.^{33,34}

Nociception. In the hot plate test, compound **1** increased dose-dependently, between 300 ng and 3 µg, latencies of both paw licking and jumping ($F(3,27) = 9.976$; $p < 0.001$ for the paw licking latency, and $F(3,24) = 7.297$; $p = 0.001$ for the jump latencies; Figure 2A,B). This result indicates that compound **1** triggers analgesia by icv administration in mice. Furthermore, the NTS2 receptor antagonist levocabastine (1350 pmol), which prevents the increase in jump latency produced by neurotensin after icv administration,¹⁸ also prevented the increase in jump latency induced by compound **1** (300 ng; interaction [levocabastine \times compound **1**]: $F(1,22) = 5.201$; $p = 0.035$). As it was already demonstrated for neurotensin,¹⁸ these data clearly established that NTS2 receptors are involved in the analgesic effect developed by compound **1** (Figure 2C).

Compound **1** was also tested in the writhing test. This test is more sensitive than the hot plate test. In the writhing test, compound **1**, injected 20 min before testing, reduced dose-dependently the number of writhes produced by acetic acid injection in mice ($F(3,37) = 9.740$; $p < 0.001$) from the dose of 30 ng ($p = 0.001$ vs saline; Figure 3). In this experiment, the ED_{50} was below this dose of 30 ng.

This test was then used for the evaluation of the analgesic activity of compound **1** by the other route of administration.

Effects of Compound 1 on Body Temperature and Nociception in Mice after i.v. Administration. Considering that compound **1** induced hypothermia and analgesia after icv administration, we have evaluated its ability to produce hypothermia and analgesia after i.v. administration.

With regard to hypothermia, the two-way repeated measures analysis of variance performed on the results of this experience indicates a significant interaction between the different doses of i.v. administered compound **1** and the different times of the measure ($F(12,114) = 19.236$; $p < 0.001$), thus, compound **1**, i.v. administered at the dose of 1 and 3 mg/kg, induced a dose and time-dependent hypothermia that lasted at least 60 min, with a maximal effect at 30 min postinjection (Figure 4).

Compound **1** produced a strong analgesic effect by i.v. administration ($F(3,42) = 7.914$; $p < 0.001$) in the writhing test from the dose of 0.3 mg/kg ($p = 0.042$ vs saline). Furthermore, at the dose of 1 mg/kg, compound **1** was close to abolish writhing in mice ($p = 0.001$ vs saline; Figure 5A).

Finally, at the dose of 0.3 mg/kg, the two-way analysis of variance indicates that compound **1**, by i.v. administration, induced a dose- and time-dependent analgesia ($F(3,78) = 4.529$; $p = 0.006$). This analgesia was still evident for 60 min (Figure

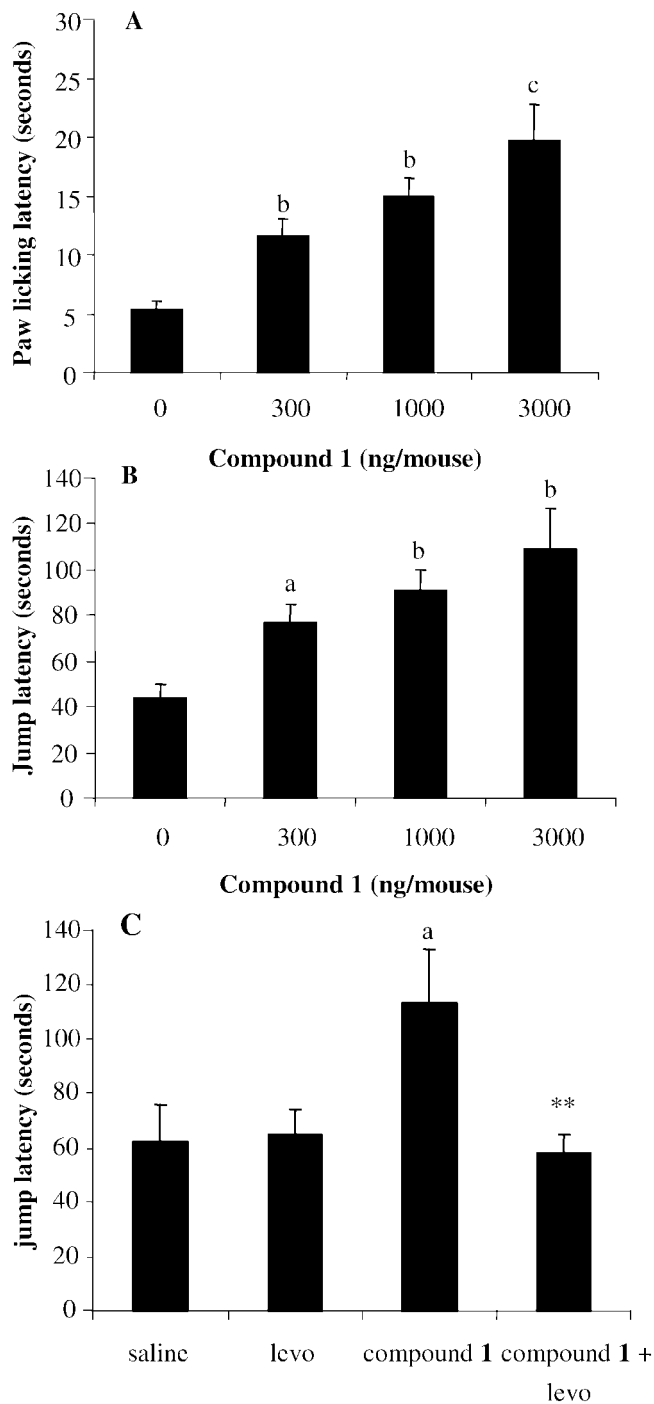


Figure 2. Dose–response relationships for the analgesic effect of icv injected compound **1** in the hot plate test. Mice were icv injected with compound **1** at various indicated doses 20 min before being placed on the hot plate at 55 °C. (A) Dose–response relationship for the paw licking latency. (B) Dose–response relationship for the jump latency. $M \pm SEM$ from 6 to 9 mice per group; (a) $p < 0.05$, (b) $p < 0.01$, and (c) $p < 0.001$ vs saline controls. (C) Effect of icv injected levocabastine on the increase in jump latency produced by icv injected compound **1**. Mice were icv injected with saline, compound **1** (300 ng), levocabastine (1350 pmol), or with a coadministration of compound **1** (300 ng) and levocabastine (1350 pmol) 20 min before being placed on the hot plate at 55 °C. $M \pm SEM$ from 6 to 8 mice per group; (a) $p < 0.05$ vs saline controls; $**p < 0.01$ vs compound **1** alone.

5B). These data indicate that compound **1** was able to cross the blood–brain barrier.

Effects of Compound 1 on Body Temperature and Nociception after s.c. Administration in Mice. The ability of

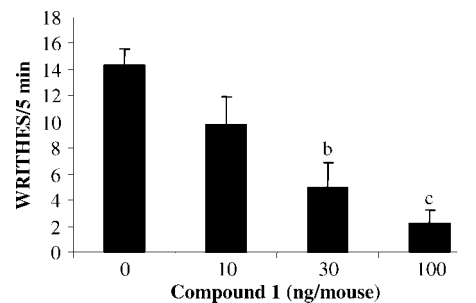


Figure 3. Dose–response relationships for the analgesic effect of icv injected compound **1** in the writhing test. Mice were icv injected with compound **1** at various indicated doses 15 min before receiving acetic acid solution 0.5% (i.p.). Mice were then placed individually in large beakers and the stretches were counted over a 5 min period 5 min after the acetic acid solution injection. $M \pm SEM$ from 8 to 14 mice per group; (b) $p < 0.01$ and (c) $p < 0.001$ vs saline controls.

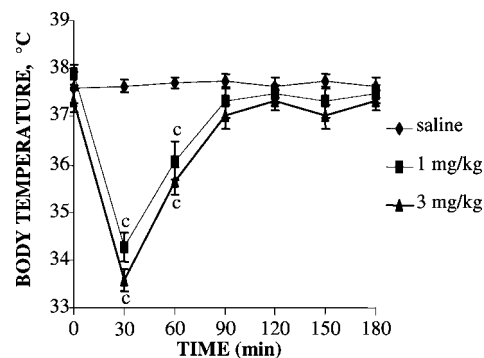


Figure 4. Time course for the hypothermic effect of i.v. injected compound **1** at various doses in the mouse. $M \pm SEM$ from 6 to 8 mice per group; (c) $p < 0.001$ vs saline controls.

compound **1** to induce hypothermia and analgesia in mice was also tested after s.c. administration.

Compound **1**, s.c. administered, produced a time- and dose-dependent hypothermia (interaction [dose \times time]: $F(24,272) = 7.647$; $p < 0.001$) with a maximal effect reached for each tested dose at 30 min postinjection (Figure 6A). This hypothermic effect lasted between 30 and 45 min for the doses of 1 and 3 mg/kg, whereas at the highest tested dose of 10 mg/kg, this hypothermia was more pronounced and still significant for more than 3 h (Figure 6A).

In the writhing test, compound **1**, between the doses of 1 and 10 mg/kg, reduces dose-dependently the number of writhes ($F(3,22) = 16.465$; $p < 0.001$) at the dose of 3 mg/kg ($p < 0.001$ vs saline; Figure 6B).

Effects of Compound 1 on Nociception after Administration per os in Mice. After oral administration, compound **1** administered at the dose of 30 mg/kg reduced significantly the number of writhes induced by the i.p. injection of an acetic acid solution (Figure 7).

Conclusion

This paper presents the synthesis and the pharmacological evaluation of a new cyclic dimeric NT derivative. This compound, c(Tyr-Ile-Leu-Lys-Lys-pro-Tyr-Ile-Leu-Lys-Lys-Pro) (**1**), exhibited analgesic and hypothermic activities after icv., i.v., s.c., and per os administration. These data suggest that this peptide, owing to its cyclic structure, resists to the NT degrading enzymes and crosses the blood–brain barrier. Moreover, the ability of levocabastine to inhibit the analgesic activity

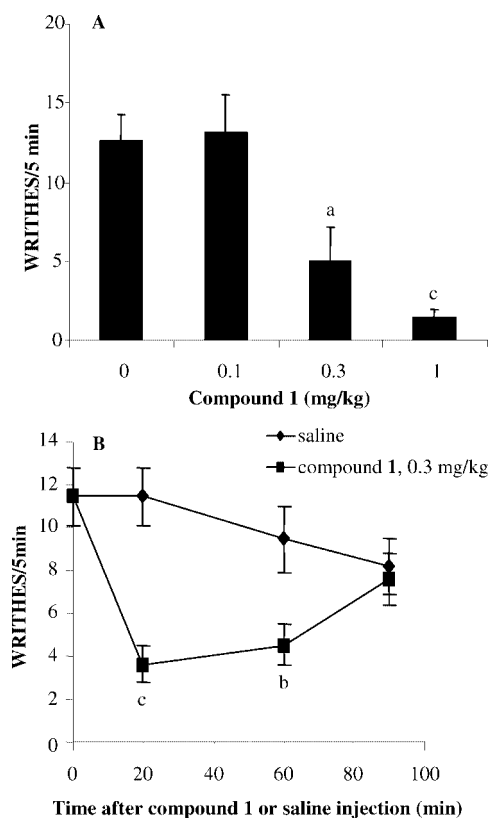


Figure 5. Dose–response and time–course relationships for the analgesic effect of i.v. injected compound **1** in the writhing test. (A) Dose–response relationships for the analgesic effect of i.v. injected compound **1** in the writhing test. Mice were i.v. injected with compound **1** at various indicated doses 15 min before receiving acetic acid solution 0.5% (i.p.). Mice were then placed individually in large beakers and the stretches were counted over a 5 min period 5 min after the acetic acid solution injection. (B) Time–course for the analgesic effect of i.v. injected compound **1** (0.3 mg/kg) in the writhing test. $M \pm SEM$ from 8 to 18 mice per group; (a) $p < 0.05$, (b) $p < 0.01$, and (c) $p < 0.001$ vs saline controls.

of compound **1** in the hot plate test also suggests that compound **1** behaves like an agonist of the NTS2 receptors. However, compound **1** probably triggers other NT receptors because it produces hypothermia in mice, a NT effect independent of the NTS2 receptors stimulation. In conclusion, compound **1** appears at this stage to be an ideal lead compound for the development of bioactive cyclic dimer more selective for the NTS2 receptors as novel analgesic drugs.

Experimental Section

The starting 2-chlorotrityl chloride resin preloaded with proline residue was purchased from Novabiochem; Fmoc-amino acids were obtained from Bachem.

HBTU, HOBt, DIEA, TEA, and piperidine were purchased from Aldrich. Water was obtained from Milli-Q plus system (Millipore), and acetonitrile and trifluoroacetic acid (TFA) were obtained from Merck. Mass spectra were obtained by electron spray ionization (ESI-MS) on a Micromass Platform II quadrupole mass spectrometer (Micromass) fitted with an electrospray source coupled with an HPLC Waters. HPLC runs were performed on Waters equipment, using columns packed with Nucleosil 100 Å, 5 μm , C18 particles, unless otherwise stated. The analytical column (250 \times 4.6 mm) operated at 1 mL/min, with a photodiode array detector 996, wavelength 214 nm. Solvent A consisted of 0.1% TFA in H_2O , and solvent B consisted of 0.1% TFA in acetonitrile. After lyophilisation, the product was stored at -20°C .

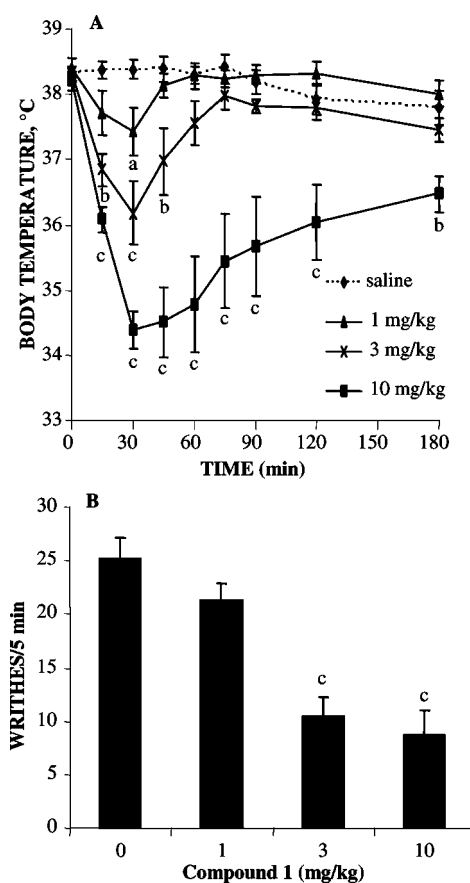


Figure 6. Time–course for the hypothermic effect of s.c. injected compound **1** and dose–response relationship for the analgesic effect of s.c. injected compound **1** in the writhing test. (A) Body temperature as a function of time after s.c. injections of saline or compound **1** at the indicated doses. $M \pm SEM$ from 8 to 10 mice per group. (B) Dose–response relationships for the analgesic effect of s.c. injected compound **1** in the writhing test. Mice were s.c. injected with compound **1** at various indicated doses 15 min before receiving acetic acid solution 0.5% (i.p.). Mice were then placed individually in large beakers and the stretches were counted over a 5 min period 5 min after the acetic acid solution injection. $M \pm SEM$ from 6 to 8 mice per group; (a) $p < 0.05$, (b) $p < 0.01$, and (c) $p < 0.001$ vs saline controls.

Preparative HPLC was performed on a Waters Delta-Prep 4000 chromatography equipped with a Waters 486 UV detector with detection at 214 nm, using a Delta-Pak C18 column (40 \times 100 mm, 15 μm , 100 Å) at a flow rate of 50 mL/min of a binary eluent system of A/B (A: H_2O , TFA 0.1%; B: CH_3CN , TFA 0.1%).

Synthesis of Protected Linear Peptide. The linear hexapeptide was synthesized by the solid-phase method on a Perkin-Elmer ABI433A automatic synthesizer on a 0.25 mmol scale with Pre-preloaded 2-chlorotrityl chloride resin (loading 0.56 mmol/g, 446 mg). The coupling reagent was a 0.45 M solution of HBTU/HOBt (2 mL). Four times excess of amino acid was used in coupling (1 mmol). Deprotection cycles were carried out in piperidine/DMF (20/80, 5 mL) and monitored by conductivity. Elongation was performed by single 30 min couplings in DMF (15 mL) with DIEA (2 M, 1 mL) as base. Washings were carried out with DMF (3 \times 15 mL) and DCM (1 \times 15 mL). Final cleavage was carried out with 0.5% TFA in DCM for 15 min (10 mL). The resin was washed extensively with DCM, then dried in vacuo, dissolved in an acetonitrile–water mixture (5/5, 10 mL), and freeze-dried. The side chain protected intermediate peptide was obtained in 89% yield (247 mg of TFA salt). $t_R = 18.4$ min (20–50% B, 30 min, C18). ES-MS $[M + H]^+$ 1017.4.

Cyclization of Protected Peptide. The resulting protected linear hexapeptide (220 mg, 0.22 mmol) was allowed to cyclize for 90 min at high concentration in DMF (2.2 mL), with HBTU (125 mg,

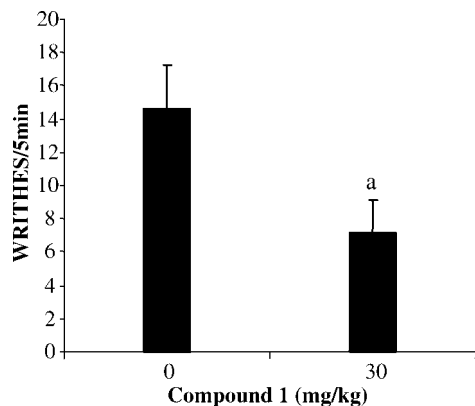


Figure 7. Analgesic effect of compound **1** administered at the dose of 30 mg/kg per os in the writhing test. Mice were treated with compound **1** 15 min before receiving acetic acid solution 0.5% (i.p.). Mice were then placed individually in large beakers and the stretches were counted over a 5 min period 5 min after the acetic acid solution injection. $M \pm SEM$ from 10 mice per group; (a) $p < 0.05$ vs saline controls.

0.33 mmol) as coupling reagent and TEA (300 μ L, 2.20 mmol) as base (Table 1). After concentration under reduced pressure, the residue was dissolved in ethyl acetate (6 mL) and then successively washed (3×1.5 mL) with 1 M aqueous solution of KH_2PO_4 , saturated NaCl aqueous solution, saturated $NaHCO_3$ aqueous solution, and water. The ethyl acetate phase was dried over $MgSO_4$, filtered off, then concentrated under reduced pressure to afford a colorless oil, which precipitated from ether/hexane (1/5) to afford a white solid (92% yield, 195 mg).

Preparation of Free Cyclic Peptide. The dried residue from the cyclization reaction (150 mg, 0.15 mmol) was dissolved in a mixture TFA/anisole (8/2, 2 mL) and stirred for 30 min. The reaction mixture was evaporated under reduced pressure and then coevaporated several times with hexane to remove residual TFA. Addition of a solution ether/hexane (1/5) allowed the peptide to precipitate as a TFA salt. The afforded solid was dried under vacuum and then purified on preparative HPLC.

These conditions afforded the expected cyclic dimer (**1**) in 85% yield, after purification. $t_R = 18.1$ min (20–50% B, 30 min, C18). ES-MS $[M + H]^+$ 1485.9.

Animals. Male Swiss albino mice (CD1, Charles River, L'Arbresle, France) weighing 20–22 g were obtained at least one week before the beginning of the experiments. The animals were housed in a room maintained at a constant temperature (21 ± 1 °C), with a regular light cycle (light on between 7 a.m. and 7 p.m.). Food and water were freely available, except at the time of testing. This study was performed in accordance with the guidelines published in the NIH Guide for the Care and Use of Laboratory Animals (National Institutes of Health No. 85-23, revised 1985), and the principles were presented in the European Communities Council Directive of 24 November 1986 (86/609/EEC).

Drugs and Solutions. c(Tyr-Ile-Leu-Lys-Lys-Pro-Tyr-Ile-Leu-Lys-Lys-Pro) **1** was dissolved in saline. Levocabastine (a generous gift from Janssen-Cilag laboratory, Beerse, Belgium) was dissolved in dimethylsulfoxide (DMSO) and cremophor EL and then diluted with saline to a final concentration of 5% DMSO and 5% cremophor.

Compound **1** was injected in mice intravenously (i.v.), subcutaneously (s.c.), and by a gastric canula (per os) in a volume of 10 mL/kg. The intracerebroventricular injections (icv.) were performed according to the method of Haley and Mc Cormick (1957)³⁵ in a volume of 10 μ L/mouse. These protocols were approved by the Regional Ethical Committee for Animal Research (Normandy) with the following numbers: N/10-04-04-12 (intracerebroventricular injection in mouse) and N/04-05-04-23 (per os injection).

Binding Experiments. Binding potencies of compound **1** were determined in competition experiments, as described previously^{9,19}

performed with homogenates freshly prepared from COS 7 cells (0.01 mg protein per tube) expressing either the human NTS1 or NTS2. Competition experiments were carried out in 250 μ L of 50 mM Tris/HCl buffer, pH 7.5, containing 0.2% BSA and 1 mM o-phenanthroline. Homogenates, 10 μ g of protein from cells, were incubated for 30 min at 25 °C with increasing concentrations of compound **1** and ^{125}I -Tyr3-NT (100 Ci/mmol, 0.05 nM). Total, specific, and nonspecific binding were determined by using the filtration method, as described previously. It was checked that membranes from untransfected COS cells were devoid of specific ^{125}I -Tyr3-NT binding.

Analgesic Tests. Hot Plate Test. This test was derived from that of Eddy and Leimbach (1953).³⁶ A plastic cylinder (height = 20 cm, diameter = 14 cm) was used to confine the mouse to the heated surface of the plate. The plate was heated to a temperature of 55 ± 0.5 °C, using a thermoregulated water circulating pump. For each animal, the paw licking and the jump latencies were determined. To avoid injury, mice that did not respond within 240 s were removed from the hot plate. Each mouse was tested only once and sacrificed immediately thereafter. This protocol was approved by the Regional Ethical Committee for Animal Research (Normandy) with the following number: N/12-04-04-14 (hot plate test).

Writhing Test. This test was derived from that of Sigmund et al. (1957).³⁷ Mice received intraperitoneally (i.p.) a 0.5% acetic acid solution in a volume of 10 mL/kg. They were then placed individually in large beakers. The stretches were counted over a 5 min period from the fifth minute after the acetic acid solution injection. A stretch was characterized by an elongation of the body, the development of tension in the abdominal muscles, and the extension of the forelimbs. This protocol was approved by the Regional Ethical Committee for Animal Research (Normandy) with the following number: N/01-05-04-20 (writhing test).

Body Temperature. Colonic temperature was measured with a thermistor probe (Thermalert TH-5, Physitemp, NJ, U.S.A.) introduced to a depth of 2 cm into the rectum. This protocol was approved by the Regional Ethical Committee for Animal Research (Normandy) with the following number: N/16-04-04-18 (measurement of colonic temperature in rat and mouse).

Statistical Analysis. The data were expressed as means \pm SEM. Results were analyzed using one-way analysis of variance or two-way analysis of variance, when appropriate, followed by Student Newman Keul's comparisons. Comparisons between two groups were analyzed by Student's *t*-test. For the study of the hypothermic effect of compound **1**, statistical analysis was performed using a two-way repeated measures followed by a Student Newman Keul's test. A *p*-value of <0.05 was considered significant, and statistical analyses were performed with SigmaStat (SPSS Inc., Chicago, IL, U.S.A.).

Acknowledgment. This work was supported by a grant from the Société Française de Pharmacologie et de Thérapeutique.

Supporting Information Available: Mass spectrometry and HPLC tracing for compound **1**. This material is available free of charge via the Internet at the <http://pubs.acs.org>.

References

- (1) Carraway, R.; Leeman, S. E. The isolation of a new hypotensive peptide, neurotensin, from bovine hypothalamus. *J. Biol. Chem.* **1973**, *248*, 6854–6861.
- (2) Kalivas, P. W.; Richardson-Carlson, R.; Duffy, P. Neuromedin N mimics the actions of neurotensin in the ventral tegmental area but not in the nucleus accumbens. *J. Pharmacol. Exp. Ther.* **1986**, *238*, 1126–1131.
- (3) Dubuc, I.; Nouel, D.; Coquerel, A.; Menard, J. F.; Kitabgi, P.; Costentin, J. Hypothermic effect of neuromedin N in mice and its potentiation by peptidase inhibitors. *Eur. J. Pharmacol.* **1988**, *151*, 117–121.
- (4) Coquerel, A.; Dubuc, I.; Kitabgi, P.; Costentin, J. Potentiation by thiophan and bestatin of the naloxone-insensitive analgesic effects of neurotensin and neuromedin N. *Neurochem. Int.* **1988**, *12*, 361–366.

- (5) Nemeroff, C. B.; Osbahr, A. J.; Manberg, P. J.; Ervin, G. N.; Prange, A. J., Jr. Alterations in nociception and body temperature after intracisternal administration of neurotensin, β -endorphin, other endogenous peptides, and morphine. *Proc. Natl. Acad. Sci. U.S.A.* **1979**, *76*, 5368–5371.
- (6) Clineschmidt, B. V.; McGuffin, J. C.; Bunting, P. B. Neurotensin: Antinociceptive action in rodents. *Eur. J. Pharmacol.* **1979**, *54*, 129–139.
- (7) Osbahr, A. J.; Nemeroff, C. B.; Luttinger, D.; Mason, G. A.; Prange, A. J., Jr. Neurotensin-induced antinociception in mice: Antagonism by thyrotropin-releasing hormone. *J. Pharmacol. Exp. Ther.* **1981**, *217*, 645–651.
- (8) Tanaka, K.; Masu, M.; Nakanishi, S. Structure and functional expression of the rat neurotensin receptor. *Neuron*. **1990**, *4*, 847–854.
- (9) Mazella, J.; Botto, J.M.; Guillemare, E.; Coppola, T.; Sarret, P.; Vincent, J. P. Structure, functional expression and cerebral localization of levocabastine-sensitive neurotensin/neuromedin N receptor from mouse brain. *J. Neurosci.* **1996**, *16*, 5613–5620.
- (10) Chalou, P.; Vita, N.; Kaghad, M.; Guillemot, M.; Bonnin, J.; Delpech, B.; Le Fur, G.; Ferrara, P.; Caput, D. Molecular cloning of a levocabastine-sensitive neurotensin site. *FEBS Lett.* **1996**, *386*, 91–94.
- (11) Mazella, J.; Zsürger, N.; Navarro, V.; Chabry, J.; Kaghad, M.; Caput, D.; Ferrara, P.; Vita, N.; Gully, D.; Maffrand, J. P.; Vincent, J. P. The 100 kDa neurotensin receptor is gp95/sortilin, a non-G-protein-coupled receptor. *J. Biol. Chem.* **1988**, *273*, 26273–26276.
- (12) Petersen, C. M.; Nielsen, M. S.; Nykjaer, A.; Jacobsen, L.; Tommerup, N.; Rasmussen, H. H.; Roigaard, H.; Gliemann, J.; Madsen, P.; Moestrup, S. K. Molecular identification of a novel candidate sorting receptor purified from human brain by receptor-associated protein affinity chromatography. *J. Biol. Chem.* **1997**, *272*, 3599–3605.
- (13) Pettibone, D. J.; Hess, J. F.; Hey, P. J.; Jacobson, M. A.; Leviten, M.; Lis, E. V.; Mallorga, P. J.; Pascarella, D. M.; Snyder, M. A.; Williams, J. B.; Zeng, Z. The effects of deleting the mouse neurotensin receptor NTS1: Central and peripheral responses to neurotensin. *J. Pharmacol. Exp. Ther.* **2002**, *300*, 305–313.
- (14) Buhler, A. V.; Choi, J.; Proudfit, H. K.; Gebhart, G. F. Neurotensin activation of the NTR1 on spinally-projecting serotonergic neurons in the rostral ventromedial medulla is antinociceptive. *Pain* **2005**, *114*, 285–294.
- (15) Sarret, P.; Esdaile, M. J.; Perron, A.; Martinez, J.; Stroth, T.; Beaudet, A. Potent spinal analgesia elicited through stimulation of NTS2 receptors. *J. Neurosci.* **2005**, *25*, 8188–8196.
- (16) Dubuc, I.; Costentin, J.; Terranova, J. P.; Barrouin, M. C.; Soubrié, P.; Le Fur, G.; Rostène, W.; Kitabgi, P. The nonpeptide neurotensin, SR48692, used as a tool to reveal putative neurotensin receptors subtypes. *Br. J. Pharmacol.* **1994**, *112*, 352–354.
- (17) Tyler, B. M.; Groshan, K.; Cusack, B.; Richelson, E. In vivo studies with low doses of levocabastine and diphenhydramine, but not pyrilamine, antagonize neurotensin-mediated antinociception. *Brain Res.* **1998**, *787*, 78–84.
- (18) Dubuc, I.; Remande, S.; Costentin, J. The partial agonist properties of levocabastine in neurotensin-induced analgesia. *Eur. J. Pharmacol.* **1999**, *381*, 9–12.
- (19) Dubuc, I.; Sarret, P.; Labbé-Jullié, C.; Botto, J. M.; Honoré, E.; Bourdel, E.; Martinez, J.; Costentin, J.; Vincent, J. P.; Kitabgi, P.; Mazella, J. Identification of the receptor subtype involved in the analgesic effect of neurotensin. *J. Neurosci.* **1999**, *19*, 503–510.
- (20) Remaury, A.; Vita, N.; Gendreau, S.; Jung, M.; Arnone, M.; Poncelet, M.; Culoussou, J. M.; Le Fur, G.; Soubrié, P.; Caput, D.; Shire, D.; Kopf, M.; Ferrara, P. Targeted inactivation of the neurotensin type 1 receptor reveals its role in body temperature control and feeding behavior but not in analgesia. *Brain Res.* **2002**, *953*, 63–72.
- (21) Yamauchi, R.; Sonoda, S.; Jinsmaa, Y.; Yoshikawa, M. Antinociception induced by β -lactotensin, a neurotensin agonist derived from β -lactoglobulin, is mediated by NT2 and D1 receptors. *Life Sci.* **2003**, *73*, 1917–1923.
- (22) Bredeloux, P.; Costentin, J.; Dubuc, I. Interactions between NTS2 and opioid receptors on two nociceptive responses assessed on the hot plate test in mice. *Behav. Brain Res.* **2006**, *175*, 399–407.
- (23) Carraway, R.; Leeman, S. E. The amino-acid sequence of a hypothalamic peptide, neurotensin. *J. Biol. Chem.* **1975**, *250*, 1907–1911.
- (24) Tokumura, T.; Tanaka, T.; Sasaki, A.; Tsuchiya, Y.; Abe, K.; Machida, R. Stability of a novel hexapeptide, (Me)Arg-Lys-Pro-Trp-tert-Leu-Leu-OEt, with neurotensin activity, in aqueous solution and in the solid state. *Chem. Pharm. Bull. (Tokyo)* **1990**, *38*, 3094–3098.
- (25) Machida, R.; Tokumura, T.; Sasaki, A.; Tsuchiya, Y.; Abe, K. High-performance liquid chromatographic determination of (Me)Arg-Lys-Pro-Trp-tert-Leu-Leu in plasma. *J. Chromatogr.* **1990**, *534*, 190–195.
- (26) Machida, R.; Tokumura, T.; Tsuchiya, Y.; Sasaki, A.; Abe, K. Pharmacokinetics of novel hexapeptides with neurotensin activity in rats. *Biol. Pharm. Bull.* **1993**, *16*, 43–47.
- (27) Pugsley, T. A.; Akunne, H. C.; Whetzel, S. Z.; Demattos, S.; Corbin, A. E.; Wiley, J. N.; Wustrow, D. J.; Wise, L. D.; Heffner, T. G. Differential effects of the nonpeptide neurotensin antagonist, SR 48692, on the pharmacological effects of neurotensin agonists. *Peptides* **1995**, *16*, 37–44.
- (28) Sarhan, S.; Hitchcock, J. M.; Grauffel, C. A.; Wettstein, J. G. Comparative antipsychotic profiles of neurotensin and a related systemically active peptide agonist. *Peptides* **1997**, *18*, 1223–1227.
- (29) Tyler-McMahon, B. M.; Stewart, J. A.; Farinas, F.; McCormick, D. J.; Richelson, E. Highly potent neurotensin analog that causes hypothermia and antinociception. *Eur. J. Pharmacol.* **2000**, *390*, 107–111.
- (30) Van Kemmel, F. M.; Dubuc, I.; Bourdel, E.; Fehrentz, J. A.; Martinez, J.; Costentin, J. A C-terminal cyclic 8–13 neurotensin fragment analog appears less exposed to neprilysin when it crosses the blood brain barrier than the cerebrospinal fluid-brain barrier in mice. *Neurosci. Lett.* **1996**, *217*, 58–60.
- (31) Erez, M.; Takemori, A.; Portoghese, P. S. Narcotic antagonistic potency of bivalent ligands which contain beta-naltrexamine. Evidence for bridging between proximal recognition sites. *J. Med. Chem.* **1982**, *25*, 847–849.
- (32) Tyler, B. M.; Douglas, C. L.; Fauq, A.; Pang, Y. P.; Stewart, J. A.; Cusack, B.; McCormick, D. J.; Richelson, E. In vitro binding and CNS effects of novel neurotensin agonists that crosses the blood-brain barrier. *Neuropharmacology* **1999**, *38*, 1027–1034.
- (33) Kitabgi, P.; Dubuc, I.; Nouel, D.; Costentin, J.; Cuber, J. C.; Fulcrand, H.; Doulut, S.; Rodriguez, M.; Martinez, J. Effects of thiorphan, bestatin and a novel metallopeptidase inhibitor JMV390-1 on the recovery of neurotensin and neuromedin N released from mouse hypothalamus. *Neurosci. Lett.* **1992**, *142*, 200–204.
- (34) Doulut, S.; Dubuc, I.; Rodriguez, M.; Vecchini, F.; Fulcrand, H.; Barelli, H.; Checler, F.; Bourdel, E.; Aumelas, A.; Lallement, J. C.; et al. Synthesis and analgesic effects of *N*-[3-[(hydroxyamino)carbonyl]-1-oxo-2(*R*)-benzylpropyl]-L-isoleucyl-L-leucine, a new potent inhibitor of multiple neurotensin/neuromedin N degrading enzymes. *J. Med. Chem.* **1993**, *36*, 1369–1379.
- (35) Haley, T. J.; McCormick, W. G. Pharmacological effects produced by intracerebral injection of drugs in the conscious mouse. *Br. J. Pharmacol. Chemother.* **1957**, *12*, 12–15.
- (36) Eddy, W.; Leimbach, D. Synthetic analgesic (II) diethenylbutenyl and diethenylbutylamine. *J. Pharmacol. Exp. Ther.* **1953**, *107*, 385–393.
- (37) Sigmund, E.; Cadmus, R.; Lu, G. Methods for evaluating both non-narcotic and narcotic analgesics. *Proc. Soc. Exp. Biol. Med.* **1957**, *95*, 725–739.

JM700925K

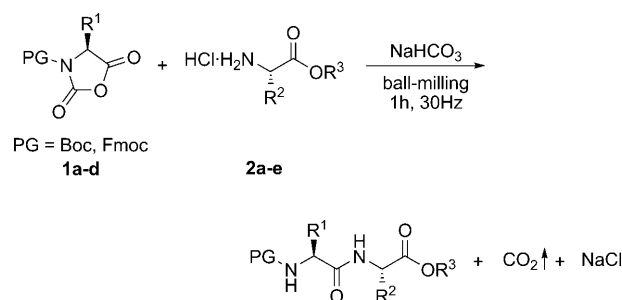
Solvent-Free Synthesis of Peptides**

Valérie Declerck, Pierrick Nun, Jean Martinez, and Frédéric Lamaty*

The chemistry of peptides has been continuously growing during the last few decades. Peptides are now not only considered as pharmacological tools but also as active pharmaceutical ingredients, in connection to their high therapeutic index and low toxicity.^[1] The market for therapeutic bulk peptides is expected to grow rapidly in the next few years.^[2] In spite of the well-established procedures^[3] for peptide synthesis by chemical ways, that is, stepwise synthesis in solution and solid-phase peptide synthesis, one of the major problems related to peptide preparation concerns the huge amount of solvent needed, particularly for synthesis on solid supports (2000–5000 kg for a large peptide). There is still a need to explore efficient, convenient, and environmentally friendly methods for peptide synthesis, particularly when the time for the scale-up of peptide production comes.

The field of “green chemistry” has recently grown at a rapid pace. Some major thematic areas have emerged: use of alternative feedstock and of innocuous reagents, employment of natural processes, use of substitute solvents, design of safer chemicals, development of alternative reaction conditions, and minimization of energy consumption.^[4] One particularly active area is in the use of substitute solvents such as aqueous, ionic, fluoruous, or supercritical fluids to replace volatile organic and chlorinated solvents and to solve the problems of treating or recycling solvent waste.^[5] An alternative approach would be to carry out chemical reactions in the absence of solvent.^[6] Techniques such as mixing, grinding, or ball-milling have proved their efficiency in the field of organic chemistry in the solid state.^[7] We report herein a new strategy for the preparation of peptides under solvent-free conditions by using ball-milling technology.^[8] This strategy has been exemplified by the synthesis of the sweetener dipeptide H–Asp–Phe–OMe (aspartame).

We have studied the coupling of urethane-protected α -amino acid *N*-carboxyanhydride (UNCA) derivatives **1** with α -amino acids, amides, or esters, while keeping in mind that all of these compounds have to remain in the solid state under the ball-milling conditions^[9] (Scheme 1). UNCAs are



Scheme 1. Synthesis of dipeptides under solvent-free conditions. Boc: *tert*-butoxycarbonyl; Fmoc: 9-fluorenylmethoxycarbonyl; PG: protecting group.

activated forms of amino acids that have proved to be useful in peptide^[10] and organic synthesis.^[11]

The reaction was tested for the coupling of Boc–Val–NCA (**1a**, 1 equiv) with HCl·H–Leu–OMe (**2a**, 1 equiv) in the presence of NaHCO₃ (1.5 equiv) in a hardened-steel vessel with steel balls. The vessel was agitated for 1 h at a frequency of 30 Hz. Analysis of the reaction mixture after this time showed the exclusive presence of the dipeptide Boc–Val–Leu–OMe, obtained in quantitative yield. To our knowledge, this represents the first example of peptide bond formation in solvent-free conditions. The results obtained with various UNCAs and amino acid derivatives are presented in Table 1.

The various UNCA derivatives do not present the same reactivity profile. Boc–Val–NCA (**1a**) reacted quantitatively with amino acid derivatives to yield the corresponding dipeptides (Table 1, entries 1–5) whereas Fmoc–Val–NCA (**1b**) gave lower conversions (Table 1, entries 6, 7, 9, and 10), except when coupling with HCl·H–Ala–OMe (**2c**; Table 1, entry 8). Excellent conversions and yields were achieved with Boc–Phe–NCA (**1c**; Table 1, entries 12–14), except for the reaction with HCl·H–Phe–OMe (Table 1, entry 15). Recovery of the product from the reaction vessel was less efficient in some cases and resulted in inferior yields (Table 1, entries 12 and 14). An amino ester, AcOH·H–Gly–OtBu was also tested and gave satisfying results (Table 1, entry 16). By contrast, the free amino acid did not react. It is worth noting that better results were obtained with freshly prepared starting materials. By reaching the maximum capacity of the ball-mill used in this study, up to 500 mg of dipeptides could be prepared. The reaction mixture was recovered directly from the milling jar, washed with water to remove the inorganic salts, and dried to provide the clean dipeptide. In the case of an incomplete reaction, maybe due to the physicochemical state of the reaction mixture (Table 1, entry 15), addition of water to the reaction mixture resulted in the opening of the UNCA. Insoluble in water, the protected dipeptide Boc–Phe–Phe–

[*] Dr. V. Declerck,^[‡] P. Nun, Prof. J. Martinez, Dr. F. Lamaty
Institut des Biomolécules Max Mousseron (IBMM)
UMR 5247 CNRS-UM1-UM2, Université Montpellier II
Place Eugène Bataillon, 34095 Montpellier Cedex 5 (France)
Fax: (+33) 4-6714-4866
E-mail: frederic.lamaty@univ-montp2.fr

[‡] Current address:
Laboratoire de Synthèse Organique et Méthodologie (LSOM)
ICMMO UMR 8182, Université Paris-Sud 11
15 Rue Georges Clemenceau, 91405 Orsay Cedex (France)

[**] We thank the MENRT and the CNRS for financial support.

Supporting information for this article is available on the WWW under <http://dx.doi.org/10.1002/anie.200903510>.

Table 1: Examples of dipeptides synthesized under solvent-free conditions.

Entry	UNCA	Amino ester	Dipeptide/Triptide	Conversion [%] ^[a]	Yield [%]
1	Boc-Val-NCA (1a)	HCl·H-Leu-OMe (2a)	Boc-Val-Leu-OMe	100	87
2		HCl·H-Leu-O t Bu (2b)	Boc-Val-Leu-O t Bu	97	85
3		HCl·H-Ala-OMe (2c)	Boc-Val-Ala-OMe	100	100
4		HCl·H-Ala-O t Bu (2d)	Boc-Val-Ala-O t Bu	100	100
5		HCl·H-Phe-OMe (2e)	Boc-Val-Phe-OMe	100	88
6	Fmoc-Val-NCA (1b)	HCl·H-Leu-OMe (2a)	Fmoc-Val-Leu-OMe	90	–
7		HCl·H-Leu-O t Bu (2b)	Fmoc-Val-Leu-O t Bu	92	–
8		HCl·H-Ala-OMe (2c)	Fmoc-Val-Ala-OMe	100	76
9		HCl·H-Ala-O t Bu (2d)	Fmoc-Val-Ala-O t Bu	78	–
10		HCl·H-Phe-OMe (2e)	Fmoc-Val-Phe-OMe	93	–
11	Boc-Phe-NCA (1c)	HCl·H-Leu-OMe (2a)	Boc-Phe-Leu-OMe	85	–
12		HCl·H-Leu-O t Bu (2b)	Boc-Phe-Leu-O t Bu	100	70
13		HCl·H-Ala-OMe (2c)	Boc-Phe-Ala-OMe	99	79
14		HCl·H-Ala-O t Bu (2d)	Boc-Phe-Ala-O t Bu	100	73
15		HCl·H-Phe-OMe (2e)	Boc-Phe-Phe-OMe	58	55
16		AcOH·H-Gly-O t Bu (2f)	Boc-Phe-Gly-O t Bu	100	90
17		Boc-Val-NCA (1a)	HCl·H-Ala-Gly-OMe	Boc-Val-Ala-Gly-OMe	100

[a] The reaction mixture was recovered in AcOEt and washed with water and analyzed by ¹H NMR spectroscopy. Calculated conversion numbers are given with a $\pm 2\%$ error.

OMe was recovered by filtration and drying, with an excellent yield based on the conversion (Table 1, entry 15).

We showed unambiguously that coupling occurred in the solid state in the presence of the three solids (UNCA, amino ester, and base) and not during the analysis process. For this purpose and as an example, we analyzed in detail the ball-milling of Boc-Phe-NCA (**1c**), HCl·H-Ala-OMe (**2c**), and NaHCO₃ (Table 1, entry 13). Firstly, ball-milling of the starting materials in the absence of NaHCO₃ did not yield the dipeptide Boc-Phe-Ala-OMe (analyzed by IR and solid-state ¹³C NMR spectroscopies). Furthermore, when the UNCA was ball-milled alone in the presence of NaHCO₃, the reaction did not occur, nor was degradation observed. Consequently, all three solids were necessary for the coupling reaction. Two analytical samples that did not involve any solvent were used for analysis: the starting materials and the crude reaction mixture taken directly from the ball-mill jar. Solid-state IR analysis showed the disappearance of the characteristic bands of Boc-Phe-NCA (**1c**; $\tilde{\nu}$ = 1817 and 1872 cm⁻¹) and the formation of the peptide bond (characteristic amide carbonyl bands in the solid state at $\tilde{\nu}$ = 1624 and 1655 cm⁻¹). We then used cross-polarization/magic-angle spinning (CP/MAS) ¹³C NMR analysis (Figure 1). The solid-state NMR analysis of the crude mixture, with no further treatment, clearly showed signals corresponding to the exclusive formation of the expected dipeptide, with consumption of the starting materials. The carbonyl region in Figure 1c shows the disappearance of the characteristic signal of **1c** (labeled as f in Figure 1a), which corresponds to the loss of CO₂ during the reaction. Complete conversion of the amino ester **2c** cannot be proved from Figure 1c because of overlapping of the signal, but complementary analysis (mass spectrometry) of the same sample confirmed the absence of **2c**. The dipeptide cannot be formed during this analysis because solid-state ¹³C NMR spectroscopy has shown the absence of **1c**. Again, no reaction was detected in the absence of NaHCO₃. These results establish without any ambiguity that the reaction took place in the solid state.

The reaction kinetics were studied at different frequencies (10, 20, and 30 Hz). Independently of the frequency, all reactions were completed, albeit with an expected longer reaction time at lower speeds (5 h at 10 Hz and 2.5 h at 20 Hz, compared with 1.25 h at 30 Hz). For each vibration speed, the profile showed apparent zero-order kinetics, in agreement with a solid-solid-state reaction mechanism.^[12]

The possible epimerization that could occur during the solid-solid coupling reaction was evaluated. An HPLC analysis of an authentic sample of Boc-D-Phe-L-Ala-OMe prepared under known nonracemizing conditions was compared to the HPLC profile of the dipeptide product from the reaction of **1c** and **2c**. No racemization was detected by HPLC analysis.

As a proof of concept and to show the suitability of this method for making larger peptides, we synthesized the tripeptide Boc-Val-Ala-Gly-OMe from HCl·H-Ala-Gly-OMe, which was coupled to Boc-Val-NCA (**1a**), as depicted in Scheme 2. Complete conversion and a quantitative yield of the expected tripeptide (Table 1, entry 17, and Scheme 2) were obtained, with the coupling step being performed without solvent and according to the standard procedure.

To demonstrate the application of this method, we prepared the commercially attractive dipeptide aspartame or α -L-aspartyl-L-phenylalanine methyl ester. Aspartame is a nutritive sweetener approximately 150 times sweeter than sucrose.^[13] To the best of our knowledge, aspartame had not been previously prepared by the UNCA route, either in the presence or absence of solvent.^[14]

By using the method described above, we considered the coupling of Boc-Asp(O t Bu)-NCA (**1d**) and HCl·H-Phe-OMe (**2e**). Acid-labile Boc and t Bu protecting groups were chosen because they can be simultaneously cleaved under acidic conditions.

First, UNCA **1d** was prepared according to the synthetic method depicted in Scheme 3. The key step in the preparation of **1d** was the cyclization of compound **3** by the Vilsmeier salt method (Scheme 3).^[15]

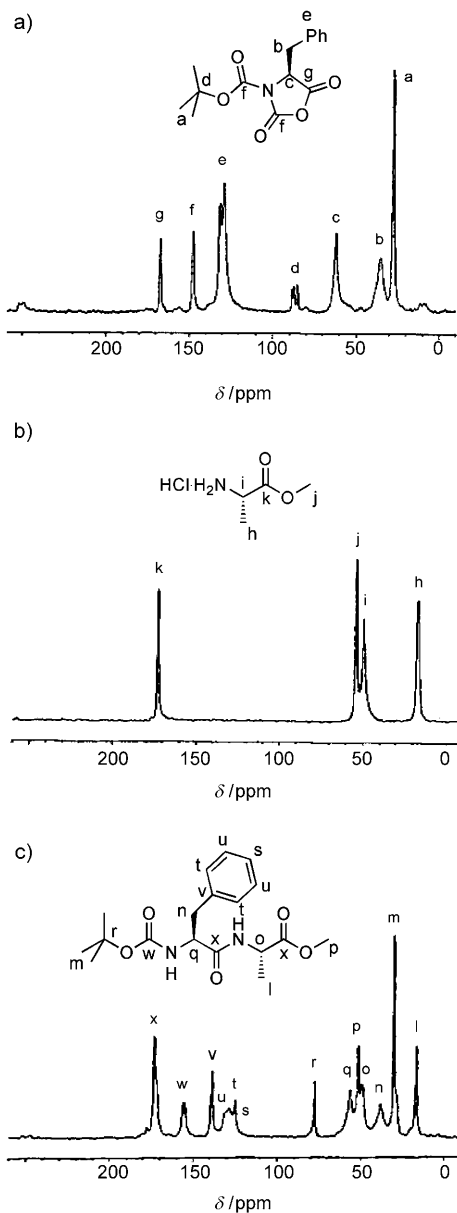
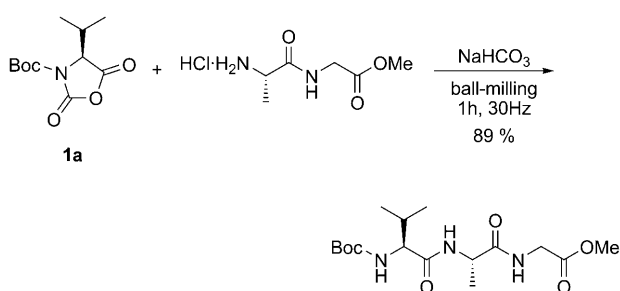
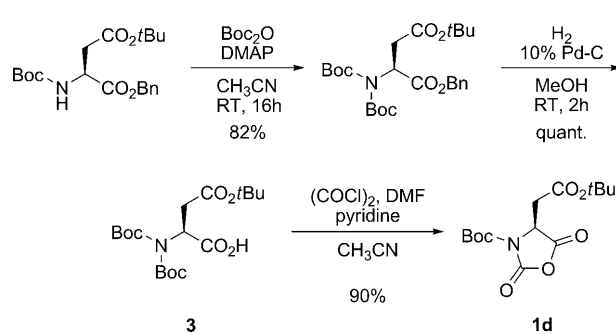


Figure 1. CP/MAS solid-state ^{13}C NMR analysis of a) Boc-Phe-NCA (**1c**), b) HCl·H₂N-Ala-OMe (**2c**), and c) crude Boc-Phe-Ala-OMe.

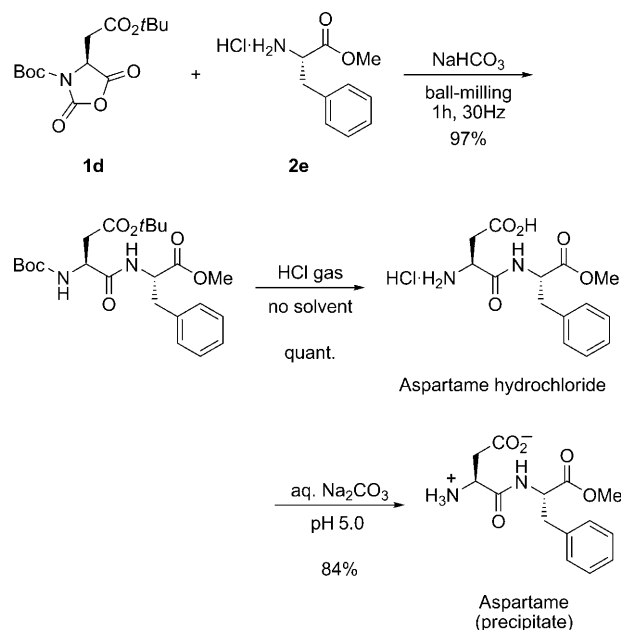


Scheme 2. Synthesis of a tripeptide under solvent-free conditions.

The procedure described above for the preparation of dipeptides was then used for the preparation of aspartame (Scheme 4). Ball-milling of Boc-Asp(O*t*Bu)-NCA (**1d**) and



Scheme 3. Synthesis of UNCA **1d**. DMAP: 4-dimethylaminopyridine; DMF: *N,N*-dimethylformamide.



Scheme 4. Synthesis of the sweetener aspartame under solvent-free conditions.

HCl·H-Phe-OMe (**2e**) for 1 h yielded the protected dipeptide as the only product, along with inorganic salts. The Boc and *t*Bu protecting groups were then cleaved under acidic conditions in a gas–solid reaction, without solvent. The protected dipeptide in solid form was placed on a fritted glass, and HCl gas was blown through for 3 h in the absence of solvent to yield the hydrochloride form of aspartame. The yield for the two steps is quantitative, and removal of the Boc and *t*Bu protecting groups under acidic conditions afforded only volatile by-products. The hydrochloride of aspartame was dissolved in water and then neutralized to the isoelectric point (pH 5.0) with an aqueous solution of Na₂CO₃.^[15] The resulting aspartame precipitated as a white powder and was filtered and dried in vacuo (84% yield).

In summary, a straightforward, high-yielding method for the preparation of peptides (including dipeptides and a tripeptide) with no epimerization and in the absence of solvent has been reported. This method involves the reaction of a UNCA with an amino ester (or amino acid amide). It was illustrated by the preparation of the aspartame sweetener.

Aspartame was obtained in pure form in three steps from Boc–Asp(OtBu)–NCA without the use of organic solvents, either for the coupling reaction or the removal of the protecting groups, and with the generation of volatile organic by-products and water-soluble inorganic salts. The only purification step consisted of a final precipitation from water to recover solid aspartame. This methodology was also exemplified by the synthesis of the tripeptide Boc–Val–Ala–Gly–OMe with good purity and excellent yield.

Received: June 29, 2009

Revised: September 8, 2009

Published online: ■ ■ ■ ■ ■, 2009



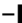



Keywords: ball-milling · peptides · peptide synthesis · solid-state reactions · solvent-free reactions

-
- [1] a) A. K. Sato, M. Viswanathan, R. B. Kent, C. R. Wood, *Curr. Opin. Biotechnol.* **2006**, *17*, 638–642; b) G. Mustata, S. M. Dinh, *Crit. Rev. Ther. Drug Carrier Syst.* **2006**, *23*, 111–135.
- [2] V. Marx, *Chem. Eng. News* **2005**, *83*, 17–24.
- [3] *Synthesis of Peptides and Peptidomimetics, Vol. E22* (Eds.: M. Goodman, A. Felix, L. Moroder, C. Toniolo), Thieme, Stuttgart, **2002**.
- [4] *Green Chemistry: Frontiers in Benign Chemical Syntheses and Processes* (Eds.: P. T. Anastas, T. C. Williamson), Oxford University Press, New York, **1999**.
- [5] J. H. Clark, S. J. Tavener, *Org. Process Res. Dev.* **2007**, *11*, 149–155.
- [6] K. Tanaka, F. Toda, *Chem. Rev.* **2000**, *100*, 1025–1074.
- [7] F. Toda, *Top. Curr. Chem.* **2005**, *254*, 1–305.
- [8] J. Martinez, F. Lamaty, V. Declerck, WO 2008125418, **2008**.
- [9] a) G. Kaupp, J. Schmeyers, J. Boy, *Tetrahedron* **2000**, *56*, 6899–6911; b) G. Kaupp, M. R. Naimi-Jamal, V. Stepanenko, *Chem. Eur. J.* **2003**, *9*, 4156–4160.
- [10] W. D. Fuller, M. Goodman, F. R. Naider, Y.-F. Zhu, *Biopolymers* **1996**, *40*, 183–205.
- [11] a) J. Hang, S.-K. Tian, L. Tang, L. Deng, *J. Am. Chem. Soc.* **2001**, *123*, 12696–12697; b) J. Hang, H. Li, L. Deng, *Org. Lett.* **2002**, *4*, 3321–3324; c) T. R. Elworthy, J. P. Dunn, J. H. Hogg, G. Lam, Y. D. Saito, T. M. P. C. Silva, D. Stefanidis, W. Woroniecki, E. Zhornisky, A. S. Zhou, K. Klumpp, *Bioorg. Med. Chem. Lett.* **2008**, *18*, 6344–6387; d) E. Dardennes, S. Labano, N. S. Simpkins, C. Wilson, *Tetrahedron Lett.* **2007**, *48*, 6380–6383; e) P. Audinn, C. Pothion, J.-A. Fehrentz, A. Loffet, J. Martinez, J. Paris, *J. Chem. Res. Synop.* **1999**, 282–283; f) P. Chevallet, J.-A. Fehrentz, K. Kiec-Kononowicz, C. Devin, J. Castel, A. Loffet, J. Martinez, *Let. Pept. Sci.* **1996**, *2*, 297–300; g) J.-A. Fehrentz, C. Genu-Dellac, M. Amblard, F. Winternitz, A. Loffet, J. Martinez, *J. Pept. Sci.* **1995**, *1*, 124–131; h) J.-A. Fehrentz, C. Pothion, J.-C. Califano, A. Loffet, J. Martinez, *Tetrahedron Lett.* **1994**, *35*, 9031–9034; i) J.-A. Fehrentz, E. Bourdel, J. C. Califano, O. Chaloin, C. Devin, P. Garrouste, A.-C. Lima-Leite, M. Llinares, F. Rieunier, J. Vizavonna, F. Winternitz, A. Loffet, J. Martinez, *Tetrahedron Lett.* **1994**, *35*, 1557–1560; j) J.-A. Fehrentz, J.-C. Califano, M. Amblard, A. Loffet, J. Martinez, *Tetrahedron Lett.* **1994**, *35*, 569–571; k) M. Mc Kiernan, J. Huck, J.-A. Fehrentz, M.-L. Roumestant, P. Viallefont, J. Martinez, *J. Org. Chem.* **2001**, *66*, 6541–6544; l) M. Paris, J.-A. Fehrentz, A. Heitz, A. Loffet, J. Martinez, *Tetrahedron Lett.* **1996**, *37*, 8489–8492; m) M. Paris, J.-A. Fehrentz, A. Heitz, J. Martinez, *Tetrahedron Lett.* **1998**, *39*, 1569–1572; n) M. Paris, C. Pothion, C. Michalak, J. Martinez, J.-A. Fehrentz, *Tetrahedron Lett.* **1998**, *39*, 6889–6890; o) C. Pothion, J.-A. Fehrentz, A. Aumelas, A. Loffet, J. Martinez, *Tetrahedron Lett.* **1996**, *37*, 1027–1030; p) C. Pothion, J.-A. Fehrentz, P. Chevallet, A. Loffet, J. Martinez, *Let. Pept. Sci.* **1997**, *4*, 241–244.
- [12] G. Kaupp, *CrystEngComm* **2003**, *5*, 117–133.
- [13] R. H. Mazur, J. M. Schlatter, A. H. Goldkamp, *J. Am. Chem. Soc.* **1969**, *91*, 2684–2691.
- [14] J. S. Tou, B. D. Vineyard, *J. Org. Chem.* **1985**, *50*, 4982–4984.
- [15] R. Mita, T. Katoh, A. Yamaguchi, T. Oura, C. Higuchi, EP 196866, **1986** [*Chem. Abstr.* **1987**, *107*, 7612].
-

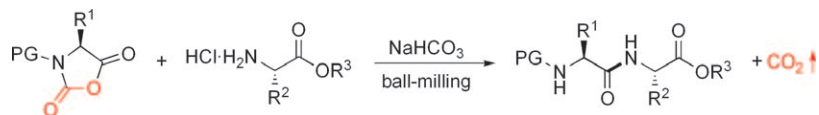
Communications



Synthetic Methods

V. Declerck, P. Nun, J. Martinez,
F. Lamaty*      

Solvent-Free Synthesis of Peptides



A crush on sweetness! The coupling of a urethane-protected *N*-carboxyanhydride of an amino acid with another amino acid derivative under ball-milling conditions gives a protected dipeptide in very high yield (see scheme; PG: protecting group).

The reaction takes place in the solid state. The synthesis was applied to the preparation of a tripeptide and the sweetener aspartame, without any organic solvent or purification.

This copy is for your personal, noncommercial use only.

Business

July 17, 2006
Volume 84, Number 29
pp. 23-25

Changing Tides

Breakthroughs in manufacturing are making large-scale synthesis of peptides a viable proposition

[Lisa M. Jarvis](#)

Though they are highly potent and generally less toxic than small-molecule pharmaceuticals, peptide-based drugs have had trouble hitting their stride. A handful of naturally occurring peptides—insulin and calcitonin to name two—are high-volume sellers, but synthetic peptides have traditionally been challenged by delivery and formulation problems, manufacturing hurdles, and cost constraints.



Roche Photo

SCALE-UP Roche scientists Chris Roberts and Rick Harrison stand in front of 1-m chromatography column used in the synthesis of Fuzeon.

Over the past several years, however, the tide has started to change. Pharmaceutical and biotechnology companies are acknowledging that the specificity and safety of peptides could allow them to address previously unattainable drug targets. Their interest in peptides coincides with technological breakthroughs that have made producing peptides, particularly longer sequences of amino acids, far more economical.

Those developments have translated into a heavier flow of peptide-based drugs through the development pipeline: At any given time, approximately 200 peptides are in clinical trials, with one to two approvals each year, according to data from peptides manufacturer [American Peptide Co.](#) Currently, more than 20 peptide-based drugs are in Phase III development, according to a study released last month by the market research firm [Drug & Market Development.](#)

The D&MD study also found that drug and biotech companies are pursuing peptides for a far wider scope of indications than previously studied. Of the 39 preclinical peptide drug candidates tracked in the study, 35 address new therapeutic targets entirely different from those of currently launched peptides. Some later stage candidates or recently launched products, in contrast, are more conveniently deliverable versions of naturally occurring peptides such as insulin.

Further evidence of heightened interest in peptides is the hefty codevelopment deal [Affymax](#) secured last month for its lead product, Hematide, a peptide that is in Phase IIb trials to treat anemia. [Takeda Pharmaceutical](#) laid out \$105 million to share U.S. rights to Hematide and will pay another \$430 million in milestones if the drug actually wins [Food & Drug Administration](#) approval.

Jane Salik, president of the contract manufacturer [PolyPeptide Laboratories](#), attributes some of the recent interest in peptides to drug company recognition that certain indications can be attacked only by a peptide or protein.

"Big Pharma has come back in a big way to peptides," Salik says. "There was a period of maybe 10 years when they were not seriously considered for new pharmaceutical indications."

Peptides had been overlooked in no small part because they have been generally administered by injection, rather than orally, and

tend to have short half-lives. "We now find more interest in peptides at big pharma companies, based on new technology in delivery and formulation," Salik adds.

Another major hindrance was cost. Peptides are made either by recombinant biotechnology or by liquid- or solid-phase synthesis, and large-scale manufacture proved economically prohibitive for some of them, particularly those composed of longer amino acid chains.

In recent years, however, a vast improvement in production economics has spurred increased use of solid-phase technology. The process, which involves building a string of amino acids off a resin support, is considered the most straightforward route to making medium- and long-chain sequences. "Over the past 10 years, cost of goods has come down dramatically," says Jim Hampton, vice president of business development at American Peptide.

Before then, recombinant technology was the only commercially viable option for a long-chain peptide drug that demanded large-scale quantities. "Ten years ago, peptides weren't as easily synthesized and scalable," Hampton says. "If you needed more than a half a kilo of product, you'd probably look at recombinant technology."

But the recombinant approach is limiting, peptide producers say, because it does not allow the introduction of unnatural amino acids. Furthermore, process development had to begin with a protracted program of selecting the right cell line to efficiently express the desired gene.

Solid-phase production, in contrast, is much more direct. "You can move into the clinic more quickly with a chemical process. We can have a few hundred grams in the clinic in four to five months, whereas with a recombinant approach it would be 18 months before that is possible," says Rodney Lax, sales and marketing director at PolyPeptide Labs.

Development speed limitations aside, recombinant manufacturing has a different set of quality issues compared with synthetic syntheses. "A synthetic universe is a known universe. You don't get anything out of it that you don't put into it," Hampton adds.

The growing prominence of solid-phase technology is driven by the need for a more economical manufacturing process to accommodate changing peptides requirements. Decades ago, peptide drug development was focused on small chain lengths that could be easily and economically manufactured through liquid-phase technology.

Today's peptides of 20 or more amino acids can't readily be manufactured in the liquid phase, says Lukas Utiger, head of exclusive synthesis at [Lonza](#). Moreover, they typically require chemical modification, such as disulfide bridges, and are often required in volumes greater than 100 kg per peptide active pharmaceutical ingredient. "The trend toward solid-phase syntheses was a logical step for both customers and CMOs," or contract manufacturing organizations, Utiger notes.

Peptide manufacturers all agree that the shift to solid-phase synthesis of longer-chain peptides was made possible by Fuzeon, the HIV medication launched by Roche and Trimeris in 2003.

The drug, a 36-amino acid peptide formerly referred to as T-20, required production capacity magnitudes beyond that of previously approved synthetic peptides. That volume—some 45 tons of raw materials are needed to make 1 ton of Fuzeon—not only brought down the prices of raw materials for Roche but changed the cost equation for all peptide contract manufacturers.

"Synthetics were given a new life because of T-20," American Peptide's Hampton notes. "We spend more now on solvents than we do on amino acids."

"The key here is bulk shopping; we are the price club of peptides," says Ralph DiLibero, director of business development at [Roche Colorado](#), the subsidiary that manufactures Fuzeon. He notes that Roche worked with suppliers to develop the chemistry that, in turn, enabled the drop in raw material and resin costs.

Although raw materials are important to the economics of peptide production, Roche says improving downstream processing has been even more critical to its ability to manufacture large quantities of synthetic peptides.

After being cleaved from the support resin, peptides are traditionally purified and then lyophilized—dehydrated through freeze-drying—for stable storage. Because of capacity limitations and time constraints, lyophilization can create a manufacturing bottleneck. Roche's response was to develop a precipitation method to replace it.

"Lyophilization is not only a very costly technique for bulk materials, but it also does not allow you to upgrade the purity of the peptide or the peptide intermediate," explains Gary W. Erickson, director of Roche Colorado's Boulder Technology Center.

In other words, "whatever is in the oven is what's going to end up in your cake," DiLibero adds. Any impurities, such as residual solvents, cannot be extracted, and the integrity of the product could even worsen if any degradation occurs during lyophilization.

Perhaps the greatest boon of the precipitation method is that it allowed Roche to synthesize certain peptide fragments in the solid phase, isolate them, and then join them with solution-phase chemistry. This hybrid approach addressed both cost and efficiency issues, and it permitted the synthetic production of longer-chain peptides that previously had been relegated to recombinant technology, peptide producers say.

To build long peptides via solid-phase chemistry alone, reactors need to be "humongous," and the coupling efficiency drops off

as the chain gets longer, explains Satish Joshi, executive vice president at [Peptisyntha](#), the peptides arm of Belgian chemicals group Solvay. The yield of a solid-phase synthesis drops exponentially as the length of the peptide increases, PolyPeptide's Lax adds.

In the hybrid process, "We can make small pieces on the solid-phase resin where coupling is very high and get extremely pure fragments," Joshi says. "Because you have large resolution, it's easy to take various fragments and put them in solution-phase mode."

Chemists can also reverse the process, making smaller pieces in solution phase and then assembling the peptide on a solid-phase resin. In either case, peptide producers say the hybrid process can be more efficient and less expensive, and it can result in a cleaner end product.

Furthermore, Roche has shown that the process can work at a large scale. With Fuzeon, "Roche Colorado has shown that you can easily make up to a ton of peptide using solid phase combined with solution phase," Joshi says.

The evolution of a more cost-effective process has more producers turning to solid-phase synthesis as a relatively quick and less expensive route to bringing peptide pharmaceuticals to market. And as the late-stage pipeline of peptide drugs fills, contract manufacturers are investing to support an expected need for commercial-scale manufacturing.

[NeoMPS](#), the peptide manufacturing unit of SNPE's Isochem custom chemicals arm, is tripling solid-phase capacity at its Strasbourg, France, site. The company currently has peptides capacity of tens of kilograms in both Strasbourg and San Diego.

With a customer's product advancing into later stage clinical trials, NeoMPS may need "over 100-kg quantities," says Robert Hagopian, director of business development at NeoMPS. Construction of a new building adjacent to the existing peptides facility in Strasbourg is expected to begin at the end of the year.

PolyPeptide recently expanded solid-phase capacity at its Torrance, Calif., facility and expects over the next few years to double capacity to enable production in the 10-100-kg range. The firm is also upgrading its European facilities, which focus on solution-phase synthesis, to add both capacity and enhanced purification capabilities.

Peptisyntha began construction on an expansion of solid-phase capacity in 2005, adding two production trains to its Torrance facility. The \$2.5 million expansion enables the firm to simultaneously manufacture multiple compounds and to support projects that are poised to progress into Phase II or III trials, Joshi says.



American Peptide Photo

CLEAN PROFILE The purification team at work at American Peptide's Vista, Calif., facility.

American Peptide is spending about \$10 million to expand its Vista, Calif., facility. The company produces two commercial peptide drugs and expects a customer will file a New Drug Application for a third product later this year. It recently secured the contract to supply clinical quantities of Affymax's Hematide. The new equipment will enable peptide production up to the 50-kg scale.

Lonza significantly fortified its position in the peptides arena in January through the \$145 million acquisition of rival producer UCB Bioproducts. In addition to adding significant capacity, the company says, the deal makes Lonza the sole peptides producer to offer all three technologies employed in peptide manufacturing.

Lonza has also boosted internal capacity at its own facility in Visp, Switzerland. The \$20 million investment, initiated in April 2005, included the construction of a midscale plant for clinical trial supplies of both peptides and oligonucleotides and the addition of related purification and lyophilization equipment.

The rash of investment is supported by growth expectations for peptides: Producers expect the market for bulk peptides to grow at roughly 15-20% per year. Successful peptide launches such as [Amylin's](#) diabetes drug Byetta, which hit the market last year and is expected to achieve blockbuster status, provide some affirmation for those lofty targets.

"Five years ago, nobody was talking about peptides being needed as much as they are needed now," NeoMPS's Hagopian says. "I'm the eternal optimist, but I think we haven't really seen the full impact of the market growth on peptides yet."

IN THE PIPELINE

Twenty companies have peptide and peptide-based drugs in Phase III development

COMPANY	PRODUCT	THERAPEUTIC TARGET
Alkermes	Inhaled insulin	Diabetes
Antigenics	Vitespen (Oncophage)	Melanoma
AVI BioPharma	CTP-37 (Avicene)	Oncology
BioMS Medical	MBP-8298	Multiple sclerosis
Cadence Pharmaceuticals	Omiganan	Antibiotic
Dyax	Ecallantide (DX-88)	Hereditary angioedema
Emisphere Technologies	Oral calcitonin	Osteoporosis
IDM Pharma	Junovan	Osteosarcoma
Jerini	Icatibant	Hereditary angiodema
Mannkind	Inhaled insulin	Diabetes
Mondobiotech	Aviptadil	Pulmonary arterial hypertension
Neurobiological Technologies	Corticotropin acetate (Xerecept)	Cerebral edema
Novo Nordisk	Inhaled insulin (AERx)	Diabetes
NPS Pharmaceuticals	Teduglutide	Short bowel syndrome
Orphan Therapeutics	Terlipressin	Heptorenal syndrome
OrthoLogic	Chrysalin	Fracture healing
Tetragenex	Netamiftide	Depression
Theratechnologies	TH9507	HIV-associated lipodystrophy
Voyager Pharmaceutical	Leuprolide	Alzheimer's disease
Xoma	Opebecan (Neuprex)	Inflammatory diseases

SOURCES: Drug & Market Development, individual companies

[View Enlarged Table](#)

Chemical & Engineering News

ISSN 0009-2347

Copyright © 2009 American Chemical Society

Related Stories

- [From Peptides To Small Molecules](#) C&EN, April 10, 2006
- [Peptide Synthesis Reinvented](#) C&EN, January 30, 2006
- [A PEPTIDE SPECIALIST](#) C&EN, July 18, 2005

- [Email this article to a friend](#)
- [Print this article](#)
- [E-mail the editor](#)

Articles By Topic

- [Latest News](#)
- [Business](#)
- [Government & Policy](#)
- [Science / Technology](#)
- [Career & Employment](#)
- [ACS News](#)
- [View All Topics](#)

Invited review

HIV entry inhibitors: a new generation of antiretroviral drugs

Elias KRAMBOVITIS^{1,3}, Filippos PORICHIS^{1,2}, Demetrios A SPANDIDOS²

¹Department of Applied Biochemistry and Immunology, Institute of Molecular Biology and Biotechnology, Vassilika Vouton, Heraklion, Crete, Greece; ²Greece Department of Virology, Medical School, University of Crete, Heraklion, Crete, Greece

Key words

highly active antiretroviral therapy; HIV receptors; HIV fusion inhibitors; HIV

³Correspondence to Prof Elias KRAMBOVITIS.
Phn 30-81-39-1020.
Fax 30-81-39-1101.
E-mail krambo@imbb.forth.gr

Received 2005-05-15
Accepted 2005-06-27

doi: 10.1111/j.1745-7254.2005.00193.x

Abstract

AIDS is presently treatable, and patients can have a good prognosis due to the success of highly active antiretroviral therapy (HAART), but it is still not curable or preventable. High toxicity of HAART, and the emergence of drug resistance add to the imperative to continue research into new strategies and interventions. Considerable progress in the understanding of HIV attachment and entry into host cells has suggested new possibilities for rationally designing agents that interfere with this process. The approval and introduction of the fusion inhibitor enfuvirtide (Fuzeon) for clinical use signals a new era in AIDS therapeutics. Here we review the crucial steps the virus uses to achieve cell entry, which merit attention as potential targets, and the compounds at pre-clinical and clinical development stages, reported to effectively inhibit cell entry.

Introduction

Acquired immunodeficiency syndrome (AIDS) was recognized in 1981, and the first human immunodeficiency virus (HIV) was isolated 2 years later, heralding a new era in the fight against pathogenic viruses^[1,2]. Since then, HIV infection has become a major public health problem worldwide, with an estimated 39.4 million infected people as at the end of 2004 (Table 1)^[3]. According to the Joint United Nations Programme on HIV/AIDS (UNAIDS) epidemic update, in 2004 there were more than 3.1 million AIDS deaths, including 500 000 children under 15 years of age^[4]. The prevalence of HIV-1 is greater in developing countries, and especially in Sub-Saharan Africa, where the infrastructure to prevent and treat the infection is limited^[5]. These “hotspots” absorb most of the attention of international committees and organizations, and a significant part of the funding for AIDS prevention and treatment goes towards attempting to scale up antiretroviral (ARV) therapy in developing and transitional countries^[6].

HIV is a lentivirus that is predominantly transmitted by sexual contact, as virus particles can cross the mucosal epithelium and infect specific cells^[7,8] expressing the CD4 receptor. Cells bearing CD4 receptors on their membrane belong to the macrophage/monocyte lineage and to a subset of T-cells^[9,10]. Initial indications were that HIV-1 used

only CD4 to identify and enter the target cells. Soon, however, it became apparent that additional co-receptors were probably required in order for the virus to complete cell entry. Subsequently, several such potential co-receptors were proposed^[11,12], but the CCR5 and CXCR4 chemokine receptors are today considered to be the major co-receptors for HIV-1 entry^[13–15]. T-cell tropic HIV strains use mainly CXCR4 as a co-receptor and are called X4 strains, whereas macrophage-

Table 1. Worldwide distribution of estimated number of people living with HIV^[4].

Region	Estimated number ¹⁾
North America	1.0 million (540 000–1.6 million)
Caribbean	440 000 (270 000–780 000)
Latin America	1.7 million (1.3–2.2 million)
Western and Central Europe	610 000 (480 000–760 000)
Eastern Europe and Central Asia	1.4 million (920 000–2.1 million)
North Africa and Middle East	540 000 (230 000–1.5 million)
Sub-Saharan Africa	25.4 million (23.4–28.4 million)
East Asia	1.1 million (560 000–1.8 million)
South and South-East Asia	7.1 million (4.4–10.6 million)
Oceania	35 000 (25 000–48 000)

¹⁾The ranges around the estimates define the boundaries within which the actual numbers lie based on the best available information^[4].

tropic strains, responsible for host-to-host transmission, use CCR5 as a co-receptor, and are referred to as R5 strains. Thus, macrophages are the principal targets for the establishment of the infection in new individuals^[16]. Although it is not always the case^[17,18], the transition from viral isolates that use the CCR5 receptor to isolates that use the CXCR4 receptor has been linked with the transition from the latent asymptomatic phase to the clinical manifestations associated with AIDS^[19,20].

The most striking feature of HIV-1 infection is the gradual depletion of circulating CD4⁺ T cells, which leads to increased sensitivity of the patient to opportunistic and chronic infections and to oncogenesis. The cause of the CD4⁺ T cell depletion is still under debate^[21–23]. It is generally accepted, however, that during the asymptomatic phase the daily replenishment rate of CD4⁺ T cells is much higher than the turnover of infective virus particles for the cytopathicity model to explain the progressive depletion of CD4⁺ T cells from circulation^[24]. An alternative hypothesis proposes that certain viral components contribute to dysfunction of a vital immune mechanism^[25].

Over the past 23 years, the main objective in the field of HIV research has been the discovery of drugs that will combat the disease. Satisfactory progress has already been made and there are now more than 20 anti-HIV drugs approved by the American Food and Drug Administration (FDA)^[26]. ARV drugs are categorized according to their mode of action into three main groups: 1) the nucleoside reverse transcriptase inhibitors (NRTI); 2) the non-nucleoside reverse transcriptase inhibitors (NNRTI)^[27,28]; and 3) the protease inhibitors (PI)^[29]. ARV drugs from these categories are now administered in combination (as cocktails) to produce more efficient treatment^[30]. This type of therapy, termed “highly active antiretroviral therapy” or HAART, has markedly decreased mortality and morbidity in the developed world. Efforts have been made by the World Health Organization (WHO) and UNAIDS

to substantially increase the number of people on HAART in developing and transitional countries^[6].

Despite the fact that current antiviral treatments have improved prognosis, drug resistance and high toxicity are serious limitations to current treatments that justify the continuation of research efforts for new strategies and interventions^[31,32]. Today, AIDS is treatable, and patients can have a good prognosis, but it is still not curable. A new generation of drugs was recently introduced that inhibit viral cell entry (to be discussed later). HIV entry inhibitors appear to be a rational step forward in ARV therapy, because they prevent the virus from infecting new host cells, and may potentially stop or significantly limit HIV transmission^[33–35]. In order to rationally design effective drugs, the pathophysiology of HIV must be better understood for ARV therapy research to target specific events in the biology of the virus within the host cell^[36,37].

HIV entry

HIV-1 predominately infects cells that have the CD4 receptor on their surface membrane, although this is not always the case^[38,39]. Achievement of infection of these cells involves three discrete steps: viral attachment, then co-receptor binding, and finally fusion (see Figure 1). Recognition of the “correct” target cell and attachment to it is primarily achieved through envelope glycoprotein gp120, which binds to CD4 molecules. Gp120 is generated within the infected host cell after cleavage of gp160 by cellular proteases into two functional proteins: gp120 and gp41. It consists of 5 variable (V1–V5) and 5 conserved (C1–C5) regions^[40]. Gp120 and gp41 are glycosylated in the Golgi apparatus, and then transported to the membrane that is later incorporated in the viral envelope during the budding of the viral particles to form mature viruses^[41]. The envelope membrane is studded with trimers of gp120-gp41 heterodimers, where gp41 forms

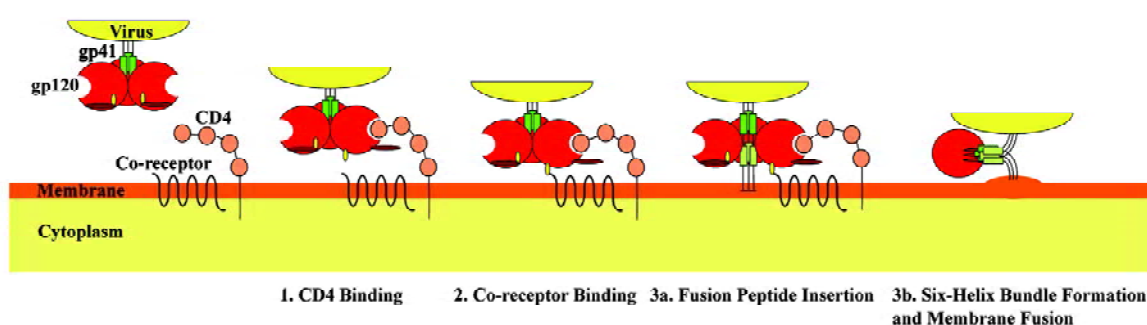


Figure 1. Schematic representation of the mechanism for HIV-1 cell entry.

the cytosolic part and gp120 the extracellular part^[42].

Binding of viral gp120 to host cell CD4 is achieved through interactions of several conserved gp120 residues with the second complementarity-determining region (CDR2) of CD4^[43,44]. This interaction alone is not sufficient to achieve cell entry, but it is necessary in order to identify the target cell and also to increase the affinity of other viral components for the co-receptor molecules. Indeed, binding of gp120 to CD4 causes conformational changes to the variable loop regions V1/V2 and V3 of gp120, causing the V3 loop to evaginate, thus becoming exposed to the co-receptors^[45] (Figure 1). The major co-receptors that HIV-1 uses are the CCR5 and CXCR4 chemokine receptors. The exact mechanism of interaction between the variable loop regions V1/V2 and V3 and the chemokine receptors is not well understood and it merits a more detailed investigation. It has been suggested, however, that the interaction between V3 and CCR5 is ionic in nature, and results in enhancement of the process of activation-induced cell death of responding effector CD4⁺ T cells during antigen presentation^[22,46,47].

The final step for viral entry requires fusion of the viral envelope components with the target surface membrane; this is achieved with the use of gp41, which is a glycoprotein consisting of 3 main domains: an intracellular domain (endodomain), a transmembrane anchor and an extracellular domain (ectodomain). The ectodomain is the key structure responsible for fusion and consists of a hydrophobic fusion peptide sequence at the N-terminal, two hydrophobic heptad repeats (HR1 and HR2) at the C-terminal, and a hinge region, where a disulfide-bond loop is formed between the two heptad repeats during fusion^[48,49]. On binding of gp120 to CD4 and subsequently to the co-receptor, further conformational changes occur that lead to gp41 dissociation from gp120. The gp41 unfolds and the hydrophobic fusion peptide sequence extends out of the viral membrane towards the host cell membrane. Insertion of the fusion peptide into the host cell membrane leads gp41 to fold into a hairpin-like structure where the two hydrophobic heptad repeats (HR1 and HR2) lie antiparallel, forming a 6-helix bundle^[50,51]. This hairpin structure is believed to be responsible for the fusion of the HIV envelope to the host cell membrane.

Enfuvirtide: the first FDA-approved fusion inhibitor

Enfuvirtide (formerly known as T-20) is the first fusion inhibitor approved by the FDA and the European Commission for the Treatment of AIDS, and is available under the trade name Fuzeon (Trimeris and Roche). It is a 36 amino

acid synthetic peptide homologous to the HR2 region of gp41 (residues 127-162)^[52,53], that has the ability to interfere with the fusion pathway by mimicking the HR2 domain^[54]. The accepted mode of action proposes that enfuvirtide targets conformational changes during fusion by binding to the HR1 domain. Recent evidence indicates that enfuvirtide interacts with multiple sites in gp41 and gp120^[55]. This binding prevents the formation of the 6-helix bundle by preventing HR2 from refolding antiparallel to HR1^[56,57]. Thus, inhibition of fusion of the viral envelope to cell membranes is achieved by blocking a critical step in the fusion pathway (Figure 2).

In the initial stages of discovery, enfuvirtide appeared to inhibit HIV-1 replication very effectively in various cell types and clinical trials proved to be very promising. Phase I/II trials provided proof that HIV entry was inhibited after treating patients with 100 mg enfuvirtide twice daily for 14 d. The levels of plasma HIV RNA after 14 d of treatment demonstrated a 1.96 lg median decline^[58]. Phase II clinical trials were performed on 71 HIV-infected individuals who were treated with 50 mg enfuvirtide together with other ARV drugs for 48 weeks. There was a 1.0 log₁₀ decline from baseline in HIV RNA and a median gain of CD4 cell counts of 84.9 cells/ μ L, with no significant toxicity^[59].

Furthermore, two TORO (T-20 vs Optimized Regimens Only) Phase III clinical trials were performed in America (TORO 1) and in Europe and Australia (TORO 2). The trials had similar protocols: they compared the efficacy and safety of enfuvirtide plus an optimized antiretroviral regimen with the efficacy and safety of an optimized antiretroviral regimen alone^[60,61]. In both studies the least-squares mean change from baseline in the plasma viral load indicated a significant difference in the decrease in the enfuvirtide group compared with the control ($P < 0.01$). In the same way, the mean count of CD4 cells/mL was significantly greater in the enfuvirtide group compared with the controls ($P < 0.01$).

Further studies are currently being performed on the exact metabolic pathway of enfuvirtide, potential drug resistance problems, and identification of synergistic interactions with other drugs. Several reports concluded that enfuvirtide does not appear to interfere with the activities of cytochrome P450, probably because it is a peptide and is easily hydrolyzed in the body^[62,63]. Enfuvirtide was found to act synergistically with other potential entry inhibitors *in vitro*, such as AMD3100 and PRO542, producing results that encouraged the use of combinations of entry inhibitors as part of a new generation of ARV strategies^[64,65]. However, HIV resistance has been reported in patients treated with enfuvirtide, indicating a hotspot from codons 36 to 38 of the HR1 domain^[66],

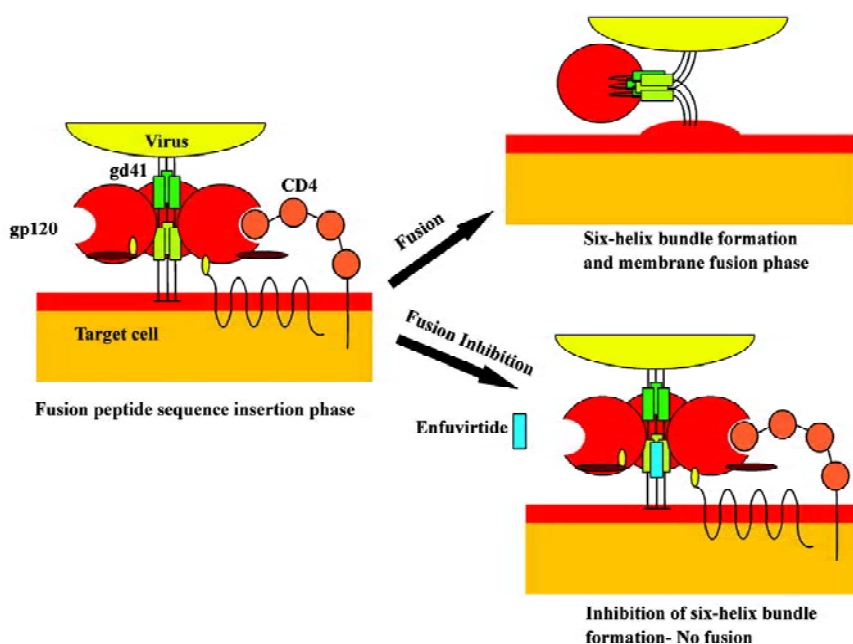


Figure 2. Mechanism of inhibition of HIV fusion to the cell membrane by enfuvirtide.

as well as other sites in gp41^[67–69]. Additionally, primary resistance has been reported, which appears to be more frequent than predicted^[70], indicating that more research is needed in this field.

Enfuvirtide obtained accelerated approval by the FDA in 2003 and became the 17th licensed ARV drug and the first to inhibit HIV entry. The drug is supplied as a lyophilized powder in single-dose vials containing 108 mg of the drug. Reconstitution of the powder in 1.1 mL sterile water for injection produces a single dose of 90 mg/mL^[71] that is injected subcutaneously. Enfuvirtide has two currently known major drawbacks. First, being a peptide, it can only be administered by injection and not orally. This makes usage more difficult, because patients must be educated for self-administration. Second, the cost of enfuvirtide is high, because it is a synthetic peptide that is manufactured by a highly complicated process involving large amounts of raw materials^[72,73]. It is estimated that the annual cost of enfuvirtide therapy is approximately US\$20 000 per patient, and if taken in combination with other ARV drugs then the cost of therapy could approach US\$30 000.

Potential drugs targeting entry and fusion

Attachment inhibitors Current novel antiretroviral drugs aim to interfere with the crucial HIV entry steps: viral attachment, co-receptor binding and fusion. One approach for interfering with viral attachment involves the use of a tetravalent fusion protein construct, consisting of a human

IgG2 in which the Fv portions of both the heavy and light chains have been replaced with the D1 and D2 domains of human CD4^[74,75]. This CD4-immunoglobulin fusion construct, called PRO 542, is suggested to bind to the viral gp120 and thus prevent the virus from interacting with CD4-bearing host cells. Phase I clinical trials indicated that PRO 542 has a half-life of 3–4 d when a relatively high dose was used (10 mg/kg), and no dose-limiting toxicities were observed^[76]. In addition, in phase II clinical trials, 12 HIV-infected patients were treated with 25 mg/kg single-dose PRO 542. The drug was well tolerated and the acute reduction caused in the HIV-1 RNA was statistically significant, even in patients with advanced AIDS^[77].

In the same way, several other compounds target either the gp120 or the CD4 receptor and interfere with HIV attachment. FP-21399 is a bis(disulfonaphthelene) derivative that binds to gp120, most probably near the third variable domain, because interactions with antibodies against the V3 loop region were blocked^[78]. A phase I study showed that it caused an increase in CD4 cell counts, and a significant decrease in viral load and minor side effects^[79]. BMS-378806, a 4-methoxy-7-azaindole derivative, is a compound that can be administered orally, and was developed by Bristol Myers Squibb^[80,81]. Despite the fact that phase I and II studies showed promising results, Bristol Myers Squibb decided to investigate similar drugs such as BMS-488043, an analogue of BMS-378806, in order to optimize its effectiveness^[82]. A series of polyanionic compounds, for example dextrin-2-sulfate, Carraguard and PRO 2000 are in clinical trials, and

are designed to be topically administered^[83–85]. Finally, TNX-355, a humanized anti-CD4 mAb that binds to CD4 without interfering with its biological function, significantly decreased viral load and increased CD4 cell counts in a phase I trial^[86].

Co-receptor binding inhibitors The most interesting target in HIV entry is the co-receptor binding phase. Current drug research is focused on designing compounds that prevent the virus interacting with the chemokine receptors. The CCR5 receptor is the principal target, and a number of potential drugs are currently being studied. SCH-C is a small molecule that inhibits the binding of gp120 to CCR5, and initial *in vitro* experiments have indicated good inhibitory activity against R5 viruses as well as synergistic effects with several ARV drugs, including enfuvirtide^[87,88]. Although it can be administered orally and clinical studies showed decreased viral loads, electrocardiographic anomalies due to arrhythmias were reported at high dosages^[89]. Another compound, SCH-D, has been found to have greater *in vitro* and *in vivo* antiviral properties, with no apparent side effects. Clinical studies for this drug are still ongoing^[90]. Interestingly, it was recently reported that V3-like peptides from X4 strains with more electropositive V3 domains were effective antagonists and potential infectivity blockers of R5 variants^[91].

TAK-779 was the first non-peptidic molecule found to inhibit co-receptor attachment by binding to CCR5 at transmembrane helices 1, 2, 3, and 7^[92,93]. It has the disadvantage of intravenous administration and because of irritations observed at the injection site, its development was discontinued. It was replaced by another compound, T-220, which can be administered orally, and shows promising anti-R5 HIV activity^[94]. Similarly, UK-427,857 is a novel CCR5 inhibitor that has acceptable pharmacokinetic and metabolic rates in mice, rats, dogs and humans, and can be administered orally^[95]. Finally, PRO 140 is one of the few monoclonal antibodies that has been used as an entry inhibitor and has been reported to block co-receptor attachment without down-modulating or inducing signaling of the CCR5 chemokine receptor^[96,97].

CXCR4, the second major HIV co-receptor, is also a target for current drug research. AMD-3100, one of the first entry inhibitors, was found to inhibit viral entry well before the discovery of co-receptor usage by HIV^[98]. It is a bicyclam compound of low molecular weight that inhibits the electrostatic interaction between CXCR4 and gp120 by ionic binding to the second extracellular loop (ECL2) and the adjacent membrane-spanning domain (TM4) of the CXCR4 receptor^[99]. Despite the fact that in phase I and II clinical trials, intravenous administration of AMD-3100 significantly reduced the

viral load^[100], it was later replaced by an orally available compound, AMD-070. A non-peptidic compound, KRH-1636, which is absorbed through the duodenum, had similar efficacies to AMD-3100^[101]. Finally, T-22 and ALX40-4C are positively charged peptides that occupy the V3 region and competitively inhibit binding of gp120 to the negatively charged amino acid residues on CXCR4^[102–104].

In conclusion, the role of the V3 region in the mechanism of cell attachment and entry in relation to the major co-receptors is being actively pursued. In addition to biological studies, physicochemical studies on the interacting protein domains are being carried out in an attempt to decipher the interface conformations between the virus and the cell^[105].

Fusion inhibitors Understanding the mechanism of fusion of the viral envelope with the host membrane played a crucial role in the development of new generation ARV drugs. This became apparent when enfuvirtide was licensed as the first viral entry inhibitor, and it is currently used in HAART. Resistance to enfuvirtide has been reported, which has led to the design of a second generation HR2 mimetic peptide. T-1249 is a 39-L-amino acid synthetic peptide that contains a pocket-binding sequence that makes the HR1 and HR2 interaction more stable. Studies on T-1249 showed that it has greater efficacy and longer half-life than enfuvirtide. Additionally, efficacy against enfuvirtide-resistant viruses has been reported, indicating that this second generation fusion inhibitor is a step forward^[106,107]. However, Roche and Trimeris decided to halt clinical development due to formulation concerns^[108].

5-Helix is a newly designed recombinant C-peptide that consists of 5 of the 6 helices that are formed during the fusion phase. A CHR domain is missing for the 6-helix bundle formation, and thus there is one exposed groove. This groove binds to a CHR domain in gp41 and inhibits fusion of the viral membrane to the host membrane^[109]. Because it is a recombinant peptide, it has a much lower cost of production compared with the synthetic enfuvirtide. Initial studies demonstrated potent antiretroviral activity, with IC₅₀ values in the low nanomolar range^[110].

Finally, N-peptides represent another group of peptides with potential inhibitory effects against HIV entry. Initial studies have indicated that they are weaker inhibitors than the C-peptides, with IC₅₀ values in the micromolar range. However, chimeric molecules composed of soluble trimeric coiled coils have shown promising results. IQN17 is one of the first such peptides with potent inhibitory effects, and the current most potent chimeric N-peptide, IQN23, is reported to have an IC₅₀ value of 15 nmol/L^[111].

Conclusion

Antiretroviral chemotherapy has recently acquired a new “weapon” in the fight against AIDS. Enfuvirtide is the first HIV entry inhibitor that was approved by FDA, and it is currently used in combination with other ARV drugs. Results from clinical trials indicated that it had potent activity against HIV strains that are resistant to other ARV drugs, although some resistance to enfuvirtide has been reported. The design of other entry inhibitors has moved forward, and every phase of HIV entry is actively pursued as a target for potential inhibitors. Probably the most exciting prospect is potential interference with co-receptor usage, particularly that of CCR5.

ARV drug development aims to produce drugs with potent antiretroviral activity, with IC_{50} values in the nanomolar range, with no or limited toxicity and that can be administered orally. Several compounds are currently in clinical trials, and we are optimistic that new, more effective drugs will be added to the ARV armory.

References

- Barre-Sinoussi F, Chermann JC, Rey F, Nugeyre MT, Chamaret S, Gruest J, *et al*. Isolation of a T-lymphotropic retrovirus from a patient at risk for acquired immune deficiency syndrome (AIDS). *Science* 1983; 220: 868–71.
- Gallo RC, Sarin PS, Gelmann EP, Robert-Guroff M, Richardson E, Kalyanaraman VS, *et al*. Isolation of human T-cell leukemia virus in acquired immune deficiency syndrome (AIDS). *Science* 1983; 220: 865–7.
- HIV/AIDS Facts and figures [database on the internet]. New Delhi: WHO Regional Office for South-East Asia . [cited 2005 Apr 20]. Available from: <http://w3.whosea.org/EN/Section10/Section18/Section348.htm#Global>
- UNAIDS/WHO. AIDS Epidemic Update. Geneva: UNAIDS; 2004.
- Gayle HD, Hill GL. Global impact of human immunodeficiency virus and AIDS. *Clin Microbiol Rev* 2001; 14: 327–35.
- UNAIDS/WHO. ‘3 by 5’ Progress Report. France: WHO; 2005.
- Bomsel M. Transcytosis of infectious human immunodeficiency virus across a tight human epithelial cell line barrier. *Nat Med* 1997; 3: 42–7.
- Ullrich R, Schmidt W, Zippel T, Schneider T, Zeitz M, Riecken EO. Mucosal HIV infection. *Pathobiology* 1998; 66: 145–50.
- Dalgleish AG, Beverley PC, Clapham PR, Crawford DH, Greaves MF, Weiss RA. The CD4 (T4) antigen is an essential component of the receptor for the AIDS retrovirus. *Nature* 1984; 312: 763–7.
- Klatzmann D, Champagne E, Chamaret S, Gruest J, Guetard D, Herceud T, *et al*. T-lymphocyte T4 molecule behaves as the receptor for human retrovirus LAV. *Nature* 1984; 312: 767–8.
- Rucker J, Samson M, Doranz BJ, Libert F, Berson JF, Yi Y, *et al*. Regions in beta-chemokine receptors CCR5 and CCR2b that determine HIV-1 cofactor specificity. *Cell* 1996; 87: 437–46.
- Roderiquez G, Oravec T, Yanagishita M, Bou-Habib DC, Mostowski H, Norcross MA. Mediation of human immunodeficiency virus type 1 binding by interaction of cell surface heparan sulfate proteoglycans with the V3 region of envelope gp120-gp41. *J Virol* 1995; 69: 2233–9.
- Berson JF, Long D, Doranz BJ, Rucker J, Jirik FR, Doms RW. A seven-transmembrane domain receptor involved in fusion and entry of T-cell-tropic human immunodeficiency virus type 1 strains. *J Virol* 1996; 70: 6288–95.
- Deng H, Liu R, Ellmeier W, Choe S, Unutmaz D, Burkhart M, *et al*. Identification of a major co-receptor for primary isolates of HIV-1. *Nature* 1996; 381: 661–6.
- Dragic T, Litwin V, Allaway GP, Martin SR, Huang Y, Nagashima KA, *et al*. HIV-1 entry into CD4+ cells is mediated by the chemokine receptor CC-CKR-5. *Nature* 1996; 381: 667–73.
- van’t Wout AB, Kootstra NA, Mulder-Kampinga GA, Albrecht-van Lent N, Scherpbier HJ, Veenstra J, *et al*. Macrophage-tropic variants initiate human immunodeficiency virus type 1 infection after sexual, parenteral, and vertical transmission. *J Clin Invest* 1994; 94: 2060–7.
- de Roda Husman AM, van Rij RP, Blaak H, Broersen S, Schuitemaker H. Adaptation to promiscuous usage of chemokine receptors is not a prerequisite for human immunodeficiency virus type 1 disease progression. *J Infect Dis* 1999; 180: 1106–15.
- Schuitemaker H, Koot M, Kootstra NA, Dercksen MW, de Goede RE, van Steenwijk RP, *et al*. Biological phenotype of human immunodeficiency virus type 1 clones at different stages of infection: progression of disease is associated with a shift from monocytotropic to T-cell-tropic virus population. *J Virol* 1992; 66: 1354–60.
- Bjorndal A, Sonnerborg A, Tscherning C, Albert J, Fenyo EM. Phenotypic characteristics of human immunodeficiency virus type 1 subtype C isolates of Ethiopian AIDS patients. *AIDS Res Hum Retroviruses* 1999; 15: 647–53.
- Richman DD, Bozzette SA. The impact of the syncytium-inducing phenotype of human immunodeficiency virus on disease progression. *J Infect Dis* 1994; 169: 968–74.
- Roumier T, Castedo M, Perfettini JL, Andreau K, Metivier D, Zamzami N, *et al*. Mitochondrion-dependent caspase activation by the HIV-1 envelope. *Biochem Pharmacol* 2003; 66: 1321–9.
- Zafiroopoulos A, Baritaki S, Sioumpara M, Spandidos DA, Krambovitis E. V3 induces in human normal cell populations an accelerated macrophage-mediated proliferation: apoptosis phenomenon of effector T cells when they respond to their cognate antigen. *Biochem Biophys Res Commun* 2001; 281: 63–70.
- Dockrell DH, Badley AD, Algeciras-Schimnich A, Simpson M, Schut R, Lynch DH, *et al*. Activation-induced CD4+ T cell death in HIV-positive individuals correlates with Fas susceptibility, CD4+ T cell count, and HIV plasma viral copy number. *AIDS Res Hum Retroviruses* 1999; 15: 1509–18.
- Graziosi C, Pantaleo G, Butini L, Demarest JF, Saag MS, Shaw GM, *et al*. Kinetics of human immunodeficiency virus type 1 (HIV-1) DNA and RNA synthesis during primary HIV-1 infection. *Proc Natl Acad Sci USA* 1993; 90: 6405–9.

- 25 Krambovitis E, Zafropoulos A, Baritaki S, Spandidos DA. Simple electrostatic interaction mechanisms in the service of HIV-1 pathogenesis. *Scand J Immunol* 2004; 59: 231–4.
- 26 De Clercq E. Antiviral drugs in current clinical use. *J Clin Virol* 2004; 30: 115–33.
- 27 Imamichi T. Action of anti-HIV drugs and resistance: reverse transcriptase inhibitors and protease inhibitors. *Curr Pharm Des* 2004; 10: 4039–53.
- 28 Zapor MJ, Cozza KL, Wynn GH, Wortmann GW, Armstrong SC. Antiretrovirals, Part II: focus on non-protease inhibitor antiretrovirals (NRTIs, NNRTIs, and fusion inhibitors). *Psychosomatics* 2004; 45: 524–35.
- 29 Dunn BM, Goodenow MM, Gustchina A, Wlodawer A. Retroviral proteases. *Genome Biol* 2002; 3: REVIEWS 3006.
- 30 Pereira CF, Paridaen JT. Anti-HIV drug development: an overview. *Curr Pharm Des* 2004; 10: 4005–37.
- 31 Johnson VA, Brun-Vezinet F, Clotet B, Conway B, D'Aquila RT, Demeter LM, *et al*. Update of the drug resistance mutations in HIV-1: 2004. *Top HIV Med* 2004; 12: 119–24.
- 32 van Heeswijk RP. Optimized antiretroviral therapy: the role of therapeutic drug monitoring and pharmacogenomics. *Expert Rev Anti Infect Ther* 2003; 1: 75–81.
- 33 Stone A. Microbicides: a new approach to preventing HIV and other sexually transmitted infections. *Nat Rev Drug Discov* 2002; 1: 977–85.
- 34 Moore JP, Shattock RJ. Preventing HIV-1 sexual transmission: not sexy enough science, or no benefit to the bottom line? *J Antimicrob Chemother* 2003; 52: 890–2.
- 35 Shattock RJ, Moore JP. Inhibiting sexual transmission of HIV-1 infection. *Nat Rev Microbiol* 2003; 1: 25–34.
- 36 Sleasman JW, Goodenow MM. 13. HIV-1 infection. *J Allergy Clin Immunol* 2003; 111: S582–92.
- 37 De Clercq E. HIV-chemotherapy and -prophylaxis: new drugs, leads and approaches. *Int J Biochem Cell Biol* 2004; 36: 1800–2.
- 38 Zerhouni B, Nelson JA, Saha K. CXCR4-dependent infection of CD8+, but not CD4+, lymphocytes by a primary human immunodeficiency virus type 1 isolate. *J Virol* 2004; 78: 12288–96.
- 39 Zerhouni B, Nelson JA, Saha K. Isolation of CD4-independent primary human immunodeficiency virus type 1 isolates that are syncytium inducing and acutely cytopathic for CD8+ lymphocytes. *J Virol* 2004; 78: 1243–55.
- 40 Farzan M, Choe H, Desjardins E, Sun Y, Kuhn J, Cao J, *et al*. Stabilization of human immunodeficiency virus type 1 envelope glycoprotein trimers by disulfide bonds introduced into the gp41 glycoprotein ectodomain. *J Virol* 1998; 72: 7620–5.
- 41 Leonard CK, Spellman MW, Riddle L, Harris RJ, Thomas JN, Gregory TJ. Assignment of intrachain disulfide bonds and characterization of potential glycosylation sites of the type 1 recombinant human immunodeficiency virus envelope glycoprotein (gp120) expressed in Chinese hamster ovary cells. *J Biol Chem* 1990; 265: 10373–82.
- 42 Yang X, Farzan M, Wyatt R, Sodroski J. Characterization of stable, soluble trimers containing complete ectodomains of human immunodeficiency virus type 1 envelope glycoproteins. *J Virol* 2000; 74: 5716–25.
- 43 Olshevsky U, Helseth E, Furman C, Li J, Haseltine W, Sodroski J. Identification of individual human immunodeficiency virus type 1 gp120 amino acids important for CD4 receptor binding. *J Virol* 1990; 64: 5701–7.
- 44 Kwong PD, Wyatt R, Robinson J, Sweet RW, Sodroski J, Hendrickson WA. Structure of an HIV gp120 envelope glycoprotein in complex with the CD4 receptor and a neutralizing human antibody. *Nature* 1998; 393: 648–59.
- 45 Sullivan N, Sun Y, Sattentau Q, Thali M, Wu D, Denisova G, *et al*. CD4-Induced conformational changes in the human immunodeficiency virus type 1 gp120 glycoprotein: consequences for virus entry and neutralization. *J Virol* 1998; 72: 4694–703.
- 46 Zafropoulos A, Baritaki S, Vlata Z, Spandidos DA, Krambovitis E. Dys-regulation of effector CD4+ T cell function by the V3 domain of the HIV-1 gp120 during antigen presentation. *Biochem Biophys Res Commun* 2001; 284: 875–9.
- 47 Baritaki S, Zafropoulos A, Sioumpara M, Politis M, Spandidos DA, Krambovitis E. Ionic interaction of the HIV-1 V3 domain with CCR5 and deregulation of T lymphocyte function. *Biochem Biophys Res Commun* 2002; 298: 574–80.
- 48 Bernstein HB, Tucker SP, Kar SR, McPherson SA, McPherson DT, Dubay JW, *et al*. Oligomerization of the hydrophobic heptad repeat of gp41. *J Virol* 1995; 69: 2745–50.
- 49 Chambers P, Pringle CR, Easton AJ. Heptad repeat sequences are located adjacent to hydrophobic regions in several types of virus fusion glycoproteins. *J Gen Virol* 1990; 71: 3075–80.
- 50 Lu M, Blacklow SC, Kim PS. A trimeric structural domain of the HIV-1 transmembrane glycoprotein. *Nat Struct Biol* 1995; 2: 1075–82.
- 51 Weissenhorn W, Dessen A, Harrison SC, Skehel JJ, Wiley DC. Atomic structure of the ectodomain from HIV-1 gp41. *Nature* 1997; 387: 426–30.
- 52 Wild C, Oas T, McDanal C, Bolognesi D, Matthews T. A synthetic peptide inhibitor of human immunodeficiency virus replication: correlation between solution structure and viral inhibition. *Proc Natl Acad Sci USA* 1992; 89: 10537–41.
- 53 Wild CT, Shugars DC, Greenwell TK, McDanal CB, Matthews TJ. Peptides corresponding to a predictive alpha-helical domain of human immunodeficiency virus type 1 gp41 are potent inhibitors of virus infection. *Proc Natl Acad Sci USA* 1994; 91: 9770–4.
- 54 Chen CH, Matthews TJ, McDanal CB, Bolognesi DP, Greenberg ML. A molecular clasp in the human immunodeficiency virus (HIV) type 1 TM protein determines the anti-HIV activity of gp41 derivatives: implication for viral fusion. *J Virol* 1995; 69: 3771–7.
- 55 Liu S, Lu H, Niu J, Xu Y, Wu S, Jiang S. Different from the HIV fusion inhibitor C34, the anti-HIV drug Fuzeon (T-20) inhibits HIV-1 entry by targeting multiple sites in gp41 and gp120. *J Biol Chem* 2005; 280: 11259–73.
- 56 Lawless MK, Barney S, Guthrie KI, Bucy TB, Petteway SR Jr., Merutka G. HIV-1 membrane fusion mechanism: structural studies of the interactions between biologically-active peptides from gp41. *Biochemistry* 1996; 35: 13697–708.
- 57 Furuta RA, Wild CT, Weng Y, Weiss CD. Capture of an early fusion-active conformation of HIV-1 gp41. *Nat Struct Biol* 1998; 5: 276–9.
- 58 Kilby JM, Hopkins S, Venetta TM, DiMassimo B, Cloud GA, Lee JY, *et al*. Potent suppression of HIV-1 replication in humans by T-20, a peptide inhibitor of gp41-mediated virus entry.

- Nat Med 1998; 4: 1302–7.
- 59 Lalezari JP, Eron JJ, Carlson M, Cohen C, DeJesus E, Arduino RC, *et al*. A phase II clinical study of the long-term safety and antiviral activity of enfuvirtide-based antiretroviral therapy. *Aids* 2003; 17: 691–8.
- 60 Lalezari JP, Henry K, O’Hearn M, Montaner JS, Piliero PJ, Trottier B, *et al*. Enfuvirtide, an HIV-1 fusion inhibitor, for drug-resistant HIV infection in North and South America. *N Engl J Med* 2003; 348: 2175–85.
- 61 Lazzarin A, Clotet B, Cooper D, Reynes J, Arasteh K, Nelson M, *et al*. Efficacy of enfuvirtide in patients infected with drug-resistant HIV-1 in Europe and Australia. *N Engl J Med* 2003; 348: 2186–95.
- 62 Zhang X, Lalezari JP, Badley AD, Dorr A, Kolis SJ, Kinchelov T, *et al*. Assessment of drug-drug interaction potential of enfuvirtide in human immunodeficiency virus type 1-infected patients. *Clin Pharmacol Ther* 2004; 75: 558–68.
- 63 Ruxrungtham K, Boyd M, Bellibas SE, Zhang X, Dorr A, Kolis S, *et al*. Lack of interaction between enfuvirtide and ritonavir or ritonavir-boosted saquinavir in HIV-1-infected patients. *J Clin Pharmacol* 2004; 44: 793–803.
- 64 Tremblay CL, Kollmann C, Giguel F, Chou TC, Hirsch MS. Strong *in vitro* synergy between the fusion inhibitor T-20 and the CXCR4 blocker AMD-3100. *J Acquir Immune Defic Syndr* 2000; 25: 99–102.
- 65 Nagashima KA, Thompson DA, Rosenfield SI, Maddon PJ, Dragic T, Olson WC. Human immunodeficiency virus type 1 entry inhibitors PRO 542 and T-20 are potently synergistic in blocking virus-cell and cell-cell fusion. *J Infect Dis* 2001; 183: 1121–5.
- 66 Rimsky LT, Shugars DC, Matthews TJ. Determinants of human immunodeficiency virus type 1 resistance to gp41-derived inhibitory peptides. *J Virol* 1998; 72: 986–93.
- 67 Wei X, Decker JM, Liu H, Zhang Z, Arani RB, Kilby JM, *et al*. Emergence of resistant human immunodeficiency virus type 1 in patients receiving fusion inhibitor (T-20) monotherapy. *Antimicrob Agents Chemother* 2002; 46: 1896–905.
- 68 Poveda E, Rodes B, Toro C, Martin-Carbonero L, Gonzalez-Lahoz J, Soriano V. Evolution of the gp41 env region in HIV-infected patients receiving T-20, a fusion inhibitor. *Aids* 2002; 16: 1959–61.
- 69 Xu L, Pozniak A, Wildfire A, Stanfield-Oakley SA, Mosier SM, Ratcliffe D, *et al*. Emergence and evolution of enfuvirtide resistance following long-term therapy involves heptad repeat 2 mutations within gp41. *Antimicrob Agents Chemother* 2005; 49: 1113–9.
- 70 Carmona R, Perez-Alvarez L, Munoz M, Casado G, Delgado E, Sierra M, *et al*. Natural resistance-associated mutations to Enfuvirtide (T20) and polymorphisms in the gp41 region of different HIV-1 genetic forms from T20 naive patients. *J Clin Virol* 2005; 32: 248–53.
- 71 Fuzeon [package insert]. Injection Instructions. Durham, NC, and Nutley, NJ: Trimeris Inc and Roche Laboratories Inc; 2003.
- 72 Steinbrook R. HIV infection: a new drug and new costs. *N Engl J Med* 2003; 348: 2171–2.
- 73 Tashima KT, Carpenter CC. Fusion inhibition: a major but costly step forward in the treatment of HIV-1. *N Engl J Med* 2003; 348: 2249–50.
- 74 Allaway GP, Davis-Bruno KL, Beaudry GA, Garcia EB, Wong EL, Ryder AM, *et al*. Expression and characterization of CD4-IgG2, a novel heterotetramer that neutralizes primary HIV type 1 isolates. *AIDS Res Hum Retroviruses* 1995; 11: 533–9.
- 75 Trkola A, Pomales AB, Yuan H, Korber B, Maddon PJ, Allaway GP, *et al*. Cross-clade neutralization of primary isolates of human immunodeficiency virus type 1 by human monoclonal antibodies and tetrameric CD4-IgG. *J Virol* 1995; 69: 6609–17.
- 76 Jacobson JM, Lowy I, Fletcher CV, O’Neill TJ, Tran DN, Ketas TJ, Trkola A, *et al*. Single-dose safety, pharmacology, and antiviral activity of the human immunodeficiency virus (HIV) type 1 entry inhibitor PRO 542 in HIV-infected adults. *J Infect Dis* 2000; 182: 326–9.
- 77 Jacobson JM, Israel RJ, Lowy I, Ostrow NA, Vassiliatos LS, Barish M, *et al*. Treatment of advanced human immunodeficiency virus type 1 disease with the viral entry inhibitor PRO 542. *Antimicrob Agents Chemother* 2004; 48: 423–9.
- 78 Ono M, Wada Y, Wu Y, Nemori R, Jinbo Y, Wang H, *et al*. FP-21399 blocks HIV envelope protein-mediated membrane fusion and concentrates in lymph nodes. *Nat Biotechnol* 1997; 15: 343–8.
- 79 Dezube BJ, Dahl TA, Wong TK, Chapman B, Ono M, Yamaguchi N, *et al*. A fusion inhibitor (FP-21399) for the treatment of human immunodeficiency virus infection: a phase I study. *J Infect Dis* 2000; 182: 607–10.
- 80 Lin PF, Blair W, Wang T, Spicer T, Guo Q, Zhou N, *et al*. A small molecule HIV-1 inhibitor that targets the HIV-1 envelope and inhibits CD4 receptor binding. *Proc Natl Acad Sci USA* 2003; 100: 11013–8.
- 81 Si Z, Madani N, Cox JM, Chruma JJ, Klein JC, Schon A, *et al*. Small-molecule inhibitors of HIV-1 entry block receptor-induced conformational changes in the viral envelope glycoproteins. *Proc Natl Acad Sci USA* 2004; 101: 5036–41.
- 82 Hanna G, Lalezari J, Hellinger J, Wohl D, Masterson T, Fiske W, *et al*. Antiviral activity, safety, and tolerability of a novel, oral small-molecule HIV-1 attachment inhibitor, BMS-488043, in HIV-1-infected subjects. In: Proceedings of the 11th conference on retroviruses and opportunistic infections; 2004 Feb 8–11, San Francisco. 2004.
- 83 Shaunak S, Thornton M, John S, Teo I, Peers E, Mason P, *et al*. Reduction of the viral load of HIV-1 after the intraperitoneal administration of dextrin 2-sulphate in patients with AIDS. *Aids* 1998; 12: 399–409.
- 84 Dezzutti CS, James VN, Ramos A, Sullivan ST, Siddig A, Bush TJ, *et al*. In vitro comparison of topical microbicides for prevention of human immunodeficiency virus type 1 transmission. *Antimicrob Agents Chemother* 2004; 48: 3834–44.
- 85 Morrow K, Rosen R, Richter L, Emans A, Forbes A, Day J, *et al*. The acceptability of an investigational vaginal microbicide, PRO 2000 Gel, among women in a phase I clinical trial. *J Womens Health (Larchmt)* 2003; 12: 655–66.
- 86 Kuritzkes DR, Jacobson J, Powderly WG, Godofsky E, DeJesus E, Haas F, *et al*. Antiretroviral activity of the anti-CD4 monoclonal antibody TNX-355 in patients infected with HIV type 1. *J Infect Dis* 2004; 189: 286–91.
- 87 Tremblay CL, Giguel F, Kollmann C, Guan Y, Chou TC, Baroudy BM, *et al*. Anti-human immunodeficiency virus interactions of SCH-C (SCH 351125), a CCR5 antagonist, with other antiret-

- roviral agents *in vitro*. *Antimicrob Agents Chemother* 2002; 46: 1336–9.
- 88 Tsamis F, Gavrilov S, Kajumo F, Seibert C, Kuhmann S, Ketas T, *et al*. Analysis of the mechanism by which the small-molecule CCR5 antagonists SCH-351125 and SCH-350581 inhibit human immunodeficiency virus type 1 entry. *J Virol* 2003; 77: 5201–8.
- 89 Reynes J, Rouzier R, Kanouni T, Baillat V, Baroudy B, Keung A. SCH C: Safety and antiviral effects of a CCR5 receptor antagonist in HIV-1-infected subjects. In: Proceedings of the 9th conference on retroviruses and opportunistic infections; 2002 Feb 24–28, San Francisco. 2002
- 90 Schurmann D, Rouzier R, Nougarede R, Reynes J, Fatkenheuer G, Raffi F, *et al*. SCH D: Antiviral activity of a CCR5 receptor antagonist. In: Proceedings of the 11th conference on retroviruses and opportunistic infections, 2004 Feb 8–11, San Francisco. 2004.
- 91 Baritaki S, Dittmar MT, Spandidos DA, Krambovitis E. *In vitro* inhibition of R5 HIV-1 infectivity by X4 V3-derived synthetic peptides. *Int J Mol Med* 2005; 16: 333–6.
- 92 Baba M, Nishimura O, Kanzaki N, Okamoto M, Sawada H, Iizawa Y, *et al*. A small-molecule, nonpeptide CCR5 antagonist with highly potent and selective anti-HIV-1 activity. *Proc Natl Acad Sci USA* 1999; 96: 5698–703.
- 93 Dragic T, Trkola A, Thompson DA, Cormier EG, Kajumo FA, Maxwell E, *et al*. A binding pocket for a small molecule inhibitor of HIV-1 entry within the transmembrane helices of CCR5. *Proc Natl Acad Sci USA* 2000; 97: 5639–44.
- 94 Iizawa Y, Kanzaki N, Takashima K, Miyake H, Tagawa Y, Sugihara Y, *et al*. Anti-HIV-1 Activity of TAK-220, a Small Molecule CCR5 Antagonist. In: Proceedings of the 10th conference on retroviruses and opportunistic infections, 2003 Feb 10–14, San Francisco. 2003.
- 95 Walker DK, Abel S, Comby P, Muirhead GJ, Nedderman AN, Smith DA. Species differences in the disposition of the CCR5 antagonist, UK-427,857, a new potential treatment for HIV. *Drug Metab Dispos* 2005; 33: 587–95.
- 96 Olson WC, Rabut GE, Nagashima KA, Tran DN, Anselma DJ, Monard SP, *et al*. Differential inhibition of human immunodeficiency virus type 1 fusion, gp120 binding, and CC-chemokine activity by monoclonal antibodies to CCR5. *J Virol* 1999; 73: 4145–55.
- 97 Trkola A, Ketas TJ, Nagashima KA, Zhao L, Cilliers T, Morris L, *et al*. Potent, broad-spectrum inhibition of human immunodeficiency virus type 1 by the CCR5 monoclonal antibody PRO 140. *J Virol* 2001; 75: 579–88.
- 98 de Clercq E, Yamamoto N, Pauwels R, Balzarini J, Witvrouw M, De Vreese K, *et al*. Highly potent and selective inhibition of human immunodeficiency virus by the bicyclam derivative JM3100. *Antimicrob Agents Chemother* 1994; 38: 668–74.
- 99 Labrosse B, Brelot A, Heveker N, Sol N, Schols D, De Clercq E, *et al*. Determinants for sensitivity of human immunodeficiency virus coreceptor CXCR4 to the bicyclam AMD3100. *J Virol* 1998; 72: 6381–8.
- 100 Hendrix CW, Flexner C, MacFarland RT, Giandomenico C, Fuchs EJ, Redpath E, *et al*. Pharmacokinetics and safety of AMD-3100, a novel antagonist of the CXCR-4 chemokine receptor, in human volunteers. *Antimicrob Agents Chemother* 2000; 44: 1667–73.
- 101 Ichiyama K, Yokoyama-Kumakura S, Tanaka Y, Tanaka R, Hirose K, *et al*. A duodenally absorbable CXC chemokine receptor 4 antagonist, KRH-1636, exhibits a potent and selective anti-HIV-1 activity. *Proc Natl Acad Sci USA* 2003; 100: 4185–90.
- 102 Doranz BJ, Grovit-Ferbas K, Sharron MP, Mao SH, Goetz MB, Daar ES, *et al*. A small-molecule inhibitor directed against the chemokine receptor CXCR4 prevents its use as an HIV-1 coreceptor. *J Exp Med* 1997; 186: 1395–400.
- 103 Murakami T, Nakajima T, Koyanagi Y, Tachibana K, Fujii N, Tamamura H, *et al*. A small molecule CXCR4 inhibitor that blocks T cell line-tropic HIV-1 infection. *J Exp Med* 1997; 186: 1389–93.
- 104 Murakami T, Zhang TY, Koyanagi Y, Tanaka Y, Kim J, Suzuki Y, *et al*. Inhibitory mechanism of the CXCR4 antagonist T22 against human immunodeficiency virus type 1 infection. *J Virol* 1999; 73: 7489–96.
- 105 Galanakis PA, Spyroulias GA, Rizos A, Samolis P, Krambovitis E. Conformational properties of HIV-1 gp120/V3 immunogenic domains. *Curr Med Chem* 2005; 12: 551–68.
- 106 Eron JJ, Gulick RM, Bartlett JA, Merigan T, Arduino R, Kilby JM, *et al*. Short-term safety and antiretroviral activity of T-1249, a second-generation fusion inhibitor of HIV. *J Infect Dis* 2004; 189: 1075–83.
- 107 Lalezari JP, Bellos NC, Sathasivam K, Richmond GJ, Cohen CJ, Myers RA, *et al*. T-1249 retains potent antiretroviral activity in patients who had experienced virological failure while on an enfuvirtide-containing treatment regimen. *J Infect Dis* 2005; 191: 1155–63.
- 108 Martin-Carbonero L. Discontinuation of the clinical development of fusion inhibitor T-1249. *AIDS Rev* 2004; 6: 61–3.
- 109 Root MJ, Kay MS, Kim PS. Protein design of an HIV-1 entry inhibitor. *Science* 2001; 291: 884–8.
- 110 Root MJ, Hamer DH. Targeting therapeutics to an exposed and conserved binding element of the HIV-1 fusion protein. *Proc Natl Acad Sci USA* 2003; 100: 5016–21.
- 111 Eckert DM, Kim PS. Design of potent inhibitors of HIV-1 entry from the gp41 N-peptide region. *Proc Natl Acad Sci USA* 2001; 98: 11187–92.

Potent HIV fusion inhibitors against Enfuvirtide-resistant HIV-1 strains

Yuxian He^{*†}, Jianwei Cheng[§], Hong Lu^{*}, Jingjing Li^{*}, Jie Hu[§], Zhi Qi^{*}, Zhonghua Liu[†], Shibo Jiang^{*}, and Qiuyun Dai^{*§}

^{*}Lindsley F. Kimball Research Institute, New York Blood Center, New York, NY 10065; [§]Institute of Biotechnology, Chinese Academy of Military Medical Sciences, Beijing 100071, China; and [†]Institute of Pathogen Biology, Chinese Academy of Medical Sciences and Peking Union Medical College, Beijing 100730, China

Edited by Robert C. Gallo, Institute of Human Virology, University of Maryland, Baltimore, MD, and approved September 3, 2008 (received for review July 29, 2008)

T20 (generic name: Enfuvirtide, brand name: Fuzeon) is the only FDA-approved HIV fusion inhibitor that is being used for treatment of HIV/AIDS patients who have failed to respond to current antiretroviral drugs. However, it rapidly induces drug resistance *in vitro* and *in vivo*. On the basis of the structural and functional information of anti-HIV peptides from a previous study, we designed an HIV fusion inhibitor named CP32M, a 32-mer synthetic peptide that is highly effective in inhibiting infection by a wide range of primary HIV-1 isolates from multiple genotypes with R5- or dual-tropic (R5X4) phenotype, including a group O virus (BCF02) that is resistant to T20 and C34 (another anti-HIV peptide). Strikingly, CP32M is exceptionally potent (at low picomolar level) against infection by a panel of HIV-1 mutants highly resistant to T20 and C34. These findings suggest that CP32M can be further developed as an antiviral therapeutic against multidrug resistant HIV-1.

drug-resistance | gp41 | peptide | six-helix bundle

In the early 1990s, a number of synthetic peptides derived from the N- and C-heptad repeat (NHR and CHR) regions of the HIV-1 envelope glycoprotein (Env) transmembrane subunit gp41 were discovered to have potent anti-HIV activity (1–6). Two of the CHR peptides, C34 and DP-178 (also known as T20), inhibit HIV infection at low nM levels. Biochemical and biophysical analyses suggest that these CHR peptides inhibit HIV-1 Env-mediated membrane fusion by interacting with the viral gp41 NHR region to form heterologous trimer of heterodimer and block gp41 six-helix bundle (6-HB) core formation, a critical step in virus–cell fusion (1, 7–9).

T20 (Enfuvirtide, Fuzeon), jointly developed by Trimeris and Roche, was licensed by the US FDA as the first member of a new class of anti-HIV drugs—HIV fusion inhibitors. Clinical data show that T20 is effective as a salvage therapy for HIV/AIDS patients who have failed to respond to current antiretroviral therapeutics, including reverse transcriptase inhibitors (RTIs) and protease inhibitors (PIs). However, T20 can easily induce drug resistance, resulting in increasing failure rates in T20-treated patients. Therefore, we sought to develop HIV fusion inhibitors that are effective against T20-resistant HIV.

Here we designed an HIV fusion inhibitory peptide, designated CP32M (Fig. 1), on the basis of findings from our previous studies on anti-HIV peptides containing a motif (⁶²¹QIWN-NMT⁶²⁷) located at the upstream region of the gp41 CHR, immediately adjacent to the pocket-binding domain (10), which is critical for 6-HB formation and stability. Surprisingly, CP32M is exceptionally potent against T20-resistant HIV-1 strains, with great potential to be further developed as an anti-HIV drug for treatment of HIV/AIDS patients, in particular those unresponsive to the first generation HIV fusion inhibitor used in clinics.

Results

Structure-Based Design of the Anti-HIV Peptide CP32M. We have recently found that the ⁶²¹QIWN-NMT⁶²⁷ motif located at the upstream region of the gp41 CHR, immediately adjacent to the

pocket-binding domain, is critical for the NHR and CHR interhelical interactions, and that the peptide CP621–652 containing the ⁶²¹QIWN-NMT⁶²⁷ motif possesses potent anti-HIV activity (10). We designed a peptide, designated CP32M, by using the peptide CP621–652 as a template, to improve the anti-HIV activity and drug-resistant profiles and the pharmacokinetics of the anti-HIV peptide with wild-type sequence. As shown in Fig. 1C, 11 of 32 residues (34.4%) in the peptide CP621–652 were mutated, while the residues that are important for the activity or stability of the peptide remained unchanged. The positively or negatively charged residues (e.g., K or E) were introduced into the CP32M to promote the formation of ion pairs (salt bridges) at the *i* to *i* + 4 position of the helical conformation (e.g., E⁶³⁶, K⁶⁴⁰, and K⁶⁴⁴). First residue Q⁶²¹ at the “a” position in the heptad repeat was replaced by a hydrophobic residue V to enhance its hydrophobic interaction with the NHR target. The residues I⁶²², N⁶²⁵, S⁶⁴⁰, and N⁶⁵¹, which are located at the *b*, *c*, *e*, and *f* positions in the α -helical wheel, were replaced by negatively or positively charged residues, E or K, respectively, to increase the hydrophilicity of the peptide. It was expected that introduction of these residues in the CP32M would improve its solubility and strengthen its ionic interactions with the NHR.

CP32M Is Highly Effective in Blocking HIV-1-Mediated Membrane Fusion and Inhibiting Infection by a Broad Spectrum of HIV-1 Isolates.

It was important to learn whether the engineered peptide CP32M maintained, or better yet improved its antiviral activity. First, we determined the inhibitory activity of CP32M on HIV-1 IIB-mediated cell–cell fusion by a dye transfer assay. As shown in Fig. 2A, CP32M inhibited cell–cell fusion with an IC₅₀ of 4 nM, approximately sevenfold more potent than T20 (IC₅₀ = 28 nM). Then, we assessed inhibitory activity of CP32M on HIV-1 IIB infection. Consistently, CP32M was found to be capable of inhibiting HIV-1 IIB infection in MT-2 cells with an IC₅₀ of 5 nM (Fig. 2B), approximately fourfold more effective than T20 (IC₅₀ = 26 nM). Further, we evaluated the inhibitory activity of CP32M on infection of peripheral blood mononuclear cells (PBMCs) by a panel of primary group M HIV-1 isolates. As shown in Table 1, CP32M potentially inhibited infection by primary viruses with distinct genotypes (subtypes A–G) and phenotypes (R5- and R5X4-tropic). Strikingly, CP32M effectively inhibited infection by HIV-1 group O virus (BCF02) with an IC₅₀ of 10 nM, whereas neither T20 nor C34 exhibited inhibitory activity even at a concentration as high as 2,000 nM (Fig. 2C). Therefore, CP32M is a potent HIV-1 fusion inhibitor against infection by

Author contributions: Y.H. and Q.D. designed research; J.C., H.L., J.L., J.H., Z.Q., and Z.L. performed research; S.J. contributed new reagents/analytic tools; Y.H. and S.J. analyzed data; and Y.H. and S.J. wrote the paper.

The authors declare no conflict of interest.

This article is a PNAS Direct Submission.

[†]To whom correspondence may be addressed. E-mail: yhe@nybloodcenter.org or qy_dai@yahoo.com.

© 2008 by The National Academy of Sciences of the USA

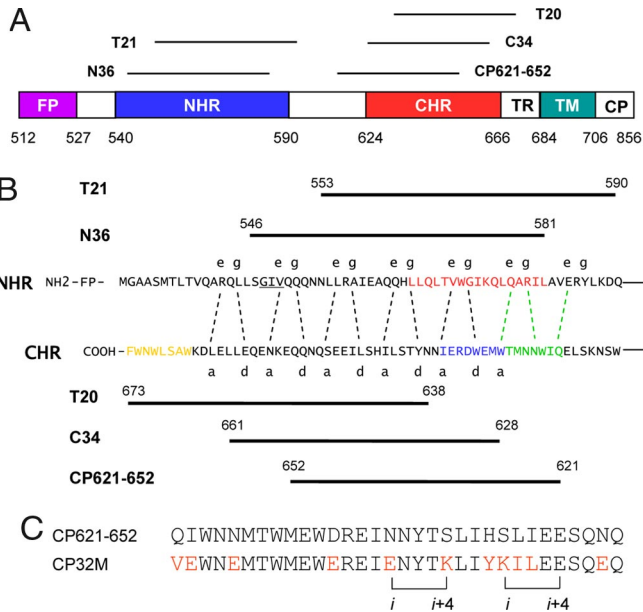


Fig. 1. Interactions of CP32M and other CHR peptides with NHR peptides. (A) Schematic view of the HIV-1_{HN} gp41 molecule. FP, fusion peptide; NHR, N-terminal heptad repeat; CHR, C-terminal heptad repeat; TR, tryptophan-rich domain; TM, transmembrane domain; CP, cytoplasmic domain. (B) In the current fusion model, the CHR region of gp41 folds back to interact with the NHR region to form a hairpin structure. Three molecules of hairpins associate with each other to form a 6-HB. The dashed lines between the NHR and CHR regions indicate the interaction between the residues located at the e, g and the a, d positions in the NHR and CHR, respectively. The interaction of the pocket-binding domain in the CHR (amino acids 628–635, in blue) with the pocket-forming domain in the NHR (amino acids 565–581, in red) is critical for stabilization of the 6-HB. Both T20 and C34 peptides contain the sequences targeting the GIV motif (in purple) in the NHR, but C34 contains the pocket-binding sequence, while T20 does not. The peptide CP621–652 overlaps the pocket-binding domain but it has no sequence targeting the GIV motif. The residues preceding the pocket-binding domain are in green. (C) Based on the CP621–652 sequence, CP32M was engineered by replacing 11 of 32 residues (the mutated residues are in red) to improve its pharmacokinetic profiles and anti-HIV activity. The positively charged residues (e.g., K) or negatively charged residues (e.g., E) were introduced to form ion pairs (salt bridges) at *i* to *i* + 4 position of the helical conformation.

both laboratory-adapted and primary HIV-1 strains with different genotypes and phenotypes.

CP32M Is Exceptionally Potent Against T20-Resistant HIV-1 Strains. Subsequently, we sought to determine whether CP32M is effective against HIV-1 strains resistant to T20. A panel of HIV-1_{NL4-3} mutants including two T20-sensitive and five T20-resistant strains (11) were used in our experiments. We found that double substitutions in the gp41 NHR (V38A/N42D, V38A/N42T, V38E/N42S, and N42T/N43K) also conferred cross-resistance to the peptide C34 (Table 2). Strikingly, CP32M was extremely active against both T20- and C34-sensitive and -resistant viruses. CP32M inhibited infection by several HIV-1_{NL4-3} mutants (N42S, V38A, and V38A/N42T) at picomolar (pM) levels. In particular, infection by HIV-1_{NL4-3} bearing V38A/N42T double mutations was shown to be effectively inhibited by CP32M with an IC_{50} of 2 pM, whereas it was highly resistant to both T20 and C34.

CP32M Interacts with the gp41 NHR Region to Form Highly Stable α -Helical Complex and Efficiently Blocks the gp41 6-HB Core Formation. We previously showed that the CHR peptide CP621–652 can interact with the NHR peptides to form typical 6-HBs (10).

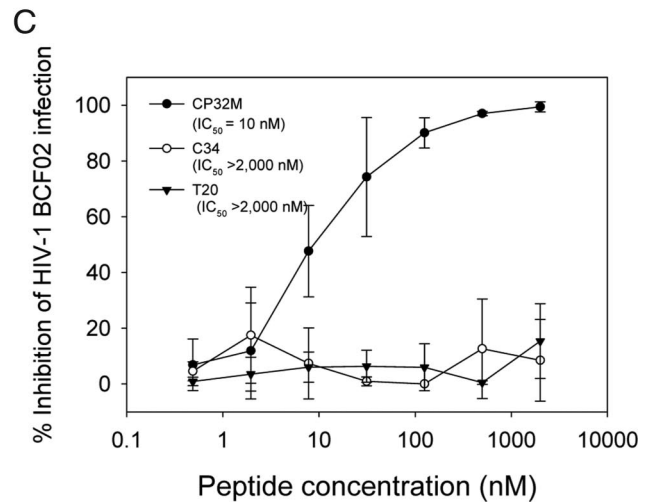
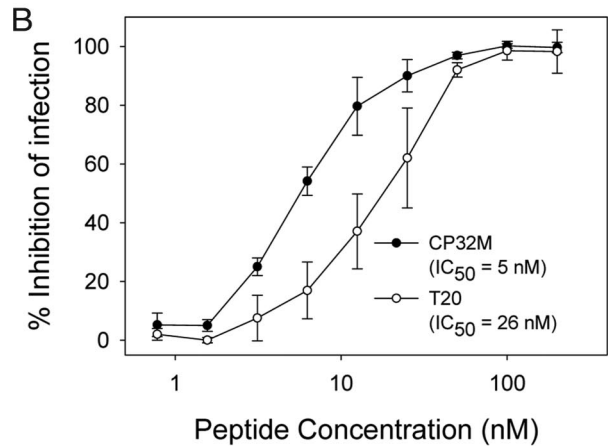
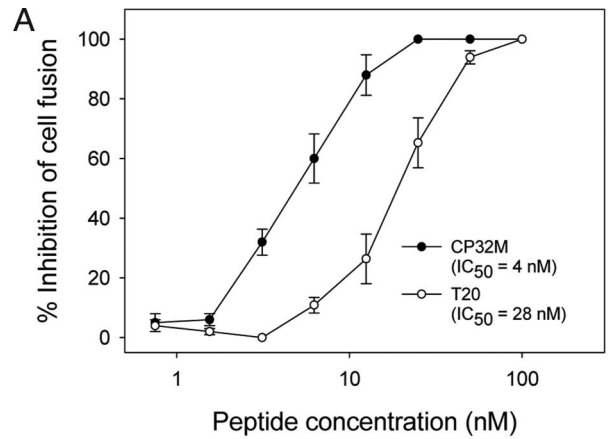


Fig. 2. Inhibition of CP32M on HIV-1-mediated cell–cell fusion (A), and on infection by HIV-1 IIIIB (B) and BCF02 (C). T20 was tested as a control. Each sample was tested in triplicate and the data are presented as mean \pm standard deviations. Numbers in parentheses indicate IC_{50} (nM) values.

It was of interest to determine whether the engineered peptide CP32M would retain its ability to interact with the NHR peptides after substitution of over one-third of its residues. As shown in Fig. 3, CP32M could form typical α -helical complexes with the NHR peptides (N36 or T21), similar to the parent peptide CP621–652 as assessed by CD spectra. Impressively, thermal denaturation analysis demonstrated that CP32M also interacted with N36 or T21 with higher thermostability (Fig. 3 B and D).

Table 1. Inhibitory activity of CP32M against infection by primary HIV-1 isolates

Virus	Subtype	Coreceptor	nM ± SD	
			IC ₅₀	IC ₉₀
RW92008	A	R5	51 ± 3	66 ± 3
94UG103	A	R5X4	30 ± 12	54 ± 14
92U5657	B	R5	235 ± 42	423 ± 40
JR-FL	B	R5	23 ± 3	37 ± 4
93IN101	C	R5	37 ± 2	80 ± 5
93MW959	C	R5	32 ± 3	83 ± 10
92UG001	D	R5X4	40 ± 6	87 ± 8
92THA009	E	R5	94 ± 16	120 ± 30
93BR020	F	R5X4	23 ± 3	105 ± 7
RU570	G	R5	84 ± 12	132 ± 30

The complex of N36/CP32M had a *T_m* value of 79°C which was 15°C higher than its wild-type bundle N36/CP621–652 (*T_m* = 64°C). The T21/CP32M complex displayed a *T_m* value (94°C) 13°C higher than the T21/CP621–652 complex (*T_m* = 81°C). As a control, the bundle N36/C34, which has been considered to be a core structure of the fusion-active gp41, had a *T_m* value of 64°C (data not shown).

We then used an N-PAGE-based method to visualize the complex formed by CP32M and counterpart peptide T21. As shown in Fig. 4A, the NHR peptide T21 shows no band in the native gel because it carries net positive charges and could migrate up and off the gel, but the negatively charged peptide CP32M shows a specific band. When CP32M was mixed with T21, a specific band corresponding to the 6-HB appeared. Their specific binding was also confirmed by size-exclusion high-performance liquid chromatography (HPLC) (Fig. 4B). Sedimentation equilibrium ultracentrifugation demonstrated that the *M_{w,app}* value of the CP32M and T21 complex was 26,600 Da (Fig. 4C). Compared to an expected molecular mass of 8,688 Da for CP32M/T21 heterodimer, we concluded that these two peptides associate to form a 6-HB structure consisting of three CP32M and T21 peptides, respectively.

The mechanism of NHR or CHR-derived anti-HIV peptides has been considered to inhibit the formation of the viral gp41 6-HB in a dominant-negative fashion (7, 12). To test whether the engineered CP32M could arrest the formation of 6-HBs, an ELISA-based method was developed, in which the 6-HB-specific mAb NC-1 was used as a capture antibody and the peptide C34 was biotinylated (see *Materials and Methods*). Consistently, NC-1 reacted specifically with the complex of N36 and C34 but not with the isolated peptides (data not shown). The results show that CP32M could efficiently inhibit the formation of 6-HB between the peptides N36 and C34-biotin in a dose-dependent manner, comparable to its parent peptide CP621–652 and C34

itself (Fig. 4D). However, T20 had no such effect at a concentration as high as 8,000 nM, consistent with our previous data (13). This result suggests that CP32M, unlike T20, is able to block 6-HB formation between the NHR and CHR in a dominant-negative fashion.

Discussion

In the present study, we designed an anti-HIV peptide, CP32M, on the basis of the structural and functional information of HIV-1 gp41 and a recently identified anti-HIV peptide (CP621–652) containing a motif (⁶²¹QIWNNMT⁶²⁷) that is critical for the 6-HB formation and stability (10). Our data have demonstrated that, like its parent peptide CP621–652 (10), the engineered CP32M maintains its potency in inhibiting HIV-1-mediated cell–cell fusion and infection by laboratory-adapted HIV-1 strains. CP32M is highly effective against a panel of primary HIV-1 strains with distinct genotypes (group M, subtypes A–G) and phenotypes (R5 and R5X4) (Table 1). Favorably, CP32M could potentially inhibit infection by BCF02, one of the HIV-1 group O isolates, having a high genetic diversity compared to the major group of HIV-1. In comparison, T20 and C34 had no inhibitory activity against infection by HIV-1_{BCF02} at a concentration as high as 2,000 nM. Therefore, the engineered peptide CP32M which has a broader anti-HIV spectrum than T20 may possess a property to overcome the genetic barrier of HIV-1 group O isolates (e.g., BCF02) and thus can be used for treatment of HIV-1 group O infection.

The most unique feature of the CP32M peptide is its exceptional potency against HIV-1 variants resistant to T20 and other CHR peptides including C34 and T1249, a second generation HIV fusion inhibitor. Although its parent peptide (CP621–652) is also effective against the drug-resistant viruses, CP32M exhibited much-improved antiviral activity against some T20-resistant mutants, with IC₅₀ in the picomolar range.

Why are CP32M and its parent peptide CP621–652 effective against HIV-1 variants resistant to T20, C34, and T1249? We believe that this is because they have different target sites in the gp41 NHR region. Early *in vitro* studies indicate that HIV-1 acquires T20 resistance by mutations in the “GIV” motif (positions 36–38 based on reference HIV-1_{HXB2} gp41 numbering, underlined in Fig. 1B) of the gp41 NHR region (11). Subsequent clinical data show that HIV-1 isolates from patients failing therapy with T20 also contain mutations in the NHR region of gp41 (amino acids 36–45: GIVQQNNLL) (14, 15). Although two changes within the amino acids 36–45 domain have been observed in some patients resistant to T20 therapy, in most cases a single mutation alone can mediate resistance (16, 17). These findings suggest that the GIV motif may be a critical binding site for T20. Indeed, Chang and colleagues have shown that the LLSGIV stretch in NHR is a crucial docking site for T20 (18, 19).

Our previous studies demonstrated that the CHR region of HIV-1 gp41 contains three functional domains (20): a pocket-

Table 2. Potent inhibitory activity of CP32M against infection by C34 and T-20-resistant viruses

HIV-1 _{NL4-3} (36G)	Phenotype*	IC ₅₀ ± SD, nM		
		T20	C34	CP32M
Parental	S	35.820 ± 14.350	3.410 ± 0.300	4.250 ± 0.130
N42S	S	28.915 ± 0.881	0.611 ± 0.142	0.042 ± 0.004
V38A	R	>2,000.000	1.686 ± 0.620	0.220 ± 0.075
V38E/N42S	R	>2,000.000	79.660 ± 4.630	4.690 ± 0.630
N42T/N43K	R	>2,000.000	119.681 ± 26.160	1.016 ± 0.359
V38A/N42T	R	>2,000.000	50.049 ± 8.305	0.002 ± 0.000
V38A/N42D	R	>2,000.000	24.474 ± 9.246	76.251 ± 11.277

*S, sensitive; R, resistant.

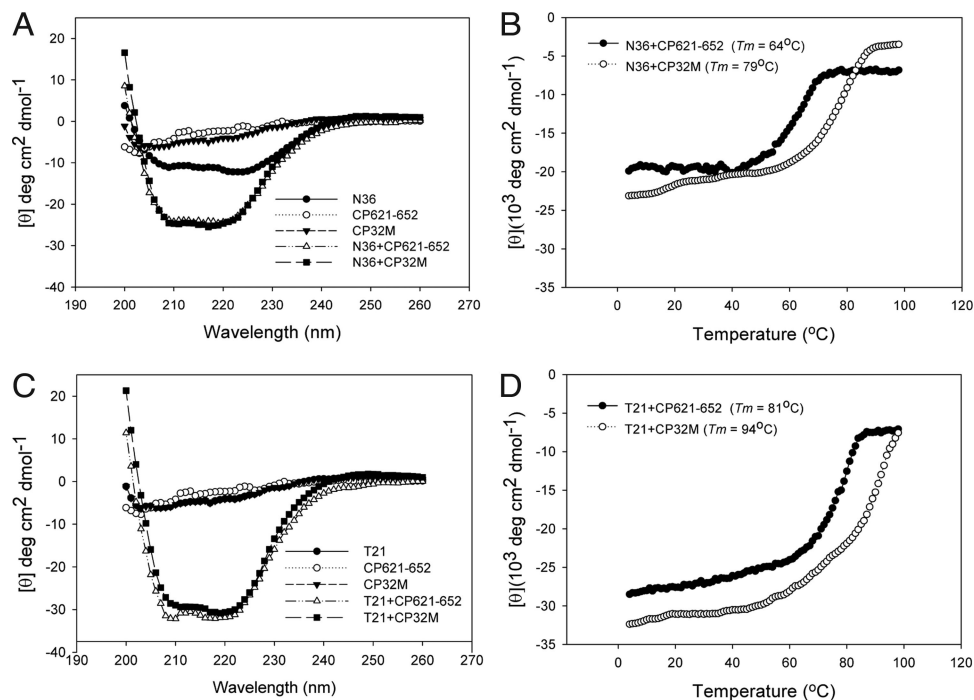


Fig. 3. Biophysical characterization of CP32M by CD spectroscopy. (A) α -helical conformation of the complex formed by N36 and CP32M or CP621–652. (B) Thermostability of the complex formed by N36 and C peptides. The unfolding temperature of each complex was scanned at 222 nm by CD spectroscopy, and their T_m values were calculated. (C) α -helical conformation of the complex formed by T21 and CP32M or CP621–652. (D) Thermostability of the complex formed by T21 and C peptides. Final concentration of each peptide in PBS is 10 μ M.

binding domain (amino acids 628–635, blue in Fig. 1B) that can bind to the pocket-forming region in NHR (red in Fig. 1B), an HR-binding domain (amino acids 628–666) which is able to interact with the 4–3 heptad repeat (HR) sequences in the gp41 NHR, and a tryptophan-rich lipid-binding domain (amino acids 666–673, orange in Fig. 1B) that has a tendency to bind lipid membranes (20). The helical packing interactions between the NHR and CHR play an essential role in viral infectivity (21–23). In particular, the hydrophobic and ionic interactions of the deep pocket region in the C terminus of the NHR groove and pocket-binding residues from the CHR can determine the conformation and stability of the fusion-active gp41 6-HB structure (1, 19, 24). T20 contains the HR- and lipid-binding domains. It inhibits HIV fusion by binding to the HR sequences in NHR, including the GIV motif, through its N-terminal HR-binding domain and interacting with the lipid membrane on the target cell, via its C-terminal lipid-binding domain (25). Mutations of the conserved GIV motif may affect the binding of T20 to the HR sequence in NHR, resulting in significant reduction of T20-mediated inhibitory activity on HIV fusion and entry. C34 contains the pocket-binding domain and shares with T20 the HR-binding sequence and thus associates with NHR to form a 6-HB through its interaction with both pocket-forming and HR-sequences in NHR. The pocket-forming region and the LLSGIV stretch in NHR are critical docking sites for C34 (18, 19). Thus, mutation of the GIV motif in viral gp41 may also affect C34 binding to the HR sequence, leading to resistance to C34. However, binding of C34 to the hydrophobic pocket region may partially compensate the decreased binding of C34 to NHR. Therefore, the viruses with GIV mutation in gp41 may be less resistant to C34 than T20 (26). T1249, a second generation HIV fusion inhibitor, contains all three functional domains, including pocket-, HR- and lipid-binding sequences. However, it functions more like T20 (25). Therefore, T20-resistant strains with GIV mutations are also insensitive to T1249 (27).

Unlike T20 and C34, CP621–652 does not contain the GIV-binding sequence, but consists of the pocket-binding domain and the 621 QIWNMT 627 motif, which is located at the upstream region of the CHR and immediately adjacent to the pocket-binding domain and is highly important for the stabilization of the gp41 core structure (10). Therefore, the mutations of the GIV motif may have little or no effect at all on the interaction of CP621–652 with the viral gp41 NHR region and consequently on the effectivity of CP621–652 against T20-resistant HIV-1 strains.

Like its parent peptide CP621–652, CP32M contains no GIV-binding sequence (Fig. 1B and C). It is expected to be efficient in inhibiting infection by T20-resistant HIV-1 variants with GIV mutations in the gp41 NHR region. After optimization of the CP621–652 sequence, the engineered CP32M demonstrated improved anti-HIV activity. Biophysical characterization showed that CP32M could form highly stable 6-HBs with the counterpart NHR peptide T21 that contains no GIV motif, and had a T_m value of 94°C, while the 6-HB formed by CP621–652 and T21 had a T_m of 81°C (Fig. 3D). This result suggests that CP32M may target the NHR with higher affinity than CP621–652. This may also explain why CP32M is much more potent than CP621–652 in inhibiting infection by HIV-1 strains resistant to T20, C34, and T1249. All these results suggest that CP32M, which has a shorter peptide sequence than T20 (36-mer) and T1249 (39-mer), has great potential to be further developed as a unique anti-HIV drug for treatment of HIV/AIDS patients who have failed to respond to the first and second generation HIV fusion inhibitors.

Materials and Methods

Peptide Synthesis. A set of peptides derived from the NHR (N36 and T21) or CHR (CP621–652, C34, and T20) of HIV-1 gp41 and CP32M (Fig. 1) were synthesized by a standard solid-phase Fmoc method using an Applied Biosystems model 433A peptide synthesizer. All peptides were acetylated at the N termini and amidated at the C termini. The peptides were purified to

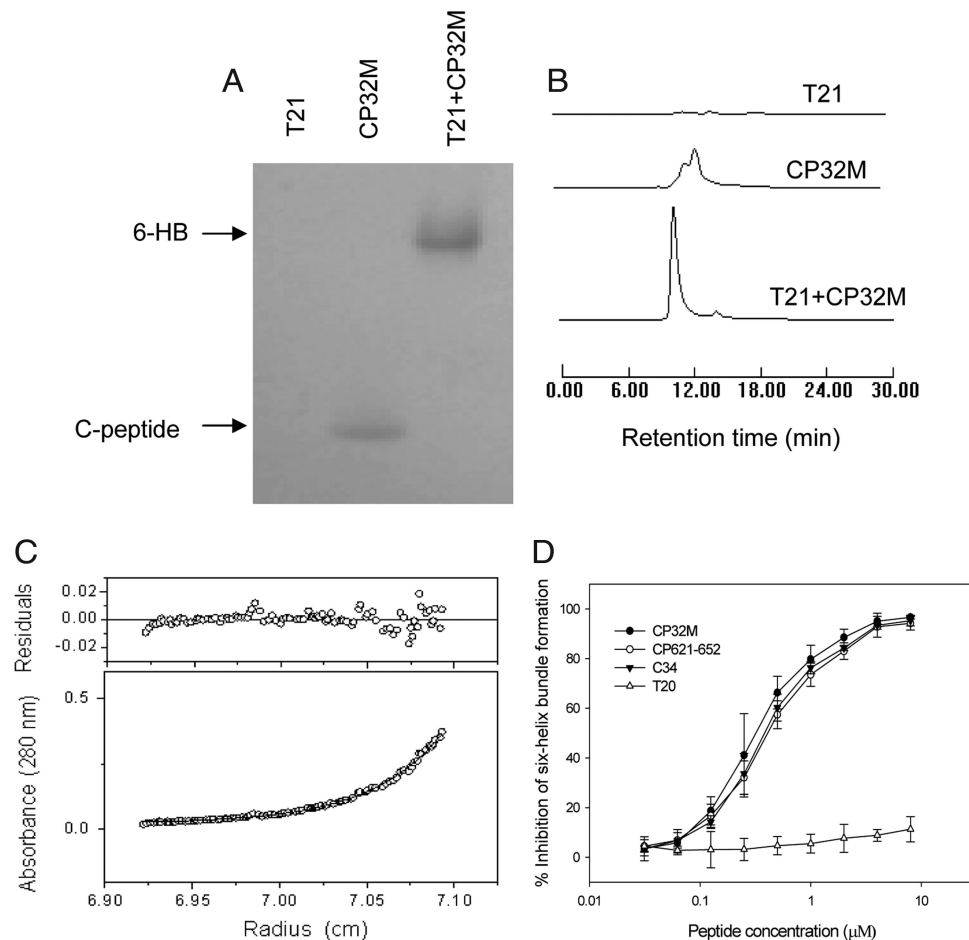


Fig. 4. Determination of the activity of CP32M to form 6-HB with T21 and to block 6-HB formation between N36 and C34. (A) N-PAGE for detection of 6-HB formation between T21 and CP32M. (B) Size-exclusion HPLC analysis for 6-HB formation between T21 and CP32M. (C) Molecular mass of the T21/CP32M complex determined by sedimentation equilibrium ultracentrifugation at concentrations of 25 μM in PBS buffer (pH 7.4) at a rotor speed of 33,000 rpm. The observed molecular mass is 26,600 Da (the calculated mass for a trimer is 26,064 Da). (D) Inhibition of C peptides on formation of 6-HB modeled by N36/C34 peptides.

homogeneity (>95% purity) by HPLC and identified by laser desorption mass spectrometry (PerSeptive Biosystems, Framingham, MA). The concentration of peptides was determined by UV absorbance and a theoretically calculated molar-extinction coefficient ϵ (280 nm) of 5500 $\text{mol/L}^{-1}\cdot\text{cm}^{-1}$ and 1490 $\text{mol/L}^{-1}\cdot\text{cm}^{-1}$ based on the number of tryptophan (Trp) residues and tyrosine (Tyr) residues (all of the peptides tested contain Trp and/or Tyr), respectively.

Circular Dichroism (CD) Spectroscopy. CD spectroscopy was performed as previously described (24). Briefly, an N peptide was incubated with a C peptide (10 μM) at 37°C for 30 min. The CD spectra of the isolated peptides and their mixtures were acquired on Jasco spectropolarimeter (Model J-715, Jasco Inc., Japan). The α -helical content was calculated from the CD signal by dividing the mean residue ellipticity at 222 nm by the value expected for 100% helix formation (i.e., 33,000° $\text{cm}^2\text{dmol}^{-1}$) according to the previous studies (28, 29). Thermal denaturation was monitored at 222 nm by applying a thermal gradient of 2°C/min in the range of 4–98°C. The melting curve was smoothed, and the midpoint of the thermal unfolding transition (T_m) values was calculated using Jasco software utilities as described previously (30).

Native Polyacrylamide Gel Electrophoresis (N-PAGE) Assay. N-PAGE was carried out to determine the 6-HB formation between the N and C peptides as described previously (31). Briefly, N peptide T21 was mixed with C peptide CP32M (40 μM) and was loaded onto a 10 \times 1.0-cm precast 18% Tris-glycine gel (Invitrogen, Carlsbad, CA). Gel electrophoresis was carried out with 125 V constant voltage at room temperature for 2 h. The gel was then stained with Coomassie Blue and imaged with a FluorChem 8800 Imaging System (Alpha Innotech).

Binding Assays by Size-Exclusion Chromatography (32). T21 was mixed with CP32M (final concentration = 0.20 mM) at a molar ratio of 1:1 in 50 mM

sodium phosphate/150 mM NaCl (pH 7.2) and incubated at 37°C for 30 min. The mixture or peptide (30 μl) was applied to the TSK-G 3000SW_{XL} HPLC column equilibrated with 50 mM sodium phosphate/150 mM NaCl and eluted at 0.8 ml/min, and fractions were monitored at 214 nm.

Sedimentation Equilibrium Centrifugation. Sedimentation equilibrium experiments were performed using an Optima XL-I analytical ultracentrifuge (Beckman) equipped with a standard two-channel cell in an An-60 Ti rotor (33). The designated peptide concentration was 25 μM in buffer consisting of 50 mM sodium phosphate/100 mM NaCl (pH 7.4), and the complex was composed of 12.5 μM N peptide (T21) and 12.5 μM C peptide (CP32M). The samples were run at 25,000 or 33,000 rpm at 20°C for 24 h. Absorbance monitoring was performed at 280 nm. The apparent molecular weight (MW_{app}) was obtained by fitting the data to self-association using the sedimentation analysis software supplied by Beckman. The partial specific volumes used for T21 and CP32M were 0.738 and 0.729 respectively, as calculated from the mass average of the partial specific volumes of the individual amino acids.

Inhibition of CP32M on 6-HB Formation. Inhibitory activity of the peptides (CP32M, CP621–652, C34, and T20) on the 6-HB formation was measured by a modified ELISA-based method as previously described (10). Briefly, a 96-well polystyrene plate was coated with a 6-HB specific monoclonal antibody NC-1 IgG (4 $\mu\text{g/ml}$ in 0.1 M Tris, pH 8.8). A test peptide at graded concentrations was mixed with C34-biotin (0.25 μM) and incubated with N36 (0.25 μM) at room temperature for 30 min. The mixture was then added to the NC-1-coated plate, followed by incubation at room temperature for 30 min and washing with a washing buffer (PBS containing 0.1% Tween 20) three times. Then, streptavidin-labeled horseradish peroxidase (Invitrogen) and the substrate 3,3',5,5'-tetramethylbenzidine (Sigma) were added sequentially. Absorbance

at 450 nm (A_{450}) was measured using an ELISA reader (Ultra 384, Tecan). The percentage of inhibition by the peptides and the IC_{50} values were calculated as previously described (34).

Cell–Cell Fusion Assay. A dye transfer assay was used for detection of HIV-1-mediated cell–cell fusion as previously described (35). Briefly, Calcein-AM-labeled H9/HIV-1_{IIIIB}-infected cells were incubated with MT-2 cells (ratio = 1:5) at 37°C for 2 h in the presence or absence of the test peptide. The fused and unfused calcein-labeled HIV-1-infected cells were counted under an inverted fluorescence microscope (Zeiss) with an eyepiece micrometer disk. The percentage of inhibition of cell–cell fusion and the IC_{50} values were calculated as described before (35).

Inhibition of HIV-1_{IIIIB} and T20-Resistant Virus. The inhibitory activity of CP32M, T20, or C34 on infection by various T20-resistant virus isolates and laboratory-adapted HIV-1 strain (HIV-1_{IIIIB}) was determined as previously described (35). In brief, 1×10^4 MT-2 cells were infected with HIV-1 isolates at 100 TCID₅₀ (50% tissue culture infective dose) in 200 μ l culture medium in the presence or absence of the test peptide overnight. Then the culture supernatants were removed and fresh media were added. On the fourth day postinfection, 100

μ l of culture supernatants were collected from each well, mixed with equal volumes of 5% Triton X-100, and assayed for p24 antigen by ELISA.

Inhibition of CP32M on Primary Viruses. The inhibitory activity of CP32M against a panel of primary HIV-1 isolates was determined as previously described (35). Briefly, the PBMCs were isolated from the blood of healthy donors using a standard density gradient (Histopaque-1077, Sigma) centrifugation. After incubation at 37°C for 2 h, the nonadherent cells were collected and resuspended at 5×10^5 /ml in RPMI medium 1640 containing 10% FBS, 5 μ g of phytohemagglutinin (PHA)/ml, and 100 U of interleukin-2/ml, followed by incubation at 37°C for 3 days. The PHA-stimulated cells were infected with the corresponding primary HIV-1 isolates at a multiplicity of infection (MOI) of 0.01 in the absence or presence of CP32M at graded concentrations. The supernatants were collected 7 days postinfection and tested for p24 antigen by ELISA.

ACKNOWLEDGMENTS. We thank Ms. Veronica Kuhlemann for editorial assistance. This work was supported by the 973 Program (Grant 2006CB504200) and 863 Program (Grant 2006A092404) from the Chinese Ministry of Science and Technology, the Nature Science Foundation of China (Grant 30870123), and the National Institutes of Health (Grant AI46221).

- Chan DC, Chutkowski CT, Kim PS (1998) Evidence that a prominent cavity in the coiled coil of HIV type 1 gp41 is an attractive drug target. *Proc Natl Acad Sci USA* 95:15613–15617.
- Jiang S, Lin K, Strick N, Neurath AR (1993) HIV-1 inhibition by a peptide. *Nature* 365:113.
- Lu M, Blacklow SC, Kim PS (1995) A trimeric structural domain of the HIV-1 transmembrane glycoprotein. *Nat Struct Biol* 2:1075–1082.
- Wild C, Oas T, McDanal C, Bolognesi D, Matthews T (1992) A synthetic peptide inhibitor of human immunodeficiency virus replication: Correlation between solution structure and viral inhibition. *Proc Natl Acad Sci USA* 89:10537–10541.
- Wild C, Greenwell T, Matthews T (1993) A synthetic peptide from HIV-1 gp41 is a potent inhibitor of virus-mediated cell–cell fusion. *AIDS Res Hum Retroviruses* 9:1051–1053.
- Wild CT, Shugars DC, Greenwell TK, McDanal CB, Matthews TJ (1994) Peptides corresponding to a predictive alpha-helical domain of human immunodeficiency virus type 1 gp41 are potent inhibitors of virus infection. *Proc Natl Acad Sci USA* 91:9770–9774.
- Chan DC, Kim PS (1998) HIV entry and its inhibition. *Cell* 93:681–684.
- Liu S, Wu S, Jiang S (2007) HIV entry inhibitors targeting gp41: From polypeptides to small-molecule compounds. *Curr Pharm Des* 13:143–162.
- Roux KH, Taylor KA (2007) AIDS virus envelope spike structure. *Curr Opin Struct Biol* 17:244–252.
- He Y, et al. (2008) Identification of a critical motif for the human immunodeficiency virus type 1 (HIV-1) gp41 core structure: Implications for designing novel anti-HIV fusion inhibitors. *J Virol* 82:6349–6358.
- Rimsky LT, Shugars DC, Matthews TJ (1998) Determinants of human immunodeficiency virus type 1 resistance to gp41-derived inhibitory peptides. *J Virol* 72:986–993.
- Weiss CD (2003) HIV-1 gp41: Mediator of fusion and target for inhibition. *AIDS Rev* 5:214–221.
- He Y, et al. (2008) Design and evaluation of Sifuvirtide, a novel HIV-1 fusion inhibitor. *J Biol Chem* 283:11126–11134.
- Mink M, et al. (2005) Impact of human immunodeficiency virus type 1 gp41 amino acid substitutions selected during enfuvirtide treatment on gp41 binding and antiviral potency of enfuvirtide in vitro. *J Virol* 79:12447–12454.
- Wei X, et al. (2002) Emergence of resistant human immunodeficiency virus type 1 in patients receiving fusion inhibitor (T-20) monotherapy. *Antimicrob Agents Chemother* 46:1896–1905.
- Greenberg ML, Cammack N (2004) Resistance to enfuvirtide, the first HIV fusion inhibitor. *J Antimicrob Chemother* 54:333–340.
- Poveda E, Briz V, Soriano V (2005) Enfuvirtide, the first fusion inhibitor to treat HIV infection. *AIDS Rev* 7:139–147.
- Chang DK, Cheng SF, Trivedi VD (1999) Biophysical characterization of the structure of the amino-terminal region of gp41 of HIV-1. Implications on viral fusion mechanism. *J Biol Chem* 274:5299–5309.
- Chang DK, Hsu CS (2007) Biophysical evidence of two docking sites of the carboxyl heptad repeat region within the amino heptad repeat region of gp41 of human immunodeficiency virus type 1. *Antiviral Res* 74:51–58.
- Liu S, et al. (2007) HIV gp41 C-terminal heptad repeat contains multifunctional domains. Relation to mechanisms of action of anti-HIV peptides. *J Biol Chem* 282:9612–9620.
- Follis KE, Larson SJ, Lu M, Nunberg JH (2002) Genetic evidence that interhelical packing interactions in the gp41 core are critical for transition of the human immunodeficiency virus type 1 envelope glycoprotein to the fusion-active state. *J Virol* 76:7356–7362.
- Liu J, Wang S, Hoxie JA, LaBranche CC, Lu M (2002) Mutations that destabilize the gp41 core are determinants for stabilizing the simian immunodeficiency virus–CPmac envelope glycoprotein complex. *J Biol Chem* 277:12891–12900.
- Lu M, et al. (2001) Structural and functional analysis of interhelical interactions in the human immunodeficiency virus type 1 gp41 envelope glycoprotein by alanine-scanning mutagenesis. *J Virol* 75:11146–11156.
- He Y, et al. (2007) Conserved residue Lys574 in the cavity of HIV-1 Gp41 coiled-coil domain is critical for six-helix bundle stability and virus entry. *J Biol Chem* 282:25631–25639.
- Eggink D, et al. (2008) Selection of T1249-resistant human immunodeficiency virus type 1 variants. *J Virol* 82:6678–6688.
- Armand-Ugon M, Gutierrez A, Clotet B, Este JA (2003) HIV-1 resistance to the gp41-dependent fusion inhibitor C-34. *Antiviral Res* 59:137–142.
- Chinnadurai R, Rajan D, Munch J, Kirchoff F (2007) Human immunodeficiency virus type 1 variants resistant to first- and second-generation fusion inhibitors and cytopathic in ex vivo human lymphoid tissue. *J Virol* 81:6563–6572.
- Shu W, et al. (2000) Helical interactions in the HIV-1 gp41 core reveal structural basis for the inhibitory activity of gp41 peptides. *Biochemistry* 39:1634–1642.
- Chen YH, Yang JT, Chau KH (1974) Determination of the helix and beta form of proteins in aqueous solution by circular dichroism. *Biochemistry* 13:3350–3359.
- Liu S, et al. (2005) Different from the HIV fusion inhibitor C34, the anti-HIV drug Fuzeon (T-20) inhibits HIV-1 entry by targeting multiple sites in gp41 and gp120. *J Biol Chem* 280:11259–11273.
- Liu S, Zhao Q, Jiang S (2003) Determination of the HIV-1 gp41 fusogenic core conformation modeled by synthetic peptides: Applicable for identification of HIV-1 fusion inhibitors. *Peptides* 24:1303–1313.
- Dai Q, Zajicek J, Castellino FJ, Prorok M (2003) Binding and orientation of conantokins in PL vesicles and aligned PL multilayers. *Biochemistry* 42:12511–12521.
- Dai Q, Castellino FJ, Prorok M (2004) A single amino acid replacement results in the Ca²⁺-induced self-assembly of a helical conantokin-based peptide. *Biochemistry* 43:13225–13232.
- Jiang SB, Lin K, Neurath AR (1991) Enhancement of human immunodeficiency virus type 1 infection by antisera to peptides from the envelope glycoproteins gp120/gp41. *J Exp Med* 174:1557–1563.
- Jiang S, et al. (2004) N-substituted pyrrole derivatives as novel human immunodeficiency virus type 1 entry inhibitors that interfere with the gp41 six-helix bundle formation and block virus fusion. *Antimicrob Agents Chemother* 48:4349–4359.



Microwave irradiation and COMU: a potent combination for solid-phase peptide synthesis

Ramon Subiros-Funosas^{a,b}, Gerardo A. Acosta^{a,b}, Ayman El-Faham^{a,c,d}, Fernando Albericio^{a,b,e,*}

^a Institute for Research in Biomedicine (IRB Barcelona), Barcelona Science Park, Baldiri Reixac 10, 08028 Barcelona, Spain

^b CIBER-BBN, Networking Centre on Bioengineering, Biomaterials and Nanomedicine, Barcelona Science Park, Baldiri Reixac 10-12, 08028 Barcelona, Spain

^c Department of Chemistry, College of Science, King Saud University, PO Box 2455, Riyadh, Saudi Arabia

^d Department of Chemistry, Faculty of Science, Alexandria University, Ibrahimia 21321, Alexandria, Egypt

^e Department of Organic Chemistry, University of Barcelona, Martí i Franqués 1-11, 08028-Barcelona, Spain

ARTICLE INFO

Article history:

Received 2 July 2009

Revised 7 August 2009

Accepted 28 August 2009

Available online 2 September 2009

Keywords:

Coupling reagents

Microwave

Peptide

Solid-phase synthesis

Oxyima

ABSTRACT

Here we demonstrate the compatibility of Oxyma-based uronium-type coupling reagent COMU with microwave-assisted peptide synthesizers. Consistent with previous reports, COMU displayed higher efficiency than benzotriazole classical immonium salts HATU and HBTU in the demanding synthesis of the Aib derivative of Leu-Enkephalin pentapeptide and did not yield Oxyma-based byproducts. Thus, the combination of microwave irradiation and COMU resulted in a similar performance in considerably shorter time to that achieved by manual synthesis.

© 2009 Elsevier Ltd. All rights reserved.

Uronium-type coupling reagent 1-[(1-(cyano-2-ethoxy-2-oxethylideneaminoxy)-dimethylamino-morpholinomethylene)] methanaminium hexafluorophosphate, **1** (COMU, Fig. 1) is a more efficient alternative to classical benzotriazole immonium salts in terms of racemization suppression, coupling effectiveness, stability, and solubility.¹ In addition to the morpholino moiety, this superiority is attributed to the introduction of ethyl 2-cyano-2-(hydroxyimino)acetate, **2** (Oxyima, Fig. 1) in its structure. Oxyma displays high control of optical purity and extension of coupling in demanding sequences.²

Both Oxyma and its related uronium salt can be handled with a considerably lower risk than its explosive benzotriazole counterparts, as determined by calorimetry techniques. However, the thermal stability of Oxyma is relatively low.^{1,2} Nonetheless, no incident has been reported during extreme coupling stability assays, carried out using microwave irradiation at 80 °C.²

Previous studies examined the stability of Oxyma toward the nucleophilic N-terminus of the growing peptide chain in extreme experiments. To enhance the likelihood of this side reaction, these experiments used a high excess of the additive in the absence of carbodiimide and Fmoc-AA-OH.² In the assay conducted at room temperature overnight, no Oxyma-based byproduct was found. In

contrast, a similar experiment with microwave irradiation gave rise to some of these undesired byproducts (Fig. 2). In that demanding experiment, the main byproduct resulted from the formylation of the amino function (**3**, 47.9%), attack of the amino group on the carboxylate (**4**) and the carbonyl of the oxime (**5**), which was also hydrolyzed (**6**). In all the cases, impurities were detected in the range 2–4%.²

In order to unequivocally determine the compatibility of the Oxyma-derived coupling reagents with microwave-assisted solid-phase peptide synthesis (SPPS), we compared the performance of COMU with that of classical immonium salts HBTU **7** and HATU **8** in the synthesis of a true peptide model conducted in an automated peptide synthesizer with microwave irradiation (Fig. 3).³

Since its first appearance in 1986, microwave irradiation has been established as a highly useful tool for solid-phase organic

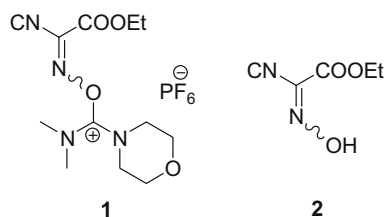


Figure 1. Structure of COMU and Oxyima.

* Corresponding author. Tel.: +11 34 93 402 9058; fax: +11 34 93 339 7878.
E-mail address: albericio@pcb.ub.es (F. Albericio).

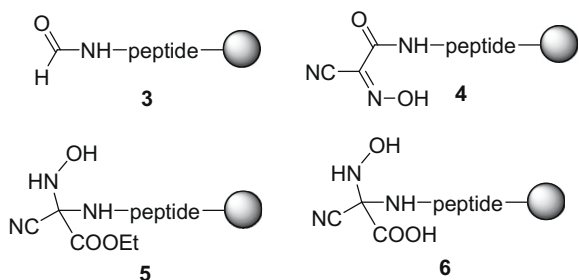


Figure 2. Side products obtained by reaction of Oxyma with a peptide in the absence of carbodiimide and Fmoc-AA-OH.

synthesis, both in academy and in industry, by increasing product yield and purity and reducing reaction times, in combination with thermal effects.^{4–6} However, few studies have reported the application of this approach in the field of peptide synthesis since the early report of Wang and co-workers in 1991.⁷ This low general acceptance could be partly attributed to the widespread belief that the acceleration rate of coupling and deprotection steps also leads to instability of coupling reagents and an increase in typical side reactions, such as racemization and aspartimide formation. Nevertheless, recent studies have confirmed that these drawbacks can be controlled with an adequate choice of reaction conditions, and also that resin loading is critical for optimal microwave-assisted peptide synthesis.^{8,9} The availability of peptide synthesizers equipped with microwave irradiation has undoubtedly contributed to the sudden increasing popularity of this tool in SPPS, which has proved compatible with both Fmoc and Boc approaches in the assembly of difficult sequences including phospho and glycopeptides, cymantrene-peptide bioconjugates, and cyclotides.^{10–16}

One of the key advantages offered by microwave irradiation (which cannot be explained by thermal effects) derives from the dipolar polarization mechanism, which provides extra energy for the rotation of the molecules with a dipolar moment, such as peptides.^{8,12} This effect is highly relevant during the elongation of long and hydrophobic peptides, since the polar peptide backbone constantly aligns with the electric field, thereby disrupting chain aggregation. Thus, peptides of up to 30-mer can be prepared easily overnight.⁸

To further demonstrate the strong performance of microwave-assisted SPPS in challenging sequences, here we report the assembly of the highly demanding Aib-analog of Leu-enkephalin pentapeptide (H-Tyr-Aib-Aib-Phe-Leu-NH₂) by means of a Liberty CEM Microwave Peptide Synthesizer. The Aib-Aib sterically hindered coupling is an excellent scenario to compare the performance of COMU **1** and benzotriazole-based HBTU **7** and HATU **8**,¹⁷ and also to study the formation of the side reactions associated with the presence of Oxyma during the coupling.

The synthesis was carried out in a 0.1 mmol scale of H-RinkAmide-ChemMatrix resin (loading = 0.42 mmol/g), a totally PEG-

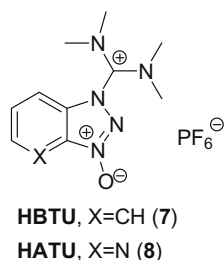


Figure 3. Structure of benzotriazole-based immonium salts HBTU and HATU.

based solid support that shows good swelling properties in both polar and non-polar solvents.^{18–21} A conditioning protocol was followed to remove any remaining base from the commercial resin before its transfer with DMF into a suitable-sized polypropylene vial. Solutions of reagents for coupling and deprotection steps were placed in appropriate vessels (Table 1).

Short single couplings were applied to introduce the five residues (6 min at 80 °C), using 1 mmol of Fmoc-amino acid (0.6 mmol for Aib, in order to enhance relative differences), 1 equiv of coupling reagent, and 2 equiv of base, relative to amino acid.²² Deprotection steps were conducted with a solution of piperidine in DMF (Table 1) at 75 °C (3 min × 2). Once automated synthesis of the pentapeptide was completed (proceeding safely with COMU **1** under the abovementioned conditions), the final cleavage from the resin was accomplished with a 2-h treatment with 90% TFA/10% H₂O at room temperature. After precipitation with cold Et₂O and lyophilization, the samples were analyzed by reverse-phase HPLC-PDA and HPLC-MS. An example of the crude mixtures obtained is shown for the synthesis with COMU **1** (Fig. 4).

Two main compounds were observed in the crude mixtures: the desired pentapeptides (H-Tyr-Aib-Aib-Phe-Leu-NH₂) and des-Aib (H-Tyr-Aib-Phe-Leu-NH₂). Only traces of other possible deletion peptides such as des-Tyr (H-Aib-Aib-Phe-Leu-NH₂) and des-Aib,Tyr (H-Aib-Phe-Leu-NH₂) were detected. Some minor peaks were observed and these were not related to the coupling reagents or deletion peptides. The relative percentages of pentapeptide/des-Aib for each coupling reagent are shown in Table 2. The highest percentage of pentapeptide was obtained with COMU **1** (92%). This performance was better than that observed for HATU **8** (79%) or HBTU **7**, (23%). The manual synthesis with COMU at room temperature afforded a higher percentage of the Aib-enkephalin pentapeptide (99.7%);¹ however, coupling times were much longer (60 min, double coupling) than those in the abovementioned microwave synthesis (6 min). These results therefore highlight the enhanced efficiency of the method presented.

In our experiment with COMU, carried out in more realistic conditions than those abovementioned, no byproducts (**4–6**) related to

Table 1
Reagents and solvents used for microwave-assisted Fmoc-SPPS

	Reagent	Concentration	Solvent
Amino acid	Fmoc-AA-OH	0.2 M	DMF
Activator	HBTU/HATU/COMU	0.5 M	DMF
Base	DIEA	2 M	DMF
Deprotection	Piperidine	20% v/v	DMF

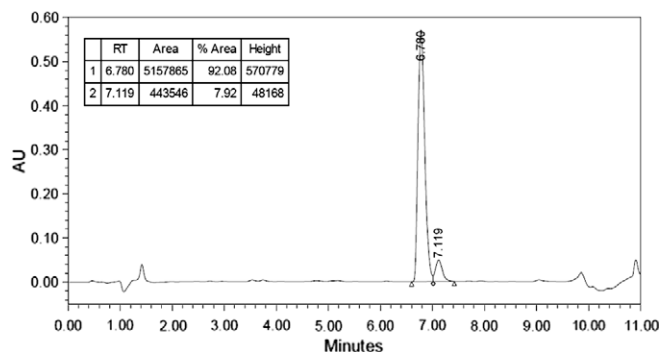


Figure 4. HPLC analysis of the crude obtained from the experiment using COMU. HPLC conditions: Waters SunFire C18 column (3.5 μm, 4.6 × 100 mm); linear gradient 20–30% of 0.036% TFA in CH₃CN/0.045% TFA in H₂O over 8 min; flow = 1.0 ml/min; detection at 220 nm; t_R (penta) = 6.780 min, [M+H]⁺ = 611.35; t_R (des-Aib) = 7.119 min, [M+H]⁺ = 526.30.

Table 2
Relative percentages of pentapeptide/des-Aib with various coupling reagents

Coupling reagent	Pentapeptide (%)	Des-Aib (%)	Yield (%)
COMU (1)	92.1	7.9	88.5
HBTU (7)	23.1	76.9	20.5
HATU (8)	79.5	20.5	76.0

the Oxyma moiety contained in the coupling reagent were detected. However, traces of guanidylation were found at the dipeptide stage²³ with each coupling reagent, during the introduction of the first Aib residue.

In summary, here we demonstrate the compatibility of Oxyma-based COMU **1** with microwave-assisted SPPS, during the automated synthesis of Aib-enkephalin pentapeptide. The Oxyma moiety contained in COMU also displayed high nucleophilic stability to the N-terminus of the growing peptide chain, as shown by the absence of Oxyma-based byproducts. Consistent with the previous reports, COMU showed better performance than classical immonium salts HATU and HBTU, which yielded lower percentages of the desired pentapeptide. On the basis of our findings, we conclude that the combination of COMU and microwave irradiation is an efficient approach for SPPS, as it yielded more than 90% of Aib-enkephalin, a highly demanding pentapeptide, in considerably less time than the conventional manual synthesis.

Acknowledgments

This work was partially supported by CICYT (CTQ2006-03794/BQU), Luxembourg Bio Technologies, Ltd., the *Generalitat de Catalunya* (2005SGR 00662), the Institute for Research in Biomedicine, and the Barcelona Science Park. R.S.-F. thanks the *Ministerio de Educación y Ciencia* for a FPU Ph.D. fellowship.

References and notes

- El-Faham, A.; Subirós-Funosas, R.; Prohens, R.; Albericio, F. *Chem. Eur. J.* in press. doi:10.1002/chem.200900615.
- Subirós-Funosas, R.; Prohens, R.; Barbas, R.; El-Faham, A.; Albericio, F. *Chem. Eur. J.* in press. doi:10.1002/chem.200900614.
- Carpino, L. A.; Imazumi, H.; El-Faham, A.; Ferrer, F. J.; Zhang, C.; Lee, Y.; Foxman, B. M.; Henklein, P.; Hanay, C.; Mügge, C.; Wenschuh, H.; Klose, J.; Beyermann, M.; Bienert, M. *Angew. Chem., Int. Ed.* **2002**, *41*, 441–445.
- Giguere, R. J.; Bray, T. L.; Duncan, S. M.; Majetich, G. *Tetrahedron Lett.* **1986**, *27*, 4945–4948.
- Lidstrom, P.; Tierney, J.; Wathey, B.; Westman, J. *Tetrahedron* **2001**, *57*, 9225–9283.
- de la Hoz, A.; Diaz-Ortiz, A.; Moreno, A. *Chem. Soc. Rev.* **2005**, *34*, 164–178.
- Chen, S. T.; Chiou, S. H.; Wang, K. T. *J. Chin. Chem. Soc.* **1991**, *38*, 85–91.
- Palasek, S. A.; Cox, Z. J.; Collins, J. M. *J. Pept. Sci.* **2007**, *13*, 143–148.
- Coantic, S.; Subra, G.; Martinez, J. *Int. J. Pept. Res. Ther.* **2008**, *14*, 143–147.
- Bacsa, B.; Desai, B.; Dibo, G.; Kappe, C. O. *J. Pept. Sci.* **2006**, *12*, 633–638.
- Katritzky, A. R.; Khashab, N. M.; Yoshioka, M.; Haase, D. N.; Wilson, K. R.; Johnson, J. V.; Chung, A.; Haskell-Luevano, C. *Chem. Biol. Drug Des.* **2007**, *70*, 465–468.
- Cemazar, M.; Craik, D. J. *J. Pept. Sci.* **2008**, *14*, 683–689.
- Brandt, M.; Gammeltoft, S.; Jensen, K. J. *Int. J. Pept. Res. Ther.* **2006**, *12*, 349–357.
- Nagaike, F.; Onuma, Y.; Kanazawa, C.; Hojo, H.; Ueki, A.; Nakahara, Y.; Nakahara, Y. *Org. Lett.* **2006**, *8*, 4465–4468.
- Peindy N'dongo, H. W.; Ott, I.; Gust, R.; Schatzschneider, U. *J. Organomet. Chem.* **2009**, *694*, 823–827.
- Leta Aboye, T.; Clark, R. J.; Craik, D. J.; Goransson, U. *ChemBioChem* **2008**, *9*, 103–113.
- El-Faham, A.; Albericio, J. *Org. Chem.* **2008**, *73*, 2731–2737.
- García-Martín, F.; Quintanar-Audelo, M.; García-Ramos, Y.; Cruz, L. J.; Gravel, C.; Furic, R.; Côté, S.; Tulla-Puche, J.; Albericio, F. *J. Comb. Chem.* **2006**, *8*, 213–220.
- García-Martín, F.; White, P.; Steinauer, R.; Côté, S.; Tulla-Puche, J.; Albericio, F. *Biopolymers (Pept. Sci.)* **2006**, *84*, 566–575.
- de la Torre, B. G.; Jakab, A.; Andreu, D. *Int. J. Pept. Res. Ther.* **2007**, *13*, 265–270.
- Frutos, S.; Tulla-Puche, J.; Albericio, F.; Giralte, E. *Int. J. Pept. Res. Ther.* **2007**, *13*, 221–227.
- Common microwave protocols were used, showing the compatibility of COMU, HATU, and HBTU with those protocols.
- Albericio, F.; Bofill, J. M.; El-Faham, A.; Kates, S. A. *J. Org. Chem.* **1998**, *63*, 9678–9683.

Synthesis and Pharmacological in Vitro and in Vivo Evaluations of Novel Triazole Derivatives as Ligands of the Ghrelin Receptor. 1

Luc Demange,[†] Damien Boeglin,[†] Aline Moulin,[†] Delphine Mousseaux,[†] Joanne Ryan,[†] Gilbert Bergé,[†] Didier Gagne,[†] Annie Heitz,[‡] Daniel Perrissoud,[§] Vittorio Locatelli,[⊥] Antonio Torsello,[⊥] Jean-Claude Galleyrand,[†] Jean-Alain Fehrentz,^{*,†,‡,⊥,⊥} and Jean Martinez^{†,⊥}

Institut des Biomolécules Max Mousseron, UMR 5247, CNRS—Universités Montpellier I et II, BP. 14491, Faculté de Pharmacie, 15 avenue Charles Flahault, 34093 Montpellier Cedex 5, France, CBS, UMR 5048, 29 rue de Navacelles 34090 Montpellier, France, Zentaris GmbH, Weismuellerstrasse 50, 60314 Frankfurt am Main, Germany, and Department of Experimental Medicine, School of Medicine, University of Milano-Bicocca, via Cadore 48, 20052 Monza (MI), Italy

Received January 9, 2007

A new series of growth hormone secretagogue (GHS) analogues based on the 1,2,4-triazole structure were synthesized and evaluated for their in vitro binding and their ability to stimulate intracellular calcium release to the cloned hGHS-1a ghrelin receptor expressed in LLC PK-1 cells. We have synthesized potent ligands of this receptor, some of them behaving as agonists, partial agonists, or antagonists. Some compounds among the most potent, i.e., agonist **29c** (JMV2873), partial agonists including **21b** (JMV2810), antagonists **19b** (JMV2866) and **19c** (JMV2844), were evaluated for their in vivo activity on food intake, after sc injection in rodents. Some compounds were found to stimulate food intake like hexarelin; some others were identified as potent hexarelin antagonists in this assay. Among the tested compounds, **21b** was identified as an in vitro ghrelin receptor partial agonist, as well as a potent in vivo antagonist of hexarelin-stimulated food intake in rodents. Compound **21b** was without effect on GH release from rat. However, in this series of compounds, it was not possible to find a clear correlation between in vitro and in vivo results.

Introduction

Growth hormone (GH) is an important endocrine regulator of growth and anabolic processes.¹ The use of recombinant human GH is beneficial in the treatment of GH-deficient children² and has been shown to reverse some of the effects of aging in the elderly.³ In recent years, the GH releasing peptides (GHRPs) and peptidomimetics have received considerable attention as potential alternatives to the expensive recombinant human GH. During their studies on enkephalin analogues Bowers et al. discovered a series of peptides able to stimulate GH release from rat pituitary, and in doing so, they opened a new avenue for research.⁴ This new family of peptides⁵ including GHRP-6, GHRP-1, GHRP-2, and hexarelin promotes the release of GH in humans. This GH releasing mechanism was found to be different from that of the endogenous growth hormone releasing hormone (GHRH)⁶ and to be mediated through a G-protein coupled receptor named growth hormone secretagogue receptor type 1a (GHS-R1a).⁷ The natural ligand for this receptor, named ghrelin, has been isolated and recently characterized from rat stomach⁸ and further identified in humans.⁹ It is constituted of a 28 amino acid peptide in which serine in position 3 is n-octanoylated. Several classes of small nonpeptide molecule secretagogues (benzolactam biphenyl tetrazoles,¹⁰ camphor derivatives,¹¹ and 4-spiropiperidines¹²) have been described and are able to release GH from the pituitary. Various peptide molecules, based on the GHRP-6 sequence, have been reported as potent GHRPs. Starting from a tripeptide EP-51389, Aib-(D)-2-Me-Trp-(D)-2-Me-Trp-NH₂,¹³

we recently described a new potent growth hormone secretagogue, namely, JMV1843¹⁴ (EP-1572),¹⁵ which is orally active in humans. As JMV1843 is a peptide derivative, we wanted to limit the inherent flexibilities of the peptide backbone and side chains. For this purpose we decided to introduce a cyclic structure as scaffold bearing the three major pharmacophores contained in JMV1843: a basic amino group (in our case included in an amino-isobutyric acid residue) and two hydrophobic regions (indole rings). Several cyclic scaffolds were tested such as piperazines, keto-piperazines, piperidines, and triazinones (unpublished results). 1,2,4-Triazoles were found to be the best templates. In this paper, we report on the identification of a new series of potent nonpeptide analogues that acted as ghrelin receptor ligands and exhibited agonist, partial agonist, or antagonist properties.

1,2,4-Triazoles have gained considerable interest among medicinal chemists because they display a wide range of antifungal¹⁶ and antibacterial¹⁷ activities. This moiety was also found in a series of potent agonist or antagonist G-protein coupled receptor ligands.^{18–21} 1,2,4-Triazole derivatives have been used as mimics^{20–23} or isosteres^{24,25} of the amide bond in an attempt to increase the bioavailability of the parent bioactive molecules. They have also been incorporated into peptides to surrogate cis amide bonds.²⁶

Chemistry

Triazole derivatives were synthesized in five steps as shown in Scheme 1, starting from Boc-(D)-Trp-OH. After coupling to an amine, the formed amide **1** was transformed into the thioamide **2** using Lawesson's reagent. The obtained thioamide **2** was then treated with 2.0 equiv of hydrazide and 1.1 equiv of mercury(II) acetate in THF, according to Hitotsuyanagi et al.²⁷ to obtain the cyclized triazole derivatives.²⁸ Completion of this step was monitored by reversed-phase HPLC, which showed that cyclization into triazoles **3** was achieved within 2

* To whom correspondence should be addressed. Phone: 33 4 67 54 86 51. Fax: 33 4 67 54 86 54. E-mail: jean-alain.fehrentz@univ-montp1.fr.

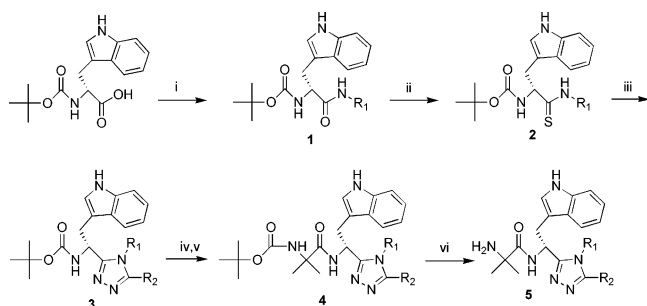
[†] CNRS—Universités Montpellier I et II.

[‡] CBS.

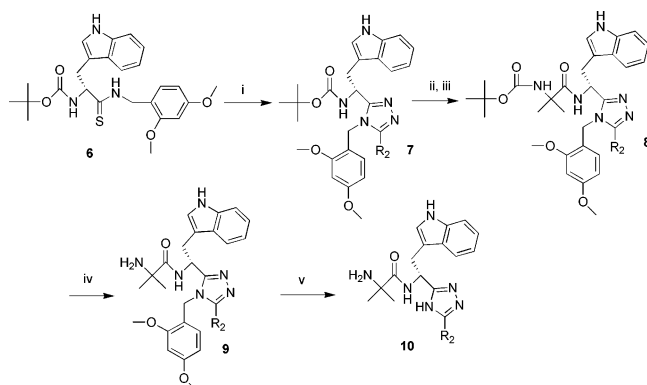
[§] Zentaris GmbH.

[⊥] University of Milano-Bicocca.

[⊥] Equal contributors.

Scheme 1. General Synthetic Scheme for the Synthesis of 3,4,5-Trisubstituted 1,2,4-Triazoles^a

^a (i) BOP, H₂N-R₁, NMM, DCM; (ii) Lawesson's Reagent, DME, 85 °C; (iii) H₂N-HN-COR₂, Hg(OAc)₂, room temperature, THF; (iv) HCl, AcOEt; (v) Boc-Aib-OH, BOP, DIPEA, DCM; (vi) HCl, AcOEt.

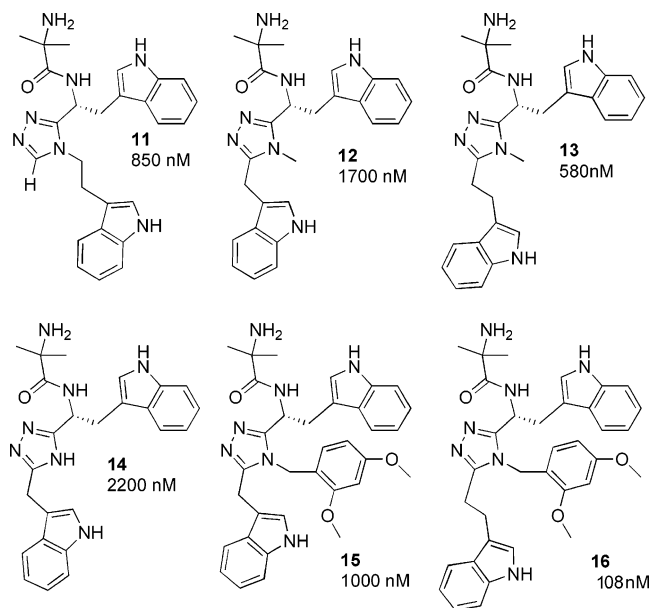
Scheme 2. General Synthetic Scheme for the Synthesis of 3,5-Disubstituted 1,2,4-Triazoles^a

^a (i) H₂N-HN-COR₂, Hg(OAc)₂, room temperature, THF; (ii) HCl, AcOEt; (iii) Boc-Aib-OH, BOP, DIPEA, DCM; (iv) HCl, AcOEt; (v) TFA, DCM.

days. Compounds were purified by silica gel column chromatography. Removing of the Boc protecting group by 4 M HCl in AcOEt and coupling with Boc-Aib-OH in the presence of BOP^{a29} and NMM in DCM produced the N-protected desired compounds **4**. The final compounds **5** were obtained after 4 M HCl in AcOEt.

When R₁ was a hydrogen atom, formation of the triazole moiety was not observed. Careful examination of LC/MS spectra revealed the presence of the corresponding nitrile derivative. This "desulfuration" of nonsubstituted thioamides already described on simple aliphatic and aromatic primary thioamides³⁰ illustrates that this synthetic pathway was not suitable for the preparation of 3,5-disubstituted 1,2,4-triazoles. We therefore decided to introduce a protecting group on the primary amide function that could be cleaved after formation of the desired triazole moiety (**7**). For this purpose, 2,4-dimethoxybenzylamine was chosen as a protecting group that did not interfere with the formation of the triazole moiety **7**. After completion of the synthesis compounds **9** and **10** were obtained, substituted or not in position 4 of the triazole moiety.

A set of six initial compounds (**11–16**, Figure 1) were synthesized as depicted in Schemes 1 and 2, all bearing an indole group in position 5 of the triazole cycle with one or two carbon atoms between the indole and the triazole.

**Figure 1.** Structure and IC₅₀ of the first synthesized triazoles.

Results and Discussion

Compounds **11–16** were tested for their ability to displace ¹²⁵I-His⁹-ghrelin from the cloned hGHS-1a receptor transiently expressed in LLC PK-1 cells. Their binding affinities were found in the micromolar range. Interestingly, comparison between compounds **12**, **13**, **14**, and **15**, respectively, showed that a two-carbon chain bearing the indole group in position 5 was well accepted by the ghrelin receptor. Substitution of the nitrogen at position 4 also had a beneficial effect (i.e., compound **16**, IC₅₀ 108 nM) (Figure 1). According to the observations that affinity for the ghrelin receptor could be modulated by substitutions at the position 4 and 5 of the triazole moiety, several compounds were synthesized to explore R₁ and R₂. Various aryl and/or alkyl groups were introduced in positions 4 and 5 (R₁ and R₂ groups). These compounds were synthesized according to Schemes 1 and 2. The synthesized compounds were tested for their ability to displace ¹²⁵I-His⁹-ghrelin from the cloned hGHS-1a receptor transiently expressed in LLC PK-1 cells. Binding affinities of human ghrelin and MK-0677 obtained with this model were in accordance with the literature. Their biological in vitro activity was then evaluated on [Ca²⁺]_i mobilization in GHS-R1a at a concentration of 10⁻⁵ M of each compound and expressed as a percent of the maximal response induced by 10⁻⁷ M ghrelin (Table 1). The best compounds were tested in vivo, for their ability to stimulate food intake or to inhibit hexarelin-stimulated food intake.

The results of their biological activity at the GHS-1a receptor are reported in Table 1. R₁ aromatic groups in position 4 of the triazole moiety were generally well tolerated for interaction with the GHS-1a receptor. As shown for compounds **16–20**, methoxy substitutions on the aromatic moiety led to potent ghrelin receptor ligands, the best compounds in this series bearing a 4-methoxybenzyl (**19b**, IC₅₀ 11 ± 4 nM; **19c**, IC₅₀ 6 ± 3 nM) or a 3-methoxybenzyl group (**18a**, IC₅₀ 18 ± 5 nM; **18b**, IC₅₀ 22 ± 4 nM) (Table 1). 2-Methoxybenzyl and dimethoxybenzyl substitution at position 4 of the triazole moiety led to derivatives presenting less affinity for the GHS-R1a compared to that of the corresponding 3- or 4-methoxy derivatives (Table 1). We then introduced various benzyl groups in position 4 of the triazole moiety. Bromide-, fluoride-, and chloride-substituted benzyl derivatives yielded less potent ligands for the GHS-1a receptor (compounds **22a–c**, **23a–c**, and **24a–c**). Electron-

^a Abbreviations: BOP, (benzotriazol-1-yloxy)-tris(dimethylamino)-phosphonium hexafluorophosphate; DME, ethylene glycol dimethyl ether; DCM, dichloromethane; NMM, *N*-methyl-morpholine. Other abbreviations used were those recommended by the IUPAC-IUB Commission [*Eur. J. Biochem.* **1984**, *138*, 9–37].

Table 1. Binding Affinities and Biological Activities of Compounds of General Formula **5** in Scheme 1

comps	R ₁	R ₂	binding IC ₅₀ (nM) ^a	% of max [Ca ²⁺] _i response at 10 μM ^b	biological activity (nM)
16	2,4-dimethoxybenzyl	1 <i>H</i> -indole-3-yl-ethyl	108 ± 17	0	antagonist; K _b , 14 ± 2
16a	2,4-dimethoxybenzyl	benzyl	560 ± 130	0	antagonist
16b	2,4-dimethoxybenzyl	1 <i>H</i> -indole-3-yl-propyl	750 ± 100	27 ± 1	partial agonist
16c	2,4-dimethoxybenzyl	phenethyl	60 ± 10	0	antagonist; K _b , 17 ± 7
17a	3,5-dimethoxybenzyl	1 <i>H</i> -indole-3-yl-ethyl	150 ± 31	22 ± 1	partial agonist
17b	3,5-dimethoxybenzyl	phenethyl	> 1000	0	antagonist
17c	3,5-dimethoxybenzyl	benzyl	110 ± 30	29 ± 1	partial agonist
18a	3-methoxybenzyl	1 <i>H</i> -indole-3-yl-ethyl	18 ± 5	63 ± 13	partial agonist; EC ₅₀ , 4 ± 1
18b	3-methoxybenzyl	1 <i>H</i> -indole-3-yl-propyl	22 ± 4	66 ± 11	partial agonist; EC ₅₀ , 18 ± 3
18c	3-methoxybenzyl	phenethyl	78 ± 15	82 ± 31	partial agonist; EC ₅₀ , 45 ± 6
18d	3-methoxybenzyl	benzyl	120 ± 20	50 ± 18	partial agonist
19a	4-methoxybenzyl	1 <i>H</i> -indole-3-yl-methyl	660 ± 40	0	antagonist
19b	4-methoxybenzyl	phenethyl	11 ± 4	0	antagonist; K _b , 5 ± 1
19c	4-methoxybenzyl	1 <i>H</i> -indole-3-yl-ethyl	6 ± 3	0	antagonist; K _b , 4 ± 1
19d	4-methoxybenzyl	phenylpropyl	12 ± 3	0	antagonist; K _b , 14 ± 4
19e	4-methoxybenzyl	benzyl	121 ± 33	0	antagonist
19f	4-methoxybenzyl	1 <i>H</i> -indole-3-yl-propyl	145 ± 30	0	antagonist; K _b , 12 ± 0.2
20a	2-methoxybenzyl	benzyl	410 ± 110	66	partial agonist
20b	2-methoxybenzyl	1 <i>H</i> -indole-3-yl-ethyl	96 ± 13	50	partial agonist
20c	2-methoxybenzyl	phenethyl	56 ± 18	80 ± 25	partial agonist; EC ₅₀ , 98 ± 17
21a	benzyl	1 <i>H</i> -indole-3-yl-ethyl	15 ± 5	73 ± 13	partial agonist; EC ₅₀ , 64 ± 14
21b	benzyl	1 <i>H</i> -indole-3-yl-propyl	33 ± 7	30 ± 4	partial agonist; EC ₅₀ , 49 ± 14
21c	benzyl	benzyl	500 ± 70	44 ± 10	partial agonist
22a	4-bromobenzyl	1 <i>H</i> -indole-3-yl-ethyl	100 ± 30	27 ± 13	partial agonist
22b	4-bromobenzyl	1 <i>H</i> -indole-3-yl-propyl	150 ± 30	25 ± 9	partial agonist
22c	4-bromobenzyl	benzyl	440 ± 50	16 ± 5	partial agonist
23a	4-fluorobenzyl	1 <i>H</i> -indole-3-yl-ethyl	66 ± 11	59 ± 16	partial agonist; EC ₅₀ , 210 ± 40
23b	4-fluorobenzyl	benzyl	170 ± 60	60 ± 3	partial agonist
23c	4-fluorobenzyl	phenethyl	400 ± 130	20 ± 9	partial agonist
24a	3,4-dichlorobenzyl	1 <i>H</i> -indole-3-yl-ethyl	55 ± 8	28 ± 1	partial agonist
24b	3,4-dichlorobenzyl	benzyl	520 ± 50	64 ± 12	partial agonist
24c	3,4-dichlorobenzyl	phenethyl	640 ± 10	53 ± 9	partial agonist
25a	phenethyl	1 <i>H</i> -indole-3-yl-ethyl	80 ± 10	25 ± 6	partial agonist
25b	phenethyl	1 <i>H</i> -indole-3-yl-methyl	300 ± 60	88 ± 30	partial agonist
25c	phenethyl	1 <i>H</i> -indole-3-yl-propyl	11 ± 4	18 ± 3	partial agonist; EC ₅₀ , 15 ± 2
25d	phenethyl	benzyl	> 1000	85 ± 26	partial agonist
25e	phenethyl	phenethyl	310 ± 30	63 ± 13	partial agonist
26a	2,2-diphenylethyl	benzyl	> 1000	60 ± 20	partial agonist
26b	2,2-diphenylethyl	1 <i>H</i> -indole-3-yl-ethyl	640 ± 250	62 ± 7	partial agonist
27a	(naphtalen-1-yl)methyl	benzyl	220 ± 30	78 ± 26	partial agonist
27b	(naphtalen-1-yl)methyl	1 <i>H</i> -indole-3-yl-propyl	140 ± 3	62 ± 2	partial agonist
27c	(naphtalen-1-yl)methyl	1 <i>H</i> -indole-3-yl-ethyl	125 ± 50	54 ± 1	partial agonist
27d	(naphtalen-1-yl)methyl	phenethyl	130 ± 1	40 ± 12	partial agonist
28a	<i>n</i> -hexyl	benzyl	470 ± 40	67 ± 6	partial agonist
28b	<i>n</i> -hexyl	1 <i>H</i> -indole-3-yl-ethyl	195 ± 35	62 ± 33	partial agonist
28c	<i>n</i> -hexyl	1 <i>H</i> -indole-3-yl-propyl	240 ± 50	32 ± 3	partial agonist
29a	1 <i>H</i> -indole-3-yl-ethyl	benzyl	700 ± 120	95 ± 9	agonist
29b	1 <i>H</i> -indole-3-yl-ethyl	1 <i>H</i> -indole-3-yl-ethyl	150 ± 5	82 ± 17	partial agonist
29c	1 <i>H</i> -indole-3-yl-ethyl	1 <i>H</i> -indole-3-yl-propyl	14 ± 2	85 ± 22	agonist; EC ₅₀ , 140 ± 30
30a	4-methylbenzyl	phenylpropyl	21 ± 2	16 ± 3	partial agonist; EC ₅₀ , 12 ± 0.7
30b	4-methylbenzyl	benzyl	840 ± 220	28 ± 4	partial agonist
30c	4-methylbenzyl	1 <i>H</i> -indole-3-yl-ethyl	28 ± 5	69 ± 6	partial agonist; EC ₅₀ , 630 ± 190
30d	4-methylbenzyl	phenethyl	140 ± 30	19 ± 15	partial agonist
31	4-ethylbenzyl	phenethyl	44 ± 17	26 ± 5	partial agonist; EC ₅₀ , 11 ± 5
32	4-nitrobenzyl	phenethyl	> 1000	10 ± 4	weak agonist
33a	(pyridin-2-yl)methyl	benzyl	> 1000	78 ± 3	partial agonist
33b	(pyridin-2-yl)methyl	phenethyl	> 1000	59 ± 20	partial agonist
34	4-methoxyphenethyl	phenethyl	550 ± 50	82 ± 40	partial agonist
35	(thiophen-2-yl)methyl	phenethyl	570 ± 40	91 ± 9	agonist
36	(furan-2-yl)methyl	phenethyl	420 ± 100	97 ± 6	agonist; EC ₅₀ , 23 ± 2
37	phenyl	1 <i>H</i> -indole-3-yl-ethyl	140 ± 20	91 ± 4	agonist; EC ₅₀ , 41 ± 3

^a Inhibition of ¹²⁵I-His⁹-ghrelin binding to membranes from *h*GHS-R1a transfected LLC cells. ^b Maximum calcium flux activity is reported relative to ghrelin at 0.1 μM.

withdrawing groups such as 4-nitro or electron-donating groups such as 4-methyl or 4-ethyl on the benzyl ring were also introduced in position 4 of the triazole moiety. It clearly appeared that electron-withdrawing groups were not tolerated at this position of the molecule (compound **32**), while electron-donating groups were privileged (**30a–d**, **31**). The significance of the length of the carbon chain between the triazole and the phenyl rings was studied. Phenyl, benzyl, and phenethyl groups

were introduced as R₁ substituents (**37**, **21a**, and **25a**). The benzyl group led to the compounds that exhibited the better affinity for the GHS-1a receptor. Naphtalen-1-yl-methyl and 2,2-diphenylethyl groups (**26a,b**, **27a–d**) were introduced. The affinity of the obtained compounds was lower than that of the benzyl-containing derivatives. Pyridin-2-yl-methyl, thiophen-2-yl-methyl, and furan-2-yl-methyl substituents led to compounds (**33a,b**, **35**, and **36**) of low affinity for the GHS-1a

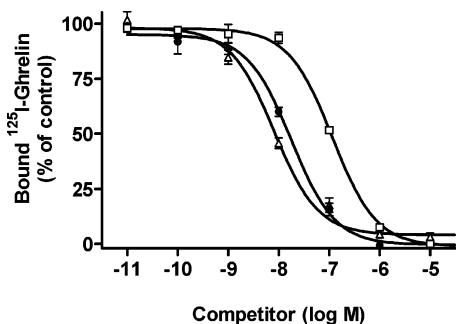


Figure 2. Ability of compounds **16** (\square), **19b** (Δ), or **25c** (\bullet) to inhibit binding of ^{125}I -His⁹-ghrelin to membranes from *hGHS-R1a*-transfected LLC cells. Results are expressed as the percentage of radioactivity bound in the absence of added nonradioactive compounds. In each experiment, each value was determined in triplicate, and the results given are means from at least three separate experiments. Nonspecific binding was determined in the presence of 10 μM ghrelin and was always less than 20% of total binding.

receptor. An indole group was also introduced at position 4 (**29a** and **29b**) without improving the affinity for the ghrelin receptor. A three-carbon chain bearing the indole group in position 5 of the triazole yielded compound **29c** with an improved binding affinity when compared with that of compound **29b**. Introducing a lipophilic chain (compounds **28a–c**) at the 4 position of the indole moiety to mimic the octanoyl group of the natural ghrelin ligand led to compounds having less affinity.

In position 5 of the triazole moiety (R_2 group), six different phenyl and indole-derived substituents were explored linked to the triazole moiety by an aliphatic chain composed of one, two, or three carbon atoms. The best compounds were obtained with a two-carbon chain length (**18a**, **19b**, **19c**, **21a**, **30c**, **31**) (IC_{50} ranging from 6 ± 3 nM for compound **19c** to 44 ± 17 nM for compound **31**). In some derivatives, a three-carbon length chain was well tolerated yielding analogues (**16b**, **18b**, **19d**, **19f**, **21b**, **22b**, **25c**, **27b**, **28c**, **29c**, and **30a**) with IC_{50} ranging from 11 ± 4 for compound **25c** to 750 ± 100 nM for compound **16b** (Table 1). When triazole derivatives substituted by benzyl or *1H*-indol-3-yl-methyl groups in position R_2 were compared, no precise rule could be defined in terms of structure–activity relationships. In some cases compounds having a benzyl group had a better affinity (**19e**, IC_{50} 121 ± 33 vs **19a**, IC_{50} 660 ± 40), in some others those having a *1H*-indol-3-yl-methyl group exhibited better affinity for the GHS-1a receptor (**25b**, IC_{50} 300 ± 60 vs **25d**, IC_{50} > 1000 nM). In general, *1H*-indole-3-yl-ethyl-containing compounds at the R_2 position were found better ligands than those with phenethyl moieties (**18a**, IC_{50} 18 ± 5 vs **18c**, IC_{50} 78 ± 15 ; **23a**, IC_{50} 66 ± 11 vs **23c**, IC_{50} 400 ± 130 ; **24a**, IC_{50} 55 ± 8 vs **24c**, IC_{50} 640 ± 10 ; **25a**, IC_{50} 80 ± 10 vs **25e**, IC_{50} 310 ± 30), although it was not always the case (**19b**, IC_{50} 11 ± 4 vs **19c**, IC_{50} 6 ± 3). However, when a three-carbon chain was placed between the triazole ring and the aromatic cycle, phenyl-containing compounds seemed to have slightly better affinity for the GHS-1a receptor (**19d**, IC_{50} 12 ± 3 vs **19f**, IC_{50} 145 ± 30). As examples of competition studies, displacement curves for compounds **16**, **19b**, and **25c** (Figure 2) are reported.

When tested for their ability to induce intracellular calcium release, most of the compounds containing a 4-methoxy group in R_1 position were not able to stimulate intracellular calcium levels (i.e., compounds **16**, **16a**, **16c**, **19a–f**). Compounds with a different substitution in the R_1 position were able to stimulate $[\text{Ca}^{2+}]_i$ accumulation, but a large majority were not fully efficacious, inducing only $16 \pm 3\%$ (for compound **30a**) to 88% (for compound **25b**) of the total response of ghrelin. The EC_{50}

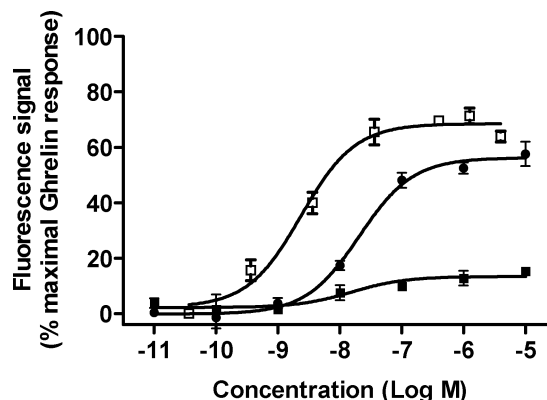


Figure 3. Effects of compounds **18a** (\square), **18b** (\bullet), and **30a** (\blacksquare) on $[\text{Ca}^{2+}]_i$ accumulation in CHO cells expressing the *hGHS-R1a*. The results are expressed as the percentage of the fluorescence signal compared to the maximal response induced by 10 μM ghrelin. In each experiment, each value was determined in triplicate, and the results given are means from at least three separate experiments.

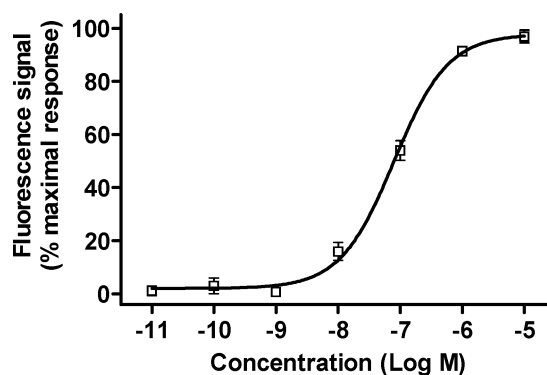


Figure 4. Effects of compound **29c** (\square) on $[\text{Ca}^{2+}]_i$ accumulation in CHO cells expressing the *hGHS-R1a*. The results are expressed as the percentage of the fluorescence signal compared to the maximal response induced by 10 μM ghrelin. In each experiment, each value was determined in triplicate, and the results given are means from at least three separate experiments.

of the best ligands for the GHS-1a receptor of these partial agonists were determined (**18a**, 63% total response, EC_{50} 4 ± 1 nM, **18b**, 66% total response, 18 ± 3 nM, **25c**, 18% total response, 15 ± 2 nM, **30a**, 16% total response, 12 ± 0.7 nM) (Table 1). As an example, the dose–response curves of compounds **18a**, **18b**, and **30a** are reported (Figure 3). On the basis of these biological results, it was not possible to establish a clear structure–activity relationship for these partial agonists. Among the compounds that behaved as full agonists (i.e., **25b**, **25d**, **29a–c**, **35**, **36**, and **37**), only **29c** exhibited high affinity for the GHS-1a receptor (IC_{50} 14 ± 2) and moderate potency on $[\text{Ca}^{2+}]_i$ accumulation (EC_{50} 120 ± 30 nM). However, it is quite clear that the presence of a phenyl, 3-methoxybenzyl, 2-methoxybenzyl, 4-fluorobenzyl, phenethyl, 2,2-diphenylethyl, (naphthalen-1-yl)-methyl, *n*-hexyl, and *1H*-indole-3-yl-ethyl group in the R_1 position was sufficient to generate derivatives with the best efficacy (particularly in the case of the *1H*-indole-3-yl-ethyl group in the R_2 position). As an example, the dose–response curve for compound **29c** is reported in Figure 4. Some of the compounds that were synthesized were not able to promote $[\text{Ca}^{2+}]_i$ accumulation, although they were able to recognize the GHS-1a receptor. For all these compounds, the R_1 group was either a 4-methoxybenzyl or a 2,4-dimethoxybenzyl (i.e., **16**, **16a**, **16c**, **19a–f**) (Table 1). These compounds were able to antagonize the $[\text{Ca}^{2+}]_i$ accumulation induced by ghrelin. Compounds **16** (K_b 14 ± 2 nM), **19b** (K_b 5 ± 1 nM),

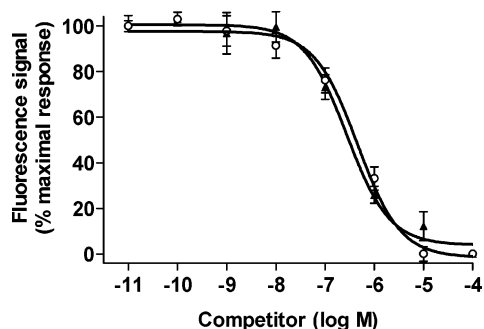


Figure 5. Ability of compounds **19c** (\blacktriangle) and **19d** (\circ) to inhibit 0.1 μM ghrelin-induced $[\text{Ca}^{2+}]_i$ accumulation in CHO cells expressing the *h*GHS-R1a. Values are expressed as the percentage of the fluorescence signal induced by 10 μM ghrelin with no added antagonist. In each experiment, each value was determined in duplicate, and the results given are means from at least three separate experiments.

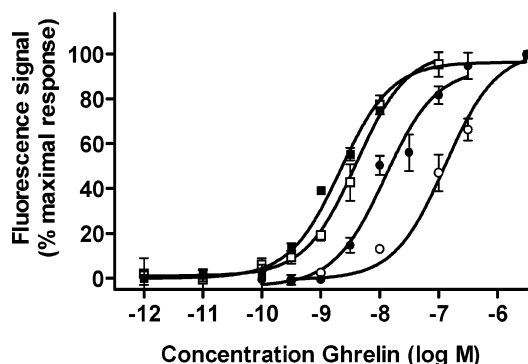


Figure 6. Effects of compound **19b** on ghrelin-induced $[\text{Ca}^{2+}]_i$ accumulation in CHO cells expressing the *h*GHS-R1a. Cells were incubated with various concentrations of ghrelin in the absence of compounds (\blacksquare) or in the presence of indicated concentrations of compound **19b** at 10^{-8} (\square), 10^{-7} (\bullet), or 10^{-6} M (\circ). Values are expressed as the percentage of the fluorescence signal induced by 10 μM ghrelin with no added antagonist. In each experiment, each value was determined in duplicate, and the results given are means from at least three separate experiments.

19c (K_b 4 ± 1 nM), and **19d** (K_b 14 ± 4 nM) were among the most potent ghrelin receptor antagonists (Figure 5 for compounds **19c** and **19d**). They were able to antagonize dose dependently ghrelin-induced $[\text{Ca}^{2+}]_i$ accumulation in CHO cells transiently transfected with the GHS-R1a. Interestingly, in the presence of various concentrations of compounds **16**, **19b**, **19c**, or **19d**, the dose–response curves of ghrelin on $[\text{Ca}^{2+}]_i$ accumulation were shifted in a parallel manner indicating a competitive antagonism (see Figure 6 for compound **19b** as an example).

Some of the compounds were tested for their activity on food intake (Table 2). Each compound was sc injected (160 $\mu\text{g}/\text{kg}$) in the rat. We selected some agonist (**29c**), partial agonists (**18c**, **20c**, **21a**, **21b**, **24a**, **25c**, **29b**, **30c**), and antagonists (**16**, **19b**, **19c**, **19e**) compounds according to their in vitro activity on the GHS-1a receptor. Compound **29c** that has been reported to be an in vitro agonist at the GHS-R1a was unable to stimulate food intake when administered alone. However, when administered with hexarelin, cumulative food intake at 6 h was increased with a variation of about 50% when compared with that of hexarelin alone. As reported in Table 2, when administered alone, compounds **24a**, **25c**, and **30a** (all in vitro partial agonists) elicited a significant increase in cumulative food intake, while all other compounds were found without effect. When administered with hexarelin, all compounds, with the exception of compounds **21a** which was without any effect and as already

Table 2. Cumulative Food Intake at 6 h after sc Administration of Compounds Alone or with Hexarelin^a

compds	cumulative food intake (g/100 g bw) at 6 h for 160 μg compd (cumulative food intake at 6 h for 80 μg hexarelin)	cumulative food intake (g/100 g bw) at 6 h for 160 μg compd + 80 μg hexarelin	% variation vs hexarelin ^b
saline	0.19 \pm 0.11	0.28 \pm 0.12	
16	0.06 \pm 0.03 (0.90 \pm 0.38)	0.33 \pm 0.22	–63
18c	0.01 \pm 0.0 (0.76 \pm 0.20)	0.48 \pm 0.23	–37
19b	0.20 \pm 0.19 (0.70 \pm 0.21)	0.63 \pm 0.20	–10
19c	0.06 \pm 0.02 (0.70 \pm 0.21)	0.48 \pm 0.22	–31
19e	0.17 \pm 0.17 (1.14 \pm 0.11)	0.79 \pm 0.33	–31
20c	0.29 \pm 0.18 (1.10 \pm 0.40)	0.47 \pm 0.41	–57
21a	0.02 \pm 0.01 (0.67 \pm 0.26)	0.64 \pm 0.01	–4
21b	0.01 \pm 0.00 (0.60 \pm 0.17)	0.02 \pm 0.01	–97
24a	0.41 \pm 0.37 (0.78 \pm 0.22)	0.43 \pm 0.20	–45
25c	0.75 \pm 0.35 (0.67 \pm 0.26)	0.53 \pm 0.33	–21
29b	0.27 \pm 0.17 (1.14 \pm 0.11)	0.85 \pm 0.41	–25
29c	0.22 \pm 0.20 (0.59 \pm 0.30)	0.91 \pm 0.36	+54
30a	0.74 \pm 0.31 (1.10 \pm 0.22)	0.49 \pm 0.17	–55
30c	0.30 \pm 0.13 (1.10 \pm 0.22)	0.56 \pm 0.21	–49

^a Results are expressed as g of food intake per 100 g of body weight (mean \pm SEM). ^b (Cumulative food intake at 6 h for compound minus cumulative food intake at 6 h for hexarelin)/cumulative food intake at 6 h for hexarelin.

Table 3. Inhibition of Hexarelin-Stimulated Cumulative Food Intake at Various sc Doses of Compound **21b** (mean \pm SEM)^a

compds	food intake at 6 h (g/100 g bw)
hexarelin 80 μg	1.01 \pm 0.19
+20 μg compound 21b	0.46 \pm 0.11
+80 μg compound 21b	0.25 \pm 0.13
+160 μg compound 21b	0.25 \pm 0.13
+320 μg compound 21b	0.08 \pm 0.05

^a Values are the mean of 7–8 determinations. Experiments have been repeated three times.

Table 4. Effect of Compound **21b** on GH Secretion in the Rat (sc Injection)^{a,b}

compd	[GH] ng/mL
solvent	2.2 \pm 0.1
hexarelin (80 μg)	170 \pm 13
21b (160 μg)	13 \pm 2
hexarelin + 21b (160 μg)	183 \pm 17

^a GH concentration was determined as described in the Experimental Section (mean \pm SEM). ^b Values are the mean of 5–7 determinations. Experiments have been repeated three times.

reported compound **29c**, were able to inhibit hexarelin-induced food intake in the rat with different potencies that were not in accordance with their in vitro potency or efficacy. Unexpectedly, the most potent compound in this series (**21b**) for the inhibition of hexarelin-stimulated food intake was not the compound presenting the best affinity for the GHS-1a receptor (IC_{50} 33 ± 7 nM), nor was it found the most potent in vitro agonist ($30 \pm 4\%$ of the maximal response on $[\text{Ca}^{2+}]_i$ accumulation, EC_{50} 49 ± 14 nM). There was no clear correlation between in vitro and in vivo results, some very potent partial agonists in recognizing the GHS-1a receptor having weak effects on food intake (i.e., **21a**), some potent partial agonist on $[\text{Ca}^{2+}]_i$ accumulation being potent antagonist of hexarelin-stimulated food intake (i.e., **20c**). A dose–response study for the most active compound (**21b**) that was able to antagonize the effects of hexarelin on food intake is reported in Table 3. A clear dose–effect could be found, compound **21b** being already active at the dose of 20 $\mu\text{g}/\text{kg}$.

Compound **21b** was evaluated for its activity on GH secretion after sc injection in the rat. As can be seen in Table 4, compound **21b** did not have any proper effect on GH release. On the other

hand, compound **21b** (160 $\mu\text{g}/\text{kg}$) was not able to modify hexarelin-stimulated GH release. Results on GH secretion are reported in Table 4.

These results indicate that compound **21b** works efficiently on the hexarelin-stimulated food intake (about 90% decrease in the cumulative 6 h period) and is without effect on GH secretion. The discrepancies observed between *in vivo* and *in vitro* activity might result from different pharmacokinetic and/or pharmacodynamic properties of compound **21b**.

Conclusion

A novel class of ghrelin receptor (GHS-R1a) ligands was identified from substituted 1,2,4-triazoles. These compounds were easily synthesized from commercially available materials. They contain only one asymmetric center that was selected at the beginning of the synthesis from the starting amino acid residue and conserved throughout the synthesis. SAR studies allowed us to improve *in vitro* binding affinity and to discover potent agonists, partial agonists, and antagonists for the GHS-1a receptor. The best *in vitro* receptor antagonists of this series were found to be compounds **19c** (JMV2844) (IC_{50} of 6 ± 3 nM, K_b of 4 ± 1 nM) and **19b** (JMV2866) (IC_{50} of 11 ± 4 nM, K_b of 5 ± 1 nM). The most potent compounds in this series were tested *in vivo* for their activity on food intake in the rat. Compound **21b** (JMV2810) that was defined *in vitro* as a partial agonist at the GHS-R1a was found the most potent compound in inhibiting hexarelin-stimulated food intake in the rat. However, it did not show any activity on GH secretion in the rat. Considering that some of the compounds tested are antagonists and some partial agonists *in vitro* at the GHS-1a receptor, this should infer that the receptor involved in the modulation of the food intake by the tested compounds depends on a more complicated mechanism.

Experimental Section

General Procedures. Ascending TLC was performed on pre-coated plates of silica gel 60 F₂₅₄ (Merck). Peptide derivatives were located with charring reagent or ninhydrine. Column chromatography was performed with silica gel Kieselguhr Merck G 0.04–0.063 mm. HPLC purifications were run on a Waters 4000 preparative apparatus on a C18 Deltapak column (100 mm \times 40 mm, 15 μm , 100 \AA), with UV detection at 214 nm, at a flow rate of 50 mL/min of a mixture of A, water with 0.1% TFA, and B, acetonitrile with 0.1% TFA in gradient mode. Analytical HPLC chromatography was performed on a Beckman Gold apparatus composed of the 126 solvent module, the 168 detector, and the 32 Karat software; runs were performed on a VWR Chromolith column (50 mm \times 3.9 mm) at a flow rate of 5 mL/min from solution A to solution B in a 3 min gradient (conditions A) or on a Symmetry Shield C18 column (50 mm \times 4.6 mm, 3.5 μm) at a flow rate of 1 mL/min from solution A to solution B in a 15 min gradient (conditions B). ¹H and ¹³C NMR spectra were recorded in DMSO-*d*₆ at 300 and 75 MHz or at 400 and 100 MHz, respectively, and at 300 K. Chemical shifts were reported as δ values (ppm) indirectly referenced to the solvent signal. Mass spectrum analyses were recorded on a Quatromicro (Micromass, Manchester, U.K.) triple-quadrupole mass spectrometer fitted with an electrospray interface. (L),(D)-Amino acids and derivatives were from Senn Chemicals, NeoMPS, or Advanced Chemtech. Human ghrelin was purchased from NeoMPS and iodinated in our laboratory. All reagents were of analytical grade.

All final compounds were purified by reversed-phase HPLC; the purity assessed by analytical reversed-phase C18 HPLC was found superior to 95%, and the structure was confirmed by MS (electrospray) and ¹H NMR and ¹³C NMR for the most interesting compounds.

General Procedure for Hydrazone Preparation. When hydrazides were not commercially available, they were synthesized in two steps via the corresponding esters as described below.

Ester Preparation. An amount of 1.0 equiv of carboxylic acid was dissolved in acetonitrile (0.5 mol/L). Then 1.2 equiv of DBU and 5.0 equiv of methyl iodide were added dropwise consecutively under stirring. After 8 h under reflux, the solvent was removed *in vacuo*. The residue was diluted in dichloromethane, washed with aqueous potassium hydrogen sulfate (1 M), saturated aqueous sodium hydrogen carbonate, and saturated aqueous sodium chloride. The organic layer was dried over sodium sulfate, filtered, and the solvent was removed *in vacuo* to afford the corresponding ester, as a colorless oil.

Methyl 3-Phenylpropanoate: 3.7 g (84%); ¹H NMR (300 MHz, DMSO-*d*₆) δ 2.58 (t, 2H, $J = 7$ Hz, CH₂–CH₂–phenyl), 2.84 (t, 2H, $J = 7$ Hz, CH₂–CH₂–phenyl), 3.55 (s, 3H, OCH₃), 7.21 (m, 5H, CH phenyl); ¹³C NMR (75 MHz, DMSO-*d*₆) δ 30.7 (CH₂–CH₂–phenyl), 35.3 (CH₂–CH₂–phenyl), 51.5 (OCH₃), 126.4 (C₄ phenyl), 128.5 (C₂ and C₆ phenyl), 128.7 (C₃ and C₅ phenyl), 140.9 (C₁ phenyl), 173.0 (CO ester); MS (ES) m/z 165.0 [M + H]⁺; HPLC t_R , 1.51 min (conditions A).

Methyl 3-(1H-Indol-3-yl)propanoate: 4.0 g (94%); ¹H NMR (300 MHz, DMSO-*d*₆) δ 2.64 (t, 2H, $J = 8$ Hz, CH₂–CH₂–indole), 2.94 (t, 2H, $J = 8$ Hz, CH₂–CH₂–indole), 3.55 (s, 3H, OCH₃), 6.95 (t, 1H, $J = 7$ Hz, H₅ indole), 7.04 (t, 1H, $J = 7$ Hz, H₆ indole), 7.08 (s, 1H, H₂ indole), 7.32 (d, 1H, $J = 8$ Hz, H₄ indole), 7.48 (d, 1H, $J = 8$ Hz, H₇ indole), 10.78 (brs, 1H, NH indole); ¹³C NMR (75 MHz, DMSO-*d*₆) δ 20.7 (CH₂–CH₂–indole), 34.7 (CH₂–CH₂–indole), 51.2 (OCH₃), 111.8 (C₇ indole), 113.5 (C₃ indole), 118.5 (C₄ and C₅ indole), 121.3 (C₆ indole), 122.7 (C₂ indole), 127.3 (C₉ indole), 136.6 (C₈ indole), 173.5 (CO ester); MS (ES) m/z 204.1 [M + H]⁺; HPLC t_R , 1.50 min (conditions A).

Methyl 4-Phenylbutanoate: 1.1 g (100%); ¹H NMR (300 MHz, DMSO-*d*₆) δ 1.79 (m, 2H, CH₂–CH₂–CH₂–phenyl), 2.26 (t, 2H, $J = 7$ Hz, CH₂–CH₂–CH₂–phenyl), 2.54 (t, 2H, $J = 7$ Hz, CH₂–CH₂–CH₂–phenyl), 3.55 (s, 3H, OCH₃), 7.13–7.16 (m, 3H, H₃, H₄, and H₅ phenyl), 7.22–7.27 (m, 2H, H₂, and H₆ phenyl); ¹³C NMR (75 MHz, DMSO-*d*₆) δ 26.6 (CH₂–CH₂–CH₂–phenyl), 33.1 (CH₂–CH₂–CH₂–phenyl), 34.7 (CH₂–CH₂–CH₂–phenyl), 51.5 (OCH₃), 126.2 (C₄ phenyl), 128.6 (C₂, C₃, C₅, and C₆ phenyl), 141.7 (C₁ phenyl), 173.4 (CO ester); MS (ES) m/z 179.1 [M + H]⁺. HPLC t_R , 1.68 min (conditions A).

Methyl 2-(1H-Indol-3-yl)acetate: 0.78 g (72%); ¹H NMR (300 MHz, DMSO-*d*₆) δ 3.58 (s, 3H, OCH₃), 3.73 (s, 2H, CH₂–indole), 6.97 (t, 1H, $J = 8$ Hz, H₅ indole), 7.07 (t, 1H, $J = 7$ Hz, H₆ indole), 7.23 (d, 1H, $J = 2$ Hz, H₂ indole), 7.35 (d, 1H, $J = 8$ Hz, H₄ indole), 7.47 (d, 1H, $J = 8$ Hz, H₇ indole), 10.92 (s, 1H, NH indole); ¹³C NMR (75 MHz, DMSO-*d*₆) δ 31.0 (CH₂–indole), 51.9 (OCH₃), 107.4 (C₃ indole), 111.8 (C₇ indole), 118.8 (C₄ indole), 118.9 (C₅ indole), 121.5 (C₆ indole), 124.5 (C₂ indole), 127.5 (C₉ indole), 136.5 (C₈ indole), 172.5 (CO ester); MS (ES) m/z 190.1 [M + H]⁺; HPLC t_R , 1.37 min (conditions A).

Methyl 4-(1H-Indol-3-yl)butanoate: 0.69 g (52%); ¹H NMR (300 MHz, DMSO-*d*₆) δ 1.87 (m, 2H, CH₂–CH₂–CH₂–indole), 2.32 (t, 2H, $J = 7$ Hz, CH₂–CH₂–CH₂–indole), 2.67 (t, 2H, $J = 7$ Hz, CH₂–CH₂–CH₂–indole), 3.55 (s, 3H, OCH₃), 6.94 (t, 1H, $J = 7$ Hz, H₅ indole), 7.03 (t, 1H, $J = 7$ Hz, H₆ indole), 7.07 (d, 1H, $J = 2$ Hz, H₂ indole), 7.31 (d, 1H, $J = 8$ Hz, H₄ indole), 7.47 (d, 1H, $J = 8$ Hz, H₇ indole), 10.74 (s, 1H, NH indole); ¹³C NMR (75 MHz, DMSO-*d*₆) δ 24.4 (CH₂–CH₂–CH₂–indole), 25.7 (CH₂–CH₂–CH₂–indole), 33.4 (CH₂–CH₂–CH₂–indole), 51.5 (OCH₃), 111.7 (C₇ indole), 114.1 (C₃ indole), 118.5 (C₄ indole), 118.6 (C₅ indole), 121.2 (C₆ indole), 122.7 (C₂ indole), 127.5 (C₉ indole), 136.5 (C₈ indole), 173.8 (CO ester); MS (ES) m/z 218.1 [M + H]⁺; HPLC t_R , 1.64 min (conditions A).

Hydrazone Preparation. An amount of 1.0 equiv of the corresponding ester and 10.0 equiv of hydrazine monohydrate were dissolved in ethanol (0.3 mol/L). The mixture was stirred overnight at reflux. The solvent was then removed *in vacuo*, and the residue was washed with diethylether and dried *in vacuo* to afford the corresponding hydrazone as a white powder.

3-Phenylpropanehydrazide: 3.3 g (91%); ¹H NMR (300 MHz, DMSO-*d*₆) δ 2.28 (t, 2H, *J* = 7 Hz, CH₂-CH₂-phenyl), 2.77 (t, 2H, *J* = 7 Hz, CH₂-CH₂-phenyl), 3.69 (brs, 2H, NH₂), 7.11-7.26 (m, 5H, CH aromatic), 8.94 (brs, 1H, NH); ¹³C NMR (75 MHz, DMSO-*d*₆) δ 31.4 (CH₂-CH₂-phenyl), 35.5 (CH₂-CH₂-phenyl), 126.3 (C₄ phenyl), 128.6 (C₂ and C₆ phenyl), 128.7 (C₃ and C₅ phenyl), 140.1 (C₁ phenyl), 173.1 (CO); MS (ES) *m/z* 165.1 [M + H]⁺; HPLC *t*_R, 0.77 min (conditions A).

3-(1H-Indol-3-yl)propanehydrazide: 3.1 g (76%); ¹H NMR (300 MHz, DMSO-*d*₆) δ 2.41 (m, 2H, CH₂-CH₂-indole), 2.90 (m, 2H, CH₂-CH₂-indole), 5.72 (brs, 2H, NH₂), 6.93 (t, 1H, *J* = 7 Hz, H₅ indole), 7.02 (t, 1H, *J* = 8 Hz, H₆ indole), 7.07 (s, 1H, H₂ indole), 7.31 (d, 1H, *J* = 8 Hz, H₄ indole), 7.48 (d, 1H, *J* = 8 Hz, H₇ indole), 9.03 (brs, 1H, NH hydrazide), 10.79 (brs, 1H, NH indole); ¹³C NMR (75 MHz, DMSO-*d*₆) δ 21.4 (CH₂-CH₂-indole), 34.7 (CH₂-CH₂-indole), 111.7 (C₇ indole), 114.1 (C₃ indole), 118.5 (C₄ indole), 118.7 (C₅ indole), 121.3 (C₆ indole), 122.5 (C₂ indole), 127.4 (C₉ indole), 136.6 (C₈ indole), 171.9 (CO); MS (ES) *m/z* 204.1 [M + H]⁺; HPLC *t*_R, 0.85 min (conditions A).

4-Phenylbutanehydrazide: 1.1 g (100%); ¹H NMR (300 MHz, DMSO-*d*₆) δ 1.84 (m, 2H, CH₂-CH₂-CH₂-phenyl), 2.00 (t, 2H, *J* = 7 Hz, CH₂-CH₂-CH₂-phenyl), 2.53 (t, 2H, *J* = 8 Hz, CH₂-CH₂-CH₂-phenyl), 4.40 (brs, 2H, NH₂), 7.09-7.16 (m, 3H, H₂, H₄, and H₆ phenyl), 7.21-7.26 (m, 2H, H₃, and H₅ phenyl), 8.90 (s, 1H, NH); ¹³C NMR (75 MHz, DMSO-*d*₆) δ 27.4 (CH₂-CH₂-CH₂-phenyl), 33.3 (CH₂-CH₂-CH₂-phenyl), 35.1 (CH₂-CH₂-CH₂-phenyl), 126.1 (C₄ phenyl), 128.7 (C₂, C₃, C₅, and C₆ phenyl), 142.1 (C₁ phenyl), 171.7 (CO); MS (ES) *m/z* 179.1 [M + H]⁺; HPLC *t*_R, 0.86 min (conditions A).

2-(1H-Indol-3-yl)acetohydrazide: 0.5 g (59%); ¹H NMR (300 MHz, DMSO-*d*₆) δ 3.46 (s, 2H, CH₂-indole), 4.25 (brs, 2H, NH₂), 6.96 (t, 1H, *J* = 7 Hz, H₅ indole), 7.05 (t, 1H, *J* = 8 Hz, H₆ indole), 7.18 (s, 1H, H₂ indole), 7.33 (d, 1H, *J* = 8 Hz, H₄ indole), 7.57 (d, 1H, *J* = 8 Hz, H₇ indole), 9.20 (brs, 1H, NH hydrazide), 10.86 (s, 1H, NH indole); ¹³C NMR (75 MHz, DMSO-*d*₆) δ 31.2 (CH₂-indole), 109.1 (C₃ indole), 111.7 (C₇ indole), 118.7 (C₄ indole), 119.2 (C₅ indole), 121.3 (C₆ indole), 124.2 (C₂ indole), 127.6 (C₉ indole), 136.5 (C₈ indole), 170.7 (CO); MS (ES) *m/z* 190.2 [M + H]⁺; HPLC *t*_R, 0.78 min (conditions A).

4-(1H-Indol-3-yl)butanehydrazide: 1.0 g (90%); ¹H NMR (300 MHz, DMSO-*d*₆) δ 1.83 (m, 2H, CH₂-CH₂-CH₂-indole), 2.06 (t, 2H, *J* = 7 Hz, CH₂-CH₂-CH₂-indole), 2.62 (t, 2H, *J* = 8 Hz, CH₂-CH₂-CH₂-indole), 4.35 (brs, 2H, NH₂), 6.92 (t, 1H, *J* = 7 Hz, H₅ indole), 7.02 (t, 1H, *J* = 7 Hz, H₆ indole), 7.06 (s, 1H, H₂ indole), 7.29 (d, 1H, *J* = 8 Hz, H₄ indole), 7.46 (d, 1H, *J* = 8 Hz, H₇ indole), 8.93 (brs, 1H, NH hydrazide), 10.72 (s, 1H, NH indole); ¹³C RMN (75 MHz, DMSO-*d*₆) δ 24.8 (CH₂-CH₂-CH₂-indole), 26.5 (CH₂-CH₂-CH₂-indole), 33.7 (CH₂-CH₂-CH₂-indole), 111.7 (C₇ indole), 114.5 (C₃ indole), 118.5 (C₄ indole), 118.7 (C₅ indole), 121.2 (C₆ indole), 122.6 (C₂ indole), 127.6 (C₉ indole), 136.7 (C₈ indole), 172.0 (CO); MS (ES) *m/z* 218.1 [M + H]⁺; HPLC *t*_R, 0.93 min (conditions A).

General Procedure for Thioamide 2 Preparation. In a solution of DCM, amine (1.0 equiv), Boc-D-Trp (1.0 equiv), NMM (2.2 equiv), and BOP (1.0 equiv) were successively added. After 1 h of stirring at room temperature, the mixture was concentrated in vacuo and dissolved in AcOEt. The organic layer was successively washed with aqueous solutions of 1 M KHSO₄, saturated NaHCO₃, and brine. The organic layer was then dried over Na₂SO₄, filtered, and concentrated in vacuo to yield amide 1 that was used without purification. To 1.0 equiv of amide 1 in DME (10 mL/mmol) was added Lawesson's reagent (0.5 equiv) under argon. The reaction mixture was heated to 85 °C for 2 h and then concentrated in vacuo. The residue was purified by chromatography on silica gel with a mixture of AcOEt/hexane 3/7 as eluent. The thioamide 2 was obtained as a white powder (yields between 35% and 70% for the two steps).

tert-Butyl (R)-1-(2-(1H-Indol-3-yl)ethylthiocarbamoyl)-2-(1H-indol-3-yl)ethylcarbamate (2a). Obtained from Boc-D-Trp and tryptamine: 1.1 g (67%). ¹H NMR (300 MHz, DMSO-*d*₆, 300 K) δ 1.27 (s, 9H, CH₃ Boc), 2.86 (m, 2H, CH₂-CH₂-indole), 2.95

(dd, 1H, *J* = 14 and 8 Hz, CH₂ βTrp), 3.11 (dd, 1H, *J* = 14 and 5 Hz, CH₂ βTrp), 3.75 (m, 2H, CH₂-CH₂-indole), 4.53 (m, 1H, CH αTrp), 6.68 (d, 1H, *J*_o = 8 Hz, H₄ Trp), 6.95 (t, 1H, *J*_o = 7 Hz, H₅ Trp), 6.96 (t, 1H, *J*_o = 8 Hz, H₅ indole), 7.03 (t, 1H, *J*_o = 6 Hz, H₆ Trp), 7.04 (m, 2H, H₆ and H₂ indole), 7.10 (d, 1H, *J* = 2 Hz, H₂ Trp), 7.12 (d, 1H, *J*_o = 8 Hz, H₄ indole), 7.30 (d, 2H, *J*_o = 8 Hz, H₇ indole and H₇ Trp), 7.57 (d, 1H, *J* = 7 Hz, NH Boc), 9.95 (brs, 1H, NH thioamide), 10.79 (s, 2H, NH indole and NH indole Trp). ¹³C NMR (75 MHz, DMSO-*d*₆, 300 K) δ 21.2 (CH₂-CH₂-indole), 28.5 (CH₃ Boc), 31.5 (C βTrp), 46.1 (CH₂-CH₂-indole), 62.0 (C αTrp), 78.6 (Cq Boc), 110.5 (C₃ indole and C₃ Trp), 111.7 (C₇ indole and C₇ Trp), 118.6 (C₄ Trp), 118.7 (C₄ indole), 119.0 (C₅ indole and C₅ Trp), 121.2 (C₆ Trp), 121.3 (C₆ indole), 123.1 (C₂ indole and C₂ Trp), 127.5 (C₉ indole), 127.8 (C₉ Trp), 136.5 (C₈ Trp), 136.7 (C₈ indole), 155.2 (CO Boc), 204.1 (CS thioamide). MS (ES) *m/z* 363.29 [M + H - 100]⁺, 406.9 [M + H - 56]⁺, 463.1 [M + H]⁺, 925.4 [2M + H]⁺. HPLC *t*_R, 2.01 min (conditions A).

tert-Butyl (R)-1-(Methylthiocarbamoyl)-2-(1H-indol-3-yl)ethylcarbamate (2b). Obtained from Boc-D-Trp and methylamine: 0.3 g (69%). ¹H NMR (300 MHz, DMSO-*d*₆, 300 K) δ 1.27 (s, 9H, CH₃ Boc), 2.91 (d, 3H, *J* = 4 Hz, NH-CH₃), 2.97 (m, 1H, CH₂ βTrp), 3.14 (dd, 1H, *J* = 14 and 5 Hz, CH₂ βTrp), 4.49 (m, 1H, CH αTrp), 6.64 (d, 1H, *J*_o = 8 Hz, H₄ Trp), 6.93 (t, 1H, *J*_o = 8 Hz, H₅ Trp), 7.03 (t, 1H, *J*_o = 8 Hz, H₆ Trp), 7.11 (s, 1H, H₂ Trp), 7.29 (d, 1H, *J*_o = 8 Hz, H₇ Trp), 7.58 (d, 1H, *J* = 8 Hz, NH Boc), 9.86 (d, 1H, *J* = 4 Hz, NH thioamide), 10.75 (s, 1H, NH indole Trp). ¹³C NMR (75 MHz, DMSO-*d*₆, 300 K) δ 28.5 (CH₃ Boc), 31.5 (C βTrp), 32.7 (NH-CH₃), 61.8 (C αTrp), 78.6 (Cq Boc), 110.5 (C₃ Trp), 111.7 (C₇ Trp), 118.6 (C₄ Trp), 118.9 (C₅ Trp), 121.2 (C₆ Trp), 124.1 (C₂ Trp), 127.8 (C₉ Trp), 136.5 (C₈ Trp), 155.2 (CO Boc), 204.8 (CS thioamide). MS (ES) *m/z* 234.4 [M + H - 100]⁺, 277.7 [M + H - 56]⁺, 334.2 [M + H]⁺, 667.3 [2M + H]⁺, 689.1 [2M + Na]⁺. HPLC *t*_R, 1.93 min (conditions A).

tert-Butyl (R)-1-(2,4-Dimethoxybenzylcarbamoyl)-2-(1H-indol-3-yl)ethylcarbamate (2c). Obtained from Boc-D-Trp and 2,4-dimethoxybenzylamine. ¹H NMR (300 MHz, DMSO-*d*₆, 300 K) δ (ppm) 1.27 (s, 9H, CH₃ Boc), 2.97 (dd, 1H, ³*J* = 8 and 14 Hz, CH₂ βTrp), 3.30 (dd, 1H, ³*J* = 4 and 14 Hz, CH₂ βTrp), 3.71 (s, 3H, CH₃O), 3.75 (s, 3H, CH₃O), 4.58 (m, 3H, CH₂-*o,p*-dimethoxybenzyl and CH αTrp), 6.37 (dd, 1H, *J*_o = 8 Hz and *J*_m = 2 Hz, H₅ *o,p*-dimethoxybenzyl), 6.53 (d, 1H, *J*_m = 2 Hz, H₃ *o,p*-dimethoxybenzyl), 6.86 (d, 1H, *J*_o = 8 Hz, H₄ Trp), 6.87 (d, 1H, *J*_o = 8 Hz, H₆ *o,p*-dimethoxybenzyl), 6.95 (t, 1H, *J*_o = 7 Hz, H₅ Trp), 7.03 (t, 1H, *J*_o = 7 Hz, H₆ Trp), 7.11 (s, 1H, H₂ Trp), 7.30 (d, 1H, *J*_o = 8 Hz, H₇ Trp), 7.60 (m, 1H, NH Trp), 9.97 (t, 1H, *J* = 6 Hz, NH-thioamide), 10.78 (s, 1H, NH indole Trp). ¹³C NMR (75 MHz, DMSO-*d*₆, 300 K) δ (ppm) 28.5 (CH₃ Boc), 31.3 (CH₂ βTrp), 44.2 (CH₂-*o,p*-dimethoxybenzyl), 55.6 (OCH₃), 55.9 (OCH₃), 61.9 (CH αTrp), 78.6 (Cq Boc), 98.7 (C₃ *o,p*-dimethoxybenzyl), 104.8 (C₅ *o,p*-dimethoxybenzyl), 110.4 (C₃ Trp), 111.7 (C₇ Trp), 116.7 (C₁ *o,p*-dimethoxybenzyl), 118.6 (C₄ Trp), 118.9 (C₅ Trp), 121.2 (C₆ Trp), 124.4 (C₂ Trp), 127.8 (C₉ Trp), 130.1 (C₆ *o,p*-dimethoxybenzyl), 136.5 (C₈ Trp), 155.5 (CO Boc), 158.6 (C₂ *o,p*-dimethoxybenzyl), 161.1 (C₄ *o,p*-dimethoxybenzyl), 210.4 (CS thioamide). MS (ES) *m/z* 470.0 [M + H]⁺. HPLC *t*_R, 1.97 min (conditions A).

General Procedure for Preparation of Triazole 3. To a solution of 1.0 equiv of thioamide 2 of tetrahydrofuran (10 mL/mmol) was added 2.0 equiv of hydrazide and then 1.1 equiv of mercury(II) acetate at room temperature. After 2 days, the mixture was filtered on Celite and the filtrate was concentrated in vacuo. The residue was purified by chromatography on silica gel with a mixture of AcOEt/MeOH 96/4 as eluent. The desired compounds were obtained as a white powder (yield ranging between 40% and 60%).

tert-Butyl (R)-1-(4-(2-(1H-Indol-3-yl)ethyl)-4H-1,2,4-triazol-3-yl)-2-(1H-indol-3-yl)ethylcarbamate (3a). Obtained from 2a and formic hydrazide. ¹H NMR (400 MHz, DMSO-*d*₆) δ 1.28 (s, 9H, Boc), 2.84 (m, 2H, CH₂-CH₂-indole), 3.29 (m, 2H, CH₂ βTrp),

4.05 (m, 2H, CH₂-CH₂-indole), 4.95 (m, 1H, CH αTrp), 6.83 (brs, 1H, H indole), 6.88–6.97 (m, 2H, H indole), 6.98–7.10 (m, 3H, H indole), 7.31 (d, 1H, *J* = 8 Hz, H indole), 7.32 (d, 1H, *J* = 8 Hz, H indole), 7.40 (d, 1H, *J* = 8 Hz, H indole), 7.48 (d, 1H, *J* = 8 Hz, H indole), 7.63 (d, 1H, *J* = 8 Hz, NH Trp), 8.21 (brs, 1H, H triazole), 10.80 (brs, 1H, NH indole), 10.85 (brs, 1H, NH indole). MS (ES) *m/z* 415.0 [M + H - 56]⁺, 471.3 [M + H]⁺, 941.3 [2M + H]⁺.

tert-Butyl (R)-1-(5-((1H-Indol-3-yl)methyl)-4-methyl-4H-1,2,4-triazol-3-yl)-2-(1H-indol-3-yl)ethylcarbamate (3b). Obtained from **2b** and 2-(1H-indol-3-yl)acetohydrazide. ¹H NMR (400 MHz, DMSO-*d*₆) δ 1.21 (s, 9H, CH₃ Boc), 3.10–3.30 (m, 5H, 3H N-CH₃ and 2H CH₂β), 4.15 (m, 2H, CH₂-indole), 4.90 (m, 1H, CH αTrp), 6.90–7.10 (m, 6H, H indole), 7.33 (d, 1H, *J* = 8 Hz, H indole), 7.35 (d, 1H, *J* = 8 Hz, H indole), 7.41–7.58 (3H, 2H indole, NH Trp), 10.75 (1H, s, NH indole), 10.90 (1H, s, NH indole). MS (ES) *m/z* 471.4 [M + H]⁺, 941.3 [2M + H]⁺.

tert-Butyl (R)-1-(5-(2-(1H-Indol-3-yl)ethyl)-4-methyl-4H-1,2,4-triazol-3-yl)-2-(1H-indol-3-yl)ethylcarbamate (3c). The title compound was obtained as previously described by reacting thioamide **2b** with 3-(1H-indol-3-yl)propanehydrazide. ¹H NMR (400 MHz, DMSO-*d*₆) δ 1.32 (s, 9H, CH₃ Boc), 2.85–3.10 (m, 4H, CH₂-CH₂-indole), 3.20 (s, 3H, N-CH₃), 3.22–3.40 (m, 2H, CH₂βTrp), 4.92 (m, 1H, CH αTrp), 6.93–7.02 (m, 2H, H indole), 7.04–7.10 (m, 2H, H indole), 7.13 (s, 1H, H indole), 7.16 (s, 1H, H indole), 7.32–7.38 (m, 2H, H indole), 7.42–7.52 (m, 3H, 2H indole and NH Trp), 10.85 (brs, 2H, NH indole). MS (ES) *m/z* 485.3 [M + H]⁺.

tert-Butyl (R)-1-(5-(2-(1H-Indol-3-yl)ethyl)-4-(2,4-dimethoxybenzyl)-4H-1,2,4-triazol-3-yl)-2-(1H-indol-3-yl)ethylcarbamate (3d). The title compound was obtained as previously described by reacting thioamide **2c** with 3-(1H-indol-3-yl)propanehydrazide: 1.2 g (65%). ¹H NMR (300 MHz, DMSO-*d*₆, 300 K) δ 1.21 (s, 9H, CH₃ Boc), 2.90 (m, 4H, CH₂-CH₂-indole), 3.28 (m, 2H, CH₂βTrp), 3.59 (s, 3H, OCH₃), 3.66 (s, 3H, OCH₃), 5.01 (m, 3H, CH₂-*o,p*-dimethoxybenzyl and CH αTrp), 6.26 (d, 1H, *J*_o = 8 Hz, H₅ *o,p*-dimethoxybenzyl), 6.49 (d, 1H, *J*_o = 8 Hz, H₆ *o,p*-dimethoxybenzyl), 6.51 (s, 1H, H₃ *o,p*-dimethoxybenzyl), 6.89 (m, 2H, H₅ Trp and H₅ indole), 7.02 (m, 2H, H₆ indole and H₆ Trp), 7.03 (s, 1H, H₂ indole), 7.05 (s, 1H, H₂ Trp), 7.26 (d, 1H, *J*_o = 8 Hz, H₄ Trp), 7.29 (m, 3H, H₄ and H₇ indole, H₇ Trp), 7.57 (d, 1H, *J* = 9 Hz, NH Boc), 10.79 (s, 1H, NH indole), 10.81 (s, 1H, NH indole Trp). ¹³C NMR (75 MHz, DMSO-*d*₆, 300 K) δ 22.4 (CH₂-CH₂-indole), 25.7 (CH₂-CH₂-indole), 28.4 (CH₃ Boc), 28.9 (C βTrp), 42.6 (CH₂-*o,p*-dimethoxybenzyl), 46.8 (C αTrp), 55.6 (OCH₃), 55.8 (OCH₃), 78.8 (Cq Boc), 98.9 (C₃ *o,p*-dimethoxybenzyl), 105.1 (C₅ *o,p*-dimethoxybenzyl), 110.0 (C₃ Trp), 111.7 (C₇ Trp), 111.8 (C₇ indole), 112.9 (C₃ indole), 114.8 (C₁ *o,p*-dimethoxybenzyl), 118.4 (C₄ indole and C₄ Trp), 118.7 (C₅ indole and C₅ Trp), 121.3 (C₆ Trp), 121.4 (C₆ indole), 123.0 (C₂ indole), 125.1 (C₂ Trp), 127.1 (C₉ indole), 127.5 (C₉ Trp), 128.5 (C₆ *o,p*-dimethoxybenzyl), 136.4 (C₈ Trp), 136.6 (C₈ indole), 155.5 (Cq triazole and CO Boc), 156.1 (Cq triazole), 157.8 (C₂ *o,p*-dimethoxybenzyl), 161.0 (C₄ *o,p*-dimethoxybenzyl). MS (ES) *m/z* 621.0 [M + H]⁺. HPLC *t*_R, 2.20 min (conditions A).

General Procedure for Preparation of Compound 5. The Boc protecting group of compound **3** was removed at room temperature for 1 h with a solution of AcOEt/HCl 4 M. The mixture was then concentrated in vacuo, diluted with MeOH, and concentrated several times in vacuo. The residue was then coupled with Boc-Aib (1.1 equiv), in the presence of BOP (1.1 equiv) and NMM (2.2 equiv) for 2 h, in DCM. The mixture was then concentrated in vacuo, and the residue was dissolved in AcOEt. The organic layer was successively washed with aqueous solutions of 1 M KHSO₄, saturated NaHCO₃, and brine. The organic layer was then dried over Na₂SO₄, filtered, and concentrated in vacuo to yield the desired compound which was then treated with AcOEt/HCl 4 M as already described. The final compound was purified by preparative HPLC on a C18 column using a water/acetonitrile/TFA 0.1% gradient (yield around 50% for the three steps).

(R)-N-(1-(4-(2-(1H-Indol-3-yl)ethyl)-4H-1,2,4-triazol-3-yl)-2-(1H-indol-3-yl)ethyl)-2-amino-2-methylpropanamide Trifluoroacetate Salt (11). Obtained from **3a**. ¹H NMR (400 MHz, DMSO-*d*₆) δ 1.29 (s, 3H, CH₃ Aib), 1.35 (s, 3H, CH₃ Aib), 2.85 (m, 1H, 1H N-CH₂-CH₂-indole), 2.89 (m, 1H, 1H, N-CH₂-CH₂-indole), 3.28 (dd, 1H, *J* = 14 Hz, *J* = 7 Hz, CH₂ βTrp), 3.40 (dd, 1H, *J* = 14 Hz and *J* = 8 Hz, CH₂ βTrp), 4.10 (m, 2H, N-CH₂-CH₂-In), 5.25 (m, 1H, CH αTrp), 6.85 (d, 1H, *J* = 2 Hz, H₂ indole), 6.90–6.98 (m, 2H, H₅ indole), 7.01 (d, 1H, *J* = 2 Hz, H₂ indole), 7.02–7.12 (m, 2H, H₆ indole), 7.30 (d, 1H, *J* = 8.2 Hz, H₇ indole), 7.33 (d, 1H, *J* = 8 Hz, H₇ indole), 7.40 (d, 1H, *J* = 8 Hz, H₄ indole), 7.47 (d, 1H, *J* = 8 Hz, H₄ indole), 8.04 (brs, 3H, NH₂ Aib, TFA salt), 8.42 (s, 1H, H triazole), 9.01 (d, 1H, *J* = 8 Hz, NH Trp), 10.81 (s, 1H, NH indole), 10.90 (s, 1H, NH indole).

(R)-N-(1-(5-((1H-Indol-3-yl)methyl)-4-methyl-4H-1,2,4-triazol-3-yl)-2-(1H-indol-3-yl)ethyl)-2-amino-2-methylpropanamide Trifluoroacetate Salt (12). Obtained from **3b**. ¹H NMR (400 MHz, DMSO-*d*₆) δ 1.20 (s, 3H, CH₃ Aib), 1.28 (s, 3H, CH₃ Aib), 3.32 (d, 3H, N-CH₃), 3.30–3.45 (m, 2H, CH₂ βTrp), 4.22 (s, 2H, CH₂-indole), 5.30 (m, 1H, CH αTrp), 6.91 (t, 1H, *J* = 8 Hz, H₅ indole), 6.94 (d, 1H, *J* = 8 Hz, H₅ indole), 7.02 (t, 1H, *J* = 8 Hz, H₆ indole), 7.05 (t, 1H, *J* = 8 Hz, H₆ indole), 7.08 (d, 1H, *J* = 2 Hz, H₂ indole), 7.12 (d, 1H, *J* = 2 Hz, H₂ indole), 7.29 (d, 1H, *J* = 8 Hz, H₇ indole), 7.33 (d, 1H, *J* = 8 Hz, H₇ indole), 7.48 (d, 1H, *J* = 8 Hz, H₄ indole), 7.57 (d, 1H, *J* = 8 Hz, H₄ indole), 8.00 (brs, 3H, NH₂ Aib, TFA salt), 8.85 (d, 1H, *J* = 8 Hz, NH amide), 10.82 (s, 1H, NH indole), 10.98 (s, 1H, NH indole).

(R)-N-(1-(5-(2-(1H-Indol-3-yl)ethyl)-4-methyl-4H-1,2,4-triazol-3-yl)-2-(1H-indol-3-yl)ethyl)-2-amino-2-methylpropanamide Trifluoroacetate Salt (13). Obtained from **3c**. ¹H NMR (400 MHz, DMSO-*d*₆) δ 1.30 (s, 3H, CH₃ Aib), 1.40 (s, 3H, CH₃ Aib), 3.00–3.20 (m, 4H, CH₂-CH₂-indole), 3.36 (s, 3H, N-CH₃), 3.45–3.50 (m, 2H, CH₂ βTrp), 5.30 (m, 1H, CH αTrp), 6.95–7.04 (t, 2H, H₅ indole), 7.06–7.13 (m, 2H, H₆ indole), 7.18 (brs, 2H, H₂ indole), 7.34 (d, 1H, *J* = 8 Hz, H₇ indole), 7.36 (d, 1H, *J* = 8 Hz, H₇ indole), 7.48 (d, 1H, *J* = 8 Hz, H₄ indole), 7.58 (d, 1H, *J* = 8 Hz, H₄ indole), 8.10 (brs, 3H, NH₂ Aib, TFA salt), 8.95 (d, 1H, *J* = 8 Hz, NH amide), 10.95 (s, 1H, NH indole), 10.96 (s, 1H, NH indole). ¹³C NMR (100 MHz, DMSO-*d*₆) 22.9 (CH₂-indole), 24.1 (CH₃ Aib), 24.3 (CH₃ Aib), 25.9 (CH₂-CH₂-indole), 28.8 (C βTrp), 30.7 (NCH₃), 46.2 (C αTrp), 57.2 (Cq Aib), 110.2 (C₃ indole), 112.3 (2C₇ indole), 113.5 (C₃ indole), 118.9–119.2 (2C₅, 2C₄ indole), 121.9 (2C₆ indole), 123.6 (C₂ indole), 125.3 (C₂ indole), 127.7 (C₉ indole), 128.0 (C₉ indole), 136.9 (C₈ indole), 137.1 (C₈ indole), 155.3 (Cq triazole), 155.8 (Cq triazole), 172.2 (CO Aib).

(R)-N-(1-(5-((1H-Indol-3-yl)methyl)-4H-1,2,4-triazol-3-yl)-2-(1H-indol-3-yl)ethyl)-2-amino-2-methylpropanamide Trifluoroacetate Salt (14). Compound **14** was obtained by treatment of compound **15** with TFA. ¹H NMR (400 MHz, DMSO-*d*₆) δ 1.31 (s, 3H, CH₃ Aib), 1.42 (s, 3H, CH₃ Aib), 3.19 (dd, 1H, *J* = 15 Hz and *J* = 10 Hz, CH₂ βTrp), 3.35 (dd, 1H, *J* = 15 Hz, *J* = 5 Hz, CH₂ βTrp), 4.15 (s, 2H, CH₂ indole), 5.26 (m, 1H, CH αTrp), 6.95 (t, 1H, H₅ Trp), 6.96 (t, 1H, H₅ indole), 7.05 (t, 1H, H₆ Trp), 7.06 (s, 1H, H₂ Trp), 7.07 (t, 1H, H₆ indole), 7.21 (s, 1H, H₂ indole), 7.32 (d, 1H, H₇ Trp), 7.37 (d, 1H, H₇ indole), 7.51 (d, 1H, *J* = 8 Hz, H₄ indole), 7.58 (d, 1H, *J* = 8 Hz, H₄ Trp), 8.00 (s, 3H, NH₂ Aib, TFA salt), 8.64 (d, 1H, *J* = 9 Hz, NH amide), 10.77 (s, 1H, NH indole Trp), 10.92 (s, 1H, NH indole). ¹³C NMR (100 MHz, DMSO-*d*₆) δ 22.9 (CH₂-indole), 23.2 (CH₃ Aib), 23.3 (CH₃ Aib), 29.4 (C βTrp), 48.3 (C αTrp), 56.3 (Cq Aib), 109.7 (C₃ indole), 110.3 (C₃ Trp), 111.2 (C₇ Trp), 111.3 (C₇ indole), 118.1 (C₄ Trp, C₅ Trp), 118.3 (C₄ indole), 118.4 (C₅ indole), 120.7 (C₆ Trp), 121.0 (C₆ indole), 123.4 (C₂ indole), 123.6 (C₂ Trp), 126.8 (C₉ indole), 127.1 (C₉ Trp), 136.0 (C₈ Trp), 136.2 (C₈ indole), 157.5 (Cq triazole), 161.7 (Cq triazole), 170.8 (CO Aib).

(R)-N-(1-(5-((1H-Indol-3-yl)methyl)-4-(2,4-dimethoxybenzyl)-4H-1,2,4-triazol-3-yl)-2-(1H-indol-3-yl)ethyl)-2-amino-2-methylpropanamide Trifluoroacetate Salt (15). ¹H NMR (400 MHz, DMSO-*d*₆) δ 1.27 (s, 3H, CH₃ Aib), 1.29 (s, 3H, CH₃ Aib), 3.25 (dd, 1H, *J* = 14 Hz, *J* = 6 Hz, CH₂ βTrp), 3.38 (dd, 1H, *J* = 14

Hz and $J = 9$ Hz, CH₂ βTrp), 3.68 (s, 3H, OCH₃), 3.72 (s, 3H, OCH₃), 4.10 (d, 1H, $J = 17$ Hz, CH₂-indole), 4.16 (d, 1H, $J = 17$ Hz, CH₂-indole), 4.96 (d, 1H, $J = 17$ Hz, CH₂ *o,p*-dimethoxybenzyl), 5.12 (d, 1H, $J = 17$ Hz, CH₂ *o,p*-dimethoxybenzyl), 5.16 (m, 1H, CH αTrp), 6.21 (dd, 1H, $J = 9$ Hz and $J = 2$ Hz, H₅ *o,p*-dimethoxybenzyl), 6.27 (d, 1H, $J = 9$ Hz, H₆ *o,p*-dimethoxybenzyl), 6.57 (d, 1H, $J = 2$ Hz, H₃ *o,p*-dimethoxybenzyl), 6.83 (t, 1H, H₅ Trp), 6.94 (t, 1H, H₅ indole), 7.02 (t, 1H, H₆ Trp), 7.05 (s, 1H, H₂ indole), 7.06 (t, 1H, H₆ indole), 7.07 (s, 1H, H₂ Trp), 7.07 (d, 1H, H₄ Trp), 7.31 (d, 1H, H₇ Trp), 7.33 (d, 1H, H₇ indole), 7.36 (d, 1H, $J = 8$ Hz, H₄ indole), 8.00 (brs, 3H, NH₂ Aib, TFA salt), 8.92 (d, 1H, $J = 8$ Hz, NH amide), 10.79 (s, 1H, NH indole Trp), 10.89 (s, 1H, NH indole). ¹³C NMR (100 MHz, DMSO-*d*₆) δ 21.2 (CH₂ indole), 23.1 (CH₃ Aib), 23.2 (CH₃ Aib), 28.6 (C βTrp), 41.4 (N-CH₂ *o,p*-dimethoxybenzyl), 45.1 (C αTrp), 55.2 (OCH₃), 55.4 (OCH₃), 56.2 (Cq Aib), 98.5 (C₃ *o,p*-dimethoxybenzyl), 104.6 (C₅ *o,p*-dimethoxybenzyl), 107.9 (C₃ indole), 109.5 (C₃ Trp), 111.2 (C₇ Trp), 111.3 (C₇ indole), 115.1 (C₁ *o,p*-dimethoxybenzyl), 117.8 (C₄ Trp), 118.1 (C₅ Trp), 118.3 (C₄ indole), 118.4 (C₅ indole), 120.8 (C₆ Trp), 121.1 (C₆ indole), 123.5 (C₂ indole), 124.3 (C₂ Trp), 126.6 (C₉ indole), 126.8 (C₉ Trp), 127.2 (C₂ *o,p*-dimethoxybenzyl), 136.0 (C₈ Trp), 136.2 (C₈ indole), 157.5 (Cq triazole), 154.9 (Cq triazole), 157.2 (C₂ *o,p*-dimethoxybenzyl), 160.3 (C₄ *o,p*-dimethoxybenzyl), 171.2 (CO Aib).

(R)-N-(1-(5-(2-(1H-Indol-3-yl)ethyl)-4-(2,4-dimethoxybenzyl)-4H-1,2,4-triazol-3-yl)-2-(1H-indol-3-yl)ethyl)-2-amino-2-methylpropanamide Trifluoroacetate Salt (16). ¹H NMR (400 MHz, DMSO-*d*₆) δ 1.32 (s, 3H, CH₃ Aib), 1.36 (s, 3H, CH₃ Aib), 2.93 (m, 2H, CH₂-CH₂-indole), 2.97 (m, 2H, CH₂-CH₂-indole), 3.31 (dd, 1H, $J = 15$ Hz and $J = 6$ Hz, CH₂ βTrp), 3.38 (dd, 1H, $J = 15$ Hz and $J = 9$ Hz, CH₂ βTrp), 3.66 (s, 3H, *o*-OCH₃), 3.72 (s, 3H, *p*-OCH₃), 4.93 (d, 1H, $J = 17$ Hz, CH₂ *o,p*-dimethoxybenzyl), 5.10 (d, 1H, $J = 17$ Hz, CH₂ *o,p*-dimethoxybenzyl), 5.23 (m, 1H, CH αTrp), 6.31 (dd, 1H, $J = 9$ Hz and $J = 2$ Hz, H₅ *o,p*-dimethoxybenzyl), 6.45 (d, 1H, $J = 9$ Hz, H₆ *o,p*-dimethoxybenzyl), 6.59 (d, 1H, $J = 2$ Hz, H₃ *o,p*-dimethoxybenzyl), 6.88 (t, 1H, $J = 8$ Hz, H₅ Trp), 6.94 (t, 1H, $J = 8$ Hz, H₅ indole), 7.04 (t, 1H, H₆ Trp), 7.06 (t, 1H, H₆ indole), 7.08 (s, 1H, H₂ indole), 7.11 (s, 1H, H₂ Trp), 7.18 (d, 1H, $J = 8$, H₄ Trp), 7.33 (3H, H₄, H₇ indole, H₇ Trp), 8.05 (s, 3H, NH₂ Aib, TFA salt), 8.95 (d, 1H, $J = 8$ Hz, NH amide), 10.80 (s, 1H, NH indole), 10.82 (s, 1H, NH indole Trp). ¹³C NMR (100 MHz, DMSO-*d*₆) δ 22.4 (CH₂-CH₂ indole), 23.2 (CH₃ Aib), 23.3 (CH₃ Aib), 25.4 (CH₂-CH₂ indole), 28.7 (C βTrp), 41.3 (CH₂-*o,p*-dimethoxybenzyl), 45.3 (C αTrp), 55.2 (*p*-OCH₃), 55.4 (*o*-OCH₃), 56.3 (Cq Aib), 98.6 (C₃ *o,p*-dimethoxybenzyl), 104.7 (C₅ *o,p*-dimethoxybenzyl), 109.5 (C₃ Trp), 111.3 (C₇ Trp, C₇ indole), 112.9 (C₃ indole), 115.2 (C₁ *o,p*-dimethoxybenzyl), 117.8 (C₄ indole), 117.9 (C₄ Trp), 118.2 (C₅ Trp, C₅ indole), 120.9 (C₆ Trp, C₆ indole), 122.4 (C₂ indole), 124.3 (C₂ Trp), 126.8 (C₉ Indole), 126.9 (C₉ Trp), 127.5 (C₆ *o,p*-dimethoxybenzyl), 136.0 (C₈ Trp), 136.2 (C₈ indole), 154.6 (2Cq triazole), 157.3 (C₂ *o,p*-dimethoxybenzyl), 160.4 (C₄ *o,p*-dimethoxybenzyl), 171.3 (CO Aib).

(R)-N-(1-(4-(2,4-Dimethoxybenzyl)-5-benzyl-4H-1,2,4-triazol-3-yl)-2-(1H-indol-3-yl)ethyl)-2-amino-2-methylpropanamide Trifluoroacetate Salt (16a). ¹H NMR (400 MHz, DMSO-*d*₆) δ 1.30 (s, 3H, CH₃ Aib), 1.33 (s, 3H, CH₃ Aib), 3.26 (dd, 1H, $J = 14$ Hz and $J = 6$ Hz, CH₂ βTrp), 3.38 (dd, 1H, $J = 14$ Hz and $J = 9$ Hz, CH₂ βTrp), 3.69 (s, 3H, OCH₃), 3.72 (s, 3H, OCH₃), 4.02 (s, 2H, CH₂-benzyl), 4.87 (d, 1H, $J = 17$ Hz, CH₂-*o,p*-dimethoxybenzyl), 5.08 (d, 1H, $J = 17$ Hz, CH₂ *o,p*-dimethoxybenzyl), 5.17 (m, 1H, CH αTrp), 6.24 (dd, 1H, $J = 8$ Hz, $J = 2$ Hz, H₅ *o,p*-dimethoxybenzyl), 6.28 (d, 1H, $J = 8$ Hz, H₆ *o,p*-dimethoxybenzyl), 6.56 (d, 1H, $J = 2$ Hz, H₃ *o,p*-dimethoxybenzyl), 6.85 (t, 1H, $J = 8$ Hz, H₅ Trp), 7.02 (t, 1H, H₆ Trp), 7.07 (m, 2H, H₂, H₆ benzyl), 7.08 (s, 1H, H₂ Trp), 7.09 (d, 1H, H₄ Trp), 7.16–7.29 (m, 3H, H₃, H₄, H₅ benzyl), 7.31 (d, 1H, $J = 8$ Hz, H₇ Trp), 8.01 (s, 3H, NH₂ Aib, TFA salt), 8.92 (d, 1H, $J = 8$ Hz, NH amide), 11.79 (s, 1H, NH indole Trp). ¹³C NMR (100 MHz, DMSO-*d*₆) δ 23.2 (2CH₃ Aib), 28.7 (C βTrp), 30.2 (CH₂-benzyl), 41.3 (CH₂-*o,p*-dimethoxybenzyl), 45.2 (C αTrp), 55.2 (OCH₃), 55.4 (OCH₃), 56.2

(Cq Aib), 98.5 (C₃ *o,p*-dimethoxybenzyl), 104.7 (C₅ *o,p*-dimethoxybenzyl), 109.5 (C₃ Trp), 111.3 (C₇ Trp), 115.1 (C₁ *o,p*-dimethoxybenzyl), 117.8 (C₄ Trp), 118.2 (C₅ Trp), 120.8 (C₆ Trp), 124.3 (C₂ Trp), 126.5 (C₄ benzyl), 126.8 (C₉ Trp), 127.3 (C₆ *o,p*-dimethoxybenzyl), 128.3 (C₂, C₃, C₅, C₆ benzyl), 135.8 (C₁ benzyl), 136.0 (C₈ Trp), 153.4 (Cq triazole), 155.0 (Cq triazole), 157.2 (C₂ *o,p*-dimethoxybenzyl), 160.3 (C₄ *o,p*-dimethoxybenzyl), 171.3 (CO Aib).

(R)-N-(1-(4-(2,4-Dimethoxybenzyl)-5-phenethyl-4H-1,2,4-triazol-3-yl)-2-(1H-indol-3-yl)ethyl)-2-amino-2-methylpropanamide Trifluoroacetate Salt (16c). ¹H NMR (300 MHz, DMSO-*d*₆, 300 K) δ (ppm) 1.26 (s, 3H, CH₃ Aib), 1.30 (s, 3H, CH₃ Aib), 2.82 (m, 4H, CH₂-CH₂-phenyl), 3.29 (t, 2H, $J = 8$ Hz, CH₂ βTrp), 3.61 (s, 3H, OCH₃), 3.68 (s, 3H, OCH₃), 4.85 (d, 1H, $J = 17$ Hz, CH₂-*o,p*-dimethoxybenzyl), 5.02 (d, 1H, $J = 17$ Hz, CH₂-*o,p*-dimethoxybenzyl), 5.18 (m, 1H, CH αTrp), 6.29 (dd, 1H, $J_o = 8$ Hz and $J_m = 2$ Hz, H₅ *o,p*-dimethoxybenzyl), 6.40 (d, 1H, $J_o = 8$ Hz, H₆ *o,p*-dimethoxybenzyl), 6.55 (d, 1H, $J_m = 2$ Hz, H₃ *o,p*-dimethoxybenzyl), 6.82 (t, 1H, $J_o = 8$ Hz, H₅ Trp), 6.99 (t, 1H, $J_o = 8$ Hz, H₆ Trp), 7.05 (s, 1H, H₂ Trp), 7.09–7.24 (m, 6H, H₄ Trp and CHar phenyl), 7.27 (d, 1H, $J_o = 8$ Hz, H₇ Trp), 7.99 (s3H, large, NH₂ Aib TFA salt), 8.89 (d, 1H, $J = 8$ Hz, NH amide), 10.77 (s, 1H, NH indole Trp). ¹³C NMR (75 MHz, DMSO-*d*₆, 300 K) δ (ppm) 23.6 (CH₃ Aib), 23.7 (CH₃ Aib), 26.5 (CH₂-CH₂-phenyl), 29.2 (CH₂ βTrp), 32.7 (CH₂-CH₂-phenyl), 41.6 (CH₂-*o,p*-dimethoxybenzyl), 45.7 (CH αTrp), 55.7 (OCH₃), 55.9 (OCH₃), 56.7 (Cq Aib), 99.1 (C₃ *o,p*-dimethoxybenzyl), 105.2 (C₅ *o,p*-dimethoxybenzyl), 110.0 (C₃ Trp), 111.8 (C₇ Trp), 115.7 (C₁ *o,p*-dimethoxybenzyl), 118.3 (C₄ Trp), 118.7 (C₅ Trp), 121.3 (C₆ Trp), 126.5 (C₂ Trp and C₆ *o,p*-dimethoxybenzyl), 127.3 (C₉ Trp), 128.1 (C₄ phenyl), 128.7 (C₂, C₃, C₅ and C₆ phenyl), 136.4 (C₈ Trp), 140.9 (C₁ phenyl), 154.5 (Cq triazole), 155.0 (Cq triazole), 157.8 (C₂ *o,p*-dimethoxybenzyl), 160.9 (C₄ *o,p*-dimethoxybenzyl), 171.7 (CO amide).

(R)-N-(1-(4-(3,5-Dimethoxybenzyl)-5-phenethyl-4H-1,2,4-triazol-3-yl)-2-(1H-indol-3-yl)ethyl)-2-amino-2-methylpropanamide Trifluoroacetate Salt (17b). ¹H NMR (300 MHz, DMSO-*d*₆, 300 K) δ (ppm) 1.24 (s, 3H, CH₃ Aib), 1.27 (s, 3H, CH₃ Aib), 2.83 (s, 4H, CH₂-CH₂-phenyl), 3.32 (m, 2H, CH₂ βTrp), 3.61 (s, 6H, OCH₃), 5.02 (m, 2H, CH₂-*m*-dimethoxybenzyl), 5.18 (m, 1H, CH αTrp), 6.07 (d, 2H, $J_m = 2$ Hz, H₂ and H₆ *m*-dimethoxybenzyl), 6.42 (brs, 1H, H₄ *m*-dimethoxybenzyl), 6.83 (t, 1H, $J_o = 7$ Hz, H₅ Trp), 6.99 (t, 1H, $J_o = 8$ Hz, H₆ Trp), 7.08 (d, 1H, $J = 2$ Hz, H₂ Trp), 7.13 (t, 3H, $J_o = 8$ Hz, H₃, H₄ and H₅ phenyl), 7.20 (d, 3H, $J_o = 7$ Hz, H₂ and H₆ phenyl, H₄ Trp), 7.28 (d, 1H, $J_o = 8$ Hz, H₇ Trp), 7.99 (brs, 3H, NH₂ Aib), 8.92 (d, 1H, $J = 8$ Hz, NH amide), 10.77 (s, 1H, NH indole). ¹³C NMR (75 MHz, DMSO-*d*₆, 300 K) δ (ppm) 23.5 (CH₃ Aib), 23.8 (CH₃ Aib), 26.5 (CH₂-CH₂-phenyl), 29.2 (CH₂ βTrp), 32.7 (CH₂-CH₂-phenyl), 45.6 (CH αTrp), 45.8 (CH₂-*m*-dimethoxybenzyl), 55.6 (OCH₃), 56.8 (Cq Aib), 99.6 (C₄ *m*-dimethoxybenzyl), 104.6 (C₂ and C₆ *m*-dimethoxybenzyl), 109.9 (C₃ Trp), 111.8 (C₇ Trp), 118.2 (C₄ Trp), 118.7 (C₅ Trp), 121.3 (C₆ Trp), 124.8 (C₂ Trp), 126.5 (C₄ phenyl), 127.3 (C₉ Trp), 128.7 (C₂, C₃, C₅ and C₆ phenyl), 136.4 (C₈ Trp), 138.6 (C₁ *m*-dimethoxybenzyl), 140.9 (C₁ phenyl), 154.6 (Cq triazole), 154.8 (Cq triazole), 161.4 (C₃ and C₅ *m*-dimethoxybenzyl), 171.8 (CO amide).

(R)-N-(1-(5-(2-(1H-Indol-3-yl)ethyl)-4-(3-methoxybenzyl)-4H-1,2,4-triazol-3-yl)-2-(1H-indol-3-yl)ethyl)-2-amino-2-methylpropanamide Trifluoroacetate Salt (18a). ¹H NMR (400 MHz, DMSO-*d*₆) δ 1.28 (s, 3H, CH₃ Aib), 1.30 (s, 3H, CH₃ Aib), 2.92 (m, 2H, CH₂-CH₂-indole), 2.98 (m, 2H, CH₂-CH₂-indole), 3.33 (dd, 1H, $J = 15$ Hz and $J = 6$ Hz, CH₂ βTrp), 3.40 (dd, 1H, $J = 15$ Hz and $J = 9$ Hz, CH₂ βTrp), 3.66 (s, 3H, OCH₃), 5.09 (m, 2H, CH₂-*m*-methoxybenzyl), 5.22 (m, 1H, CH αTrp), 6.38 (d, 1H, $J = 8$ Hz, H₆ *m*-methoxybenzyl), 6.59 (s, 1H, H₂ *m*-methoxybenzyl), 6.86 (t, 1H, H₅ Trp), 6.87 (d, 1H, H₄ *m*-methoxybenzyl), 6.92 (t, 1H, $J = 7.5$ Hz, H₅ indole), 7.03 (t, 1H, $J = 7.9$ Hz, H₆ Trp), 7.05 (t, 1H, H₆ indole), 7.07 (s, 1H, H₂ indole), 7.11 (s, 1H, H₂ Trp), 7.18 (t, 1H, H₅ *m*-methoxybenzyl), 7.19 (d, 1H, H₄ Trp), 7.31 (1H, H₄ indole), 7.32 (2H, H₇ Trp, H₇ indole), 8.00 (s, 3H, NH₂ Aib,

TFA salt), 8.96 (d, 1H, $J = 8$ Hz, NH amide), 10.78 (s, 1H, NH indole), 10.80 (s, 1H, NH indole Trp). ^{13}C NMR (100 MHz, DMSO- d_6) δ 22.4 ($\text{CH}_2\text{-CH}_2\text{-indole}$), 23.1 (CH_3 Aib), 23.3 (CH_3 Aib), 25.4 ($\text{CH}_2\text{-CH}_2\text{-indole}$), 28.7 ($\text{C } \beta$ Trp), 45.3 (CH_2 *m*-methoxybenzyl), 45.4 (C α Trp), 55.0 (OCH_3), 56.3 (Cq Aib), 109.5 (C₃ Trp), 111.3 (C₇ Trp, C₇ indole), 112.0 (C₂ *m*-methoxybenzyl), 113.0 (C₄ *m*-methoxybenzyl, C₃ indole), 117.8 (C₄ Trp, C₆ *m*-methoxybenzyl), 118.0 (C₄ indole), 118.2 (C₅ indole), 118.3 (C₅ Trp), 120.8 (C₆ indole), 120.9 (C₆ Trp), 122.4 (C₂ indole), 124.3 (C₂ Trp), 126.7 (C₉ indole), 126.9 (C₉ Trp), 130.0 (C₅ *m*-methoxybenzyl), 136.0 (C₈ indole), 136.1 (C₈ Trp), 137.2 (C₁ *m*-methoxybenzyl), 154.3 (2Cq triazole), 159.6 (C₃ *m*-methoxybenzyl), 171.4 (CO amide).

(R)-N-(1-(5-(3-(1H-Indol-3-yl)propyl)-4-(3-methoxybenzyl)-4H-1,2,4-triazol-3-yl)-2-(1H-indol-3-yl)ethyl)-2-amino-2-methylpropanamide Trifluoroacetate Salt (18b). ^1H NMR (400 MHz, DMSO- d_6) δ 1.27 (s, 3H, CH₃ Aib), 1.30 (s, 3H, CH₃ Aib), 1.92 (m, 2H, CH₂-CH₂-CH₂-indole), 2.62 (m, 2H, CH₂-CH₂-CH₂-indole), 2.68 (m, 2H, CH₂-CH₂-CH₂-indole), 3.24 (dd, 1H, $J = 14.5$, $J = 5.8$, CH₂ β Trp), 3.39 (dd, 1H, $J = 14.5$, $J = 9.0$, CH₂ β Trp), 3.66 (s, 3H, *m*-OCH₃), 5.07 (s, 2H, CH₂ *m*-methoxybenzyl), 5.18 (m, 1H, CH α Trp), 6.35 (d, 1H, $J = 7.5$, H₆ *m*-methoxybenzyl), 6.54 (brs, 1H, H₂ *m*-methoxybenzyl), 6.84 (t, 1H, $J = 7.5$, H₅ Trp), 6.87 (dd, 1H, $J = 8.0$, $J = 2.1$, H₄ *m*-methoxybenzyl), 6.94 (t, 1H, $J = 7.3$, H₅ indole), 7.02 (t, 1H, H₆ Trp), 7.02 (s, 1H, H₂ indole), 7.05 (t, 1H, $J = 7.8$, H₆ indole), 7.08 (d, 1H, $J = 2.1$, H₂ Trp), 7.13 (d, 1H, $J = 8.1$, H₄ Trp), 7.17 (t, 1H, $J = 8.1$, H₅ *m*-methoxybenzyl), 7.30 (d, 1H, H₇ Trp), 7.32 (d, 1H, $J = 8$, H₇ indole), 7.42 (d, 1H, $J = 7.6$, H₄ indole), 7.98 (brs, 3H, NH₂ Aib, TFA salt), 8.93 (d, 1H, $J = 8.2$, NH amide), 10.71 (s, 1H, NH indole), 10.77 (s, 1H, NH indole Trp). ^{13}C NMR (100 MHz, DMSO- d_6) δ 23.1 (CH₃ Aib), 23.3 (CH₃ Aib), 23.9 (CH₂-CH₂-CH₂-indole), 24.8 (CH₂-CH₂-CH₂-indole), 27.4 (CH₂-CH₂-CH₂-indole), 28.3 (C β Trp), 45.2 (CH₂ *m*-methoxybenzyl), 45.4 (C α Trp), 55.1 (*m*-OCH₃), 56.3 (Cq Aib), 109.5 (C₃ Trp), 111.3 (C₇ Trp, C₇ indole), 111.8 (C₂ *m*-methoxybenzyl), 113.0 (C₄ *m*-methoxybenzyl), 113.8 (C₃ indole), 117.8 (C₆ *m*-methoxybenzyl), 117.9 (C₄ Trp), 118.1 (C₅ indole), 118.2 (C₅ Trp, C₄ indole), 120.8 (C₆ Trp), 120.9 (C₆ indole), 122.2 (C₂ indole), 124.3 (C₂ Trp), 126.8 (C₉ Trp), 127.0 (C₉ indole), 130.0 (C₅ *m*-methoxybenzyl), 136.0 (C₈ Trp), 136.2 (C₈ indole), 137.4 (C₁ *m*-methoxybenzyl), 154.3 (Cq triazole), 154.6 (Cq triazole), 159.7 (C₃ *m*-methoxybenzyl), 171.4 (CO amide).

(R)-N-(1-(4-(3-Methoxybenzyl)-5-phenethyl-4H-1,2,4-triazol-3-yl)-2-(1H-indol-3-yl)ethyl)-2-amino-2-methylpropanamide Trifluoroacetate Salt (18c). ^1H NMR (300 MHz, DMSO- d_6 , 300 K) δ (ppm) 1.24 (s, 3H, CH₃ Aib), 1.27 (s, 3H, CH₃ Aib), 2.82 (m, 4H, CH₂-CH₂-phenyl), 3.32 (m, 2H, CH₂ β Trp), 3.63 (s, 3H, OCH₃), 5.08 (m, 2H, CH₂-*m*-methoxybenzyl), 5.18 (m, 1H, CH α Trp), 6.35 (d, 1H, $J_0 = 8$ Hz, H₆ *m*-methoxybenzyl), 6.57 (s, 1H, H₂ *m*-methoxybenzyl), 6.82 (t, 1H, $J_0 = 8$ Hz, H₅ Trp), 6.84 (d, 1H, $J_0 = 8$ Hz, H₄ *m*-methoxybenzyl), 6.99 (t, 1H, $J_0 = 8$ Hz, H₆ Trp), 7.08 (m, 1H, H₄ phenyl), 7.11–7.16 (m, 5H, H₂ and H₄ Trp, H₂ and H₆ phenyl, H₅ *m*-methoxybenzyl), 7.20 (m, 2H, H₃ and H₅ phenyl), 7.27 (d, 1H, $J_0 = 8$ Hz, H₇ Trp), 8.01 (brs, 3H, NH₂ Aib, TFA salt), 8.96 (d, 1H, $J = 8$ Hz, NH amide), 10.81 (d, 1H, $J = 2$ Hz, NH indole Trp). ^{13}C NMR (75 MHz, DMSO- d_6 , 300 K) δ (ppm) 23.5 (CH₃ Aib), 23.8 (CH₃ Aib), 26.4 (CH₂-CH₂-phenyl), 29.1 (CH₂ β Trp), 32.7 (CH₂-CH₂-phenyl), 45.7 (CH α Trp), 45.8 (CH₂-*m*-methoxybenzyl), 55.5 (OCH₃), 56.7 (Cq Aib), 109.8 (C₃ Trp), 111.8 (C₇ Trp), 112.5 (C₂ *m*-methoxybenzyl), 113.5 (C₄ *m*-methoxybenzyl), 118.2 (C₄ Trp), 118.4 (C₆ *m*-methoxybenzyl), 118.7 (C₅ Trp), 121.3 (C₆ Trp), 124.8 (C₂ Trp), 126.5 (C₄ phenyl), 127.3 (C₉ Trp), 128.7 (C₂, C₃, C₅, and C₆ phenyl), 130.5 (C₅ *m*-methoxybenzyl), 136.4 (C₈ Trp), 137.7 (C₁ *m*-methoxybenzyl), 140.9 (C₁ phenyl), 154.6 (Cq triazole), 154.9 (Cq triazole), 160.1 (C₃ *m*-methoxybenzyl), 171.9 (CO amide).

(R)-N-(1-(4-(3-Methoxybenzyl)-5-benzyl-4H-1,2,4-triazol-3-yl)-2-(1H-indol-3-yl)ethyl)-2-amino-2-methylpropanamide Trifluoroacetate Salt (18d). ^1H NMR (400 MHz, DMSO- d_6) δ 1.25 (s, 3H, CH₃ Aib), 1.29 (s, 3H, CH₃ Aib), 3.24 (dd, 1H, $J = 14.3$, $J = 5.8$, CH₂ β Trp), 3.38 (dd, 1H, $J = 14.3$, $J = 9.1$, CH₂ β Trp),

3.61 (s, 3H, *m*-OCH₃), 4.04 (m, 2H, CH₂ benzyl), 5.07 (d, 1H, $J = 17.4$, CH₂ *m*-methoxybenzyl), 5.13 (d, 1H, $J = 17.4$, CH₂ *m*-methoxybenzyl), 5.14 (m, 1H, CH α Trp), 6.32 (d, 1H, $J = 7.8$, H₆ *m*-methoxybenzyl), 6.40 (m, 1H, H₂ *m*-methoxybenzyl), 6.82 (t, 1H, H₅ Trp), 6.83 (d, 1H, $J = 7.8$, H₄ *m*-methoxybenzyl), 7.01 (t, 1H, $J = 8.2$, H₆ Trp), 7.04 (d, 1H, $J = 8.2$, H₄ Trp), 7.06 (d, 1H, $J = 2.0$, H₂ Trp), 7.12 (m, 2H, H₂, H₆ benzyl), 7.13 (t, 1H, $J = 7.9$, H₅ *m*-methoxybenzyl), 7.20 (m, 1H, H₄ benzyl), 7.24 (m, 2H, H₃, H₅ benzyl), 7.29 (d, 1H, $J = 8.2$, H₇ Trp), 7.99 (brs, 3H, NH₂ Aib, TFA salt), 8.92 (d, 1H, $J = 8.2$, NH amide), 10.77 (s, 1H, NH indole Trp). ^{13}C NMR (100 MHz, DMSO- d_6) δ 23.0 (CH₃ Aib), 23.3 (CH₃ Aib), 28.6 (C β Trp), 30.1 (CH₂ benzyl), 45.2 (C α Trp), 45.6 (CH₂-*m*-methoxybenzyl), 54.9 (*m*-OCH₃), 56.2 (Cq Aib), 109.4 (C₃ Trp), 111.2 (C₇ Trp), 111.7 (C₂ *m*-methoxybenzyl), 113.1 (C₄ *m*-methoxybenzyl), 117.9 (C₄ Trp, C₆ *m*-methoxybenzyl), 118.2 (C₅ Trp), 120.8 (C₆ Trp), 124.3 (C₂ Trp), 126.6 (C₄ benzyl), 126.8 (C₉ Trp), 128.3 (C₃, C₅ benzyl), 128.4 (C₂, C₆ benzyl), 129.9 (C₅ *m*-methoxybenzyl), 135.9 (C₁ benzyl, C₈ Trp), 137.0 (C₁ *m*-methoxybenzyl), 153.5 (Cq triazole), 154.8 (Cq triazole), 159.5 (C₃ *m*-methoxybenzyl), 171.3 (CO amide).

(R)-N-(1-(5-((1H-Indol-3-yl)methyl)-4-(4-methoxybenzyl)-4H-1,2,4-triazol-3-yl)-2-(1H-indol-3-yl)ethyl)-2-amino-2-methylpropanamide Trifluoroacetate Salt (19a). ^1H NMR (300 MHz, DMSO- d_6) δ (ppm) 1.22 (s, 3H, CH₃ Aib), 1.25 (s, 3H, CH₃ Aib), 3.22 (dd, 1H, $J = 14$ and 6 Hz, CH₂ β Trp), 3.34 (dd, 1H, $J = 14$ and 9 Hz, CH₂ β Trp), 3.68 (s, 3H, OCH₃), 4.11 (m, 2H, CH₂-indole), 5.09 (m, 3H, CH α Trp and CH₂-*p*-methoxybenzyl), 6.70 (s, 4H, CHar *p*-methoxybenzyl), 6.78 (m, 2H, H₅ indole and H₅ Trp), 6.93 (m, 2H, H₆ indole and H₆ Trp), 7.01–7.06 (m, 3H, H₂ indole, H₂ and H₄ Trp), 7.31 (m, 3H, H₄ and H₇ indole, H₇ Trp), 7.98 (brs, 3H, NH₂ Aib, TFA salt), 8.92 (d, 1H, $J = 8$ Hz, NH amide), 10.77 (s, 1H, NH indole), 10.89 (s, 1H, NH indole Trp). ^{13}C NMR (75 MHz, DMSO- d_6) δ (ppm) 21.7 (CH₂-indole), 23.5 (CH₃ Aib), 23.7 (CH₃ Aib), 28.9 (C β Trp), 45.6 (C α Trp), 45.8 (CH₂-*p*-methoxybenzyl), 55.5 (OCH₃), 56.7 (Cq Aib), 108.1 (C₃ indole), 109.7 (C₃ Trp), 111.7 (C₇ Trp), 111.9 (C₇ indole), 114.5 (C₃ and C₅ *p*-methoxybenzyl), 118.3 (C₄ Trp), 118.7 (C₄ indole), 118.8 (C₅ indole), 118.9 (C₅ Trp), 121.3 (C₆ indole), 121.6 (C₆ Trp), 124.2 (C₂ indole), 125.3 (C₂ Trp), 127.1 (C₉ indole), 127.2 (C₉ Trp), 127.6 (C₁ *p*-methoxybenzyl), 127.8 (C₂ and C₆ *p*-methoxybenzyl), 136.4 (C₈ Trp), 136.7 (C₈ indole), 154.2 (Cq triazole), 155.2 (Cq triazole), 159.2 (C₄ *p*-methoxybenzyl), 171.9 (CO amide).

(R)-N-(1-(4-(4-Methoxybenzyl)-5-phenethyl-4H-1,2,4-triazol-3-yl)-2-(1H-indol-3-yl)ethyl)-2-amino-2-methylpropanamide Trifluoroacetate Salt (19b). ^1H NMR (300 MHz, DMSO- d_6) δ (ppm) 1.28 (s, 3H, CH₃ Aib), 1.32 (s, 3H, CH₃ Aib), 2.46 (m, 2H, CH₂-CH₂-phenyl), 2.82 (m, 2H, CH₂-CH₂-phenyl), 3.35 (d, 2H, $J = 7$ Hz, CH₂ β Trp), 3.68 (s, 3H, OCH₃), 5.02 (s, 2H, CH₂-*p*-methoxybenzyl), 5.22 (m, 1H, CH α Trp), 6.73–6.81 (s, 4H, CHar *p*-methoxybenzyl), 6.84 (t, 1H, $J_0 = 7$ Hz, H₅ Trp), 7.00 (t, 1H, $J_0 = 7$ Hz, H₆ Trp), 7.05–7.11 (m, 4H, H₂ and H₆ phenyl, H₂ and H₄ Trp), 7.14–7.22 (m, 3H, H₃, H₄ and H₅ phenyl), 7.29 (d, 1H, $J_0 = 8$ Hz, H₇ Trp), 8.09 (brs, 3H, NH₂ Aib, TFA salt), 8.99 (d, 1H, $J = 8$ Hz, NH amide), 10.83 (s, 1H, NH indole Trp). ^{13}C NMR (75 MHz, DMSO- d_6) δ (ppm) 23.5 (CH₃ Aib), 23.8 (CH₃ Aib), 26.5 (CH₂-CH₂-phenyl), 29.1 (C β Trp), 32.6 (CH₂-CH₂-phenyl), 45.5 (CH₂-*p*-methoxybenzyl), 45.7 (C α Trp), 55.5 (OCH₃), 56.8 (Cq Aib), 109.7 (C₃ Trp), 111.8 (C₇ Trp), 114.6 (C₃ and C₅ *p*-methoxybenzyl), 118.3 (C₄ Trp), 118.7 (C₅ Trp), 121.3 (C₆ Trp), 124.9 (C₂ Trp), 126.6 (C₄ phenyl), 127.3 (C₉ Trp), 127.6 (C₁ *p*-methoxybenzyl), 128.0 (C₂ and C₆ *p*-methoxybenzyl), 128.7 (C₂, C₃, C₅, and C₆ phenyl), 136.4 (C₈ Trp), 140.8 (C₁ phenyl), 154.5 (Cq triazole), 154.8 (Cq triazole), 159.2 (C₄ *p*-methoxybenzyl), 172.0 (CO amide).

(R)-N-(1-(5-(2-(1H-Indol-3-yl)ethyl)-4-(4-methoxybenzyl)-4H-1,2,4-triazol-3-yl)-2-(1H-indol-3-yl)ethyl)-2-amino-2-methylpropanamide Trifluoroacetate Salt (19c). ^1H NMR (400 MHz, DMSO- d_6) δ 1.30 (s, 3H, CH₃ Aib), 1.33 (s, 3H, CH₃ Aib), 2.91 (m, 2H, CH₂-CH₂-indole), 2.97 (m, 2H, CH₂-CH₂-indole), 3.37 (d, 2H, CH₂ β Trp), 3.71 (s, 3H, OCH₃), 5.02 (s, 2H, CH₂-*p*-

methoxybenzyl), 5.23 (m, 1H, CH α Trp), 6.78 (s, 4H, CHar *p*-methoxybenzyl), 6.87 (t, 1H, *J* = 8 Hz, H₅ Trp), 6.93 (t, 1H, *J* = 8 Hz, H₅ indole), 7.03 (t, 1H, H₆ Trp), 7.05 (t, 1H, H₆ indole), 7.07 (s, 1H, H₂ indole), 7.09 (s, 1H, H₂ Trp), 7.21 (d, 1H, *J* = 8 Hz, H₄ Trp), 7.32 (3H, H₄, H₇ indole, H₇ Trp), 8.02 (brs, 3H, NH₂ Aib, TFA salt), 8.97 (d, 1H, *J* = 8 Hz, NH amide), 10.77 (s, 1H, NH indole), 10.80 (s, 1H, NH indole Trp). ¹³C NMR (100 MHz, DMSO-*d*₆) δ (ppm) 22.4 (CH₂-CH₂ indole), 23.1 (CH₃ Aib), 23.4 (CH₃ Aib), 25.5 (CH₂-CH₂ indole), 28.9 (C β Trp), 44.9 (CH₂ *p*-methoxybenzyl), 45.3 (C α Trp), 55.0 (OCH₃), 56.3 (Cq Aib), 109.5 (C₃ Trp), 111.3 (C₇ Trp, C₇ indole), 113.0 (C₃ indole), 114.1 (C₃, C₅ *p*-methoxybenzyl), 117.9 (C₄ Trp), 118.0 (C₄ indole), 118.2 (C₅ indole), 118.3 (C₅ Trp), 120.9 (C₆ indole, C₆ Trp), 122.0 (C₂ indole), 124.4 (C₂ Trp), 126.7 (C₉ indole), 126.9 (C₉ Trp), 127.3 (C₂, C₆ *p*-methoxybenzyl), 127.4 (C₁ *p*-methoxybenzyl), 135.9 (C₈ Trp), 136.1 (C₈ indole), 154.2 (Cq triazole), 154.5 (Cq triazole), 158.4 (C₄ *p*-methoxybenzyl), 171.4 (CO amide).

(R)-N-(1-(4-(4-Methoxybenzyl)-5-(3-phenylpropyl)-4H-1,2,4-triazol-3-yl)-2-(1H-indol-3-yl)ethyl)-2-amino-2-methylpropanamide Trifluoroacetate Salt (19d). ¹H NMR (300 MHz, DMSO-*d*₆, 300 K) δ (ppm) 1.27 (s, 3H, CH₃ Aib), 1.31 (s, 3H, CH₃ Aib), 1.73 (m, 2H, CH₂-CH₂-CH₂-phenyl), 2.47 (m, 2H, CH₂-CH₂-CH₂-phenyl), 2.52 (t, 2H, ³*J* = 7 Hz, CH₂-CH₂-CH₂-phenyl), 3.35 (d, 2H, *J* = 7 Hz, CH₂ β Trp), 3.68 (s, 3H, OCH₃), 4.98 (s, 2H, CH₂-*p*-methoxybenzyl), 5.20 (m, 1H, CH α Trp), 6.75 (s, 4H, CHar *p*-methoxybenzyl), 6.82 (t, 1H, *J*_o = 7 Hz, H₅ Trp), 6.99 (t, 1H, *J*_o = 7 Hz, H₆ Trp), 7.04-7.07 (m, 4H, H₂ and H₆ phenyl, H₂ and H₄ Trp), 7.13-7.24 (m, 3H, H₃, H₄, and H₅ phenyl), 7.29 (d, 1H, *J*_o = 8 Hz, H₇ Trp), 8.03 (brs, 3H, NH₂ Aib, TFA salt), 8.96 (d, 1H, *J* = 8 Hz, NH amide), 10.80 (d, 1H, *J* = 2 Hz, NH indole Trp). ¹³C NMR (75 MHz, DMSO-*d*₆, 300 K) δ (ppm) 23.6 (CH₃ Aib), 23.6 (CH₃ Aib), 24.06 (CH₂-CH₂-CH₂-phenyl), 28.5 (CH₂-CH₂-CH₂-phenyl), 29.2 (CH₂ β Trp), 34.7 (CH₂-CH₂-CH₂-phenyl), 45.5 (CH₂-*p*-methoxybenzyl), 45.8 (CH α Trp), 55.5 (OCH₃), 56.8 (Cq Aib), 109.8 (C₃ Trp), 111.8 (C₇ Trp), 114.6 (C₃ and C₅ *p*-methoxybenzyl), 118.3 (C₄ Trp), 118.7 (C₅ Trp), 121.3 (C₆ Trp), 124.9 (C₂ Trp), 126.2 (C₄ phenyl), 127.3 (C₉ Trp), 127.8 (C₁ *p*-methoxybenzyl), 127.9 (C₂ and C₆ *p*-methoxybenzyl), 128.7 (C₂, C₃, C₅, and C₆ phenyl), 136.4 (C₈ Trp), 141.7 (C₁ phenyl), 154.8 (2Cq triazole), 159.2 (C₄ *p*-methoxybenzyl), 171.9 (CO amide).

(R)-N-(1-(4-(4-Methoxybenzyl)-5-benzyl-4H-1,2,4-triazol-3-yl)-2-(1H-indol-3-yl)ethyl)-2-amino-2-methylpropanamide Trifluoroacetate Salt (19e). ¹H NMR (300 MHz, DMSO-*d*₆, 300 K) δ (ppm) 1.24 (s, 3H, CH₃ Aib), 1.28 (s, 3H, CH₃ Aib), 3.26 (dd, 1H, ³*J* = 14 and 6 Hz, CH₂ β Trp), 3.31 (dd, 1H, ³*J* = 14 and 9 Hz, CH₂ β Trp), 3.67 (s, 3H, OCH₃), 3.99 (s, 2H, CH₂ benzyl), 4.99 (s, 2H, CH₂-*p*-methoxybenzyl), 5.12 (m, 1H, CH α Trp), 6.67 (s, 4H, CHar *p*-methoxybenzyl), 6.80 (t, 1H, *J*_o = 8 Hz, H₅ Trp), 6.98 (t, 1H, *J*_o = 8 Hz, H₆ Trp), 7.02-7.06 (m, 4H, H₂ and H₆ benzyl, H₂ and H₄ Trp), 7.12-7.25 (m, 3H, H₃, H₄, and H₅ benzyl), 7.26 (d, 1H, *J*_o = 8 Hz, H₇ Trp), 8.01 (brs, 3H, NH₂ Aib, TFA salt), 8.92 (d, 1H, *J* = 8 Hz, NH amide), 10.77 (s, 1H, NH indole Trp). ¹³C NMR (75 MHz, DMSO-*d*₆, 300 K) δ (ppm) 23.5 (CH₃ Aib), 23.7 (CH₃ Aib), 29.1 (CH₂ β Trp), 30.6 (CH₂-benzyl), 45.7 (CH₂-*p*-methoxybenzyl), 45.7 (CH α Trp), 55.5 (OCH₃), 56.7 (Cq Aib), 109.8 (C₃ Trp), 111.7 (C₇ Trp), 114.5 (C₃ and C₅ *p*-methoxybenzyl), 118.3 (C₄ Trp), 118.7 (C₅ Trp), 121.3 (C₆ Trp), 124.8 (C₂ Trp), 127.1 (C₂ and C₆ benzyl), 127.3 (C₉ Trp), 127.6 (C₁ *p*-methoxybenzyl), 127.8 (C₂ and C₆ *p*-methoxybenzyl), 128.8 (C₃, C₄, and C₅ benzyl), 136.3 (C₁ benzyl), 136.4 (C₈ Trp), 153.8 (Cq triazole), 155.2 (Cq triazole), 159.1 (C₄ *p*-methoxybenzyl), 171.9 (CO amide).

(R)-N-(1-(5-(3-(1H-Indol-3-yl)propyl)-4-(4-methoxybenzyl)-4H-1,2,4-triazol-3-yl)-2-(1H-indol-3-yl)ethyl)-2-amino-2-methylpropanamide Trifluoroacetate Salt (19f). ¹H NMR (300 MHz, DMSO-*d*₆, 300 K) δ (ppm) 1.27 (s, 3H, CH₃ Aib), 1.30 (s, 3H, CH₃ Aib), 1.84 (m, 2H, CH₂CH₂CH₂-indole), 2.58 (m, 2H, CH₂-CH₂CH₂-indole), 2.65 (m, 2H, CH₂CH₂CH₂-indole), 3.34 (d, 2H, ³*J* = 7 Hz, CH₂ β Trp), 3.67 (s, 3H, OCH₃), 4.96 (s, 2H, CH₂-*p*-methoxybenzyl), 5.19 (m, 1H, CH α Trp), 6.71 (s, 4H, CH ar *p*-methoxybenzyl), 6.89 (t, 1H, *J*_o = 7 Hz, H₅ Trp), 6.92 (t, 1H, *J*_o

= 7 Hz, H₅ indole), 6.96 (m, 2H, H₆ indole, H₆ Trp), 7.02 (s, 1H, H₂ indole), 7.05 (s, 1H, H₂ Trp), 7.14 (d, 1H, *J*_o = 8 Hz, H₄ Trp), 7.33 (m, 3H, H₄ indole, H₇ Trp, H₇ indole), 7.90 (d, 1H, *J* = 8 Hz, NH amide), 8.02 (brs, 3H, NH₂ Aib, TFA salt), 10.73 (s, 1H, NH indole), 10.79 (s, 1H, NH indole Trp). ¹³C NMR (75 MHz, DMSO-*d*₆, 300 K) δ (ppm) 23.6 (CH₃ Aib), 23.8 (CH₃ Aib), 24.3 (CH₂-CH₂CH₂-indole), 24.8 (CH₂CH₂CH₂-indole), 27.7 (CH₂CH₂CH₂-indole), 29.1 (C β Trp), 45.5 (CH₂-*p*-methoxybenzyl), 45.8 (C α Trp), 55.5 (OCH₃), 56.8 (Cq Aib), 109.8 (C₃ Trp), 111.7 (C₇ Trp, C₇ indole), 114.0 (C₃ indole), 114.5 (C₃, C₅ *p*-methoxybenzyl), 118.3 (C₄ indole, C₄ Trp), 118.5 (C₅ indole), 118.8 (C₅ Trp), 121.3 (C₆ indole, C₆ Trp), 127.3 (C₉ indole), 127.4 (C₉ Trp), 127.6 (C₁ *p*-methoxybenzyl), 127.9 (C₂, C₆ *p*-methoxybenzyl, C₂ Trp, C₂ indole), 136.1 (C₈ indole), 136.4 (C₈ Trp), 154.7 (Cq triazole), 155.1 (Cq triazole), 159.2 (C₄ *p*-methoxybenzyl), 171.9 (CO amide).

(R)-N-(1-(4-(2-Methoxybenzyl)-5-benzyl-4H-1,2,4-triazol-3-yl)-2-(1H-indol-3-yl)ethyl)-2-amino-2-methylpropanamide Trifluoroacetate Salt (20a). ¹H NMR (300 MHz, DMSO-*d*₆, 300 K) δ (ppm) 1.24 (s, 3H, CH₃ Aib), 1.27 (s, 3H, CH₃ Aib), 3.20 (dd, 1H, *J* = 14 and 5 Hz, CH₂ β Trp), 3.33 (dd, 1H, *J* = 14 and 9 Hz, CH₂ β Trp), 3.68 (s, 3H, OCH₃), 4.00 (s, 2H, CH₂-phenyl), 4.95 (d, 1H, *J* = 17 Hz, CH₂-*o*-methoxybenzyl), 5.07 (m, 1H, CH α Trp), 5.18 (d, 1H, *J* = 17 Hz, CH₂-*o*-methoxybenzyl), 6.27 (d, 1H, *J*_o = 8 Hz, H₃ *o*-methoxybenzyl), 6.67 (t, 1H, *J*_o = 7 Hz, H₅ Trp), 6.77 (t, 1H, *J*_o = 6 Hz, H₆ Trp), 6.92-7.05 (m, 6H, H₂ Trp, H₂ and H₆ phenyl, H₄, H₅, and H₆ *o*-methoxybenzyl), 7.14-7.26 (m, 5H, H₄ and H₇ Trp, H₃, H₄, and H₅ phenyl), 8.03 (brs, 3H, NH₂ Aib, TFA salt), 8.91 (d, 1H, *J* = 8 Hz, NH amide), 10.78 (s, 1H, NH indole Trp). ¹³C NMR (75 MHz, DMSO-*d*₆, 300 K) δ (ppm) 23.5 (CH₃ Aib), 23.6 (CH₃ Aib), 29.1 (C β Trp), 30.5 (CH₂-phenyl), 42.1 (CH₂-*o*-methoxybenzyl), 45.7 (CH α Trp), 55.9 (OCH₃), 56.7 (Cq Aib), 109.8 (C₃ Trp), 111.3 (C₃ *o*-methoxybenzyl), 111.7 (C₇ Trp), 118.2 (C₄ Trp), 118.7 (C₅ Trp), 120.9 (C₅ *o*-methoxybenzyl), 121.2 (C₆ Trp), 123.3 (C₁ *o*-methoxybenzyl), 124.8 (C₂ Trp), 126.6 (C₄ phenyl), 127.1 (C₄ *o*-methoxybenzyl), 127.2 (C₉ Trp), 128.8 (C₂, C₃, C₅ and C₆ phenyl), 129.5 (C₆ *o*-methoxybenzyl), 136.0 (C₁ phenyl), 136.4 (C₈ Trp), 154.0 (Cq triazole), 155.6 (Cq triazole), 156.5 (C₂ *o*-methoxybenzyl), 171.8 (CO amide).

(R)-N-(1-(5-(2-(1H-Indol-3-yl)ethyl)-4-(2-methoxybenzyl)-4H-1,2,4-triazol-3-yl)-2-(1H-indol-3-yl)ethyl)-2-amino-2-methylpropanamide Trifluoroacetate Salt (20b). ¹H NMR (300 MHz, DMSO-*d*₆, 300 K) δ (ppm) 1.27 (s, 3H, CH₃ Aib), 1.29 (s, 3H, CH₃ Aib), 2.90 (m, 2H, CH₂-CH₂-indole), 2.96 (m, 2H, CH₂-CH₂-indole), 3.29 (m, 2H, CH₂ β Trp), 3.65 (s, 3H, OCH₃), 5.09 (m, 3H, CH₂-*o*-methoxybenzyl and CH α Trp), 6.49 (d, 1H, *J*_o = 8 Hz, H₃ *o*-methoxybenzyl), 6.76 (t, 1H, *J*_o = 8 Hz, H₅ Trp), 6.81 (t, 1H, *J*_o = 8 Hz, H₅ indole), 6.89 (t, 1H, *J*_o = 7 Hz, H₆ Trp), 6.96 (t, 1H, *J*_o = 8 Hz, H₆ indole), 6.98 (s, 1H, H₂ indole), 7.02 (m, 3H, H₄, H₅, and H₆ *o*-methoxybenzyl), 7.07 (d, 1H, *J*_o = 6 Hz, H₄ Trp), 7.18 (d, 1H, H₄ indole), 7.29 (m, 2H, H₇ indole and H₇ Trp), 8.07 (brs, 3H, NH₂ Aib, TFA salt), 8.97 (d, 1H, *J* = 8 Hz, NH amide), 10.80 (s, 1H, NH indole), 10.82 (s, 1H, NH indole Trp). ¹³C NMR (75 MHz, DMSO-*d*₆, 300 K) δ (ppm) 22.8 (CH₂-CH₂-indole), 23.6 (CH₃ Aib), 23.7 (CH₃ Aib), 25.8 (CH₂-CH₂-indole), 29.1 (C β Trp), 42.3 (CH₂-*o*-methoxybenzyl), 45.7 (C α Trp), 55.8 (OCH₃), 56.7 (Cq Aib), 109.8 (C₃ Trp), 111.5 (C₃ *o*-methoxybenzyl), 111.8 (C₇ indole and C₇ Trp), 113.2 (C₃ indole), 118.2 (C₄ Trp), 118.4 (C₄ indole), 118.7 (C₅ indole and C₅ Trp), 121.0 (C₆ indole), 121.3 (C₆ Trp), 121.4 (C₅ *o*-methoxybenzyl), 123.0 (C₂ indole and C₂ Trp), 123.3 (C₁ *o*-methoxybenzyl), 127.0 (C₄ *o*-methoxybenzyl), 127.1 (C₉ indole), 127.3 (C₉ Trp), 129.8 (C₆ *o*-methoxybenzyl), 136.4 (C₈ indole), 136.6 (C₈ Trp), 155.2 (2Cq triazole), 156.6 (C₂ *o*-methoxybenzyl), 171.9 (CO amide).

(R)-N-(1-(4-(2-Methoxybenzyl)-5-phenethyl-4H-1,2,4-triazol-3-yl)-2-(1H-indol-3-yl)ethyl)-2-amino-2-methylpropanamide Trifluoroacetate Salt (20c). ¹H NMR (300 MHz, DMSO-*d*₆, 300 K) δ (ppm) 1.26 (s, 3H, CH₃ Aib), 1.29 (s, 3H, CH₃ Aib), 2.78-2.92 (m, 4H, CH₂-CH₂-phenyl), 3.29 (m, 2H, CH₂ β Trp), 3.65 (s, 3H, OCH₃), 4.97-5.21 (m, 3H, CH α Trp and CH₂-*o*-methoxybenzyl), 6.52 (d, 1H, *J*_o = 7 Hz, H₃ *o*-methoxybenzyl), 6.78 (t, 1H, *J*_o = 7

Hz, H₅ Trp), 6.82 (t, 1H, *J*₆ = 8 Hz, H₆ Trp), 6.84–7.04 (m, 3H, H₂ and H₆ phenyl, H₂ Trp), 7.04–7.10 (m, 3H, H₄, H₅, and H₆ *o*-methoxybenzyl), 7.15 (d, 1H, *J*₀ = 7 Hz, H₄ Trp), 7.19–7.29 (m, 4H, H₃, H₄ and H₅ phenyl, H₇ Trp), 8.03 (brs, 3H, NH₂ Aib, TFA salt), 8.94 (d, 1H, *J* = 8 Hz, NH amide), 10.82 (s, 1H, NH indole Trp). ¹³C NMR (75 MHz, DMSO-*d*₆, 300 K) δ (ppm) 23.6 (CH₃ Aib), 23.7 (CH₃ Aib), 26.3 (CH₂-CH₂-phenyl), 29.0 (C βTrp), 32.5 (CH₂-CH₂-phenyl), 42.3 (CH₂-*o*-methoxybenzyl), 45.7 (C αTrp), 55.8 (OCH₃), 56.7 (Cq Aib), 109.7 (C₃ Trp), 111.5 (C₇ Trp), 111.8 (C₃ *o*-methoxybenzyl), 118.2 (C₄ Trp), 118.7 (C₅ Trp), 121.0 (C₆ Trp), 121.3 (C₅ *o*-methoxybenzyl), 123.2 (C₁ *o*-methoxybenzyl), 124.9 (C₂ Trp), 126.6 (C₄ phenyl), 127.2 (C₉ Trp and C₄ *o*-methoxybenzyl), 128.7 (C₂, C₃, C₅ and C₆ phenyl), 129.9 (C₆ *o*-methoxybenzyl), 136.4 (C₈ Trp), 140.6 (C₁ phenyl), 154.8 (Cq triazole), 155.2 (Cq triazole), 156.7 (C₂ *o*-methoxybenzyl), 171.9 (CO amide).

(*R*)-*N*-(1-(5-(2-(1*H*-Indol-3-yl)ethyl)-4-benzyl-4*H*-1,2,4-triazol-3-yl)-2-(1*H*-indol-3-yl)ethyl)-2-amino-2-methylpropanamide Trifluoroacetate Salt (21a). ¹H NMR (400 MHz, DMSO-*d*₆) δ 1.29 (s, 3H, CH₃ Aib), 1.30 (s, 3H, CH₃ Aib), 2.88 (m, 2H, CH₂-CH₂-indole), 2.97 (m, 2H, CH₂-CH₂-indole), 3.37 (m, 2H, CH₂ βTrp), 5.11 (s, 2H, CH₂-benzyl), 5.21 (m, 1H, CH αTrp), 6.86 (t, 1H, *J* = 7 Hz, H₅ Trp), 6.88 (2H, H₂, H₆ benzyl), 6.92 (t, 1H, *J* = 8 Hz, H₅ indole), 7.03 (t, 1H, *J* = 8 Hz, H₆ Trp), 7.05 (2H, H₆ indole, H₂ indole), 7.09 (d, 1H, *J* = 2 Hz, H₂ Trp), 7.17 (d, 1H, *J* = 8 Hz, H₄ Trp), 7.26 (2H, H₃, H₅ benzyl), 7.27 (1H, H₄ benzyl), 7.30 (1H, H₄ indole), 7.32 (2H, H₇ Trp, H₇ indole), 8.03 (brs, 3H, NH₂ Aib, TFA salt), 8.95 (d, 1H, *J* = 8 Hz, NH amide), 10.77 (s, 1H, NH indole), 10.81 (s, 1H, NH indole Trp). ¹³C NMR (100 MHz, DMSO-*d*₆) δ 22.4 (CH₂-CH₂ indole), 23.1 (CH₃ Aib), 23.3 (CH₃ Aib), 25.4 (CH₂-CH₂ indole), 28.7 (C βTrp), 45.3 (C αTrp, CH₂-benzyl), 56.3 (Cq Aib), 109.5 (C₃ Trp), 111.3 (C₇ Trp, C₇ indole), 113.0 (C₃ indole), 117.8 (C₄ Trp), 118.0 (C₄ indole), 118.2 (C₅ indole), 118.3 (C₅ Trp), 120.9 (C₆ Trp, C₆ indole), 122.4 (C₂ indole), 124.3 (C₂ Trp), 125.9 (C₄ benzyl), 126.7 (C₉ indole), 126.9 (C₉ Trp), 127.6 (C₂, C₆ benzyl), 128.8 (C₃, C₅ benzyl), 135.7 (C₁ benzyl), 136.0 (C₈ Trp), 136.1 (C₈ indole), 154.3 (Cq triazole), 154.5 (Cq triazole), 171.4 (CO amide).

(*R*)-*N*-(1-(5-(3-(1*H*-Indol-3-yl)propyl)-4-benzyl-4*H*-1,2,4-triazol-3-yl)-2-(1*H*-indol-3-yl)ethyl)-2-amino-2-methylpropanamide Trifluoroacetate Salt (21b). ¹H NMR (400 MHz, DMSO-*d*₆) δ 1.29 (s, 3H, CH₃ Aib), 1.31 (s, 3H, CH₃ Aib), 1.90 (m, 2H, CH₂-CH₂-CH₂-indole), 2.61 (m, 2H, CH₂-CH₂-CH₂-indole), 2.69 (m, 2H, CH₂-CH₂-CH₂-indole), 3.37 (m, 2H, CH₂ βTrp), 5.09 (s, 2H, CH₂ Bzl), 5.20 (m, 1H, CH αTrp), 6.85 (m, 3H, H₂, H₆ Bzl, H₅ Trp), 6.94 (t, 1H, *J* = 7.5, H₅ indole), 7.01 (s, 1H, H₂ indole), 7.02 (t, 1H, *J* = 7.8, H₆ Trp), 7.05 (t, 1H, *J* = 8, H₆ indole), 7.08 (d, 1H, *J* = 2.0, H₂ Trp), 7.14 (d, 1H, *J* = 8.0, H₄ Trp), 7.25 (m, 3H, H₃, H₄, H₅ benzyl), 7.31 (d, 1H, *J* = 8.0, H₇ Trp), 7.32 (d, 1H, *J* = 8.0, H₇ indole), 7.42 (d, 1H, *J* = 7.8, H₄ indole), 8.03 (brs, 3H, NH₂ Aib, TFA salt), 8.95 (d, 1H, *J* = 8.1, NH Trp), 10.73 (s, 1H, NH indole), 10.80 (d, 1H, *J* = 2.0, NH indole Trp). ¹³C NMR (100 MHz, DMSO-*d*₆) δ 23.1 (CH₃ Aib), 23.3 (CH₃ Aib), 23.8 (CH₂-CH₂-CH₂-indole), 24.1 (CH₂-CH₂-CH₂-indole), 27.2 (CH₂-CH₂-CH₂-indole), 28.7 (C βTrp), 45.4 (C αTrp), 45.5 (CH₂ benzyl), 56.3 (Cq Aib), 109.4 (C₃ Trp), 111.3 (C₇ Trp, C₇ indole), 113.6 (C₃ indole), 117.8 (C₄ Trp), 118.0 (C₅ indole), 118.2 (C₄ indole), 118.3 (C₅ Trp), 120.8 (C₆ indole, C₆ Trp), 122.2 (C₂ indole), 124.3 (C₂ Trp), 125.9 (C₄ benzyl), 126.8 (C₉ Trp), 127.0 (C₉ indole), 127.7 (C₂, C₆ benzyl), 128.7 (C₃, C₅ benzyl), 135.5 (C₁ benzyl), 136.0 (C₈ Trp), 136.2 (C₈ indole), 154.3 (Cq triazole), 154.7 (Cq triazole), 171.4 (CO amide).

2-Amino-*N*-(*R*)-1-(4,5-dibenzyl-4*H*-1,2,4-triazol-3-yl)-2-(1*H*-indol-3-yl)ethyl)-2-methylpropanamide Trifluoroacetate Salt (21c). ¹H NMR (300 MHz, DMSO-*d*₆, 300 K) δ (ppm) 1.23 (s, 3H, CH₃ Aib), 1.26 (s, 3H, CH₃ Aib), 3.23 (dd, 1H, *J* = 14 and 6 Hz, CH₂ βTrp), 3.35 (dd, 1H, *J* = 14 and 9 Hz, CH₂ βTrp), 3.99 (s, 2H, C-CH₂-phenyl), 5.10 (m, 3H, N-CH₂-phenyl and CH αTrp), 6.77 (m, 3H, H₅ Trp, H₂ and H₆ phenyl from N-CH₂-phenyl), 6.99 (m, 2H, H₂ and H₆ Trp), 7.01–7.07 (m, 3H, H₄ Trp, H₂ and H₆ from C-CH₂-phenyl), 7.15–7.23 (m, 6H, H₃, H₄, and

H₅ phenyl from N-CH₂-phenyl and from C-CH₂-phenyl), 7.25 (d, 1H, *J* = 8 Hz, H₇ Trp), 8.01 (brs, 3H, NH₂ Aib, TFA salt), 8.91 (d, 1H, *J* = 8 Hz, NH amide), 10.78 (s, 1H, NH indole Trp). ¹³C NMR (75 MHz, DMSO-*d*₆, 300 K) δ (ppm) 23.5 (CH₃ Aib), 23.7 (CH₃ Aib), 29.0 (C βTrp), 30.6 (C-CH₂-phenyl), 45.7 (C αTrp), 46.1 (N-CH₂-phenyl), 56.7 (Cq Aib), 109.8 (C₃ Trp), 111.7 (C₇ Trp), 118.3 (C₄ Trp), 118.7 (C₅ Trp), 121.2 (C₆ Trp), 124.8 (C₂ Trp), 126.3 (C₄ phenyl from N-CH₂-phenyl), 127.0 (C₄ phenyl from C-CH₂-phenyl), 127.2 (C₉ Trp), 128.0 (C₂, C₆ phenyl from N-CH₂-phenyl), 128.8 (C₂, C₃, C₅, and C₆ from C-CH₂-phenyl), 128.9 (C₃ and C₅ phenyl from N-CH₂-phenyl), 135.8 (C₁ phenyl from N-CH₂-phenyl), 136.2 (C₁ phenyl from C-CH₂-phenyl), 136.4 (C₈ Trp), 153.9 (Cq triazole), 155.3 (Cq triazole), 171.9 (CO amide).

(*R*)-*N*-(1-(5-(2-(1*H*-Indol-3-yl)ethyl)-4-(4-bromobenzyl)-4*H*-1,2,4-triazol-3-yl)-2-(1*H*-indol-3-yl)ethyl)-2-amino-2-methylpropanamide Trifluoroacetate Salt (22a). ¹H NMR (400 MHz, DMSO-*d*₆) δ 1.28 (s, 3H, CH₃ Aib), 1.30 (s, 3H, CH₃ Aib), 2.90 (m, 2H, CH₂-CH₂-indole), 3.00 (m, 2H, CH₂-CH₂-indole), 3.37 (m, 2H, CH₂ βTrp), 5.10 (s, 2H, CH₂ *p*-bromobenzyl), 5.13 (m, 1H, CH αTrp), 6.75 (d, 2H, *J* = 8.1, H₂, H₆ *p*-bromobenzyl), 6.88 (t, 1H, *J* = 7.3, H₅ Trp), 6.93 (t, 1H, *J* = 7.5, H₅ indole), 7.03 (t, 1H, *J* = 7.0, H₆ Trp), 7.05 (m, 1H, H₆ indole), 7.07 (d, 1H, *J* = 1.7, H₂ indole), 7.09 (d, 1H, *J* = 1.8, H₂ Trp), 7.12 (d, 1H, *J* = 8.2, H₄ Trp), 7.28 (d, 1H, *J* = 7.9, H₄ indole), 7.32 (d, 2H, *J* = 8.2, H₇ Trp, H₇ indole), 7.41 (d, 2H, *J* = 8.1, H₃, H₅ *p*-bromobenzyl), 8.01 (brs, 3H, NH₂ Aib, TFA salt), 8.95 (d, 1H, *J* = 7.9, NH amide), 10.77 (brs, 1H, NH indole), 10.80 (brs, 1H, NH indole Trp). ¹³C NMR (100 MHz, DMSO-*d*₆) δ 22.4 (CH₂-CH₂ indole), 23.1 (CH₃ Aib), 23.4 (CH₃ Aib), 25.4 (CH₂-CH₂ indole), 28.7 (C βTrp), 44.8 (CH₂ *p*-bromobenzyl), 45.2 (C αTrp), 56.3 (Cq Aib), 109.4 (C₃ Trp), 111.3 (C₇ Trp, C₇ indole), 113.0 (C₃ indole), 117.8 (C₄ Trp), 118.0 (C₄ indole), 118.2 (C₅ indole), 118.3 (C₅ Trp), 120.8 (C₄ *p*-bromobenzyl), 120.9 (C₆ Trp, C₆ indole), 122.5 (C₂ indole), 124.4 (C₂ Trp), 126.7 (C₉ indole), 126.8 (C₉ Trp), 128.0 (C₂, C₆ *p*-bromobenzyl), 131.6 (C₃, C₅ *p*-bromobenzyl), 135.1 (C₁ *p*-bromobenzyl), 136.1 (C₈ Trp, C₈ indole), 154.2 (Cq triazole), 154.5 (Cq triazole), 171.4 (CO amide).

N-(*R*)-1-(4-(4-Bromobenzyl)-5-benzyl-4*H*-1,2,4-triazol-3-yl)-2-(1*H*-indol-3-yl)ethyl)-2-amino-2-methylpropanamide Trifluoroacetate Salt (22c). ¹H NMR (300 MHz, DMSO-*d*₆, 300 K) δ (ppm) 1.23 (s, 3H, CH₃ Aib), 1.25 (s, 3H, CH₃ Aib), 3.26 (dd, 1H, ³*J* = 14 and 6 Hz, CH₂ Trp), 3.34 (dd, 1H, ³*J* = 14 and 9 Hz, CH₂ βTrp), 4.01 (m, 2H, CH₂-benzyl), 5.01 (m, 1H, CH αTrp), 5.08 (s, 2H, CH₂-*p*-bromobenzyl), 6.59 (d, 2H, *J*₀ = 8 Hz, H₂ and H₆ *p*-bromobenzyl), 6.81 (t, 1H, *J*₀ = 7 Hz, H₅ Trp), 6.94 (s, 1H, H₂ Trp), 6.98 (t, 1H, *J*₀ = 7 Hz, H₆ Trp), 7.06 (m, 2H, H₂ and H₆ benzyl), 7.12 (d, 1H, *J*₀ = 7 Hz, H₄ Trp), 7.16–7.20 (m, 3H, H₃, H₄, and H₅ benzyl), 7.26 (d, 1H, *J*₀ = 8 Hz, H₇ Trp), 7.29 (d, 2H, *J*₀ = 8 Hz, H₃ and H₅ *p*-bromobenzyl), 8.00 (brs, 3H, NH₂ Aib, TFA salt), 8.92 (d, 1H, *J* = 8 Hz, NH amide), 10.78 (s, 1H, NH indole Trp). ¹³C NMR (75 MHz, DMSO-*d*₆, 300 K) δ (ppm) 23.5 (CH₃ Aib), 23.8 (CH₃ Aib), 29.0 (C βTrp), 30.5 (CH₂-benzyl), 45.6 (CH₂-*p*-bromobenzyl), 45.7 (C αTrp), 56.7 (Cq Aib), 109.7 (C₃ Trp), 111.8 (C₇ Trp), 118.2 (C₄ Trp), 118.7 (C₅ Trp), 121.2 (C₄ *p*-bromobenzyl), 121.3 (C₆ Trp), 124.9 (C₂ Trp), 127.0 (C₂ and C₆ benzyl), 127.2 (C₉ Trp), 128.4 (C₂ and C₆ *p*-bromobenzyl), 128.9 (C₃, C₄ and C₅ benzyl), 131.9 (C₃ and C₅ *p*-bromobenzyl), 135.2 (C₁ *p*-bromobenzyl), 136.2 (C₈ Trp), 136.4 (C₁ benzyl), 153.9 (Cq triazole), 155.3 (Cq triazole), 171.9 (CO amide).

(*R*)-*N*-(1-(4-(4-Fluorobenzyl)-5-benzyl-4*H*-1,2,4-triazol-3-yl)-2-(1*H*-indol-3-yl)ethyl)-2-amino-2-methylpropanamide Trifluoroacetate Salt (23b). ¹H NMR (300 MHz, DMSO-*d*₆, 300 K) δ (ppm) 1.27 (s, 3H, CH₃ Aib), 1.29 (s, 3H, CH₃ Aib), 3.33 (m, 2H, CH₂ βTrp), 4.02 (s, 2H, CH₂-benzyl), 5.10 (m, 3H, CH₂-*p*-fluorobenzyl and CH αTrp), 6.71 (m, 2H, H₃ and H₅ *p*-fluorobenzyl), 6.80 (t, 1H, *J*₀ = 8 Hz, H₅ Trp), 6.90 (d, 2H, *J*₀ = 8 Hz, H₂ and H₆ *p*-fluorobenzyl), 6.94 (t, 1H, *J*₀ = 8 Hz, H₆ Trp), 6.99–7.10 (m, 4H, H₂ and H₄ Trp, H₂ and H₆ benzyl), 7.20 (m, 3H, H₃, H₄ and H₅ benzyl), 7.27 (d, 1H, *J*₀ = 8 Hz, H₇ Trp), 8.09 (brs, 3H, NH₂ Aib, TFA salt), 8.97 (d, 1H, *J* = 8 Hz, NH amide), 10.79 (s,

1H, NH indole Trp). ¹³C NMR (75 MHz, DMSO-*d*₆, 300 K) δ (ppm) 23.5 (CH₃ Aib), 23.8 (CH₃ Aib), 29.0 (C β Trp), 31.1 (CH₂-benzyl), 45.7 (CH₂-*p*-fluorobenzyl), 45.8 (C α Trp), 56.8 (Cq Aib), 109.6 (C₃ Trp), 111.8 (C₇ Trp), 115.6 and 115.9 (C₃ and C₅ *p*-fluorobenzyl), 118.2 (C₄ Trp), 118.7 (C₅ Trp), 121.3 (C₆ Trp), 124.8 (C₂ Trp), 127.1 (C₄ benzyl), 127.2 (C₉ Trp), 128.8 and 128.9 (C₂ and C₆ *p*-fluorobenzyl), 129.4 (C₂, C₃, C₅, and C₆ benzyl), 131.6 (C₁ *p*-fluorobenzyl), 135.9 (C₁ benzyl), 136.4 (C₈ Trp), 154.0 (C₄ *p*-fluorobenzyl), 155.3 (2Cq triazole), 172.0 (CO amide).

***N*-(*(R)*-1-(4-(4-Fluorobenzyl)-5-phenethyl-4*H*-1,2,4-triazol-3-yl)-2-(1*H*-indol-3-yl)ethyl)-2-amino-2-methylpropanamide Trifluoroacetate Salt (23c).** ¹H NMR (300 MHz, DMSO-*d*₆, 300 K) δ (ppm) 1.27 (s, 3H, CH₃ Aib), 1.28 (s, 3H, CH₃ Aib), 2.82 (m, 4H, CH₂-CH₂-phenyl), 3.34 (m, 2H, CH₂ β Trp), 5.06 (s, 2H, CH₂-*p*-fluorobenzyl), 5.16 (m, 1H, CH α Trp), 6.85 (m, 3H, H₅ Trp, H₃ and H₅ *p*-fluorobenzyl), 6.98–7.04 (m, 4H, H₂ and H₆ Trp, H₂ and H₆ phenyl), 7.09–7.11 (m, 2H, H₂ and H₆ *p*-fluorobenzyl), 7.15 (d, 1H, *J*₀ = 6 Hz, H₄ Trp), 7.19 (t, 3H, *J*₀ = 8 Hz, H₃, H₄ and H₅ phenyl), 7.29 (d, 1H, *J*₀ = 8 Hz, H₇ Trp), 8.01 (brs, 3H, NH₂ Aib, TFA salt), 8.94 (d, 1H, *J* = 8 Hz, NH amide), 10.78 (s, 1H, NH indole Trp). ¹³C NMR (75 MHz, DMSO-*d*₆, 300 K) δ (ppm) 23.5 (CH₃ Aib), 23.8 (CH₃ Aib), 26.5 (CH₂-CH₂-phenyl), 29.2 (C β Trp), 32.7 (CH₂-CH₂-phenyl), 45.4 (CH₂-*p*-fluorobenzyl), 45.7 (C α Trp), 56.8 (Cq Aib), 109.8 (C₃ Trp), 111.8 (C₇ Trp), 115.9 and 116.2 (C₃ and C₅ *p*-fluorobenzyl), 118.3 (C₄ Trp), 118.7 (C₅ Trp), 121.3 (C₆ Trp), 124.8 (C₂ Trp), 126.5 (C₄ phenyl), 127.3 (C₉ Trp), 128.5 (C₂ and C₆ *p*-fluorobenzyl), 128.7 (C₂, C₃, C₅ and C₆ phenyl), 132.2 (C₁ *p*-fluorobenzyl), 136.4 (C₈ Trp), 140.9 (C₁ phenyl), 154.5 (Cq triazole), 154.7 (Cq triazole), 160.3 (C₄ *p*-fluorobenzyl), 171.9 (CO amide).

(*R*)-*N*-(1-(5-(2-(1*H*-Indol-3-yl)ethyl)-4-(3,4-dichlorobenzyl)-4*H*-1,2,4-triazol-3-yl)-2-(1*H*-indol-3-yl)ethyl)-2-amino-2-methylpropanamide Trifluoroacetate Salt (24a). ¹H NMR (300 MHz, DMSO-*d*₆, 300 K) δ (ppm) 1.26 (s, 6H, CH₃ Aib), 2.87 (m, 2H, CH₂-CH₂-indole), 2.96 (m, 2H, CH₂-CH₂-indole), 3.32 (m, 2H, CH₂ β Trp), 5.13 (m, 3H, CH α Trp and CH₂-*m,p*-dichlorobenzyl), 6.58 (d, 1H, *J*₀ = 8 Hz, H₆ *m,p*-dichlorobenzyl), 6.85 (t, 1H, *J*₀ = 7 Hz, H₅ Trp), 6.96 (t, 1H, *J*₀ = 7 Hz, H₅ indole), 7.01 (m, 2H, H₆ indole and H₆ Trp), 7.04 (s, 1H, H₂ Trp), 7.08 (s, 1H, H₂ indole), 7.13 (d, 1H, *J*₀ = 8 Hz, H₅ *m,p*-dichlorobenzyl), 7.20–7.30 (m, 4H, H₄ and H₇ indole, H₇ Trp and H₂ *m,p*-dichlorobenzyl), 7.36 (d, 1H, *J*₀ = 8 Hz, H₄ Trp), 8.08 (brs, 3H, NH₂ Aib, TFA salt), 8.98 (d, 1H, *J* = 8 Hz, NH amide), 10.80 (s, 1H, NH indole), 10.82 (s, 1H, NH indole Trp). ¹³C NMR (75 MHz, DMSO-*d*₆, 300 K) δ (ppm) 22.8 (CH₂-CH₂-indole), 23.4 (CH₃ Aib), 23.8 (CH₃ Aib), 25.8 (CH₂-CH₂-indole), 29.0 (C β Trp), 44.8 (CH₂-*m,p*-dichlorobenzyl), 45.6 (C α Trp), 56.8 (Cq Aib), 109.7 (C₃ indole), 111.8 (C₇ indole and C₇ Trp), 113.3 (C₃ Trp), 118.1 (C₄ Trp), 118.4 (C₅ indole), 118.6 (C₄ indole and C₅ Trp), 121.3 (C₆ indole and C₆ Trp), 123.0 (C₂ indole and C₂ Trp), 126.4 (C₆ *m,p*-dichlorobenzyl), 127.1 (C₉ Trp), 127.3 (C₉ indole), 128.6 (C₂ *m,p*-dichlorobenzyl), 130.9 (C₄ *m,p*-dichlorobenzyl), 131.3 (C₅ *m,p*-dichlorobenzyl), 132.0 (C₃ *m,p*-dichlorobenzyl), 136.4 (C₈ Trp), 136.6 (C₈ indole), 137.2 (C₁ *m,p*-dichlorobenzyl), 154.7 (Cq triazole), 155.1 (Cq triazole), 172.0 (CO amide).

***N*-(*(R)*-1-(4-(3,4-Dichlorobenzyl)-5-benzyl-4*H*-1,2,4-triazol-3-yl)-2-(1*H*-indol-3-yl)ethyl)-2-amino-2-methylpropanamide Trifluoroacetate Salt (24b).** ¹H NMR (300 MHz, DMSO-*d*₆, 300 K) δ (ppm) 1.24 (s, 3H, CH₃ Aib), 1.25 (s, 3H, CH₃ Aib), 3.33 (m, 2H, CH₂ β Trp), 4.04 (s, 2H, CH₂-benzyl), 5.05 (m, 1H, CH α Trp), 5.12 (s, 2H, CH₂-*m,p*-dichlorobenzyl), 6.49 (dd, 1H, *J*₀ = 8 Hz and *J*_m = 2 Hz, H₆ *m,p*-dichlorobenzyl), 6.80 (t, 1H, *J*₀ = 8 Hz, H₅ Trp), 6.87 (d, 1H, *J*_m = 2 Hz, H₂ Trp), 6.98 (t, 1H, *J*₀ = 7 Hz, H₆ Trp), 7.02–7.10 (m, 3H, H₂ and H₆ benzyl, H₅ *m,p*-dichlorobenzyl), 7.18 (m, 4H, H₃, H₄ and H₅ benzyl, H₂ *m,p*-dichlorobenzyl), 7.26 (m, 2H, H₄ and H₇ Trp), 8.04 (brs, 3H, NH₂ Aib, TFA salt), 8.94 (d, 1H, *J* = 9 Hz, NH amide), 10.81 (s, 1H, NH indole Trp). ¹³C NMR (75 MHz, DMSO-*d*₆, 300 K) δ (ppm) 23.4 (CH₃ Aib), 23.8 (CH₃ Aib), 29.0 (C β Trp), 30.4 (CH₂-benzyl), 45.1 (CH₂-*m,p*-dichlorobenzyl), 45.6 (C α Trp), 56.7 (Cq Aib), 109.6 (C₃ Trp), 111.8 (C₇ Trp), 118.1 (C₄ Trp), 118.6 (C₅ Trp), 121.3 (C₆ Trp),

124.9 (C₂ Trp), 126.4 (C₆ *m,p*-dichlorobenzyl and C₄ benzyl), 127.0 (C₂ *m,p*-dichlorobenzyl), 127.2 (C₉ Trp), 128.4 (C₂, C₃, C₅ and C₆ benzyl), 130.7 (C₄ and C₅ *m,p*-dichlorobenzyl), 131.8 (C₃ *m,p*-dichlorobenzyl), 136.0 (C₁ benzyl), 136.4 (C₈ Trp), 136.7 (C₁ *m,p*-dichlorobenzyl), 154.1 (Cq triazole), 155.2 (Cq triazole), 172.0 (CO amide).

***N*-(*(R)*-1-(4-(3,4-Dichlorobenzyl)-5-phenethyl-4*H*-1,2,4-triazol-3-yl)-2-(1*H*-indol-3-yl)ethyl)-2-amino-2-methylpropanamide Trifluoroacetate Salt (24c).** ¹H NMR (300 MHz, DMSO-*d*₆, 300 K) δ (ppm) 1.25 (s, 3H, CH₃ Aib), 1.26 (s, 3H, CH₃ Aib), 2.84 (m, 4H, CH₂-CH₂-phenyl), 3.34 (d, 2H, *J* = 7 Hz, CH₂ β Trp), 5.11 (m, 3H, CH α Trp and CH₂-*m,p*-dichlorobenzyl), 6.63 (dd, 1H, *J*₀ = 8 Hz and *J*_m = 2 Hz, H₆ *m,p*-dichlorobenzyl), 6.83 (t, 1H, *J*₀ = 8 Hz, H₅ Trp), 6.99 (t, 1H, *J*₀ = 8 Hz, H₆ Trp), 7.05 (d, 1H, *J* = 2 Hz, H₂ Trp), 7.12 (m, 5H, CHar phenyl), 7.17 (d, 1H, *J*₀ = 8 Hz, H₄ Trp), 7.21 (s, 1H, H₂ *m,p*-dichlorobenzyl), 7.27 (d, 1H, *J*₀ = 8 Hz, H₅ *m,p*-dichlorobenzyl), 7.39 (d, 1H, *J*₀ = 8 Hz, H₇ Trp), 8.02 (brs, 3H, NH₂ Aib, TFA salt), 8.94 (d, 1H, *J* = 8 Hz, NH amide), 10.78 (s, 1H, NH indole Trp). ¹³C NMR (75 MHz, DMSO-*d*₆, 300 K) δ (ppm) 23.5 (CH₃ Aib), 23.8 (CH₃ Aib), 26.4 (CH₂-CH₂-phenyl), 29.1 (C β Trp), 32.6 (CH₂-CH₂-phenyl), 44.7 (CH₂-*m,p*-dichlorobenzyl), 45.6 (C α Trp), 56.7 (Cq Aib), 109.7 (C₃ Trp), 111.8 (C₇ Trp), 118.1 (C₄ Trp), 118.7 (C₅ Trp), 121.3 (C₆ Trp), 124.9 (C₂ Trp), 126.5 (C₄ phenyl and C₆ *m,p*-dichlorobenzyl), 127.2 (C₉ Trp), 128.7 (C₂, C₃, C₅, and C₆ phenyl, C₂ *m,p*-dichlorobenzyl), 130.9 (C₄ *m,p*-dichlorobenzyl), 131.4 (C₅ *m,p*-dichlorobenzyl), 132.0 (C₃ *m,p*-dichlorobenzyl), 136.4 (C₈ Trp), 137.2 (C₁ *m,p*-dichlorobenzyl), 140.8 (C₁ phenyl), 154.5 (Cq triazole), 154.7 (Cq triazole), 171.9 (CO amide).

***N*-(*(R)*-1-(5-(1*H*-Indol-3-yl)methyl)-4-phenethyl-4*H*-1,2,4-triazol-3-yl)-2-(1*H*-indol-3-yl)ethyl)-2-amino-2-methylpropanamide Trifluoroacetate Salt (25b).** ¹H NMR (300 MHz, DMSO-*d*₆, 300 K) δ (ppm) 1.27 (s, 3H, CH₃ Aib), 1.29 (s, 3H, CH₃ Aib), 2.39–2.53 (m, 4H, CH₂-CH₂-phenyl), 3.74 (m, 1H, CH₂ β Trp), 3.92 (m, 1H, CH₂ β Trp), 3.99 (s, 2H, CH₂-indole), 5.21 (m, 1H, CH α Trp), 6.74 (m, 2H, H₅ indole and H₅ Trp), 6.90 (t, 1H, *J*₀ = 8 Hz, H₆ Trp), 6.92 (t, 1H, *J*₀ = 8 Hz, H₆ indole), 7.01–7.06 (m, 4H, H₂ and H₆ phenyl, H₂ indole and H₂ Trp), 7.16 (m, 3H, H₃, H₄ and H₅ phenyl), 7.27 (d, 1H, *J*₀ = 8 Hz, H₄ Trp), 7.32 (d, 1H, *J*₀ = 8 Hz, H₇ Trp), 7.36 (d, 1H, *J*₀ = 8 Hz, H₇ indole), 7.50 (d, 1H, *J*₀ = 8 Hz, H₄ indole), 7.99 (brs, 3H, NH₂ Aib, TFA salt), 9.02 (s, 1H, *J* = 8 Hz, NH amide), 10.79 (s, 1H, NH indole Trp), 10.94 (s, 1H, NH indole). ¹³C NMR (75 MHz, DMSO-*d*₆, 300 K) δ (ppm) 21.4 (CH₂-indole), 23.5 (CH₃ Aib), 23.8 (CH₃ Aib), 29.5 (C β Trp), 35.8 (CH₂-CH₂-phenyl), 44.5 (CH₂-CH₂-phenyl), 45.8 (C α Trp), 56.7 (Cq Aib), 108.5 (C₃ indole), 109.9 (C₃ Trp), 114.0 (C₇ indole and C₇ Trp), 118.4 (C₄ Trp), 118.8 (C₄ indole and C₅ Trp), 119.0 (C₅ indole), 121.4 (C₆ Trp), 121.7 (C₆ indole), 124.0 (C₂ indole and C₂ Trp), 127.1 (C₄ phenyl), 127.7 (C₉ indole and C₉ Trp), 128.8 (C₂ and C₆ phenyl), 129.1 (C₃ and C₅ phenyl), 136.5 (C₈ Trp), 136.6 (C₈ indole), 137.5 (C₁ phenyl), 153.6 (Cq triazole), 155.0 (Cq triazole), 171.8 (CO amide).

(*R*)-*N*-(1-(5-(3-(1*H*-Indol-3-yl)propyl)-4-phenethyl-4*H*-1,2,4-triazol-3-yl)-2-(1*H*-indol-3-yl)ethyl)-2-amino-2-methylpropanamide Trifluoroacetate Salt (25c). ¹H NMR (300 MHz, DMSO-*d*₆) δ (ppm) 1.32 (s, 3H, CH₃ Aib), 1.37 (s, 3H, CH₃ Aib), 1.86 (m, 2H, CH₂-CH₂-CH₂-indole), 2.38 (m, 2H, CH₂-CH₂-CH₂-indole), 2.65 (m, 4H, CH₂-CH₂-CH₂-indole and CH₂-CH₂-phenyl), 3.38 (m, 2H, CH₂-CH₂-phenyl), 3.74 (m, 1H, CH₂ β Trp), 3.92 (m, 1H, CH₂ β Trp), 5.23 (m, 1H, CH α Trp), 6.78 (m, 2H, H₅ indole and H₅ Trp), 6.93 (t, 1H, *J*₀ = 8 Hz, H₆ Trp), 7.01 (m, 3H, H₆ indole, H₂ and H₆ phenyl), 7.05 (d, 1H, *J* = 2 Hz, H₂ Trp), 7.08 (d, 1H, *J* = 2 Hz, H₂ indole), 7.15 (m, 3H, H₃, H₄ and H₅ phenyl), 7.29 (d, 1H, *J*₀ = 8 Hz, H₄ Trp), 7.31 (d, 1H, *J*₀ = 8 Hz, H₇ Trp), 7.44 (d, 1H, *J*₀ = 8 Hz, H₇ indole), 7.46 (d, 1H, *J*₀ = 8 Hz, H₄ indole), 8.06 (brs, 3H, NH₂ Aib, TFA salt), 9.05 (d, 1H, 8 Hz, NH amide), 10.76 (s, 1H, NH indole), 10.85 (d, 1H, *J* = 2 Hz, NH indole Trp). ¹³C NMR (75 MHz, DMSO-*d*₆) δ (ppm) 23.5 (CH₃ Aib), 23.6 (CH₂-CH₂-CH₂-indole), 23.9 (CH₃ Aib), 24.5 (CH₂-CH₂-CH₂-indole), 27.3 (CH₂-CH₂-CH₂-indole), 29.4 (C β Trp), 35.7 (CH₂-CH₂-phenyl), 44.5 (CH₂-CH₂-phenyl), 46.1 (C

α Trp), 56.8 (C_q Aib), 109.6 (C₃ Trp), 111.8 (C₇ Trp), 111.9 (C₇ indole), 113.9 (C₃ indole), 118.3 (C₄ Trp), 118.6 (C₅ indole), 118.7 (C₄ indole), 118.9 (C₅ Trp), 121.3 (C₆ Trp), 121.4 (C₆ indole), 122.8 (C₂ indole and C₂ Trp), 127.1 (C₄ phenyl), 127.3 (C₉ Trp), 127.5 (C₉ indole), 128.8 (C₂ and C₆ phenyl), 129.1 (C₃ and C₅ phenyl), 136.5 (C₁ phenyl), 136.8 (C₈ Trp), 137.2 (C₈ indole), 154.7 (2C_q triazole), 172.0 (CO amide).

***N*-(*R*)-2-(1*H*-Indol-3-yl)-1-(4,5-diphenethyl-4*H*-1,2,4-triazol-3-yl)ethyl)-2-amino-2-methylpropanamide Trifluoroacetate Salt (25e).** ¹H NMR (300 MHz, DMSO-*d*₆, 300 K) δ (ppm) 1.32 (s, 3H, CH₃ Aib), 1.37 (s, 3H, CH₃ Aib), 2.59 (m, 4H, C-CH₂-CH₂-phenyl), 2.83 (t, 2H, *J* = 8 Hz, N-CH₂-CH₂-phenyl), 3.38 (m, 2H, N-CH₂-CH₂-phenyl), 3.84 (m, 1H, CH₂ β Trp), 3.94 (m, 1H, CH₂ β Trp), 5.23 (m, 1H, CH α Trp), 6.84 (m, 2H, H₄ phenyl from C-CH₂-CH₂-phenyl and H₄ phenyl from N-CH₂-CH₂-phenyl), 6.93 (t, 1H, *J*_o = 8 Hz, H₅ Trp), 7.00 (t, 1H, *J*_o = 8 Hz, H₆ Trp), 7.07 (d, 1H, *J* = 2 Hz, H₂ Trp), 7.11–7.27 (m, 9H, H₂, H₃, H₅ and H₆ phenyl from C-CH₂-CH₂-phenyl, H₂, H₃, H₅ and H₆ phenyl from N-CH₂-CH₂-phenyl and H₄ Trp), 7.50 (d, 1H, *J*_o = 8 Hz, H₇ Trp), 8.07 (brs, 3H, NH₂ Aib, TFA salt), 9.04 (d, 1H, *J* = 8 Hz, NH amide), 10.85 (s, 1H, NH indole Trp). ¹³C NMR (75 MHz, DMSO-*d*₆, 300 K) δ (ppm) 23.5 (CH₃ Aib), 23.8 (CH₃ Aib), 25.9 (C-CH₂-CH₂-phenyl), 29.5 (C β Trp), 32.4 (C-CH₂-CH₂-phenyl), 35.8 (N-CH₂-CH₂-phenyl), 44.2 (N-CH₂-CH₂-phenyl), 45.9 (C α Trp), 56.8 (C_q Aib), 109.7 (C₃ Trp), 111.9 (C₇ Trp), 118.4 (C₄ Trp), 118.9 (C₅ Trp), 121.4 (C₆ Trp), 124.8 (C₂ Trp), 126.6 (C₄ phenyl from C-CH₂-CH₂-phenyl), 127.2 (C₄ phenyl from N-CH₂-CH₂-phenyl), 127.4 (C₉ Trp), 128.7 (C₂ and C₆ phenyl from C-CH₂-CH₂-phenyl, C₂ and C₆ phenyl from N-CH₂-CH₂-phenyl), 128.8 (C₃ and C₅ phenyl from C-CH₂-CH₂-phenyl, C₃ and C₅ phenyl from N-CH₂-CH₂-phenyl), 136.5 (C₁ phenyl from N-CH₂-CH₂-phenyl), 137.5 (C₁ phenyl from C-CH₂-CH₂-phenyl), 140.8 (C₈ Trp), 154.1 (C_q triazole), 154.7 (C_q triazole), 171.9 (CO amide).

2-Amino-*N*-(*R*)-1-(5-benzyl-4-(2,2-diphenylethyl)-4*H*-1,2,4-triazol-3-yl)-2-(1*H*-indol-3-yl)ethyl)-2-methylpropanamide Trifluoroacetate Salt (26a). ¹H NMR (300 MHz, DMSO-*d*₆, 300 K) δ (ppm) 1.29 (s, 3H, CH₃ Aib), 1.34 (s, 3H, CH₃ Aib), 3.37 (m, 4H, CH₂ β Trp and CH₂-benzyl), 3.74 (t, 1H, *J* = 7 Hz, CH₂-CH(Phe)₂), 4.21 (dd, 1H, *J* = 14 and 8 Hz, CH₂-CH(Phe)₂), 4.51 (dd, 1H, *J* = 14 and 8 Hz, CH₂-CH(Phe)₂), 5.08 (m, 1H, CH α Trp), 6.72 (m, 2H, H₂ and H₆ benzyl), 6.86–6.93 (m, 5H, H₃, H₄ and H₅ benzyl, H₅ and H₆ Trp), 7.03 (s, 1H, H₂ Trp), 7.06–7.25 (m, 10H, CHar phenyl from CH(Phe)₂), 7.33 (d, 1H, *J*_o = 8 Hz, H₄ Trp), 7.47 (d, 1H, *J*_o = 8 Hz, H₇ indole), 8.10 (brs, 3H, NH₂ Aib, TFA salt), 8.98 (d, 1H, *J* = 8 Hz, NH amide), 10.94 (s, 1H, NH indole Trp). ¹³C NMR (75 MHz, DMSO-*d*₆, 300 K) δ (ppm) 23.5 (CH₃ Aib), 23.7 (CH₃ Aib), 29.4 (C β Trp), 30.1 (CH₂-benzyl), 46.0 (C α Trp), 47.7 (CH₂-CH(Phe)₂), 51.3 (CH(Phe)₂), 56.8 (C_q Aib), 109.8 (C₃ Trp), 112.0 (C₇ Trp), 118.5 (C₄ Trp), 119.0 (C₅ Trp), 121.5 (C₆ Trp), 124.8 (C₂ Trp), 127.1 (C₄ phenyl from CH(Phe)₂), 127.4 (C₉ Trp, C₄ benzyl), 128.3 (C₂ and C₆ phenyl from CH(Phe)₂), 128.8–129.1 (C₃ and C₅ phenyl from CH(Phe)₂, C₂, C₃, C₅, and C₆ benzyl), 136.2 (C₁ benzyl), 136.5 (C₈ Trp), 141.0 (C₁ phenyl from CH(Phe)₂), 153.5 (C_q triazole), 155.1 (C_q triazole), 172.0 (CO amide).

***N*-(*R*)-1-(5-(2-(1*H*-Indol-3-yl)ethyl)-4-(2,2-diphenylethyl)-4*H*-1,2,4-triazol-3-yl)-2-(1*H*-indol-3-yl)ethyl)-2-amino-2-methylpropanamide Trifluoroacetate Salt (26b).** ¹H NMR (300 MHz, DMSO-*d*₆, 300 K) δ (ppm) 1.34 (s, 3H, CH₃ Aib), 1.38 (s, 3H, CH₃ Aib), 2.06 (m, 1H, CH₂-CH₂-indole), 2.30 (m, 1H, CH₂-CH₂-indole), 2.78 (m, 2H, CH₂-CH₂-indole), 3.35 (dd, 1H, *J* = 14 and 7 Hz, CH₂ β Trp), 3.46 (dd, 1H, *J* = 14 and 9 Hz, CH₂ β Trp), 3.58 (t, 1H, *J* = 7 Hz, CH₂-CH(Phe)₂), 4.14 (dd, 1H, *J* = 14 and 8 Hz, CH₂-CH(Phe)₂), 4.39 (dd, 1H, *J* = 14 and 7 Hz, CH₂-CH(Phe)₂), 5.12 (m, 1H, CH α Trp), 6.50 (m, 2H, H₅ indole and H₅ Trp), 6.76 (m, 2H, H₆ indole and H₆ Trp), 6.87 (m, 2H, H₂ indole and H₂ Trp), 6.89–6.96 (m, 2H, H₄ phenyl), 7.03–7.15 (m, 8H, H₂, H₃, H₅ and H₆ phenyl), 7.33 (m, 3H, H₄ indole, H₄ and H₇ Trp), 7.47 (d, 1H, *J* = 8 Hz, H₇ indole), 8.11 (brs, 3H, NH₂ Aib, TFA salt), 9.04 (d, 1H, *J* = 8 Hz, NH amide), 10.76 (s, 1H, NH

indole), 10.96 (s, 1H, NH indole Trp). ¹³C NMR (75 MHz, DMSO-*d*₆, 300 K) δ (ppm) 22.4 (CH₂-CH₂-indole), 23.6 (CH₃ Aib), 23.8 (CH₃ Aib), 24.9 (CH₂-CH₂-indole), 29.6 (C β Trp), 46.1 (C α Trp), 47.5 (CH₂-CH(Phe)₂), 51.5 (CH₂-CH(Phe)₂), 56.8 (C_q Aib), 109.8 (C₃ Trp), 111.8 (C₇ Trp), 112.1 (C₇ indole), 113.5 (C₃ indole), 118.4 (C₄ Trp), 118.7 (C₄ and C₅ indole), 119.0 (C₅ Trp), 121.4 (C₆ indole and C₆ Trp), 122.8 (C₂ indole), 125.0 (C₂ Trp), 127.2 (C₉ indole and C₉ Trp), 127.3 (C₄ phenyl), 128.2 (C₂ and C₆ phenyl), 128.7 (C₃ and C₅ phenyl), 136.6 (C₈ indole and C₈ Trp), 141.0 (C₁ phenyl), 154.6 (2 C_q triazole), 172.0 (CO amide).

(*R*)-2-Amino-*N*-(1-(5-benzyl-4-(naphthalen-1-ylmethyl)-4*H*-1,2,4-triazol-3-yl)-2-(1*H*-indol-3-yl)ethyl)-2-methylpropanamide Trifluoroacetate Salt (27a). ¹H NMR (300 MHz, DMSO-*d*₆, 300 K) δ (ppm) 1.18 (s, 3H, CH₃ Aib), 1.24 (s, 3H, CH₃ Aib), 3.17 (dd, 1H, *J* = 14 and 5 Hz, CH₂ β Trp), 3.36 (dd, 1H, *J* = 14 and 9 Hz, CH₂ β Trp), 4.05 (m, 2H, CH₂-benzyl), 4.90 (m, 1H, CH α Trp), 5.65 (d, 1H, *J* = 18 Hz, CH₂-naphtyl), 5.81 (d, 1H, *J* = 18 Hz, CH₂-naphtyl), 6.12 (d, 1H, *J*_o = 7 Hz, H₂ naphtyl), 6.38 (t, 1H, *J*_o = 7 Hz, H₅ Trp), 6.47 (d, 1H, *J*_o = 8 Hz, H₄ Trp), 6.85 (t, 1H, *J*_o = 8 Hz, H₆ Trp), 7.03 (d, 1H, *J* = 2 Hz, H₂ Trp), 7.05–7.12 (m, 5H, CHar benzyl), 7.15 (d, 1H, *J*_o = 8 Hz, H₇ Trp), 7.19 (d, 1H, *J*_o = 8 Hz, H₃ naphtyl), 7.58 (m, 2H, H₆ and H₇ naphtyl), 7.81 (d, 1H, *J*_o = 8 Hz, H₄ naphtyl), 7.89–8.01 (m, 5H, NH₂ Aib TFA salt, H₅ and H₈ naphtyl), 8.92 (d, 1H, *J* = 8 Hz, NH amide), 10.73 (s, 1H, NH indole Trp). ¹³C NMR (75 MHz, DMSO-*d*₆, 300 K) δ (ppm) 23.5 (CH₃ Aib), 23.6 (CH₃ Aib), 29.2 (C β Trp), 30.5 (CH₂-benzyl), 44.0 (CH₂-naphtyl), 45.6 (C α Trp), 56.6 (C_q Aib), 109.7 (C₃ Trp), 111.7 (C₇ Trp), 117.9 (C₄ Trp), 118.4 (C₅ Trp), 121.1 (C₆ Trp), 122.1 (C₂ naphtyl), 122.8 (C₈ naphtyl), 124.9 (C₂ Trp), 125.7 (C₃ naphtyl), 126.7 (C₆ naphtyl), 126.9 (C₉ Trp), 127.0 (C₇ naphtyl), 128.2 (C₄ benzyl), 128.7–129.1 (C₂, C₃, C₅, and C₆ benzyl, C₄ and C₅ naphtyl), 129.9 (C₉ naphtyl), 131.5 (C₁ naphtyl), 133.5 (C₁₀ naphtyl), 136.2 (C₁ benzyl), 136.4 (C₈ Trp), 154.2 (C_q triazole), 155.7 (C_q triazole), 171.9 (CO amide).

(*R*)-*N*-(1-(5-(3-(1*H*-Indol-3-yl)propyl)-4-(naphthalen-1-ylmethyl)-4*H*-1,2,4-triazol-3-yl)-2-(1*H*-indol-3-yl)ethyl)-2-amino-2-methylpropanamide Trifluoroacetate Salt (27b). ¹H NMR (300 MHz, DMSO-*d*₆, 300 K) δ (ppm) 1.20 (s, 3H, CH₃ Aib), 1.25 (s, 3H, CH₃ Aib), 1.93 (m, 2H, CH₂-CH₂-indole), 2.66 (m, 4H, CH₂-CH₂-indole), 3.25 (dd, 1H, *J* = 14 and 5 Hz, CH₂ β Trp), 3.40 (dd, 1H, *J* = 14 and 9 Hz, CH₂ β Trp), 4.95 (m, 1H, CH α Trp), 5.66 (d, 1H, *J* = 18 Hz, CH₂-naphtyl), 5.81 (d, 1H, *J* = 18 Hz, CH₂-naphtyl), 6.37 (d, 1H, *J*_o = 7 Hz, H₂ naphtyl), 6.43 (t, 1H, *J*_o = 7 Hz, H₅ Trp), 6.59 (d, 1H, *J*_o = 8 Hz, H₄ Trp), 6.86 (m, 3H, H₅ and H₆ indole, H₆ Trp), 6.95 (d, 1H, *J* = 2 Hz, H₂ indole), 7.00 (d, 1H, *J*_o = 8 Hz, H₄ indole), 7.06 (d, 1H, *J* = 2 Hz, H₂ Trp), 7.20–7.33 (m, 3H, H₇ indole, H₇ Trp, H₃ naphtyl), 7.60 (m, 2H, H₆ and H₇ naphtyl), 7.87 (d, 1H, *J*_o = 8 Hz, H₄ naphtyl), 7.99 (m, 5H, NH₂ Aib TFA salt, H₅ and H₈ naphtyl), 8.95 (d, 1H, *J* = 8 Hz, NH amide), 10.70 (s, 1H, NH indole), 10.77 (s, 1H, NH indole Trp). ¹³C NMR (75 MHz, DMSO-*d*₆, 300 K) δ (ppm) 23.5 (CH₃ Aib), 23.6 (CH₃ Aib), 24.1 (CH₂-CH₂-indole), 24.5 (CH₂-CH₂-indole), 27.6 (CH₂-CH₂-indole), 29.1 (C β Trp), 44.1 (CH₂-naphtyl), 45.7 (C α Trp), 56.7 (C_q Aib), 109.7 (C₃ Trp), 111.7 (C₇ indole and C₇ Trp), 113.9 (C₃ indole), 117.9 (C₄ Trp), 118.5 (C₄ indole, C₅ Trp), 118.6 (C₅ indole), 121.1 (C₆ Trp), 121.2 (C₆ indole), 122.1 (C₂ naphtyl), 122.7 (C₂ indole), 122.9 (C₈ naphtyl), 125.0 (C₂ Trp), 125.9 (C₃ naphtyl), 126.8 (C₆ naphtyl), 127.0 (C₉ indole), 127.1 (C₇ naphtyl), 127.4 (C₉ Trp), 128.5 (C₄ naphtyl), 129.2 (C₅ naphtyl), 129.9 (C₉ naphtyl), 131.6 (C₁ naphtyl), 133.6 (C₁₀ naphtyl), 136.4 (C₈ Trp), 136.7 (C₈ indole), 155.4 (2C_q triazole), 171.9 (CO amide).

(*R*)-*N*-(1-(5-(2-(1*H*-Indol-3-yl)ethyl)-4-(naphthalen-1-ylmethyl)-4*H*-1,2,4-triazol-3-yl)-2-(1*H*-indol-3-yl)ethyl)-2-amino-2-methylpropanamide Trifluoroacetate Salt (27c). ¹H NMR (400 MHz, DMSO-*d*₆) δ (ppm) 1.25 (s, 3H, CH₃ Aib), 1.28 (s, 3H, CH₃ Aib), 2.93 (m, 2H, CH₂-CH₂-indole), 3.01 (m, 2H, CH₂-CH₂-indole), 3.30 (dd, 1H, *J* = 14.3, *J* = 5.8, CH₂ β Trp), 3.40 (dd, 1H, *J* = 14.3, *J* = 8.8, CH₂ β Trp), 5.03 (m, 1H, CaH Trp), 5.62 (d, 1H, *J* = 18.0, CH₂-naphtyl), 5.76 (d, 1H, *J* = 18.0, CH₂-naphtyl), 6.36 (d, 1H, *J* = 7.2, H₂ naphtyl), 6.51 (t, 1H, *J* = 7.4, H₅ Trp), 6.72 (d, 1H, *J*

= 7.9, H₄ Trp), 6.76 (t, 1H, *J* = 7.5, H₅ indole), 6.92 (t, 1H, *J* = 7.5, H₆ Trp), 7.0 (t, 1H, *J* = 7.5, H₆ indole), 7.02 (d, 1H, *J* = 2.0, H₂ indole), 7.09 (d, 1H, *J* = 2.0, H₂ Trp), 7.13 (d, 1H, *J* = 7.9, H₄ indole), 7.26 (d, 1H, *J* = 7.9, H₇ Trp), 7.27 (t, 1H, *J* = 8.2, H₃ naphthyl), 7.29 (d, 1H, H₇ indole), 7.58–7.64 (m, 2H, H₆, H₇ naphthyl), 7.88 (d, 1H, *J* = 8.2, H₄ naphthyl), 7.93 (d, 1H, *J* = 7.9, H₈ naphthyl), 7.98 (brs, 2H, NH₂ Aib, TFA salt), 8.03 (d, 1H, *J* = 8.2, H₅ naphthyl), 8.96 (d, 1H, *J* = 7.9, NH Trp), 10.75 (brs, 1H, NH indole), 10.77 (brs, 1H, NH indole Trp). ¹³C NMR (100 MHz, DMSO-*d*₆) δ 22.6 (CH₂–CH₂ indole), 23.1 (CH₃ Aib), 23.2 (CH₃ Aib), 25.3 (CH₂–CH₂ indole), 28.8 (C βTrp), 43.3 (CH₂–naphthyl), 45.3 (C αTrp), 56.2 (Cq Aib), 109.4 (C₃ Trp), 111.2 (C₇ Trp, C₇ indole), 112.9 (C₃ indole), 117.5 (C₄ Trp), 117.8 (C₄ indole), 118.0 (C₅ Trp), 118.1 (C₅ indole), 120.7 (C₆ Trp), 120.8 (C₆ indole), 121.6 (C₂ naphthyl), 122.5 (C₂ indole, C₈ naphthyl), 124.4 (C₂ Trp), 125.4 (C₃ naphthyl), 126.3 (C₆ naphthyl), 126.6 (C₉ Indole, C₉ Trp, C₇ naphthyl), 127.9 (C₄ naphthyl), 128.6 (C₅ naphthyl), 129.5 (C₉ naphthyl), 131.4 (C₁ naphthyl), 133.1 (C₁₀ naphthyl), 135.9 (C₈ Trp), 136.1 (C₈ indole), 154.7 (2Cq triazole), 171.4 (CO amide).

(R)-N-(2-(1H-Indol-3-yl)-1-(4-(naphthalen-1-ylmethyl)-5-phenethyl-4H-1,2,4-triazol-3-yl)ethyl)-2-amino-2-methylpropanamide Trifluoroacetate Salt (27d). ¹H NMR (300 MHz, DMSO-*d*₆, 300 K) δ (ppm) 1.21 (s, 3H, CH₃ Aib), 1.25 (s, 3H, CH₃ Aib), 2.46 (m, 2H, CH₂–CH₂–phenyl), 2.88 (m, 2H, CH₂–CH₂–phenyl), 3.26 (dd, 2H, ³*J* = 14 and 6 Hz, CH₂ βTrp), 3.36 (dd, 2H, ³*J* = 14 and 9 Hz, CH₂ βTrp), 4.99 (m, 1H, CH αTrp), 5.65 (d, 1H, ³*J* = 18 Hz, CH₂–naphthyl), 5.78 (d, 1H, ³*J* = 18 Hz, CH₂–naphthyl), 6.29 (d, 1H, *J*_o = 7 Hz, H₂ naphthyl), 6.45 (t, 1H, *J*_o = 7 Hz, H₅ Trp), 6.62 (d, 1H, *J*_o = 8 Hz, H₄ Trp), 6.88 (t, 1H, *J*_o = 8 Hz, H₆ Trp), 7.04–7.06 (m, 4H, H₂ and H₇ Trp, H₂ and H₆ phenyl), 7.07–7.25 (m, 4H, H₃ naphthyl, H₃, H₄ and H₅ phenyl), 7.57–7.60 (m, 2H, H₆ and H₇ naphthyl), 7.86 (d, 1H, *J*_o = 8 Hz, H₄ naphthyl), 7.98–8.00 (m, 5H, H₅ and H₈ naphthyl, NH₂ Aib, TFA salt), 8.96 (d, 1H, *J* = 8 Hz, NH amide), 10.77 (s, 1H, NH indole Trp). ¹³C NMR (75 MHz, DMSO-*d*₆, 300 K) δ (ppm) 23.5 (CH₃ Aib), 23.6 (CH₃ Aib), 26.3 (CH₂CH₂–phenyl), 29.2 (C βTrp), 32.6 (CH₂–CH₂–phenyl), 43.8 (CH₂–naphthyl), 45.6 (C αTrp), 56.7 (Cq Aib), 109.7 (C₃ Trp), 111.7 (C₇ Trp), 117.9 (C₄ Trp), 118.4 (C₅ Trp), 121.1 (C₆ Trp), 122.1 (C₂ naphthyl), 123.0 (C₈ naphthyl), 124.9 (C₂ Trp), 125.9 (C₃ naphthyl), 126.5 (C₆ naphthyl), 126.9 (C₄ phenyl), 127.0 (C₉ Trp and C₇ naphthyl), 127.1 (C₄ naphthyl), 128.4 (C₅ naphthyl), 128.7 (C₂, C₃, C₅, and C₆ phenyl), 130.0 (C₉ naphthyl), 131.7 (C₁ naphthyl), 133.6 (C₁₀ naphthyl), 136.4 (C₈ Trp), 140.8 (C₁ phenyl), 154.8 (Cq triazole), 155.3 (Cq triazole), 171.9 (CO amide).

2-Amino-N-((R)-1-(5-benzyl-4-hexyl-4H-1,2,4-triazol-3-yl)-2-(1H-indol-3-yl)ethyl)-2-methylpropanamide Trifluoroacetate Salt (28a). ¹H NMR (300 MHz, DMSO-*d*₆, 300 K) δ (ppm) 0.71 (t, 3H, ³*J* = 7 Hz, (CH₂)₅–CH₃), 0.87 (m, 4H, 2 CH₂), 0.95 (m, 2H, CH₂–CH₃), 1.00 (m, 2H, N–CH₂–CH₂), 1.36 (s, 6H, CH₃ Aib), 3.36 (dd, 1H, ³*J* = 14 and 7 Hz, CH₂ βTrp), 3.41 (dd, 1H, ³*J* = 14 and 7 Hz, CH₂ βTrp), 3.50 (m, 1H, N–CH₂), 3.65 (m, 1H, N–CH₂), 4.11 (s, 2H, CH₂–benzyl), 5.14 (m, 1H, CH αTrp), 6.90 (t, 1H, *J*_o = 7 Hz, H₅ Trp), 7.01 (t, 1H, *J*_o = 7 Hz, H₆ Trp), 7.04 (s, 1H, H₂ Trp), 7.09 (m, 2H, H₂ and H₆ benzyl), 7.17–7.29 (m, 4H, H₄ Trp, H₃, H₄ and H₅ benzyl), 7.47 (d, 1H, *J*_o = 8 Hz, H₇ Trp), 8.10 (brs, 3H, NH₂ Aib, TFA salt), 9.05 (d, 1H, *J* = 7 Hz, NH amide), 10.84 (s, 1H, NH indole Trp). ¹³C NMR (75 MHz, DMSO-*d*₆, 300 K) δ (ppm) 14.1 ((CH₂)₅–CH₃), 22.1 (CH₂–CH₃), 23.8 (CH₃ Aib), 23.5 (CH₃ Aib), 25.8 (CH₃–CH₂–CH₂–CH₂), 29.5 (C βTrp), 30.3 (N–CH₂–CH₂), 30.8 (CH₂–benzyl and CH₃–CH₂–CH₂), 43.3 (N–CH₂–CH₂), 46.1 (C αTrp), 56.8 (Cq Aib), 109.6 (C₃ Trp), 111.9 (C₇ Trp), 118.2 (C₄ Trp), 118.8 (C₅ Trp), 121.4 (C₆ Trp), 124.7 (C₂ Trp), 127.2 (C₄ benzyl), 127.3 (C₉ Trp), 128.8 (C₂, C₃, C₅ and C₆ benzyl), 136.2 (C₁ benzyl), 136.5 (C₈ Trp), 153.1 (Cq triazole), 155.1 (Cq triazole), 171.9 (CO amide).

(R)-N-(1-(5-(2-(1H-Indol-3-yl)ethyl)-4-hexyl-4H-1,2,4-triazol-3-yl)-2-(1H-indol-3-yl)ethyl)-2-amino-2-methylpropanamide Trifluoroacetate Salt (28b). ¹H NMR (400 MHz, DMSO-*d*₆) δ 0.77 (t, 3H, *J* = 7.2 (CH₂)₅–CH₃), 1.01 (m, 4H, 2CH₂), 1.11 (m, 2H, CH₂–CH₃), 1.14 (m, 1H, N–CH₂–CH₂), 1.33 (m, 1H, N–CH₂–CH₂), 1.40 (s, 3H, CH₃ Aib), 1.42 (s, 3H, CH₃ Aib), 3.05 (m, 2H,

CH₂–CH₂–indole), 3.10 (m, 2H, CH₂–CH₂–indole), 3.37 (dd, 1H, *J* = 14.2, *J* = 7.6, CH₂ βTrp), 3.44 (dd, 1H, *J* = 14.2, *J* = 7.6, CH₂ βTrp), 3.58 (m, 1H, 1H N–CH₂), 3.71 (m, 1H, N–CH₂), 5.21 (m, 1H, CH αTrp), 6.96 (t, 1H, H₅ Trp), 6.97 (t, 1H, H₅ indole), 7.06 (t, 2H, H₆ Trp, H₆ indole), 7.09 (s, 1H, H₂ Trp), 7.13 (s, 1H, H₂ indole), 7.34 (d, 2H, H₇ Trp, H₇ indole), 7.48 (d, 1H, d, H₄ indole), 7.50 (d, 1H, H₄ Trp), 8.14 (brs, 3H, NH₂ Aib, TFA salt), 9.08 (d, 1H, *J* = 7.8, NH amide), 10.84 (s, 1H, NH indole), 10.88 (s, 1H, NH indole Trp). ¹³C NMR (100 MHz, DMSO-*d*₆) δ 13.7 (CH₂)₅–CH₃, 21.7 (CH₂–CH₃), 22.4 (CH₂–CH₂ indole), 23.1 (CH₃ Aib), 23.3 (CH₃ Aib), 25.1 (CH₂–CH₂ indole), 25.5 (CH₃–CH₂–CH₂–CH₂), 29.1 (C βTrp), 29.3 (N–CH₂–CH₂), 30.4 (CH₃–CH₂–CH₂), 42.6 (N–CH₂–CH₂), 45.6 (C αTrp), 56.3 (Cq Aib), 109.2 (C₃ Trp), 111.4 (C₇ Trp, C₇ indole), 112.8 (C₃ indole), 117.7 (C₄ Trp), 118.0 (C₅ indole), 118.2 (C₄ indole), 118.4 (C₅ Trp), 120.9 (C₆ indole, C₆ Trp), 122.6 (C₂ Trp), 124.3 (C₂ Trp), 126.8 (C₉ Trp), 126.9 (C₉ indole), 136.0 (C₈ Trp), 136.2 (C₈ indole), 154.0 (Cq triazole), 154.1 (Cq triazole), 171.4 (CO amide).

(R)-N-(1-(5-(3-(1H-Indol-3-yl)propyl)-4-hexyl-4H-1,2,4-triazol-3-yl)-2-(1H-indol-3-yl)ethyl)-2-amino-2-methylpropanamide Trifluoroacetate Salt (28c). ¹H NMR (300 MHz, DMSO-*d*₆, 300 K) δ (ppm) 0.74 (t, 3H, *J* = 6 Hz, CH₃–CH₂–CH₂–CH₂–CH₂–CH₂), 0.95 (brs, 4H, CH₃–CH₂–CH₂–CH₂–CH₂–CH₂), 1.06 (m, 3H, CH₃–CH₂–CH₂–CH₂–CH₂–CH₂ and N–CH₂–CH₂), 1.38 (s, 7H, CH₃ Aib and N–CH₂–CH₂), 1.97 (m, 2H, CH₂–CH₂–CH₂–indole), 2.71 (m, 4H, CH₂–CH₂–CH₂–indole), 3.37 (m, 2H, CH₂ βTrp), 3.56 (m, 2H, N–CH₂), 5.15 (m, 1H, CH αTrp), 6.91 (m, 2H, H₅ indole and H₅ Trp), 7.00 (m, 2H, H₆ indole and H₆ Trp), 7.07 (s, 2H, H₂ indole and H₂ Trp), 7.29 (d, 2H, *J*_o = 8 Hz, H₇ indole and H₇ Trp), 7.45 (d, 2H, *J* = 7 Hz, H₄ indole and H₄ Trp), 8.15 (brs, 3H, NH₂ Aib, TFA salt), 9.10 (d, 1H, *J* = 6 Hz, NH amide), 10.77 (s, 1H, NH indole), 10.85 (s, 1H, NH indole Trp). ¹³C NMR (75 MHz, DMSO-*d*₆, 300 K) δ (ppm) 14.2 (CH₃–CH₂–CH₂–CH₂–CH₂–CH₂), 22.2 (CH₃–CH₂–CH₂–CH₂–CH₂–CH₂ and CH₂–CH₂–CH₂–indole), 23.6 (CH₃ Aib), 23.7 (CH₃ Aib), 24.5 (CH₂–CH₂–CH₂–indole), 25.9 (CH₃–CH₂–CH₂–CH₂–CH₂–CH₂), 27.5 (C βTrp and CH₂–CH₂–CH₂–indole), 29.7 (N–CH₂–CH₂), 30.8 (CH₃–CH₂–CH₂–CH₂–CH₂–CH₂), 43.2 (N–CH₂), 46.1 (C αTrp), 56.8 (Cq Aib), 109.5 (C₃ Trp), 111.8 (C₇ Trp), 111.9 (C₇ indole), 113.9 (C₃ indole), 118.1 (C₄ Trp), 118.5 (C₅ indole), 118.6 (C₄ indole), 118.9 (C₅ Trp), 121.3 (C₆ indole and C₆ Trp), 122.8 (C₂ indole and C₂ Trp), 127.3 (C₉ Trp), 127.4 (C₉ indole), 136.5 (C₈ Trp), 136.8 (C₈ indole), 154.7 (2Cq triazole), 172.0 (CO amide).

N-((R)-1-(4-(2-(1H-Indol-3-yl)ethyl)-5-benzyl-4H-1,2,4-triazol-3-yl)-2-(1H-indol-3-yl)ethyl)-2-amino-2-methylpropanamide Trifluoroacetate Salt (29a). ¹H NMR (400 MHz, DMSO-*d*₆, 300 K) δ (ppm) 1.31 (s, 3H, CH₃ Aib), 1.35 (s, 3H, CH₃ Aib), 2.51 (m, 2H, CH₂–CH₂–indole), 3.37 (m, 2H, CH₂ βTrp), 3.76–3.90 (m, 4H, CH₂–benzyl and CH₂–CH₂–indole), 5.25 (m, 1H, CH αTrp), 6.88 (t, 2H, *J*_o = 7 Hz, H₅ indole and H₅ Trp), 6.95 (t, 2H, *J*_o = 7 Hz, H₆ indole and H₆ Trp), 7.03 (m, 4H, H₂ Trp, H₂ indole, H₂ and H₆ benzyl), 7.16 (d, 2H, *J*_o = 8 Hz, H₄ indole and H₄ Trp), 7.20–7.30 (m, 4H, H₇ indole, H₃, H₄ and H₅ benzyl), 7.47 (d, 1H, *J*_o = 8 Hz, H₇ Trp), 8.05 (brs, 3H, NH₂ Aib, TFA salt), 9.05 (d, 1H, *J* = 8 Hz, NH amide), 10.83 (s, 1H, NH indole), 10.88 (s, 1H, NH indole Trp). ¹³C NMR (100 MHz, DMSO-*d*₆, 300 K) δ (ppm) 23.5 (CH₃ Aib), 23.7 (CH₃ Aib), 29.6 (C βTrp), 30.3 (CH₂–benzyl and CH₂–CH₂–indole), 44.1 (CH₂–CH₂–indole), 46.1 (C αTrp), 56.8 (Cq Aib), 109.8 (C₃ Trp), 109.9 (C₃ indole), 111.9 (C₇ indole and C₇ Trp), 118.3 (C₄ Trp), 118.4 (C₄ indole), 118.9 (C₅ indole and C₅ Trp), 121.3 (C₆ Trp), 121.5 (C₆ indole), 123.7 (C₂ indole), 124.7 (C₂ Trp), 127.0 (C₉ indole), 127.2 (C₄ benzyl), 127.4 (C₉ Trp), 128.8 (C₃ and C₅ benzyl), 129.0 (C₂ and C₆ benzyl), 136.3 (C₁ benzyl), 136.4 (C₈ indole and C₈ Trp), 153.1 (Cq triazole), 155.3 (Cq triazole), 171.8 (CO amide).

(R)-N-(1-(4,5-bis(2-(1H-Indol-3-yl)ethyl)-4H-1,2,4-triazol-3-yl)-2-(1H-indol-3-yl)ethyl)-2-amino-2-methylpropanamide Trifluoroacetate Salt (29b). ¹H NMR (300 MHz, DMSO-*d*₆, 300 K) δ (ppm) 1.30 (s, 3H, CH₃ Aib), 1.37 (s, 3H, CH₃ Aib), 2.50 (m, 2H, N–CH₂–CH₂–indole), 2.68 (t, 2H, *J*_o = 8 Hz, C–CH₂–CH₂–

indole), 2.91 (t, 2H, $J_0 = 8$ Hz, C-CH₂-CH₂-indole), 3.34 (m, 2H, N-CH₂-CH₂-indole), 3.93 (m, 2H, CH₂ βTrp), 5.25 (m, 1H, CH αTrp), 6.72–6.94 (m, 4H, H₅ and H₆ Trp, H₅ indole from C-CH₂-CH₂-indole and H₅ indole from N-CH₂-CH₂-indole), 6.98–7.04 (m, 4H, H₂ Trp, H₆ indole from C-CH₂-CH₂-indole, H₂ and H₆ indole from N-CH₂-CH₂-indole), 7.11 (s, 1H, H₂ indole from C-CH₂-CH₂-indole), 7.19 (d, 1H, $J_0 = 8$ Hz, H₄ indole from N-CH₂-CH₂-indole), 7.28 (m, 3H, H₄ and H₇ Trp, H₇ indole from N-CH₂-CH₂-indole), 7.40 (d, 1H, $J_0 = 8$ Hz, H₇ indole from C-CH₂-CH₂-indole), 7.44 (d, 1H, $J_0 = 8$ Hz, H₄ indole from C-CH₂-CH₂-indole), 8.04 (brs, 3H, NH₂ Aib, TFA salt), 9.69 (d, 1H, $J = 8$ Hz, NH amide), 10.73 (s, 1H, NH indole from C-CH₂-CH₂-indole), 10.82 (d, 1H, $J = 2$ Hz, NH indole Trp), 10.84 (s, 1H, NH indole from N-CH₂-CH₂-indole). ¹³C NMR (75 MHz, DMSO-*d*₆, 300 K) δ (ppm) 22.7 (C-CH₂-CH₂-indole), 23.6 (CH₃ Aib), 23.8 (CH₃ Aib), 25.4 (C-CH₂-CH₂-indole), 26.0 (N-CH₂-CH₂-indole), 29.6 (C βTrp), 43.9 (N-CH₂-CH₂-indole), 46.0 (C αTrp), 56.8 (Cq Aib), 109.5 (C₃ indole from N-CH₂-CH₂-indole), 109.9 (C₃ Trp), 111.7 (C₇ Trp), 111.9 (C₇ indole from N-CH₂-CH₂-indole and C₇ indole from C-CH₂-CH₂-indole), 113.5 (C₃ indole from C-CH₂-CH₂-indole), 118.3 (C₄ indole from N-CH₂-CH₂-indole), 118.4 (C₄ Trp), 118.5 (C₅ indole from C-CH₂-CH₂-indole), 118.7 (C₄ indole from C-CH₂-CH₂-indole), 118.9 (C₅ Trp), 119.0 (C₅ indole from N-CH₂-CH₂-indole), 121.3 (C₆ Trp), 121.5 (C₆ indole from C-CH₂-CH₂-indole and C₆ indole from N-CH₂-CH₂-indole), 122.8 (C₂ Trp, C₂ indole from C-CH₂-CH₂-indole and C₂ indole from N-CH₂-CH₂-indole), 127.1 (C₉ Trp), 127.2 (C₉ indole from C-CH₂-CH₂-indole), 127.4 (C₉ indole from N-CH₂-CH₂-indole), 136.5 (C₈ Trp and C₈ indole from C-CH₂-CH₂-indole), 136.6 (C₈ indole from N-CH₂-CH₂-indole), 154.5 (Cq triazole), 154.8 (Cq triazole), 171.8 (CO amide).

(R)-N-(1-(4-(2-(1H-Indol-3-yl)ethyl)-5-(3-(1H-indol-3-yl)propyl)-4H-1,2,4-triazol-3-yl)-2-(1H-indol-3-yl)ethyl)-2-amino-2-methylpropanamide Trifluoroacetate Salt (29c). ¹H NMR (300 MHz, DMSO-*d*₆) δ (ppm) 1.29 (s, 3H, CH₃ Aib), 1.35 (s, 3H, CH₃ Aib), 1.78 (m, 2H, CH₂-CH₂-CH₂-indole), 2.34 (m, 2H, CH₂-CH₂-CH₂-indole), 2.48 (m, 2H, N-CH₂-CH₂-indole), 2.80 (m, 2H, CH₂-CH₂-CH₂-indole), 3.34 (m, 2H, N-CH₂-CH₂-indole), 3.94 (m, 2H, CH₂ βTrp), 5.27 (m, 1H, CH αTrp), 6.73–6.94 (m, 4H, H₅ and H₆ Trp, H₅ indole from N-CH₂-CH₂-indole and H₅ indole from CH₂-CH₂-CH₂-indole), 6.99–7.04 (m, 5H, H₂ Trp, H₂ and H₆ indole from N-CH₂-CH₂-indole, H₂ and H₆ indole from CH₂-CH₂-CH₂-indole), 7.20 (d, 1H, $J_0 = 8$ Hz, H₄ indole from N-CH₂-CH₂-indole), 7.29 (m, 3H, H₄ and H₇ Trp, H₇ indole from N-CH₂-CH₂-indole), 7.40 (d, 1H, $J_0 = 8$ Hz, H₇ indole from CH₂-CH₂-CH₂-indole), 7.44 (d, 1H, $J_0 = 8$ Hz, H₄ indole from CH₂-CH₂-CH₂-indole), 8.05 (brs, 3H, NH₂ Aib, TFA salt), 9.07 (d, 1H, $J = 8$ Hz, NH amide), 10.75 (s, 1H, NH indole from CH₂-CH₂-CH₂-indole), 10.86 (s, 1H, NH indole Trp), 10.90 (s, 1H, NH indole from N-CH₂-CH₂-indole). ¹³C NMR (75 MHz, DMSO-*d*₆) δ (ppm) 23.6 (CH₃ Aib), 23.8 (CH₃ Aib), 24.5 (CH₂-CH₂-CH₂-indole), 25.8 (CH₂-CH₂-CH₂-indole), 27.2 (CH₂-CH₂-CH₂-indole), 29.4 (C βTrp), 44.1 (N-CH₂-CH₂-indole), 46.0 (C αTrp), 52.9 (N-CH₂-CH₂-indole), 56.8 (Cq Aib), 109.7 (C₃ Trp and C₃ indole from N-CH₂-CH₂-indole), 111.8 (C₇ Trp), 111.9 (C₇ indole from N-CH₂-CH₂-indole and C₇ indole from CH₂-CH₂-CH₂-indole), 114.0 (C₃ indole from CH₂-CH₂-CH₂-indole), 118.2 (C₄ indole from N-CH₂-CH₂-indole), 118.3 (C₄ Trp), 118.5 (C₅ indole from CH₂-CH₂-CH₂-indole), 118.6 (C₄ indole from CH₂-CH₂-CH₂-indole), 118.9 (C₅ Trp), 119.0 (C₅ indole from N-CH₂-CH₂-indole), 121.3 (C₆ Trp), 121.4 (C₆ indole from CH₂-CH₂-CH₂-indole), 121.6 (C₆ indole from N-CH₂-CH₂-indole), 122.7 (C₂ Trp, C₂ indole from N-CH₂-CH₂-indole and C₂ indole from CH₂-CH₂-CH₂-indole), 127.1 (C₉ Trp), 127.4 (C₉ indole from N-CH₂-CH₂-indole and C₉ indole from CH₂-CH₂-CH₂-indole), 136.4 (C₈ Trp), 136.5 (C₈ indole from CH₂-CH₂-CH₂-indole), 136.7 (C₈ indole from N-CH₂-CH₂-indole), 154.7 (Cq triazole), 171.9 (CO amide).

(R)-N-(1-(4-(4-Methylbenzyl)-5-(3-phenylpropyl)-4H-1,2,4-triazol-3-yl)-2-(1H-indol-3-yl)ethyl)-2-amino-2-methylpropan-

amide Trifluoroacetate Salt (30a). ¹H NMR (300 MHz, DMSO-*d*₆) δ (ppm) 1.25 (s, 3H, CH₃ Aib), 1.28 (s, 3H, CH₃ Aib), 1.73 (m, 2H, CH₂-CH₂-CH₂-phenyl), 2.23 (s, 3H, CH₃ *p*-methylbenzyl), 2.49–2.54 (m, 4H, CH₂-CH₂-CH₂-phenyl), 3.33 (m, 2H, CH₂ βTrp), 5.04 (s, 2H, CH₂-*p*-methylbenzyl), 5.16 (m, 1H, CH αTrp), 6.74 (d, 2H, $J_0 = 8$ Hz, H₃ and H₅ *p*-methylbenzyl), 6.80 (t, 1H, $J_0 = 7$ Hz, H₅ Trp), 6.98 (t, 1H, $J_0 = 7$ Hz, H₆ Trp), 7.03 (d, 1H, $J = 2$ Hz, H₂ Trp), 7.06 (m, 5H, CHar phenyl), 7.14 (d, 1H, $J_0 = 7$ Hz, H₄ Trp), 7.20 (d, 2H, $J_0 = 7$ Hz, H₂ and H₆ *p*-methylbenzyl), 7.27 (d, 1H, $J_0 = 8$ Hz, H₇ Trp), 8.01 (brs, 3H, NH₂ Aib, TFA salt), 8.95 (d, 1H, $J = 8$ Hz, NH amide), 10.80 (d, 1H, $J = 2$ Hz, NH indole Trp). ¹³C NMR (75 MHz, DMSO-*d*₆) δ (ppm) 21.0 (CH₃ *p*-methylbenzyl), 23.5 (CH₃ Aib), 23.8 (CH₃ Aib), 24.0 (CH₂-CH₂-CH₂-phenyl), 28.5 (CH₂-CH₂-CH₂-phenyl), 29.1 (C βTrp), 34.7 (CH₂-CH₂-CH₂-phenyl), 45.7 (C αTrp), 45.8 (CH₂-*p*-methylbenzyl), 56.8 (Cq Aib), 109.8 (C₃ Trp), 111.8 (C₇ Trp), 118.3 (C₄ Trp), 118.7 (C₅ Trp), 121.3 (C₆ Trp), 124.9 (C₂ Trp), 126.2 (C₄ phenyl), 126.4 (C₃ and C₅ *p*-methylbenzyl), 127.3 (C₉ Trp), 128.7 (C₂, C₃, C₅ and C₆ phenyl), 129.8 (C₂ and C₆ *p*-methylbenzyl), 133.0 (C₁ *p*-methylbenzyl), 136.4 (C₈ Trp), 137.5 (C₄ *p*-methylbenzyl), 141.7 (C₁ phenyl), 154.8 (2Cq triazole), 171.9 (CO amide).

(R)-N-(1-(4-(4-Methylbenzyl)-5-(3-benzyl)-4H-1,2,4-triazol-3-yl)-2-(1H-indol-3-yl)ethyl)-2-amino-2-methylpropanamide Trifluoroacetate Salt (30b). ¹H NMR (300 MHz, DMSO-*d*₆, 300 K) δ (ppm) 1.22 (s, 3H, CH₃ Aib), 1.27 (s, 3H, CH₃ Aib), 2.22 (s, 3H, CH₃ *p*-methylbenzyl), 3.22 (dd, 1H, $J = 14$ and 6 Hz, CH₂ βTrp), 3.33 (dd, 1H, $J = 14$ and 9 Hz, CH₂ βTrp), 3.99 (s, 2H, CH₂-benzyl), 5.04 (s, 2H, CH₂-*p*-methylbenzyl), 5.09 (m, 1H, CH αTrp), 6.64 (d, 2H, $J_0 = 8$ Hz, H₃ and H₅ *p*-methylbenzyl), 6.78 (t, 1H, $J_0 = 7$ Hz, H₅ Trp), 6.98 (t, 4H, $J_0 = 7$ Hz, H₆ Trp, H₃, H₄ and H₅ benzyl), 7.01 (d, 1H, $J = 2$ Hz, H₂ Trp), 7.07 (d, 2H, $J_0 = 7$ Hz, H₂ and H₆ *p*-methylbenzyl), 7.20 (m, 3H, H₄ Trp, H₂ and H₆ benzyl), 7.26 (d, 1H, $J_0 = 8$ Hz, H₇ Trp), 7.98 (brs, 3H, NH₂ Aib, TFA salt), 8.89 (d, 1H, $J = 8$ Hz, NH amide), 10.74 (s, 1H, NH indole Trp). ¹³C NMR (75 MHz, DMSO-*d*₆, 300 K) δ (ppm) 21.0 (CH₃ *p*-methylbenzyl), 23.5 (CH₃ Aib), 23.7 (CH₃ Aib), 29.1 (C βTrp), 30.6 (CH₂-benzyl), 45.7 (C αTrp), 46.0 (CH₂-*p*-methylbenzyl), 56.7 (Cq Aib), 109.8 (C₃ Trp), 111.7 (C₇ Trp), 118.3 (C₄ Trp), 118.6 (C₅ Trp), 121.2 (C₆ Trp), 124.8 (C₂ Trp), 126.3 (C₃ and C₅ *p*-methylbenzyl), 127.0 (C₄ benzyl), 127.2 (C₉ Trp), 128.9 (C₂, C₃, C₅, and C₆ benzyl), 129.7 (C₂ and C₆ *p*-methylbenzyl), 132.9 (C₁ *p*-methylbenzyl), 136.3 (C₄ *p*-methylbenzyl), 136.4 (C₈ Trp), 137.4 (C₁ benzyl), 153.9 (Cq triazole), 155.3 (Cq triazole), 171.8 (CO amide).

(R)-N-(1-(5-(2-(1H-Indol-2-yl)ethyl)-4-(4-methylbenzyl)-4H-1,2,4-triazol-3-yl)-2-(1H-indol-3-yl)ethyl)-2-amino-2-methylpropanamide Trifluoroacetate Salt (30c). ¹H NMR (300 MHz, DMSO-*d*₆, 300 K) δ (ppm) 1.25 (s, 3H, CH₃ Aib), 1.28 (s, 3H, CH₃ Aib), 2.23 (s, 3H, CH₃-*p*-methylbenzyl), 2.84–2.97 (m, 4H, CH₂-CH₂-indole), 3.32 (m, 2H, CH₂ βTrp), 5.04 (s, 2H, CH₂-*p*-methylbenzyl), 5.16 (m, 1H, CH αTrp), 6.79–6.86 (m, 4H, CH ar *p*-methylbenzyl), 6.99–7.05 (m, 4H, H₅ and H₆ indole, H₅ and H₆ Trp), 7.08 (m, 3H, H₂ indole, H₂ and H₄ Trp), 7.25–7.30 (m, 3H, H₄ and H₇ indole, H₇ Trp), 8.00 (brs, 3H, NH₂ Aib, TFA salt), 8.94 (d, 1H, $J = 8$ Hz, NH amide), 10.76 (s, 1H, NH indole), 10.78 (s, 1H, NH indole Trp). ¹³C NMR (75 MHz, DMSO-*d*₆, 300 K) δ (ppm) 21.0 (CH₃-*p*-methylbenzyl), 22.8 (CH₂-CH₂-indole), 23.8 (CH₃ Aib), 23.9 (CH₃ Aib), 25.9 (CH₂-CH₂-indole), 28.5 (C βTrp), 45.7 (CH₂-*p*-methylbenzyl and C αTrp), 56.7 (Cq Aib), 109.9 (C₃ Trp), 111.8 (C₇ indole and C₇ Trp), 113.4 (C₃ indole), 118.1 (C₄ Trp), 118.3 (C₄ indole), 118.5 (C₅ indole), 118.7 (C₅ Trp), 120.9 (C₆ indole and C₆ Trp), 121.3 (C₂ indole and C₂ Trp), 126.3 (C₃ and C₅ *p*-methylbenzyl), 127.2 (C₉ indole), 127.3 (C₉ Trp), 129.8 (C₂ and C₆ *p*-methylbenzyl), 133.1 (C₁ *p*-methylbenzyl), 135.8 (C₈ indole, C₈ Trp), 136.4 (C₄ *p*-methylbenzyl), 154.8 (Cq triazole), 155.0 (Cq triazole), 171.9 (CO amide).

(R)-N-(1-(4-(4-Methylbenzyl)-5-phenethyl-4H-1,2,4-triazol-3-yl)-2-(1H-indol-3-yl)ethyl)-2-amino-2-methylpropanamide Trifluoroacetate Salt (30d). ¹H NMR (300 MHz, DMSO-*d*₆, 300 K) δ (ppm) 1.25 (s, 3H, CH₃ Aib), 1.28 (s, 3H, CH₃ Aib), 2.23 (s,

3H, CH₃ *p*-methylbenzyl), 2.83 (m, 4H, CH₂-CH₂-phenyl), 3.32 (m, 2H, CH₂ βTrp), 5.05 (s, 2H, CH₂-*p*-methylbenzyl), 5.18 (m, 1H, CH αTrp), 6.75 (d, 2H, J_o = 8 Hz, H₃ and H₅ *p*-methylbenzyl), 6.82 (t, 1H, J_o = 8 Hz, H₅ Trp), 6.99 (t, 1H, J_o = 8 Hz, H₆ Trp), 7.02–7.11 (m, 6H, H₂ Trp and CHar phenyl), 7.15 (d, 1H, J_o = 7 Hz, H₄ Trp), 7.20 (d, 2H, J_o = 7 Hz, H₂ and H₆ *p*-methylbenzyl), 7.28 (d, 1H, J_o = 8 Hz, H₇ Trp), 8.01 (brs, 3H, NH₂ Aib, TFA salt), 8.93 (d, 1H, J = 8 Hz, NH amide), 10.77 (s, 1H, NH indole Trp). ¹³C NMR (75 MHz, DMSO-*d*₆, 300 K) δ (ppm) 21.0 (CH₃ *p*-methylbenzyl), 23.6 (CH₃ Aib), 23.8 (CH₃ Aib), 26.5 (CH₂-CH₂-phenyl), 29.1 (C βTrp), 32.7 (CH₂-CH₂-phenyl), 45.7 (C αTrp and CH₂-*p*-methylbenzyl), 56.8 (Cq Aib), 109.8 (C₃ Trp), 111.8 (C₇ Trp), 118.3 (C₄ Trp), 118.7 (C₅ Trp), 121.3 (C₆ Trp), 124.8 (C₂ Trp), 126.4 (C₃ and C₅ *p*-methylbenzyl), 126.6 (C₄ phenyl), 127.3 (C₉ Trp), 128.7 (C₂, C₃, C₅, and C₆ phenyl), 129.8 (C₂ and C₆ *p*-methylbenzyl), 133.0 (C₁ *p*-methylbenzyl), 136.4 (C₈ Trp), 137.5 (C₄ *p*-methylbenzyl), 140.9 (C₁ phenyl), 154.5 (Cq triazole), 154.9 (Cq triazole), 171.9 (CO amide).

(R)-N-(1-(4-(4-Ethylbenzyl)-5-phenethyl-4H-1,2,4-triazol-3-yl)-2-(1H-indol-3-yl)ethyl)-2-amino-2-methylpropanamide Trifluoroacetate Salt (31). ¹H NMR (300 MHz, DMSO-*d*₆, 300 K) δ (ppm) 1.10 (t, 3H, J = 8 Hz, CH₃-CH₂ *p*-ethylbenzyl), 1.25 (s, 3H, CH₃ Aib), 1.28 (s, 3H, CH₃ Aib), 2.53 (q, 2H, J = 8 Hz, CH₃-CH₂ *p*-ethylbenzyl), 2.83 (m, 4H, CH₂-CH₂-phenyl), 3.34 (m, 2H, CH₂ βTrp), 5.07 (s, 2H, CH₂-*p*-ethylbenzyl), 5.19 (m, 1H, CH αTrp), 6.77 (d, 2H, J_o = 8 Hz, H₃ and H₅ *p*-ethylbenzyl), 6.81 (t, 1H, J_o = 7 Hz, H₅ Trp), 6.99 (t, 1H, J_o = 8 Hz, H₆ Trp), 7.05–7.10 (m, 7H, CHar phenyl, H₂ and H₆ *p*-ethylbenzyl), 7.13 (d, 1H, J = 2 Hz, H₂ Trp), 7.20 (d, 1H, J_o = 7 Hz, H₄ Trp), 7.28 (d, 1H, J_o = 8 Hz, H₇ Trp), 8.03 (brs, 3H, NH₂ Aib, TFA salt), 8.94 (d, 1H, J = 8 Hz, NH amide), 10.79 (s, 1H, NH indole Trp). ¹³C NMR (75 MHz, DMSO-*d*₆, 300 K) δ (ppm) 15.9 (CH₃-CH₂ *p*-ethylbenzyl), 23.5 (CH₃ Aib), 23.8 (CH₃ Aib), 26.5 (CH₂-CH₂-phenyl), 28.1 (CH₃-CH₂ *p*-ethylbenzyl), 29.1 (C βTrp), 32.7 (CH₂-CH₂-phenyl), 45.7 (C αTrp), 45.8 (CH₂-*p*-ethylbenzyl), 56.8 (Cq Aib), 109.8 (C₃ Trp), 111.8 (C₇ Trp), 118.3 (C₄ Trp), 118.7 (C₅ Trp), 121.3 (C₆ Trp), 124.9 (C₂ Trp), 126.5 (C₃ and C₅ *p*-ethylbenzyl), 126.6 (C₄ phenyl), 127.3 (C₉ Trp), 128.6 (C₂ and C₆ *p*-ethylbenzyl), C₂, C₃, C₅, and C₆ phenyl), 133.1 (C₁ *p*-ethylbenzyl), 136.5 (C₈ Trp), 140.8 (C₁ phenyl), 143.8 (C₄ *p*-ethylbenzyl), 154.6 (Cq triazole), 154.9 (Cq triazole), 171.9 (CO amide).

N-((R)-1-(4-(4-Nitrobenzyl)-5-phenethyl-4H-1,2,4-triazol-3-yl)-2-(1H-indol-3-yl)ethyl)-2-amino-2-methylpropanamide Trifluoroacetate Salt (32). ¹H NMR (300 MHz, DMSO-*d*₆, 300 K) δ (ppm) 1.28 (s, 3H, CH₃ Aib), 1.29 (s, 3H, CH₃ Aib), 2.77–2.94 (m, 4H, CH₂-CH₂-phenyl), 3.28 (dd, 1H, ³J = 14 and 8 Hz, CH₂ βTrp), 3.43 (dd, 1H, ³J = 14 and 7 Hz, CH₂ βTrp), 5.05 (m, 1H, CH αTrp), 5.25 (d, 2H, J = 7 Hz, CH₂-*p*-nitrobenzyl), 6.72 (t, 1H, J_o = 7 Hz, H₅ Trp), 6.89 (d, 2H, J_o = 9 Hz, H₂ and H₆ *p*-nitrobenzyl), 6.92 (t, 1H, J_o = 7 Hz, H₆ Trp), 7.00 (d, 1H, J_m = 2 Hz, H₂ Trp), 7.08–7.15 (m, 4H, H₄ and H₇ Trp, H₂ and H₆ phenyl), 7.17 (t, 2H, J_o = 7 Hz, H₃ and H₅ phenyl), 7.24 (t, 1H, J_o = 8 Hz, H₄ phenyl), 7.92 (d, 2H, J_o = 9 Hz, H₃ and H₅ *p*-nitrobenzyl), 8.06 (brs, 3H, NH₂ Aib, TFA salt), 8.98 (d, 1H, J = 8 Hz, NH amide), 10.79 (s, 1H, NH indole Trp). ¹³C NMR (75 MHz, DMSO-*d*₆, 300 K) δ (ppm) 23.5 (CH₃ Aib), 23.8 (CH₃ Aib), 26.4 (CH₂-CH₂-phenyl), 29.1 (C βTrp), 32.6 (CH₂-CH₂-phenyl), 45.3 (CH₂-*p*-nitrobenzyl), 45.7 (C αTrp), 56.8 (Cq Aib), 109.6 (C₃ Trp), 111.8 (C₇ Trp), 118.1 (C₄ Trp), 118.5 (C₅ Trp), 121.2 (C₆ Trp), 124.1 (C₂ and C₆ *p*-nitrobenzyl), 124.8 (C₂ Trp), 126.5 (C₄ phenyl), 127.2 (C₉ Trp, C₃ and C₅ *p*-nitrobenzyl), 128.7 (C₂, C₃, C₅, and C₆ phenyl), 136.4 (C₈ Trp), 140.8 (C₁ phenyl), 143.5 (C₁ *p*-nitrobenzyl), 147.1 (C₄ *p*-nitrobenzyl), 154.5 (Cq triazole), 154.8 (Cq triazole), 172.0 (CO amide).

(R)-2-Amino-N-(1-(5-benzyl-4-(pyridin-2-ylmethyl)-4H-1,2,4-triazol-3-yl)-2-(1H-indol-3-yl)ethyl)-2-methylpropanamide Trifluoroacetate Salt (33a). ¹H NMR (300 MHz, DMSO-*d*₆, 300 K) δ (ppm) 1.23 (s, 3H, CH₃ Aib), 1.27 (s, 3H, CH₃ Aib), 3.34 (dd, 1H, J = 14 and 6 Hz, CH₂ βTrp), 3.43 (dd, 1H, J = 14 and 9 Hz, CH₂ βTrp), 4.13 (s, 2H, CH₂-benzyl), 5.22 (s, 1H, CH αTrp), 5.35

(s, 2H, CH₂-*o*-pyridyl), 6.80 (t, 1H, J_o = 8 Hz, H₅ Trp), 6.92 (t, 1H, J_o = 8 Hz, H₅ pyridyl), 6.97 (t, 1H, J_o = 8 Hz, H₆ Trp), 7.04 (d, 1H, J_o = 8 Hz, H₄ Trp), 7.07 (d, 1H, J = 2 Hz, H₂ Trp), 7.10–7.16 (m, 5H, CHar benzyl), 7.19 (s, 1H, H₃ *o*-pyridyl), 7.26 (d, 1H, J_o = 8 Hz, H₇ Trp), 7.57 (t, 1H, J_o = 9 Hz, H₄ *o*-pyridyl), 8.16 (brs, 3H, NH₂ Aib, TFA salt), 8.36 (d, 1H, J_{αβ} = 5 Hz, H₆ *o*-pyridyl), 9.01 (d, 1H, J = 8 Hz, NH amide), 10.85 (s, 1H, NH indole Trp). ¹³C NMR (75 MHz, DMSO-*d*₆, 300 K) δ (ppm) 23.4 (CH₃ Aib), 23.7 (CH₃ Aib), 28.6 (C βTrp), 30.4 (CH₂-benzyl), 45.7 (C αTrp), 47.7 (CH₂-*o*-pyridyl), 56.7 (Cq Aib), 109.8 (C₃ Trp), 111.8 (C₇ Trp), 118.3 (C₄ Trp), 118.6 (C₅ Trp), 121.2 (C₆ Trp), 121.7 (C₃ *o*-pyridyl), 123.3 (C₅ *o*-pyridyl), 124.8 (C₂ Trp), 127.1 (C₄ benzyl), 127.3 (C₉ Trp), 128.8 (C₂ and C₆ benzyl), 129.0 (C₃ and C₅ benzyl), 135.6 (C₁ benzyl), 136.4 (C₈ Trp), 137.5 (C₄ *o*-pyridyl), 149.5 (C₆ *o*-pyridyl), 154.1 (Cq triazole), 154.2 (Cq triazole), 155.7 (C₂ *o*-pyridyl), 172.0 (CO amide).

(R)-2-Amino-N-(1-(5-phenethyl-4-(pyridin-2-ylmethyl)-4H-1,2,4-triazol-3-yl)-2-(1H-indol-3-yl)ethyl)-2-methylpropanamide Trifluoroacetate Salt (33b). ¹H NMR (300 MHz, DMSO-*d*₆, 300 K) δ (ppm) 1.26 (s, 3H, CH₃ Aib), 1.29 (s, 3H, CH₃ Aib), 2.95 (m, 4H, CH₂-CH₂-phenyl), 3.40 (m, 2H, CH₂ βTrp), 5.26 (m, 1H, CH αTrp), 5.37 (s, 2H, CH₂-*o*-pyridyl), 6.83 (t, 1H, J_o = 7 Hz, H₅ Trp), 6.98 (t, 1H, J_o = 8 Hz, H₆ Trp), 7.11–7.30 (m, 10H, H₂, H₄ and H₇ Trp, CHar phenyl, H₃ and H₅ *o*-pyridyl), 7.71 (t, 1H, J_o = 7 Hz, H₄ *o*-pyridyl), 8.22 (brs, 3H, NH₂ Aib, TFA salt), 8.42 (d, 1H, J_{αβ} = 4 Hz, H₆ *o*-pyridyl), 9.05 (d, 1H, J = 8 Hz, NH amide), 10.87 (s, 1H, NH indole Trp). ¹³C NMR (75 MHz, DMSO-*d*₆, 300 K) δ (ppm) 23.4 (CH₃ Aib), 23.7 (CH₃ Aib), 26.4 (CH₂-CH₂-phenyl), 28.6 (C βTrp), 32.5 (CH₂-CH₂-phenyl), 45.7 (C αTrp), 47.6 (CH₂-*o*-pyridyl), 56.8 (Cq Aib), 109.8 (C₃ Trp), 111.8 (C₇ Trp), 118.3 (C₄ Trp), 118.6 (C₅ Trp), 121.2 (C₆ Trp), 122.0 (C₃ *o*-pyridyl), 123.6 (C₅ *o*-pyridyl), 126.3 (C₂ Trp), 126.6 (C₄ phenyl), 127.3 (C₉ Trp), 128.7 (C₂, C₃, C₅, and C₆ phenyl), 136.4 (C₈ tryptophane), 137.7 (C₄ *o*-pyridyl), 140.7 (C₁ phenyl), 150.1 (C₆ *o*-pyridyl), 154.9 (Cq triazole), 155.2 (Cq triazole), 158.7 (C₂ *o*-pyridyl), 172.0 (CO amide).

N-((R)-1-(4-(4-Methoxyphenethyl)-5-phenethyl-4H-1,2,4-triazol-3-yl)-2-(1H-indol-3-yl)ethyl)-2-amino-2-methylpropanamide Trifluoroacetate Salt (34). ¹H NMR (300 MHz, DMSO-*d*₆, 300 K) δ (ppm) 1.30 (s, 3H, CH₃ Aib), 1.35 (s, 3H, CH₃ Aib), 2.55 (m, 4H, CH₂-CH₂-phenyl and CH₂-CH₂-*p*-methoxybenzyl), 2.83 (t, 2H, J = 8 Hz, CH₂-CH₂-phenyl), 3.37 (m, 2H, CH₂-CH₂-*p*-methoxybenzyl), 3.65 (s, 3H, OCH₃), 3.77 (m, 1H, CH₂ βTrp), 3.89 (m, 1H, CH₂ βTrp), 5.20 (m, 1H, CH αTrp), 6.72 (s, 4H, CHar *p*-methoxybenzyl), 6.94 (t, 1H, J_o = 7 Hz, H₅ Trp), 7.02 (t, 1H, J_o = 8 Hz, H₆ Trp), 7.05 (d, 1H, J = 2 Hz, H₂ Trp), 7.11 (d, 2H, J_o = 7 Hz, H₂ and H₆ phenyl), 7.16 (d, 1H, J_o = 7 Hz, H₄ Trp), 7.25 (m, 3H, H₃, H₄, H₅ phenyl), 7.50 (d, 1H, J_o = 8 Hz, H₇ Trp), 8.05 (brs, 3H, NH₂ Aib, TFA salt), 9.02 (d, 1H, J = 8 Hz, NH amide), 10.83 (d, 1H, J = 2 Hz, NH indole Trp). ¹³C NMR (75 MHz, DMSO-*d*₆, 300 K) δ (ppm) 23.5 (CH₃ Aib), 23.8 (CH₃ Aib), 26.0 (CH₂-CH₂-phenyl), 29.5 (C βTrp), 32.5 (CH₂-CH₂-phenyl), 35.0 (CH₂-CH₂-*p*-methoxybenzyl), 44.4 (CH₂-CH₂-*p*-methoxybenzyl), 45.8 (C αTrp), 55.4 (OCH₃), 56.8 (Cq Aib), 109.9 (C₃ Trp), 111.9 (C₇ Trp), 114.2 (C₃ and C₅ *p*-methoxybenzyl), 118.4 (C₄ Trp), 118.9 (C₅ Trp), 121.4 (C₆ Trp), 124.7 (C₂ Trp), 126.5 (C₄ phenyl), 127.4 (C₉ Trp), 128.7 (C₂, C₃, C₅, and C₆ phenyl), 129.4 (C₁ *p*-methoxybenzyl), 130.3 (C₂ and C₆ *p*-methoxybenzyl), 136.5 (C₈ Trp), 141.0 (C₁ phenyl), 154.0 (Cq triazole), 154.5 (Cq triazole), 158.6 (C₄ *p*-methoxybenzyl), 171.8 (CO amide).

In Vitro hGHSR-1a Evaluation. Transient transfection of LLC PK-1 cells and membrane preparation were performed as previously described.³¹ LLC PK-1 cells were grown at 37 °C, 5% CO₂ in Dulbecco's modified eagle's medium (DMEM) supplemented with 10% FCS (v/v), glutamine (2 mM), and antibiotics (50 units/mL penicillin and 50 μg/mL streptomycin). LLC PK-1 cells were transiently transfected with 1 μg of hGHSR-1a using electroporation (Easyject Optima apparatus, Equibio) according to the manufacturer's protocol (Equibio). Electroporation was carried out at room temperature according to the manufacturer's instructions with the following parameters: 250 V, 1500 μF, and infinite internal

resistance. Transfected cells were plated in 10 cm culture dishes containing complete growth medium without phenol red. Approximately 48 h post-transfection, cells were washed three times with phosphate-buffered saline, pH 6.95, once with 10 mL of homogenization buffer (HB) containing 50 mM Tris (pH 7.3), 5 mM MgCl₂, 2.5 mM EDTA, and 30 μg/mL bacitracin, and were then collected by scrapping. The cells underwent two cycles of freeze/thawing and were then centrifuged at 10 000g for 20 min at 4 °C. The membrane pellet was then resuspended in a minimal volume of HB, aliquoted, and stored at -80 °C until use. Membrane protein concentration was determined by the Bradford method using the Bio-Rad protein assay kit.

Receptor Binding Studies. Isolated plasma membranes from LLC PK-1 cells (10 μg of protein) were incubated in HB for 60 min at 25 °C (steady-state conditions) with 60 pM [¹²⁵I]-His⁹-ghrelin (Amersham) in the presence or absence of competing compounds. Nonspecific binding was defined using an excess (1 μM) of ghrelin and was always less than 20% of total binding. The binding reaction was stopped by addition of 4 mL of ice-cold HB followed by rapid filtration over Whatman GF/C filters presoaked with 0.5% polyethyleneimine to prevent excessive binding of radioligand to the filters. Filters were rinsed three times with 3 mL of ice-cold wash buffer (50 mM Tris (pH 7.3), 10 mM MgCl₂, 2.5 mM EDTA, and 0.015% (w/v) Triton X-100), and the radioactivity bound to membranes was measured in a γ counter.

Intracellular Calcium Mobilization Assay. The calcium experiments were performed using the benchtop scanning fluorometer FlexStation II machine (pharmacologie and screening platform of the Institut Fédératif de Recherche 3, Montpellier, France). CHO cells were transiently transfected with the hGHS-1a receptor, using electroporation, and were then plated into 96-well black-bottom plates (80 000 cells/well). Twenty-four hours later the cells were washed with 150 μL buffer A (Hanks' balanced salt solution, 0.5% BSA, 20 mM CaCl₂, 2.5 mM probenecid, pH 7.4) and were then loaded with 1 μM of the fluorescent calcium indicator Fluo-4AM prepared in buffer A, containing 0.06% pluronic acid (a mild ionic detergent which facilitates Fluo-4AM ester loading). The cells were left to incubate for 1 h in the dark at 37 °C. Following the incubation, excess Fluo-4AM was removed from the cells by washing twice with 100 μL of buffer A, and 50 μL of the same buffer was then added to each well. The cells were left at room temperature for 30 min to allow complete de-esterification of intracellular Fluo-4AM esters. The black-bottom plate containing the cells, as well as the plate containing the compounds to be tested, was then placed into the temperature-regulated FlexStation machine. The machine records the fluorescence output over a period of 60 s, with the compounds being automatically distributed into the wells containing the cells after 15 s. The Fluo-4AM exhibits a large fluorescence intensity increase on binding of calcium, and therefore the fluorescence output is used directly as a measure of intracellular calcium mobilization. The excitation and emission wavelengths were 485 and 525 nm, respectively. The basal fluorescence intensity of dye-loaded cells was 800–1200 arbitrary units, and the fluorescence peak upon maximal response was 5000–7000 units. To assess the ability of each of the compounds to induce calcium mobilization, they were tested at a concentration of 10 μM in triplicate, in at least two independent experiments. In each case, the change in fluorescence upon addition of the compound was compared with the basal fluorescence output measured with the control (addition of buffer A only). The maximum fluorescent output was equivalent to that achieved when the cells were stimulated with 1 μM ghrelin. For the compounds behaving as agonists and displaying a high affinity binding for hGHS-R1a in radiolabeled binding experiments, the EC₅₀ (the molar concentration of the agonist producing 50% of the maximal possible effect of that agonist) was determined using a dose–response curve. In the case of high affinity antagonists, the IC₅₀ and K_b were determined using antagonist inhibition curves in the presence of 0.1 μM ghrelin (submaximal concentration). The IC₅₀ was calculated as the molar concentration of antagonist that reduced the maximal response of ghrelin by 50%, and an estimation of the K_b was made using the

Cheng–Prusoff equation.³² Schild analysis³³ was also used to determine the EC₅₀ of ghrelin in the presence of different concentrations of antagonist, and from this the pA₂ and the exact K_b were determined.

In Vivo Experiments in the Rat. A. Growth Hormone Assay. Compounds were dissolved in DMSO (10⁻² M) and brought to the final volume with saline. Animals, male 10-day-old Sprague–Dawley rats weighing about 25 g (Charles River, Calco, Italy), were used. Rat pups were received on the fifth day after birth and were housed in our facilities under controlled conditions (22 ± 2 °C, 65% humidity, and artificial light from 06:00 to 20:00 h). A standard dry diet and water were available ad libitum to the dams. One hour before the experiments, pups were separated from their respective dams and were divided randomly into groups of eight each. All the experiments were performed in accordance with the Italian Guidelines for the Use of Animals in Medical Research.

Pups were acutely challenged with solvent (DMSO, final dilution 1:300), hexarelin (80 μg/kg sc), or the compound to be tested (160 μg/kg sc). For combined treatments (test compounds plus hexarelin), test compounds were administered 10 min before hexarelin. Pups were killed by decapitation 15 min later. Trunk blood was collected and centrifuged immediately. Plasma samples were stored at -20 °C until assayed for the determination of plasma GH concentrations. GH was assayed in plasma using a commercial rat GH enzyme immunoassay kit (Spibio, Montigny le Bretonneux, France). Values are expressed in terms of NIDDK–rat–GHRP-2 standard (potency 2 IU/mg) as ng/mL plasma. The minimum detectable value of rat GH was about 1.0 ng/mL, and intra-assay variability was about 6%.

B. Experiments on Food Intake. Young adult male Sprague–Dawley rats (Charles River Laboratories, Calco, Italy) weighing 125–150 g were used. All rats were housed in single cages under controlled conditions (22 ± 2 °C, 65% humidity, artificial light from 08:00 to 20:00 h) with ad libitum access to standard rat chow and water. Rats had 1 week of acclimation in individual home cages and animal room conditions. The following week, they were trained daily to mimic the experimental procedure. At the end of training, rats were administered sc (around 10:00–11:00 a.m.) with graded doses of the compounds to test (0, 20, 80, 160, 320 μg/kg) at time -10 min and hexarelin (80 μg/kg) at time 0 to stimulate the feeding behavior. Immediately after, the animals were returned to their home cages, which contained a known amount of standard rat chow and ad libitum water. The remaining food was carefully collected and weighed to the nearest 0.1 g every hour for the following 6 h. In all the experiments hexarelin stimulated the intake of about 1 g of standard dry pellet food per 100 g of body weight of rats. Food intake was normalized for the body weight of the animals and expressed as g of food eaten for 100 g of body weight. Statistical analysis of food intake eaten in the first 2 h and in the total period of observation of 6 h was performed by one-way ANOVA followed by Dunnett's *t* test for multiple comparisons. A *P* value less than 0.05 was considered significant.

Acknowledgment. We gratefully acknowledge Mr. Pierre Sanchez for providing MS analytical data. The authors thank Aeterna-Zentaris and the CNRS for the financial support of this work and for providing a Research Grant for the Ph.D. Thesis of A.M. (BDI 752776/01).

Supporting Information Available: Displacement curves of [¹²⁵I]-His⁹-ghrelin for compounds **18a**, **19d**, **21a**, and **29c**; inhibition curves of ghrelin-induced [Ca²⁺]_i accumulation by compounds **16** and **19b**; [Ca²⁺]_i accumulation dose–response curves of ghrelin in the presence of increasing concentrations of compounds **16**, **19c**, and **19d**; physicochemical properties of all final compounds. This material is available free of charge via the Internet at <http://pubs.acs.org>.

References

- (1) For a review on GH see: Strobl, J. S.; Thomas, M. J. Human growth hormone. *Pharmacol. Rev.* **1994**, *46*, 1–34.

- (2) Blethen, S. L.; Baptista, J.; Kuntze, J.; Foley, T.; LaFranchi, S.; Johanson, A. Adult height in growth hormone (GH)-deficient children treated with biosynthetic GH. *J. Clin. Endocrinol. Metab.* **1997**, *82*, 418–420.
- (3) Bouillanne, O.; Rainfray, M.; Tissandier, O.; Nasr, A.; Lahlou, A.; Cnockaert, X.; Piette, F. Growth hormone therapy in elderly people: An age-delaying drug? *Fundam. Clin. Pharmacol.* **1996**, *10*, 416–430.
- (4) Bowers, C. Y.; Chang, J.; Momany, F.; Folkers, K. Effects of the Enkephalins and Enkephalin Analogs on Release of Pituitary Hormones in Vitro. In *Molecular Endocrinology*; Macintyne, I., Ed.; Elsevier: Amsterdam, The Netherlands, 1977; pp 287–292.
- (5) For recent reviews on GHRP see: (a) Ghigo, E.; Arvat, E.; Muccioli, G.; Camanni, F. Growth hormone-releasing peptides. *Eur. J. Endocrinol.* **1997**, *136*, 445–460. (b) Thorner, M. O.; Chapman, I. M.; Gaylinn, B. D.; Pezzoli, S. S.; Hartman, M. L. Growth hormone-releasing hormone and growth hormone-releasing peptide as therapeutic agents to enhance growth hormone secretion in disease and aging. *Recent Prog. Horm. Res.* **1997**, *52*, 215–44.
- (6) Bowers, C. Y. GH releasing peptides—structure and kinetics. *J. Pediatr. Endocrinol.* **1993**, *6*, 21–31.
- (7) Howard, A. D.; Feighner, S. D.; Cully, D. F.; Arena, J. P.; Liberato, P. A.; Rosenblum, C. I.; Hamelin, M. J.; Hreniuk, D. L.; Palyha, O. C.; Anderson, J.; Paress, P. S.; Diaz, C.; Chou, M.; Liu, K.; Mckee, K. K.; Pong, S. S.; Chung, L. Y.; Elbrecht, A.; Heavens, R.; Rigby, M.; Sirinathsinghji, D. J. S.; Dean, D. C.; Melillo, D. G.; Patchett, A. A.; Nargund, R.; Griffin, P. R.; DeMartino, J. A.; Gupta, S. K.; Schaeffer, J. M.; Smith, R. G.; Van Der Ploeg, L. H. T. A receptor in pituitary and hypothalamus that functions in growth hormone release. *Science* **1996**, *273*, 974–977.
- (8) Kojima, M.; Hosoda, H.; Date, Y.; Nakazato, M.; Matsuo, H.; Kangawa, K. Ghrelin is a growth-hormone-releasing acylated peptide from stomach. *Nature* **1999**, *402*, 656–660.
- (9) Ariyasu, H.; Takaya, K.; Tagami, T.; Ogawa, Y.; Hosoda, K.; Akamizu, T.; Suda, M.; Koh, T.; Natsui, K.; Toyooka, S.; Shirakami, G.; Usui, T.; Shimatsu, A.; Doi, K.; Hosoda, H.; Kojima, M.; Kangawa, K.; Nakao, K. Stomach is a major source of circulating ghrelin, and feeding state determines plasma ghrelin-like immunoreactivity levels in humans. *J. Clin. Endocrinol.* **2001**, *86*, 4753–4758.
- (10) Smith, R. G.; Cheng, K.; Schoen, W. R.; Pong, S. S.; Hickey, G.; Jacks, T.; Butler, B.; Chan, W. W. S.; Chung, L. Y. P.; Judith, F.; Taylor, J.; Wyvratt, M. J.; Fisher, M. H. A nonpeptidyl growth hormone secretagogue. *Science* **1993**, *260*, 1640–1643.
- (11) Nargund, R. P.; Barakat, K. H.; Cheng, K.; Chan, W. W. S.; Butler, B. R.; Smith, R. G.; Patchett, A. A. Synthesis and biological activities of camphor-based non-peptide growth hormone secretagogues. *Bioorg. Med. Chem. Lett.* **1996**, *6*, 1265–1270.
- (12) Patchett, A. A.; Nargund, R. P.; Tata, J. R.; Chen, M. H.; Barakat, K. J.; Johnston, D. B.; Cheng, K.; Chan, W. W.; Butler, B.; Hickey, G.; Jacks, T.; Schleich, K.; Pong, S. S.; Chung, L. Y. P.; Chen, H. Y.; Frazier, E.; Leung, K. H.; Chiu, S. H. L.; Smith, R. G. Design and biological activities of L-163,191 (MK-0677): a potent, orally active growth hormone secretagogue. *Proc. Natl. Acad. Sci. U.S.A.* **1995**, *92*, 7001–7005.
- (13) Locatelli, V.; Rossoni, G.; Schweiger, F.; Torsello, A.; De Gennaro Colonna, V.; Bernareggi, M.; Deghenghi, R.; Mueller, E. E.; Berti, F. Growth hormone-independent cardioprotective effects of hexarelin in the rat. *Endocrinology* **1999**, *140*, 4024–4031.
- (14) Guerlavais, V.; Boeglin, D.; Mousseaux, D.; Oiry, C.; Heitz, A.; Deghenghi, R.; Locatelli, V.; Torsello, A.; Ghe, C.; Catapano, F.; Muccioli, G.; Galleyrand, J. C.; Fehrentz, J. A.; Martinez, J. New active series of growth hormone secretagogues. *J. Med. Chem.* **2003**, *46*, 1191–203.
- (15) Broglio, F.; Boutignon, F.; Benso, A.; Gottero, C.; Prodam, F.; Arvat, E.; Ghe, C.; Catapano, F.; Torsello, A.; Locatelli, V.; Muccioli, G.; Guerlavais, V.; Boeglin, D.; Fehrentz, J. A.; Martinez, J.; Ghigo, E.; Deghenghi, R. EP1572: a novel peptido-mimetic GH secretagogue with potent and selective GH-releasing activity in man. *J. Endocrinol. Invest.* **2002**, *25*, R26–R29.
- (16) Collin, X.; Sauleau, A.; Coulon, J. 1,2,4-Triazole mercapto and aminonitriles as potent antifungal agents. *Bioorg. Med. Chem. Lett.* **2003**, *13*, 2601–2605.
- (17) Papakonstantinou-Garoufalias, S.; Pouli, N.; Marakos, P.; Chytyroglou-Ladas, A. Synthesis antimicrobial and antifungal activity of some new 3 substituted derivatives of 4-(2,4-dichlorophenyl)-5-adamantyl-1H-1,2,4-triazole. *Farmaco* **2002**, *57*, 973–977.
- (18) Starck, D.; Treiber, H.-J.; Unger, L.; Neumann-Schultz, B.; Blumbach, K.; Schobel, D. Preparation of 3-[(aminoalkyl)thio]-1,2,4-triazoles as dopamine D3 receptor ligands. International Patent WO 2000042038, 2000.
- (19) Chen, C.; Dagnino, R.; Huang, C. Q.; McCarthy, J. R.; Grigoriadis, D.; E. 1-Alkyl-3-amino-5-aryl-1H-[1,2,4]triazoles: novel synthesis via cyclization of *N*-acyl-*S*-methylisothioureas with alkylhydrazines and their potent corticotropin-releasing factor-1 (CRF₁) receptor antagonist activities. *Bioorg. Med. Chem. Lett.* **2001**, *11*, 3165–3168.
- (20) Wadsworth, H. J.; Jenkins, S. M.; Orlek, B. S.; Cassidy, F.; Clark, M. S. G.; Brown, F.; Riley, G. J.; Graves, D.; Hawlins, J.; Naylor, C. B. Synthesis and muscarinic activities of quinuclidin-3-yltriazole and -tetrazole derivatives. *J. Med. Chem.* **1992**, *35*, 1280–1290.
- (21) Jenkins, S. M.; Wadsworth, H. J.; Bromidge, S.; Orlek, B. S.; Wyman, P. A.; Riley, G. J.; Hawkins, J. Substituent variation in azabicyclic triazole- and tetrazole-based muscarinic receptor ligands. *J. Med. Chem.* **1992**, *35*, 2392–2406.
- (22) Burrell, G.; Evans, J. M.; Hadley, M. S.; Hicks, F.; Stemp, G. Benzopyran potassium channel activators related to cromakalim—heterocyclic amide replacements at position 4. *Bioorg. Med. Chem. Lett.* **1994**, *4*, 1285–1290.
- (23) Tully, W. R.; Gardner, C. R.; Gillespie, R. J.; Westwood, R. 2-(Oxadiazolyl)- and 2-(thiazolyl)imidazo[1,2-a]pyrimidines as agonists and inverse agonists at benzodiazepine receptors. *J. Med. Chem.* **1991**, *34*, 2060–2067.
- (24) Thompson, S. K.; Eppley, A. M.; Frazee, J. S.; Darcy, M. G.; Lum, R. T.; Tomaszek, T. A.; Ivanoff, L. A.; Morris, J. F.; Sternberg, E. J.; Lambert, D. M.; Fernandez, A. V.; Petteway, S. R.; Meek, T. D.; Metclaff, B. W.; Gleason, J. G. Synthesis and antiviral activity of a novel class of HIV-1 protease inhibitors containing a heterocyclic P₁–P₂ amide bond isostere. *Bioorg. Med. Chem. Lett.* **1994**, *4*, 2441–2446.
- (25) Boyd, S. A.; Fung, A. K. L.; Baker, W. R.; Mantei, R. A.; Stein, H. H.; Cohen, J.; Barlow, J. L.; Klinghofer, V.; Wessale, J. L.; Verburg, K. M.; Polakowski, J. S.; Adler, A. L.; Calzadilla, S. V.; Kovar, P.; Yao, Z.; Hutchins, C. W.; Denissen, J. F.; Grabowski, B. A.; Cepa, S.; Hoffman, D. J.; Garren, K. W.; Kleinert, H. D. Nonpeptide renin inhibitors with good intraduodenal bioavailability and efficacy in dog. *J. Med. Chem.* **1994**, *37*, 2991–3007.
- (26) Duncia, J. V.; Santella, J. B., III; Higley, A.; VanAtten, M. K.; Weber, P. C.; Alexander, R. S.; Kettner, C. A.; Pruitt, J. R.; Liauw, A. Y.; Quan, M. L.; Knabb, R. M.; Wexler, R. R. Pyrazoles, 1,2,4-triazoles, and tetrazoles as surrogates for *cis*-amide bonds in boronate ester thrombin inhibitors. *Bioorg. Med. Chem. Lett.* **1998**, *8*, 775–780.
- (27) Hitotsuyanagi, Y.; Motegi, S.; Fukaya, H.; Takeya, K. A *cis* amide bond surrogate incorporating 1,2,4-triazole. *J. Org. Chem.* **2002**, *67*, 3266–3271.
- (28) Boeglin, D.; Cantel, S.; Heitz, A.; Martinez, J.; Fehrentz, J.-A. Solution and solid-supported synthesis of 3,4,5-trisubstituted 1,2,4-triazole-based peptidomimetics. *Org. Lett.* **2003**, *5*, 4465–4468.
- (29) Castro, B.; Dormoy, J. R.; Evin, G.; Selve, C. Reactifs de couplage peptidique I l'hexafluorophosphate de benzotriazolyl *N*-oxytrisdimethylamino phosphonium (B.O.P.). *Tetrahedron Lett.* **1975**, *16*, 1219–1222.
- (30) Avalos, M.; Babiano, R.; Cintas, P.; Duran, C. J.; Higes, F. J.; Jiménez, J. L.; Lopez, I.; Palacios, J. C. Reactions of thioamides with metal carboxylates in organic media. *Tetrahedron* **1997**, *53*, 14463–14480.
- (31) Mousseaux, D.; Le Gallic, L.; Ryan, J.; Oiry, C.; Gagne, D.; Fehrentz, J.-A.; Galleyrand, J.-C.; Martinez, J. Regulation of ERK1/2 activity by ghrelin-activated growth hormone secretagogue receptor 1A involves a PLC/PKC pathway. *Br. J. Pharmacol.* **2006**, *148*, 350–365.
- (32) Cheng, Y.-C.; Prusoff, W. H. Relationship between the inhibition constant (K_i) and the concentration of inhibitor which causes 50 percent inhibition (IC₅₀) of an enzymatic reaction. *Biochem. Pharmacol.* **1973**, *22*, 3099–3108.
- (33) Schild, H. O. pA_x and competitive drug antagonism. *Br. J. Pharmacol.* **1949**, *4*, 277–280.

Transannular rearrangement of activated 2,5-diketopiperazines: a key route to original scaffolds†

Daniel Farran,^a Isabelle Parrot,^a Loïc Toupet,^b Jean Martinez^a and Georges Dewynter^{*a}

Received 18th June 2008, Accepted 24th July 2008

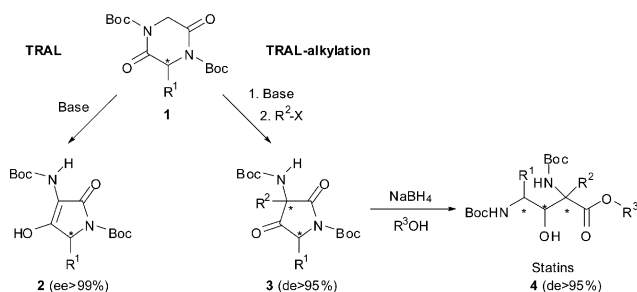
First published as an Advance Article on the web 3rd September 2008

DOI: 10.1039/b810352f

An efficient and original stereocontrolled transannular rearrangement starting from activated 2,5-diketopiperazines has been developed, an opportunity for the medicinal chemistry field, which requests access to novel biological scaffolds. This powerful ring contraction, which can be related to a stereoselective aza-version of the Chan rearrangement, allows for example the one-step synthesis of various tetramic acids, access to 2-disubstituted statins, or the synthesis of relevant lactam-constrained dipeptide mimetics using a TRAL–RCM sequence.

Introduction

Access to new therapeutic entities depends greatly on the discovery of original and pertinent scaffolds, connected with the development of innovative synthetic reactions. In the perpetual quest for pioneering compounds, we recently described an unprecedented ring contraction reaction. The transannular rearrangement of activated lactams (TRAL) leads to 4-hydroxy-3-pyrrolin-2-ones **2** starting from suitable Boc-activated 2,5-diketopiperazines **1** (Scheme 1).¹ This powerful rearrangement could be seen as a new intramolecular N→C acyl migration reaction of cyclic imides. It can be related to a highly stereocontrolled aza-version of the Chan rearrangement,² or to the interesting reaction of acyclic imides described by Hamada *et al.*³



Scheme 1 TRAL and TRAL-alkylation. Access to statins.

By adding an alkylating agent during the course of the TRAL, bis-Boc *cyclo*-[Gly-X] **1** can be easily converted into its dialkylated pyrrolidine-2,4-dione **3** in an exceptionally diastereoselective manner (TRAL-alkylation, Scheme 1). This regioselective ring contraction allows then the one-step synthesis of various

substituted pyrrolidine-2,4-diones or tetramic acids, key patterns founded in several biological compounds.⁴ Moreover, the first successful application of the TRAL leads to a highly selective synthesis of various novel 2-disubstituted statins **4**.^{5,6}

After a full account of our results on the TRAL/TRAL-alkylation, including a debate on various activating groups of the 2,5-diketopiperazines (DKPs), we will extend the discussion to the postulated mechanism and then report on original applications of TRAL, such as the asymmetric synthesis of original lactam-constrained dipeptide mimetics as a key route to promising heterocyclic scaffolds.

Results and discussion

The transannular rearrangement of activated lactams (TRAL): a serendipitous finding

Stereoselective ring contraction of DKPs into 3-aminotetramates

While our efforts were initially devoted to the stereoselective 3- or 6-alkylation of bis-(*N*-*tert*-butoxycarbonyl)-DKPs (bis-Boc-DKPs), by taking advantage of the electrophilicity of such substituted lactams, we made an unexpected observation. Instead of displaying a predictable protecting group character, under certain basic conditions, the two Boc moieties acted as electron withdrawing activators, allowing the unusual transformation of symmetrical and unsymmetrical bis-Boc-DKPs **1** into the corresponding 3-aminopyrrolidine-2,4-diones **2** (Scheme 1).

A preliminary study has concentrated on the reaction with diprotected bis-Boc-DKPs **5a–f**, in the presence of *t*-BuOK (Table 1).

Contradictorily to the few examples described in the literature concerning the reactions on Boc-protected DKPs under basic conditions,^{7,8} we highlighted a new kind of reactivity. According to chiral HPLC analyses, ¹H NMR and ¹³C NMR studies, we observed that the keto–enolic equilibrium of pyrrolidine-2,4-diones was always shifted towards the enol formation. We noticed a totally regioselective ring contraction which allows the exclusion from the ring system of the Boc-*N*1 of the DKPs, leading to the formation of the corresponding aminotetramates **6a–f** in good yields with

^aInstitut des Biomolécules Max Mousseron, UMR CNRS 5247, Université Montpellier 1, Université Montpellier 2, Place Eugène Bataillon, 34095 Montpellier Cedex 5, France. E-mail: dewynter@univ-montp2.fr

^bGroupe Matière Condensée et Matériaux, UMR 6626, Université de Rennes 1, Campus de Beaulieu, 35042 Rennes Cedex, France

† CCDC reference number 643845. For crystallographic data in CIF or other electronic format see DOI: 10.1039/b810352f

Table 1 Stereocontrolled ring contraction of activated DKPs

Entry	5	R ¹	R ²	6/7	Yield ^a (%)	ee ^b (%)
1	5a	H	Boc	6a	72	—
2	5b	Me (<i>S</i>)	Boc	6b	60	>99
3	5c	Me (<i>R</i>)	Boc	6c	64	>99
4	5d	<i>i</i> Pr (<i>S</i>)	Boc	6d	82	>99
5	5e	<i>i</i> Pr (<i>R</i>)	Boc	6e	84	>99
6	5f	<i>s</i> Bu (<i>S</i>)	Boc	6f	71	>95
7	5g	<i>i</i> Pr (<i>S</i>)	Z	6g	0	—
8	5h	H	Bz	6h	69	—
9	5i	<i>i</i> Pr (<i>S</i>)	Bz	6i	98	87
10	5j	<i>i</i> Pr (<i>R</i>)	Bz	6j	98	87
11	5k	H	Ac	7	37	—

^a Yield of product isolated by flash chromatography. ^b The ee values were determined by HPLC on a chiral phase.

excellent enantioselectivities and with absolute retention of the initial configuration.

The examination of the feasibility of this serendipitous rearrangement was then extended to other conventional N-protecting groups that could be perceived as lactamic activators of the TRAL. While no reaction was detected with a bis-Z-DKP (entry 7, Table 1), the reaction of bis-Bz-DKPs occurred with higher yields but lower stereoselectivity, contrasting with the exceptional enantioselectivity described for the bis-Boc-DKPs (entries 8–10, Table 1). This tiny fall in stereoselectivity could be explained by the increased facility of racemisation of the bis-Bz-DKPs in alkaline media.

Interestingly, when we investigated the switch to bis-Ac-DKP **5k**, the tris-acetylated DKP **7** was produced in moderate yield with no trace of the corresponding tetramate (entry 11, Table 1). Ascribing this to an intermolecular acetyl migration, since unprotected DKP was simultaneously generated, we then exploited this peculiarity for the synthesis of an interesting scaffold. The reduction of the DKP **7** using LiAlH(O*t*Bu)₃ allowed us access to the dehydro product **8**, in good yield, in a Perkin-like elimination with concomitant cleavage of the neighboring acetyl group. The *Z*-stereochemistry of this compound was established using ¹H NMR spectra by comparison with previously described analyses.⁹

Further applications of the TRAL to other symmetrical DKPs, such as di-protected *cyclo*-[X-X] (X = Ala, Val, Glu(OMe)), provide original substituted pyrrolidine-2,4-diones, in which the two alkyl chains belong to the same half-space of the heterocyclic moiety (Table 2).

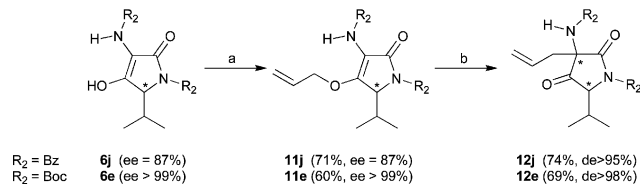
Table 2 TRAL on symmetrical DKPs

Entry	9	R	10	Yield ^a (%)	de ^b (%)
1	9a	Me (<i>S</i>)	10a	66	67
2	9b	<i>i</i> Pr (<i>S</i>)	10b	68	>95
3	9c	MeO ₂ C(CH ₂) (<i>S</i>)	10c	29	>95

^a Yield of product isolated by flash chromatography. ^b The de values were determined by HPLC of the crude product.

Claisen-like rearrangement applied to the TRAL products (obtained from unsymmetrical DKPs)

With the scope of the TRAL on unsymmetrical DKPs established, the synthetic value of the tetramate adducts was then investigated. The asymmetric Claisen-like rearrangement described for 3-*O*-allyl(*isopropylidene*)ascorbate¹⁰ was successfully transposed to the bis-Bz-pyrrolidine-2,4-dione **6j** and to the bis-Boc-pyrrolidine-2,4-dione **6e**. After an appropriate *O*-allylation, derivatives **11j** and **11e** followed a sigmatropic rearrangement to yield **12j** and **12e** in a stereocontrolled manner (Scheme 2).



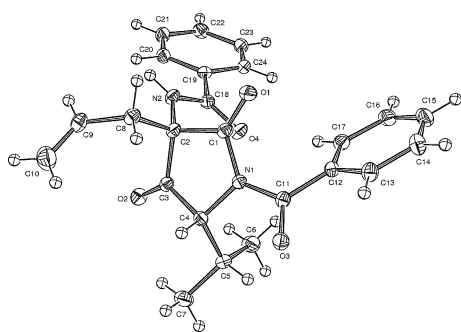
Scheme 2 Claisen-like rearrangement. *Reagents and conditions:* (a) KOH, DMSO, CH₂=CHCH₂Br; (b) microwave irradiation, toluene–DMSO, 170 °C, 30 min.

The stereochemistry of this Claisen-like rearrangement was unambiguously determined by X-ray diffraction crystal analysis of the major compound **12j** enantioenriched by recrystallization (Scheme 3).[‡]

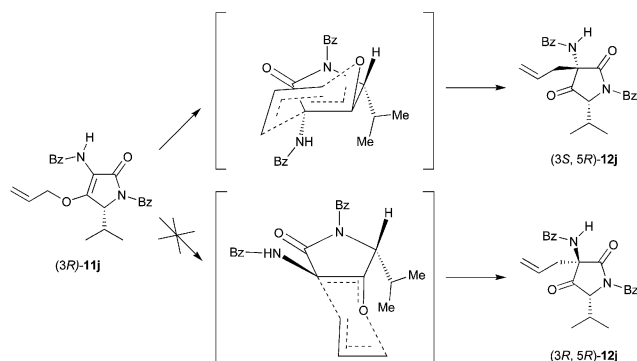
The high diastereoselectivity of this sigmatropic rearrangement could be easily explained by the structural parameters of the Zimmermann–Traxler chair transition state, as illustrated by Scheme 4.

In agreement with our preliminary studies on TRAL, benzoyl groups also appear to be a suitable alternative to Boc activating groups here.

[‡] C₂₄H₂₄O₄N₂, Mr = 404.45, orthorhombic, P2₁2₁2₁, a = 10.4911(5), b = 12.2289(6), c = 16.1319(7) Å, V = 2069.6(2) Å³, Z = 4, D_x = 1.298 Mg·m⁻³, λ(Mo Kα) = 0.71073 Å, μ = 0.89 cm⁻¹, F(000) = 856, T = 110(1) K. CCDC 643845. These data can also be obtained free of charge from The Cambridge Crystallographic Data Centre via www.ccdc.cam.uk/data_request/cif.



Scheme 3 X-Ray analysis of (3*S*,5*R*)-12*j*.



Scheme 4 Zimmermann–Traxler chair transition state.

Stereoselective ring contraction of DKPs in the presence of an alkylating agent: the TRAL-alkylation

To improve the access to more functionalized tetramates, we have already described a viable route for the relevant regioselective and stereoselective ring contraction of DKPs into pyrrolidine-2,4-diones in the presence of an alkylating agent. By using symmetrical or unsymmetrical DKPs, we could obtain a range of derivatives bearing the two side chains R_1 and R_2 on the same face of the heterocyclic ring (Table 3).

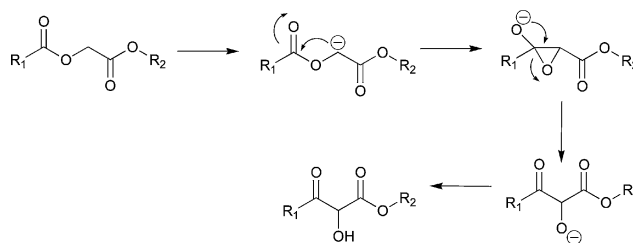
Table 3 TRAL-alkylation of unsymmetrical and symmetrical DKPs

Entry	5	R^1	R^2X	R	13	Yield ^a (%)	de ^b (%)
1	5a	H	$CH_2=CHCH_2Br$	$= R^2$	13a	62	>95
2	5a	H	BnBr	$= R^2$	13b	57	>95
3	5e	<i>i</i> Pr (<i>R</i>)	CH_3I	$= R^1$	13c	60	>95
4	5e	<i>i</i> Pr (<i>R</i>)	BnBr	$= R^1$	13d	72	>95
5	5e	<i>i</i> Pr (<i>R</i>)	EtO_2CCH_2I	$= R^1$	13e	69	>95
6	5e	<i>i</i> Pr (<i>R</i>)	$CH_2=CHCH_2Br$	$= R^1$	13f	76	>99
7	5e	<i>i</i> Pr (<i>R</i>)	$(CH_3)_2C=CHCH_2Br$	$= R^1$	13g	84	>95
8	5f	<i>i</i> Bu (<i>S</i>)	$CH_2=CHCH_2Br$	$= R^1$	13h	68	>95

^a Yield of product isolated by flash chromatography. ^b The ^{13}C NMR spectra gave only one set of peaks.

Towards a plausible mechanism to explain the stereoselectivity of the TRAL

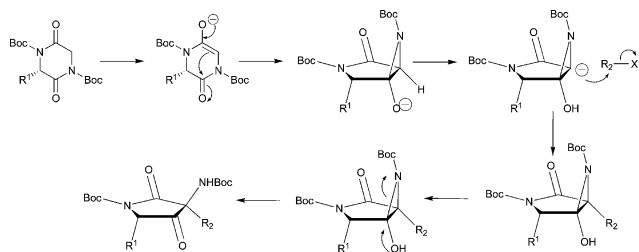
The transannular rearrangement of activated lactams (TRAL), an intramolecular acylation of an imide enolate, could be related to the Dieckmann and Gabriel–Colman reactions or to the early step of the Dakin–West reaction. However, a better match could be made with the Chan reaction,² a rearrangement of an acyloxyacetate to a 2-hydroxy-3-keto-ester in the presence of a strong base (Scheme 5). Its aza-version has been developed on acyclic imides by Hamada *et al.*³ and extended to biological hits by Wipf and Methot,¹¹ and White *et al.*,^{12,13} as illustrated by the Holton Taxol total synthesis.¹⁴



Scheme 5 The Chan rearrangement.

As suggested by Wipf and co-workers, only the *s*-cis conformation of the ester and the tertiary amide of the incriminated imide moiety is able to undergo the Chan rearrangement. A transposition of this interpretation could allow us to connect the success of the TRAL to the unique presence of the *s*-cis conformation, since bis-Boc-DKPs could be likened to constrained cyclic systems of two imides.

Concerning the mechanism of the TRAL, we anticipated that the TRAL of activated DKPs could sensibly follow the Chan–Hamada reaction (Scheme 6). We proposed that after a suitable deprotonation of the activated DKP under basic conditions, the kinetic enolate would be formed. The transannular attack of the enolate, and nucleophilic acyl substitution with the adjacent carbonyl of the imide group could afford an aziridine intermediate,



Scheme 6 Postulated mechanism for the TRAL, by analogy with the Chan reaction.

in accordance with the oxirane formation described for the Chan reaction.

To explain the exceptional stereoselectivity of the TRAL, we could postulate that the aziridine ring would be positioned on the less bulky half-space rather than on the face containing the side chain R^1 . Prototropy on the oxanion could lead to the anionic intermediate shown. In the presence of an alkylating reagent such as R^2-X , we have anticipated that the constrained ring system could hinder the attack of the sp^3 carbanion on the face where the Boc-aziridine moiety is located. The electrophile could then only add to the open half-space of the heterocycle, where the R^1 group is pointed away from the Boc-aziridine moiety. In the last step, the opening of the aziridine affords the resulting bis-Boc 3-aminopyrrolidine-2,4-dione or its enolic form. The possibility of immediate ring opening of the *in situ* formed aziridine intermediate could be also considered. This opening could be induced by the alkoxide anion, followed by prototropy to the nitrogen anion, affording an anionic intermediate which could attack the electrophile R^2-X . Taking into account the high reactivity of 2-oxyaziridines, the ring opening of the proposed 2-hydroxyaziridine intermediate in a final stage of the process is less likely.¹⁵

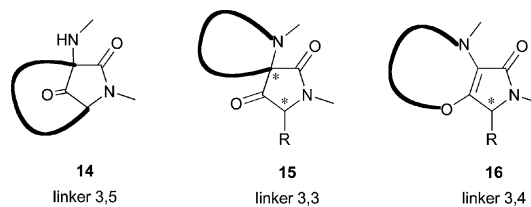
TRAL: a key route to promising scaffolds

Besides the first described application of the TRAL leading to the synthesis of statin analogues, we describe here an original access to promising heterocyclic scaffolds, using a tandem TRAL–metathesis approach.

Asymmetric synthesis of original lactam-constrained dipeptide mimetics

The concept of conformational constraint has emerged as the favourite method in medicinal chemistry of “freezing” the bioactive conformation of the initial peptide in order to optimize its activity, its receptor selectivity or the duration of its action.^{16–26} Since the lactam-bridged dipeptides described by Freidinger *et al.* have been well recognized to be a significant type of conformational constraint in peptides^{27,28} and since the ring-closing metathesis reaction has been shown to be a powerful method of accessing rigidified dipeptides of biological interest,^{29–32} we chose to design a new and efficient method leading to original lactam-constrained dipeptide mimetics.

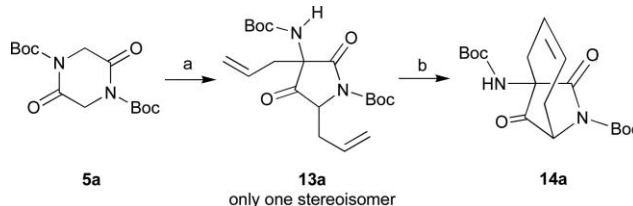
Using a highly stereoselective chemical sequence, TRAL followed by a ring-closing metathesis reaction (RCM), we have been able to access unprecedented heterocyclic scaffolds **14–16** (Scheme 7), that could be received as dipeptide mimetics.



Scheme 7 Lactam-constrained dipeptide mimetics.

Furthermore, the presence of a quaternary stereogenic carbon center enhances the significance of these bicyclic derivatives, regarding the fact that aza-cyclic α -aminoacids with quaternary stereocenters are part of biologically active natural products with therapeutic potential,^{33–35} and are useful building blocks for natural product synthesis and enantioselective syntheses.^{36–40}

In order to add more constraints on the pyrrolidine-2,4-dione moieties, we first imagined linking the side chains of the dipeptide mimetic, taking the opportunity given by the TRAL to choose their spatial arrangement. First of all, as we already demonstrated, the bis-Boc *cyclo*-[Gly-Gly] **5a** can be easily converted into its dialkylated pyrrolidine-2,4-dione **13a** in a diastereoselective manner (Scheme 8). With both allyl chains being in the same half-space and properly positioned for cyclization, the use of a Grubbs' catalyst **II** in the second step leads to the over-constrained derivative **14a** in good yield.



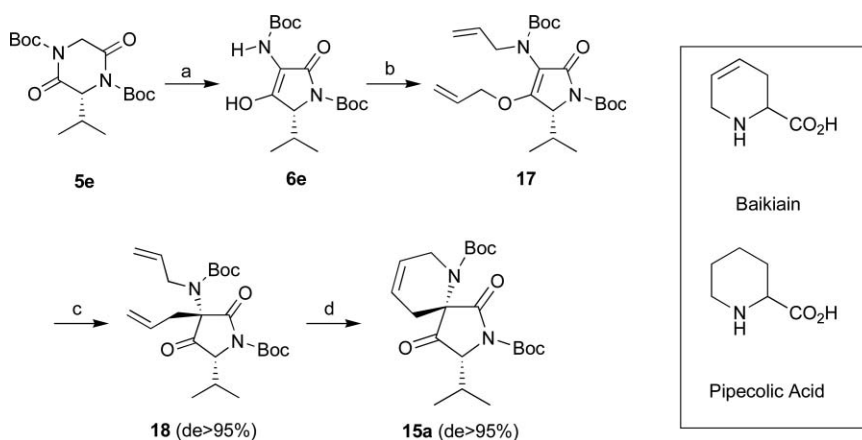
Scheme 8 Synthesis of bicyclo-compound **14a** starting from bis-Boc *cyclo*-[Gly-Gly]. *Reagents and conditions:* (a) (i) LiHMDS, -78°C , THF (ii) $\text{CH}_2=\text{CHCH}_2\text{Br}$, 62%; (b) 2% mol Grubbs' catalyst II, CH_2Cl_2 , r.t., 84%. About **14a**: the ^{13}C NMR spectrum of the crude material gave only one set of peaks.

In the quest for novel heterocyclic scaffolds and encouraged by the efficiency of this pioneering ring-closing metathesis on pyrrolidine-2,4-dione derivatives, we decided to expand our strategy to the synthesis of *spiro*-derivatives.

By taking advantage of the potential for high stereoselectivity of one of our previously reported synthetic sequences, the TRAL and *O*-allylation followed by a Claisen-like rearrangement, we already knew how to access 3-allyl-3-aminopyrrolidine-2,4-dione **12e** from bis-Boc *cyclo*-[Gly-*D*-Val] **5e** (Scheme 2).

Taking a bet on this totally diastereoselective sequence, we were then able to transpose it to the *O,N*-diallyl derivative **17**, which could be accessed from the same aminotetramate intermediate **6e** by using two equivalents of base and allyl bromide. The sigmatropic rearrangement provided the new *C,N*-diallyl **18** in good yield in a stereocontrolled manner. This reaction was carried out under microwave conditions, which appeared to be more efficient than thermal conditions.

A suitable intramolecular cyclization by ring-closing metathesis of the pyrrolidine-2,4-dione **18**, allowed the new stereoselective

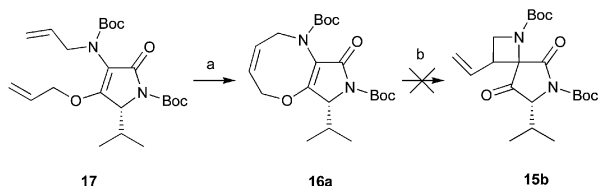


Scheme 9 TRAL and *O*-allylation followed by a Claisen-like rearrangement. *Reagents and conditions:* (a) *t*BuOK, THF, r.t., 84%; (b) KOH (2.0 equiv.), DMSO, CH₂=CHCH₂Br (2.0 equiv.), 76%; (c) microwave irradiation, toluene–DMSO, 170 °C, 30 min, 73%; (d) 2% mol Grubbs' catalyst II, DCM, r.t., 88%. About **15a**: the ¹³C NMR spectrum of the crude material gave only one set of peaks.

construction of the innovative [5 + 6] *spiro*-derivative **15a** in excellent yield (Scheme 9).

This unprecedented *spiro*-scaffold could be classified as a significant lactam-constrained dipeptide mimetic. In addition it could be also considered a more complex derivative of Baikiain, a cyclic α -amino acid isolated from the heartwood of Rhodesian teak (*Baikiaea plurijuga*).⁴¹ This interesting natural compound is an unsaturated derivative of pipecolic acid, which is a non-proteinogenic amino acid present in pharmacologically active molecules such as immunosuppressors or antitumor antibiotics.⁴²

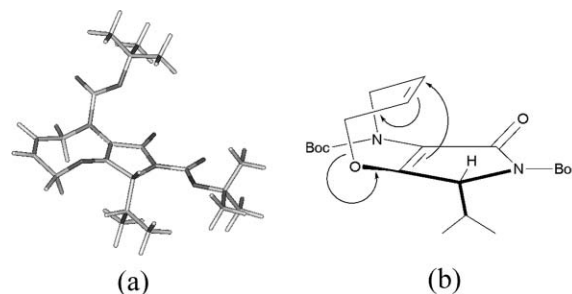
Finally, regarding the fact that using RCM to synthesize an eight-membered cycle is still challenging,^{43,44} we performed the cyclization starting from the intermediate compound **16a**, to build the [5 + 4] *spiro*-derivative **15b**, another lactam-constrained dipeptide mimetic (Scheme 10). We were delighted to observe that the aminotetramate **17** was easily converted into the novel *bicyclo*-derivative **16a**, in good yield, probably helped by the steric constraints induced by the *N*-Boc group. This optically active compound **16a** can be considered as an interesting *bicyclo*- and dehydro- quaternary dipeptide mimetic.



Scheme 10 Synthesis of a [5 + 4] *spiro*-derivative. *Reagents and conditions:* (a) 2% mol Grubbs' catalyst II, CH₂Cl₂, r.t., 78%; (b) microwave irradiation, toluene–DMSO, 170 °C, 30 min.

Interestingly, under microwaves or thermal conditions, the sigmatropic rearrangement of **16a** was unsuccessful, leading to a partial cleavage of the Boc protecting group. In order to give an explanation, we first postulated two ring-conformations for **16a**, the chair-like and boat-like conformations. A careful examination of the ¹H NMR spectrum of the eight-membered ring part of the cyclic system, showed unambiguously that the

allylic methylene protons on the nitrogen side possess anisochrony, exhibited as a significant splitting of signals ($\Delta\delta = 1.42$ ppm). This allowed us to conclude on a chair-like favorite conformation. This observation was also confirmed by molecular modelling studies on **16a** (Scheme 11a).⁴⁵ We then had to admit that the boat-like conformer was critical for the transannular reaction (Scheme 11b).



Scheme 11 (a) The predicted lower energy conformation of **16a**: the chair-like favorite conformation observed by molecular modelling studies and ¹H NMR; (b) the boat-like conformer probably crucial for the transannular Claisen rearrangement reaction.

Conclusions

In conclusion, we have devised a powerful method for accessing new lactam-constrained dipeptide mimetics, new chemical entities that could be of broad interest in the quest for original scaffolds for drug discovery. The success of this strategy is closely linked to the access to suitable building blocks for the ring-closing metathesis, which can only be obtained by the highly stereocontrolled TRAL. The association of the TRAL and an unprecedented ring-closing metathesis on pyrrolidine-2,4-dione derivatives provided lactam-constrained dipeptide mimetics in good yields with remarkable stereoselectivity. We believe that this study will offer a strong incentive for the construction of larger or structurally modified dipeptide mimetics and potentially novel biological hits.

Experimental

General procedures

All solvents were dried and freshly distilled prior to use. TLC was performed with Merck-Kieselgel 60 F₂₅₄ plates, and spots were visualized with UV light and/or by staining with ninhydrin solution followed by heating. Flash chromatography was performed on Merck-Kieselgel 60 (230–400 mesh). Melting points were recorded on Buchi 510 melting apparatus. Optical rotations were measured with a 1 cm cell (concentration *c* given in g 100mL⁻¹ solvent) on a Perkin Elmer Polarimeter at 20 °C with a sodium lamp (589 nm). HPLC analyses were performed on a Waters-Millennium (column 250 × 4.6 mm Nucleosil C18 5 μ, detection UV). High resolution mass spectra (HRMS) were obtained on a JEOL JMS-SX-102 high resolution magnetic sector mass spectrometer. ¹H NMR and ¹³C NMR spectra were recorded with Bruker 200 MHz, Bruker AC250 MHz, Bruker Advance 300 MHz or Bruker A DRX 400 MHz spectrometers. Chemical shifts are reported in δ relative to an internal standard of residual chloroform (δ = 7.26 for ¹H NMR and 77.16 for ¹³C NMR) or DMSO-*d*₆ (δ = 2.50 for ¹H NMR and 39.52 for ¹³C NMR). The reported ¹H NMR signals were assigned using standard 2D NMR techniques or by direct comparison to the ¹H NMR spectra of the corresponding starting materials. The reported ¹³C NMR signals were assigned using DEPT-135 and HMQC techniques or by direct comparison of the ¹³C NMR spectra of the corresponding starting materials.

1,4-Di(benzoyl)-piperazine-2,5-dione 5h

Typical procedure for the benzoylation of DKP. A solution of piperazine-2,5-dione (0.198 g, 1.74 mmol) and benzoic anhydride (1.572 g, 6.95 mmol) in toluene (2 mL) was irradiated for 20 min at 180 °C (Biotage Initiator apparatus). The medium was then concentrated *in vacuo* and 10 mL of CH₂Cl₂ were added. The organic layer was washed with a saturated solution of NaHCO₃, dried over MgSO₄ and concentrated *in vacuo*. The crude residue was purified by column chromatography (CH₂Cl₂–AcOEt (100 : 0 → 90 : 10)), providing 1,4-di(benzoyl)-piperazine-2,5-dione **5h** in 56% yield (0.318 g) as a white powder. Mp (decomposed) = 207 °C; ¹H NMR (CDCl₃, 400 MHz): δ 4.54 (s, 4H), 7.39–7.65 (m, 10H); ¹³C NMR (CDCl₃, 100 MHz): δ 48.8, 128.5, 128.9, 133.1, 133.8, 166.6, 170.9; HRMS (FAB+) *m/z* calcd for C₁₈H₁₄N₂O₄ [M + H⁺] 323.1032, found 323.1042.

(3R)-1,4-Di(benzoyl)-3-isopropylpiperazine-2,5-dione 5j

Mp = 77 °C; [α]_D²⁰ = –17.6 (*c* = 1.08, CH₂Cl₂); ¹H NMR (CDCl₃, 300 MHz): δ 1.18 (t, 6H), 2.22–2.41 (m, 1H), 4.48 (d, 1H, *J*_{AB} = 18.8 Hz), 4.88 (d, 1H, *J*_{AB} = 18.8 Hz), 4.94 (d, 1H, *J* = 8.4 Hz), 7.40–7.71 (m, 10H); ¹³C NMR (CDCl₃, 75 MHz): δ 19.5, 19.7, 32.6, 48.5, 64.2, 128.3 to 132.9, 134.1, 134.3, 167.0, 167.9, 171.1, 171.6; HRMS (FAB+) *m/z* calcd for C₂₁H₂₀N₂O₄ [M + H⁺] 365.1501, found 365.1514.

1-(Benzoyl)-3-[(benzoyl)amino]-4-hydroxy-3-pyrrolin-2-one 6h

Typical procedure for the rearrangement. To a solution of 1,4-di(benzoyl)-piperazine-2,5-dione **5h** (0.077 g, 0.24 mmol) in dry THF (5 mL) was added *t*BuOK (0.030 g, 0.26 mmol) at r.t. The

solution was stirred for 12 hours under an argon atmosphere. The medium was then diluted with AcOEt (10 mL), washed with a solution of 0.1 N HCl (20 mL), and dried over anhydrous MgSO₄. The solvent was removed *in vacuo* and the desired compound was obtained (0.054 g, 69% yield) as a yellow oil. ¹H NMR (CDCl₃, 300 MHz): δ 4.44 (s, 2H), 7.21–8.05 (m, 11H), 12.50 (m, 1H); ¹³C NMR (CDCl₃, 75 MHz): δ 46.8, 104.2, 127.4 to 133.4, 131.0, 134.3, 156.5, 165.3, 167.2, 168.3; HRMS (FAB+) *m/z* calcd for C₁₈H₁₄N₂O₄ [M + H⁺] 323.1032, found 323.1026.

(5R)-1-(Benzoyl)-3-[(benzoyl)amino]-4-hydroxy-5-isopropyl-3-pyrrolin-2-one 6j

Mp = 94 °C; [α]_D²⁰ = –137.3 (*c* = 1.02, CH₂Cl₂); ¹H NMR (CDCl₃, 300 MHz): δ 0.96 (d, 3H, *J* = 7.0 Hz), 1.16 (d, 3H, *J* = 7.1 Hz), 2.39–2.55 (m, 1H), 4.89 (d, 1H, *J* = 2.8 Hz), 7.29–8.02 (m, 11H), 12.57 (m, 1H); ¹³C NMR (CDCl₃, 75 MHz): δ 16.6, 18.0, 29.3, 61.4, 103.9, 127.4 to 133.2, 131.0, 134.9, 160.1, 165.8, 167.2, 168.7; HRMS (FAB+) *m/z* calcd for C₂₁H₂₀N₂O₄ [M + H⁺] 365.1501, found 365.1495.

1,4-Di(acetyl)-piperazine-2,5-dione 5k

A solution of piperazine-2,5-dione (0.424 g, 3.72 mmol) in acetic anhydride (2 mL) was irradiated for 26 min at 180 °C (Biotage Initiator apparatus). The medium was then concentrated *in vacuo* and purified by column chromatography (CH₂Cl₂–AcOEt (100 : 0 → 90 : 10)), providing 1,4-diacetyl-piperazine-2,5-dione in 76% yield (0.560 g) as white crystals. Mp = 97 °C; ¹H NMR (CDCl₃, 400 MHz): δ 2.52 (s, 6H), 4.55 (s, 4H); ¹³C NMR (CDCl₃, 100 MHz): δ 26.7, 47.1, 166.0, 170.8; HRMS (FAB+) *m/z* calcd for C₈H₁₀N₂O₄ [M + H⁺] 199.0719, found 199.0730.

1,2,4-Tri(acetyl)-piperazine-2,5-dione 7

To a solution of 1,4-di(acetyl)-piperazine-2,5-dione **5k** (0.070 g, 0.35 mmol) in dry THF (5 mL) was added *t*BuOK (0.044 g, 0.39 mmol) at r.t. The solution was stirred for 12 hours under an argon atmosphere. The medium was then diluted with AcOEt (10 mL), washed with a solution of 0.1 N HCl (20 mL), dried over anhydrous MgSO₄ and concentrated *in vacuo*. The crude residue was purified by column chromatography (CH₂Cl₂–AcOEt, 100 : 0 → 96 : 4). The desired compound was obtained (0.031 g, 37% yield) as a colorless oil. ¹H NMR (CDCl₃, 400 MHz): δ 2.41 (s, 3H), 2.52 (s, 3H), 2.55 (s, 3H), 3.82 (d, 1H, *J*_{AB} = 18.1 Hz), 4.95 (d, 1H, *J*_{AB} = 18.1 Hz), 6.08 (s, 1H); ¹³C NMR (CDCl₃, 100 MHz): δ 26.6, 26.9, 27.4, 46.5, 68.5, 162.3, 165.0, 170.6, 171.2, 197.5; HRMS (FAB+) *m/z* calcd for C₁₀H₁₂N₂O₅ [M + H⁺] 241.0824, found 241.0825.

(Z)-1-Acetyl-3-ethylene-piperazine-2,5-dione 8

To a solution of 1,2,4-tri(acetyl)-piperazine-2,5-dione **7** (0.162 g, 0.68 mmol) in 10 mL of dry THF was added LiAlH(O*t*Bu)₃ (1.01 mmol) at r.t. under stirring and an argon atmosphere. After 2 hours, AcOEt (30 mL) was added. The organic layer was washed with 0.1 N HCl, dried over MgSO₄ and concentrated *in vacuo*. The crude residue was then purified by silica gel column chromatography (CH₂Cl₂–MeOH (100 : 0 → 96 : 4)). The desired compound was obtained (0.103 g, 83% yield) as a white powder.

Mp = 145 °C; ¹H NMR (CDCl₃, 300 MHz): δ 1.80 (d, 3H, *J* = 7.6 Hz), 2.54 (s, 3H), 4.37 (s, 2H), 6.34 (q, *J* = 7.6 Hz), 8.66 (br s, 1H); ¹³C NMR (CDCl₃, 75 MHz): δ 11.7, 27.1, 45.9, 119.4, 127.3, 159.7, 163.9, 172.6; HRMS (FAB+) *m/z* calcd for C₈H₁₀N₂O₃ [M + H⁺] 183.0770, found 183.0775.

(5*R*)-4-Allyloxy-1-benzoyl-3-[(benzoyl)amino]-5-isopropyl-3-pyrrolin-2-one 11j

To a solution of (5*R*)-1-(benzoyl)-3-[(benzoyl)amino]-4-hydroxy-5-isopropyl-3-pyrrolin-2-one **6j** (0.152 g, 0.42 mmol) in dry DMSO (5 mL) was added KOH in powder form (0.021 g, 0.37 mmol) with stirring. Gentle warming was necessary for dissolution. The mixture changed color from pink to deep violet. Allyl bromide (0.03 mL, 0.38 mmol) was then added and the medium was allowed to stir under an argon atmosphere for 6 h. AcOEt (10 mL) was then added. The organic layer was washed with 0.1 N HCl (10 mL), dried over MgSO₄ and concentrated *in vacuo*. The crude residue was purified by column chromatography (CH₂Cl₂-AcOEt, 100 : 0 → 80 : 20), providing the derivative **11j** (0.120 g) as a colorless oil in 71% yield. [α]_D²⁰ = -160.4 (*c* = 1.11, CH₂Cl₂); ¹H NMR (CDCl₃, 300 MHz): δ 1.10 (d, 3H, *J* = 7.0 Hz), 1.23 (d, 3H, *J* = 7.1 Hz), 2.45–2.59 (m, 1H), 4.77–4.92 (m, 2H), 5.00 (d, 1H, *J* = 2.5 Hz), 5.24–5.39 (m, 2H), 5.85–6.02 (m, 1H), 7.33–7.82 (m, 11H); ¹³C NMR (CDCl₃, 75 MHz): δ 17.3, 18.0, 29.7, 61.8, 71.5, 103.1, 119.1, 127.4 to 132.3, 132.7, 134.9, 168.1, 168.2, 168.3, 169.0; HRMS (FAB+) *m/z* calcd for C₂₄H₂₄N₂O₄ [M + H⁺] 405.1814, found 405.1819.

(3*S*,5*R*)-3-Allyl-1-(benzoyl)-3-[(benzoyl)amino]-5-isopropylpyrrolidine-2,4-dione 12j

A solution of (5*R*)-4-allyloxy-1-benzoyl-3-[(benzoyl)amino]-5-isopropyl-3-pyrrolin-2-one **11j** (0.020 g, 0.05 mmol) in toluene (3 mL) with some drops of DMSO was irradiated for 30 min at 170 °C (Biotage Initiator apparatus). The medium was then concentrated *in vacuo* and the crude residue was purified by column chromatography (CH₂Cl₂-AcOEt, 100 : 0 → 95 : 5), providing **12j** in 74% yield (0.015 g) as a colorless oil. ¹H NMR (CDCl₃, 300 MHz): δ 1.17 (d, 3H, *J* = 6.9 Hz), 1.19 (d, 3H, *J* = 6.6 Hz), 2.50–2.62 (m, 3H), 4.73 (d, 1H, *J* = 4.4 Hz), 5.20–5.36 (m, 2H), 5.64–5.81 (m, 1H), 6.51 (br s, 1H), 7.32–7.95 (m, 10H); ¹³C NMR (CDCl₃, 75 MHz): δ 18.9, 19.4, 29.8, 38.2, 62.6, 67.3, 123.0, 127.4 to 133.9, 166.7, 170.2, 171.0, 205.1.

1-*tert*-Butoxycarbonylamino-8,9-dioxo-7-aza-bicyclo[4.2.1]non-3-ene-7-carboxylic acid *tert*-butyl ester 14a

To a stirred solution of 3,5-*trans*-diallyl-1-(*tert*-butoxycarbonyl)-3-[(*tert*-butoxycarbonyl)amino]pyrrolidine-2,4-dione **13a** (0.226 g, 0.57 mmol) in dichloromethane (8 mL) was added Grubbs' catalyst (2% mol of benzylidene-[1,3-bis-(2,4,6-trimethylphenyl)-2-imidazolidinylidene]-dichloro (tricyclohexyl phosphane) ruthenium, 0.010 g in 2 mL of dichloromethane, 0.0115 mmol). The reaction mixture was stirred for 2 h. DMSO (0.04 mL, 0.48 mmol, 50 equiv. related to catalyst) was then added and the solution was stirred for an additional 12 hours. After concentration *in vacuo*, the residue was purified by flash chromatography on silica gel (CH₂Cl₂-AcOEt, 100 : 0 → 85 : 15) to give the compound **14a** (0.176 g, 84% yield) as a solid. Mp = 104 °C; *t*_r = 10.937 min; ¹H

NMR (CDCl₃, 200 MHz): δ 1.35 (s, 9H), 1.54 (s, 9H), 2.22–2.33 (m, 1H), 2.55–2.68 (m, 1H), 2.36–2.48 (m, 1H), 2.80–2.92 (m, 1H), 4.70 (m, 1H), 5.40 (s, 1H), 5.46–5.61 (m, 2H); ¹³C NMR (CDCl₃, 100 MHz): δ 28.0, 28.2, 30.3, 33.7, 62.0, 64.4, 81.6, 84.2, 121.9, 124.5, 148.4, 154.6, 170.3, 204.7. HRMS (FAB+) *m/z* calcd for C₁₈H₂₆N₂O₆ [M + H⁺] 367.4092, found 367.4101.

(5*R*)-4-Allyloxy-3-[allyl-(*tert*-butoxycarbonyl)amino]-1-(*tert*-butoxycarbonyl)-5-isopropyl-3-pyrrolin-2-one 17

To a stirred solution of (5*R*)-1-(*tert*-butoxycarbonyl)-3-[(*tert*-butoxycarbonyl)amino]-4-hydroxy-5-isopropyl-3-pyrrolin-2-one **6e** (0.713 g, 2.00 mmol) in dry DMSO (8 mL) was added KOH powder (0.280 g, 5.01 mmol). Gentle warming was necessary for total dissolution. The mixture turned from pink to deep violet. Allyl bromide (0.44 mL, 5.01 mmol) was then added and the medium was stirred under an argon atmosphere for 12 hours. The reaction mixture was diluted with AcOEt (16 mL) and then washed with 0.1 N HCl (16 mL). The organic layer was dried over anhydrous MgSO₄ and concentrated *in vacuo*. The crude residue was purified by flash chromatography on silica gel (CH₂Cl₂-AcOEt, 100 : 0 → 80 : 20), providing the derivative **17** (0.665 g) as a colorless oil in 76% yield. [α]_D²⁰ = -46.0 (*c* = 2.20, CH₂Cl₂); *t*_r = 14.549 min; ¹H NMR (CDCl₃, 400 MHz): δ 0.79 (d, 3H, *J* = 6.9 Hz), 1.10 (d, 3H, *J* = 7.2 Hz), 1.41 (s, 9H), 1.53 (s, 9H), 2.38–2.50 (m, 1H), 3.79–4.34 (m, 2H), 4.28 (s, 1H), 4.68–4.87 (m, 2H), 5.10–5.40 (m, 4H), 5.81–6.00 (m, 2H); ¹³C NMR (CDCl₃, 100 MHz): δ 16.4, 18.9, 28.2, 28.4, 29.5, 52.1, 62.2, 71.5, 81.1, 82.8, 109.3, 119.0, 131.7, 133.2, 149.3, 154.9, 166.9, 167.9; HRMS (FAB+) *m/z* calcd for C₂₃H₃₆N₂O₆ [M + H⁺] 437.2652, found 437.2627.

(3*S*,5*R*)-3-Allyl-3-[allyl-(*tert*-butoxycarbonyl)amino]-1-(*tert*-butoxycarbonyl)-5-isopropylpyrrolidine-2,4-dione 18

A solution of (5*R*)-4-allyloxy-3-[allyl-(*tert*-butoxycarbonyl)amino]-1-(*tert*-butoxycarbonyl)-5-isopropyl-3-pyrrolin-2-one **17** (0.180 g, 0.45 mmol) in toluene (3 mL) containing some drops of DMSO, was irradiated for 30 min at 170 °C (Biotage Initiator apparatus). The medium was then concentrated *in vacuo* and the crude residue was purified by column chromatography on silica gel (CH₂Cl₂-AcOEt, 100 : 0 → 95 : 5), providing compound **18** as a colorless oil (0.143 g, 73% yield). [α]_D²⁰ = -98.0 (*c* = 1.48, CH₂Cl₂); *t*_r = 15.413 min; ¹H NMR (CDCl₃, 300 MHz): δ 1.06 (d, 3H, *J* = 7.1 Hz), 1.18 (d, 3H, *J* = 6.9 Hz), 1.40 (s, 9H), 1.55 (s, 9H), 2.39–2.52 (m, 1H), 2.39–2.67 (m, 2H), 3.93 (d, 1H, *J* = 5.9 Hz), 4.01 (br s, 2H), 5.10–5.23 (m, 2H), 5.10–5.40 (m, 2H), 5.48–5.62 (m, 1H), 5.81–5.98 (m, 1H); ¹³C NMR (CDCl₃, 75 MHz): δ 18.6, 21.4, 28.0, 28.1, 31.4, 37.4, 46.3, 68.4, 69.4, 81.8, 83.4, 115.8, 122.1, 128.4, 135.6, 150.0, 155.3, 171.8, 206.8; HRMS (FAB+) *m/z* calcd for C₂₃H₃₆N₂O₆ [M + H⁺] 437.2652, found 437.2649.

Baikiaian spiro-derivative 15a

To a stirred solution of (3*S*,5*R*)-3-allyl-3-[allyl-(*tert*-butoxycarbonyl)amino]-1-(*tert*-butoxycarbonyl)-5-isopropylpyrrolidine-2,4-dione **18** (0.105 g, 0.24 mmol) in dichloromethane (5 mL) was added Grubbs' catalyst (2% mol of benzylidene-[1,3-bis-(2,4,6-trimethylphenyl)-2-imidazolidinylidene]-dichloro (tricyclohexyl phosphane) ruthenium, 0.004 g, in 2 mL of dichloromethane, 0.0048 mmol). The reaction mixture was stirred for 2 hours.

DMSO (0.02 mL, 0.24 mmol, 50 equiv. related to catalyst) was then added and the solution was stirred for an additional 12 hours. After concentration *in vacuo*, the residue was purified by flash chromatography on silica gel (CH₂Cl₂-AcOEt, 100 : 0 → 98 : 2) to produce the compound **15a** (0.086 g, 88% yield) as a solid. Mp = 124 °C; *t*_r = 14.275 min; [α]_D²⁰ = -89.0 (*c* = 1.90, CH₂Cl₂); ¹H NMR (CDCl₃, 300 MHz): δ 1.04 (d, 3H, *J* = 7.0 Hz), 1.08 (d, 3H, *J* = 7.2 Hz), 1.35 (s, 9H), 1.50 (s, 9H), 2.24–2.36 (m, 1H), 2.40–2.52 (m, 2H), 3.98–4.02 (m, 2H), 4.23 (d, 1H, *J* = 4.5 Hz), 5.60–5.70 (m, 1H), 5.86–5.94 (m, 1H); ¹³C NMR (CDCl₃, 75 MHz): δ 19.1, 19.2, 28.0, 28.2, 30.6, 30.9, 43.6, 62.8, 67.0, 81.7, 83.8, 118.5, 126.0, 150.0, 155.1, 171.1, 206.2; HRMS (FAB+) *m/z* calcd for C₂₁H₃₂N₂O₆ [M + H⁺] 409.2339, found 409.2347.

(3R)-3-isoPropyl-1-oxo-1,3,5,8-tetrahydro-4-oxa-2,9-diaza-cyclopentacyclooctene-2,9-dicarboxylic acid di-*tert*-butyl ester **16a**

To a stirred solution of (5R)-4-allyloxy-3-[allyl-(*tert*-butoxycarbonyl)amino]-1-(*tert*-butoxycarbonyl)-5-isopropyl-3-pyrrolidin-2-one **17** (0.403 g, 0.92 mmol) in dichloromethane (20 mL) was added Grubbs' catalyst (2% mol of benzylidene-[1,3-bis-(2,4,6-trimethylphenyl)-2-imidazolidinylidene]-dichloro (tricyclohexyl phosphane) ruthenium, 0.016 g, in 2 mL of dichloromethane, 0.0185 mmol). The reaction mixture was stirred for 2 h. DMSO (0.08 mL, 0.92 mmol, 50 equiv. related to catalyst) was then added and the solution was stirred for an additional 12 hours. After concentration *in vacuo*, the residue was purified by flash chromatography on silica gel (CH₂Cl₂-AcOEt, 100 : 0 → 80 : 20) to produce the compound **16a** (0.295 g, 78% yield) as a colorless oil. The ¹H NMR spectrum of compound **16a** gave two sets of peaks for the methyl protons of one Boc and also two sets of peaks for the isopropyl group. A high-temperature ¹H NMR study in DMSO-*d*₆ allowed us to correlate this observation with E/Z isomerisation of the *N*1-Boc. Coalescence of the proton resonances occurred at 120 °C. Once back at room temperature, the splitting of the signals returned and the NMR spectrum was identical to the initial spectrum, allowing us to prove that the compound was not damaged. [α]_D²⁰ = -66.9 (*c* = 1.45, CH₂Cl₂); *t*_r = 13.428 min; ¹H NMR (DMSO-*d*₆, 400 MHz) at 25 °C: δ 0.60 (m, 1H), 0.72 (d, 2H, *J* = 7.0 Hz), 0.90 (m, 1H), 0.97 (d, 2H, *J* = 7.2 Hz), 1.28 (s, 3H), 1.34 (s, 6H), 1.53 (s, 9H), 2.18–2.37 (m, 1H), 3.39–3.61 (m, 1H), 4.17 (d, 1H, *J* = 2.5 Hz), 4.42–5.15 (m, 3H), 5.72–5.92 (m, 2H); ¹³C NMR (CDCl₃, 100 MHz) at 25 °C: δ 16.0, 18.5, 18.8, 28.1, 28.3, 29.8, 30.2, 49.7, 62.2, 63.6, 81.2, 81.5, 82.6, 109.0, 121.2, 136.5, 149.3, 154.6, 166.3, 167.3; HRMS (FAB+) *m/z* calcd for C₂₁H₃₂N₂O₆ [M + H⁺] 409.2339, found 409.2324.

Notes and references

- 1 D. Farran, I. Parrot, J. Martinez and G. Dewynter, *Angew. Chem., Int. Ed.*, 2007, **46**, 7488.
- 2 S. D. Lee, T. H. Chan and K. S. Kwon, *Tetrahedron Lett.*, 1984, **25**, 3399.
- 3 O. Hara, M. Ito and Y. Hamada, *Tetrahedron Lett.*, 1998, **39**, 5537.
- 4 B. J. L. Royle, *Chem. Rev.*, 1995, **95**, 1981.
- 5 D. Farran, L. Toupet, J. Martinez and G. Dewynter, *Org. Lett.*, 2007, **9**, 4833.
- 6 T. Coursindel, D. Farran, J. Martinez and G. Dewynter, *Tetrahedron Lett.*, 2008, **49**, 906.

- 7 C. Alcaraz, M. Dolores Fernandez, M. Pilar de Frutos, J. L. Marco, M. Bernabé, C. Foces-Foces and F. H. Cano, *Tetrahedron*, 1994, **50**, 12443.
- 8 M. Oba, T. Terauchi, Y. Owari, Y. Imai, I. Motoyama, and K. Nishiyama, *J. Chem. Soc., Perkin Trans. 1*, 1998, 1275.
- 9 C. Gallina and A. Liberatori, *Tetrahedron*, 1974, **30**, 667.
- 10 K. Wimalasena and M. P. D. Mahindaratne, *J. Org. Chem.*, 1994, **59**, 3427.
- 11 P. Wipf and J.-L. Methot, *Org. Lett.*, 2001, **3**, 1261.
- 12 J. D. White and S. C. Jeffrey, *J. Org. Chem.*, 1996, **61**, 2600.
- 13 J. D. White, M. A. Avery, S. C. Choudhry, O. P. Dhingra, B. D. Gray, M. C. Kang, S. C. Kuo and A. J. Whittle, *J. Am. Chem. Soc.*, 1989, **111**, 790.
- 14 R. A. Holton, C. Somoza, H. B. Kim, F. Liang, R. J. Biediger, D. Boatman, M. Shindo, C. C. Smith, S. Kim, H. Nadizadeh, Y. Suzuki, C. Tao, P. Vu, S. Tang, P. Zhang, K. K. Murthy, L. N. Gentile and J. H. Liu, *J. Am. Chem. Soc.*, 1994, **116**, 1597.
- 15 G. S. Singh, M. D'hooghe and N. De Kimpe, *Chem. Rev.*, 2007, **107**, 2080.
- 16 M. Goodman and S. Ro, in *Burger's Medicinal Chemistry and Drug Discovery Volume I: Principles and Practice*, ed. M. E. Wolff, John Wiley & Sons, New York, 5th edn, 1995, vol. 1, pp. 833–838.
- 17 P. A. Hart, in *The Practice of Medicinal Chemistry*, ed. C. J. Wermuth, Academic Press, London, 1996, pp. 393–412.
- 18 T. K. Sawyer, in *Structure-Based Drug Design: Targets, Techniques and Developments*, ed. P. Veerapandian, Marcel Dekker, New York, 1997, vol. 1, pp. 559–634.
- 19 V. J. Hruby and P. S. Hill, in *Conformational Analysis of Medium-Sized Heterocycles*, ed. R. S. Glass, VCH, New York, 1998, pp. 217–260.
- 20 A. Félix, in *Houben-Weyl Methods in Organic Chemistry: Synthesis of Peptides and Peptidomimetics*, ed. M. Goodman, A. Félix, L. Moroder and C. Toniolo, Georg Thieme Verlag, Stuttgart, 2004, vol. E22c.
- 21 A. Giannis and T. Kolter, *Ang. Chem., Int. Ed. Engl.*, 1993, **32**, 1244.
- 22 J. Gante, *Ang. Chem., Int. Ed. Engl.*, 1994, **33**, 1699.
- 23 P. Gillespie, J. Cicariello and G. L. Olson, *Biopolymers*, 1997, **43**, 191.
- 24 S. Hanessian, G. McNaughton-Smith, H.-G. Lombart and W. D. Lubell, *Tetrahedron*, 1997, **53**, 12789.
- 25 A. S. Ripka and D. H. Rich, *Curr. Opin. Chem.*, 1998, 441.
- 26 O. Labbuda-Dawidowska, T. H. Wierzbza, A. Prah, W. Kowalczyk, L. Gawinski, M. Plackova, J. Slaninova and B. Lammek, *J. Med. Chem.*, 2005, **48**, 8055.
- 27 R. M. Freidinger, D. F. Veber, D. S. Perlow, J. R. Brooks and R. Saperstein, *Science*, 1980, **210**, 656.
- 28 R. M. Freidinger, D. S. Perlow and D. F. Veber, *J. Org. Chem.*, 1982, **47**, 104.
- 29 S. J. Miller, H. E. Blackwell and R. H. Grubbs, *J. Am. Chem. Soc.*, 1996, **118**, 9606.
- 30 F. P. J. T. Rutjes and H. E. Schoemaker, *Tetrahedron Lett.*, 1997, **38**, 677.
- 31 A. J. Phillips and A. D. Abell, *Aldrichimica Acta*, 1999, **32**, 75.
- 32 C. J. Creighton and A. B. Reitz, *Org. Lett.*, 2001, **3**, 893.
- 33 R. D. Long and K. D. Moeller, *J. Am. Chem. Soc.*, 1997, **119**, 12394.
- 34 D. Trancard, J. B. Tout, T. Giard, I. Chichaoui, D. Cahard and J.-C. Plaquevent, *Tetrahedron Lett.*, 2000, **41**, 3843.
- 35 M. Gutiérrez-Rodríguez, M. T. Garcia-Lopez and R. Herranz, *Tetrahedron*, 2004, **60**, 5177.
- 36 C. Catiuela and M.-D. Diaz-de-Villegas, *Tetrahedron: Asymmetry*, 2000, **11**, 645.
- 37 J. S. Clark and M. D. Middleton, *Org. Lett.*, 2002, **4**, 765.
- 38 K.-P. Park and M. J. Kurth, *Tetrahedron*, 2002, **58**, 8629.
- 39 T. Kawabata, S. Kawakami and S. Majumdar, *J. Am. Chem. Soc.*, 2003, **125**, 13012.
- 40 T. Ooi, T. Miki and K. Maruoka, *Org. Lett.*, 2005, **7**, 191.
- 41 F. E. King, T. J. King, and A. J. Warwick, *J. Chem. Soc.*, 1950, 3590.
- 42 L. A. Watanabe, S. Haranaka, B. Jose, M. Yoshida, T. Kato, M. Moriguchi, K. Soda and N. Nishino, *Tetrahedron: Asymmetry*, 2005, **16**, 903.
- 43 R. H. Grubbs and S. Chang, *Tetrahedron*, 1998, **54**, 4413.
- 44 S. J. Miller, S.-H. Kim, Z.-R. Chen and R. H. Grubbs, *J. Am. Chem. Soc.*, 1995, **117**, 2108.
- 45 Experiments were performed on Silicon Graphics Indigo using Discover Molecular Simulation program, Biosym/MSI (Accelrys, San Diego, USA).